

AD-A169 113 COORDINATED RESEARCH PROGRAM IN PULSED POWER PHYSICS

143

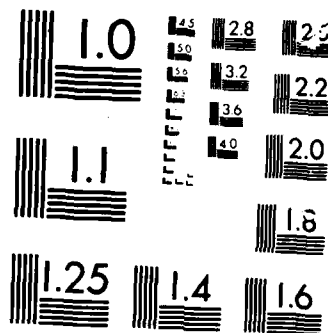
(U) TEXAS TECH UNIV LUBBOCK PULSED POWER LAB

H KRISTIANSEN ET AL. 20 DEC 85 AFOSR-TR-86-0305  
AFOSR-84-0032 F/G

UNCLASSIFIED AFOSR-84-0032

F/G 10/2

NL



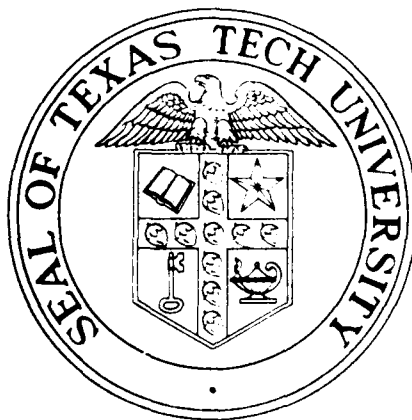
MICROCOPY

CHART

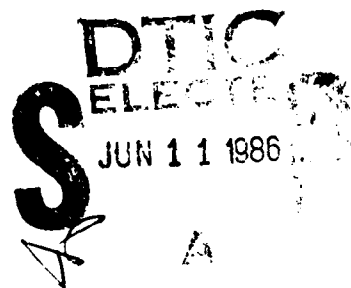
*(Handwritten mark)*

on  
COORDINATED RESEARCH PROGRAM  
in  
PULSED POWER PHYSICS

December 20, 1985



Air Force Office of Scientific Research  
Grant No. 84-0032



Approved for public release;  
distribution unlimited.

[ PULSED POWER LABORATORY  
Department of Electrical Engineering  
TEXAS TECH UNIVERSITY

Lubbock, Texas 79409

86 6 10 123

ORIGINAL COPY

AD-A169113

REPORT DOCUMENTATION PAGE

1a. REPORT SECURITY CLASSIFICATION <b>Unclassified</b>		1b. RESTRICTIVE MARKINGS	
2a. SECURITY CLASSIFICATION AUTHORITY		3. DISTRIBUTION/AVAILABILITY OF REPORT <b>Approved for public release; distribution unlimited.</b>	
2b. DECLASSIFICATION/DOWNGRADING SCHEDULE <b>N/A</b>		4. PERFORMING ORGANIZATION REPORT NUMBER(S)	
5. MONITORING ORGANIZATION REPORT NUMBER(S)		6a. NAME OF PERFORMING ORGANIZATION <b>Texas Tech University</b>	
6b. OFFICE SYMBOL (If applicable) <b>EE</b>		7a. NAME OF MONITORING ORGANIZATION <b>Air Force Office of Scientific Research</b>	
6c. ADDRESS (City, State and ZIP Code) <b>Department of Electrical Engineering P.O. Box 4439, Texas Tech University Lubbock, TX 79409</b>		7b. ADDRESS (City, State and ZIP Code) <b>Bldg. 410 Bolling Air Force Base Washington, DC 20332</b>	
8a. NAME OF FUNDING/SPONSORING ORGANIZATION <b>Air Force Office of Scientific Res.</b>		8b. OFFICE SYMBOL (If applicable)	
9. PROCUREMENT INSTRUMENT IDENTIFICATION NUMBER <b>AFOSR 84-0032</b>		10. SOURCE OF FUNDING NOS.	
11. TITLE (Include Security Classification) <b>See Front Cover</b>		PROGRAM ELEMENT NO. <b>61102F</b>	
		PROJECT NO. <b>2301</b>	
		TASK NO. <b>A7</b>	
		WORK UNIT NO.	
12. PERSONAL AUTHOR(S) <b>M. Kristiansen, G. Schaefer, K. Schoenbach, and H. Krompholz</b>			
13a. TYPE OF REPORT <b>Annual</b>		13b. TIME COVERED <b>10/ FROM 10/1/84 TO 31/85</b>	
		14. DATE OF REPORT (Yr., Mo., Day) <b>1985/12/20</b>	
		15. PAGE COUNT <b>205</b>	
16. SUPPLEMENTARY NOTATION			
17. CCSATI CODES		18. SUBJECT TERMS (Continue on reverse if necessary and identify by block number)	
FIELD	GROUP	SUB. GR.	
19. ABSTRACT (Continue on reverse if necessary and identify by block number)			
<p>The work on three programs, elements, related to pulsed power research, is described. The program is a multi-investigator program whose main emphasis is on gaining a better understanding of repetitive opening and closing switch phenomena. The main effort is on diffuse discharge opening switches but considerable progress has also been made on understanding and describing fundamental, transient discharge phenomena. Some effort has also been given to studies of electrode erosion and insulator damage in high power closing switches. In addition several smaller studies have considered various novel ideas and concepts to determine their potential for further investigations.</p>			
20. DISTRIBUTION/AVAILABILITY OF ABSTRACT <b>UNCLASSIFIED/UNLIMITED</b> <input type="checkbox"/> SAME AS RPT. <input checked="" type="checkbox"/> DTIC USERS <input type="checkbox"/>		21. ABSTRACT SECURITY CLASSIFICATION <b>Unclassified</b>	
22a. NAME OF RESPONSIBLE INDIVIDUAL <b>Major B. Smith</b>		22b. TELEPHONE NUMBER (Include Area Code) <b>202/767-4908</b>	
		22c. OFFICE SYMBOL <b>AFOSR/NP</b>	



Annual Report  
on  
COORDINATED RESEARCH PROGRAM  
IN  
PULSED POWER PHYSICS

AFOSR Grant #84-0032

December 20, 1985

Program Director: M. Kristiansen

Principal Investigators: M. Kristiansen  
H. Krompholz  
G. Schaefer  
K. Schoenbach

Associate Investigator: L. Hatfield

Research Associates: K. Zinsmeyer

Administrative Secretary: M. Byrd  
Secretary III: J. Davis

Graduate Students: A. Donaldson M. Ingram  
G. Hutcheson R. Cooper  
H. Harjes E. Strickland  
L. Thurmond D. Skaggs  
R. Korzekwa

AIR FORCE OFFICE OF SCIENTIFIC RESEARCH (AFOSR)  
NOTICE OF TECHNICAL REPORT  
This report is the property of the Air Force Office of Scientific Research and is  
loaned to you for your use only. It is not to be distributed outside your organization.  
AFOSR-12.  
MATTHEW S. REISER  
Chief, Technical Information Division

By	
Date	
Project Number	
Project Title	
Project Codes	
Project Manager	
Project Status	
Project Budget	
Project Personnel	
Project Equipment	
Project Materials	
Project Facilities	
Project Other	

QUALITY  
SELECTED  
3

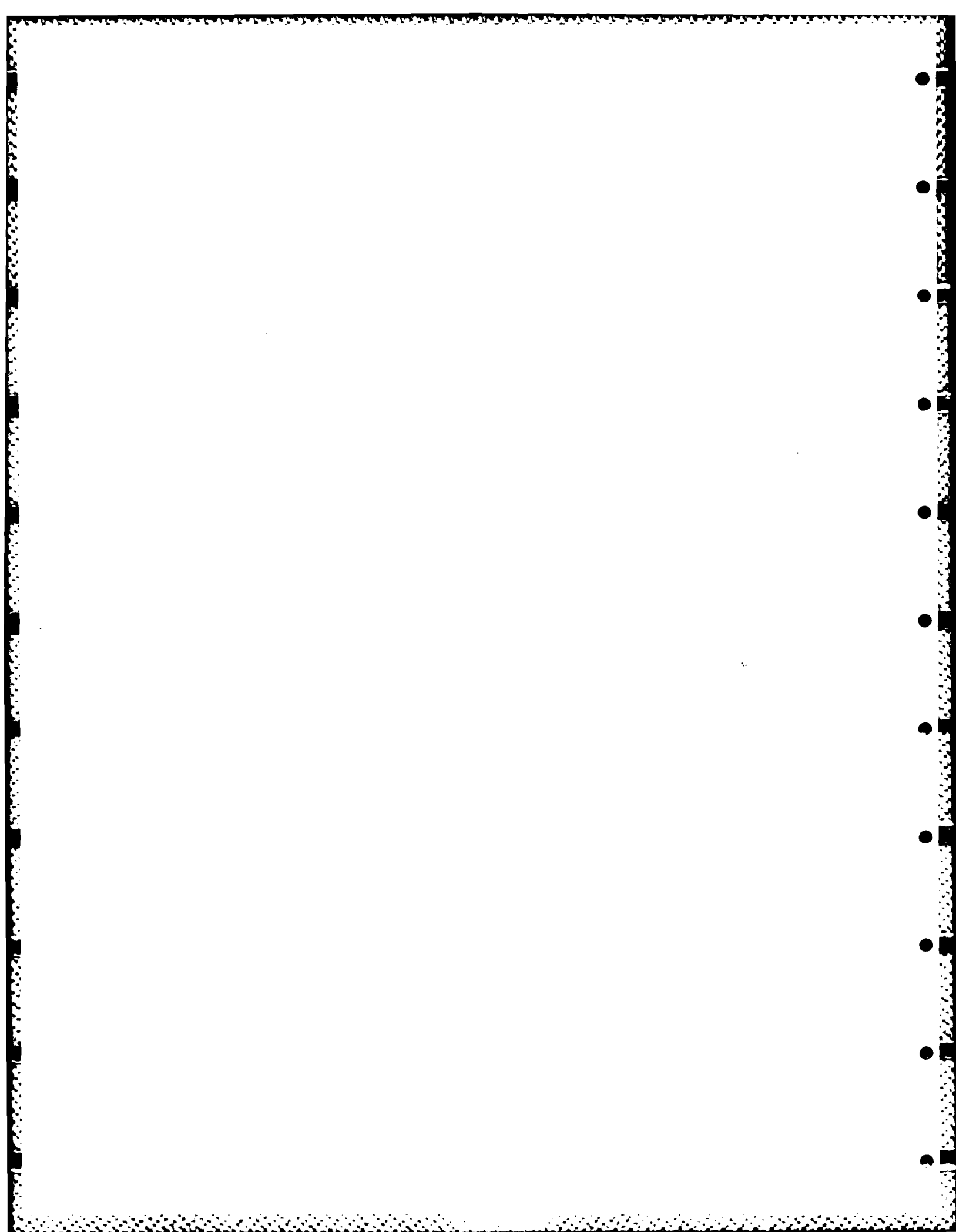


## TABLE OF CONTENTS

Summary of Research Objectives for 1984-85 . . . . .	1
Introduction . . . . .	3
Opening Switches . . . . .	4
Spark Gap and Arc Discharge Investigations . . . . .	8
Exploratory Concepts . . . . .	44
Faculty Publication, 1984-85 . . . . .	50
Interactions, 1984-85 . . . . .	53
Advanced Degrees Awarded, 1984-85 . . . . .	57
Seminars, 1984-85 . . . . .	58
Guests, 1984-85 . . . . .	59

## SUMMARY OF RESEARCH OBJECTIVES

for

1984-85

OPENING SWITCHES

1. Investigations of repetitive e-beam controlled discharges with respect to gas properties.
2. Investigation of optogalvanic effects with respect to their use as discharge control mechanisms.
3. Studies of concepts for optically assisted, e-beam sustained, diffuse discharge switches.
4. Modeling of diffuse discharges, including control mechanisms.
5. Feasibility studies of novel opening switch concepts.

SPARK GAP AND ARC DISCHARGE INVESTIGATIONS

1. Optical diagnostic methods will be developed to investigate propagation phenomena associated with streamers in detail. The emphasis will be on polarity effects (positive and negative streamers) and their influence on gap closing as a function of parameters. The influence of x-ray preionization on the propagation velocity will be investigated.

2. General scaling laws for the breakdown delay will be formulated, defining requirements for multichannel operation. The requirements will be tested experimentally.
3. Theoretical investigations will be continued with the aim of formulating general scaling laws describing the properties of streamer formation and propagation, yielding a quantitative understanding of the basic phenomena in overvolted spark gaps.

#### EXPLORATORY CONCEPTS

Some of the previous year's investigations may be carried over to the second year. In addition we specifically propose (if the needed Raman shifter becomes available) to:

Determine the feasibility of using Stark shifts in admixtures of  $H_2$  to determine the electric fields at localized points in pulsed power systems\*.

In addition, as in previous years, new projects will be added as new ideas are generated.

---

\* Funds for the Raman shifter were not awarded so the emphasis changed towards injector problems for railguns.

## INTRODUCTION

The Coordinated Research Program in Pulsed Power Physics is a multi-investigator Program involving 4 Principal Investigators, 1 Associate Investigator and 9 Graduate Students. Other faculty investigators from Electrical Engineering, Physics and Chemistry, also interacted and cooperated at various times. The program is jointly sponsored by AFOSR and ARO. Some 4 refereed journal articles and 11 conference proceedings papers were published last year. Several other papers were prepared or submitted for publication. Some of these are reproduced in the Appendices. The main projects are Opening Switches, Spark Gap and Arc Discharge Investigations, and Exploratory Concepts.

## OPENING SWITCHES

(C. Harjes, G.Z. Hutcheson, R.A. Korzekwa, D. Skaggs,  
E. Strickland, G. Schaefer, M. Kristiansen,  
K.H. Schoenbach, and H. Krompholz)

### I. Summary

The primary objective of this work is to study control processes in externally sustained or controlled diffuse discharges, with respect to their application as opening switches. Concepts for diffuse discharge opening switches have been developed, experimental facilities have been assembled and experiments have been performed to investigate the applicability of these concepts. Computer codes have been developed and applied to different systems to allow optimization and scaling.

The major research areas of the last year in the field of diffuse discharge opening switches were:

- concepts for diffuse discharge opening switches (Section II)
- the electron-beam sustained diffuse discharge (Section III)
- the optically controlled diffuse discharge, where optical control either means increased conductivity of the discharge by means of laser radiation or optical stimulation of loss processes (Section IV)

For the investigation of the electron-beam sustained discharge an apparatus was designed, operated, and improved, which allows investigations of repetitive opening in the time range of 100 ns at current levels of up to 10 kA.

Experiments performed with this device during the last year concentrated on investigations with gases recommended by the group of L.G. Christophorou at Oak Ridge National Laboratories, such as gas mixtures with Argon and  $\text{CH}_4$  as buffer gases and admixtures of attachers, such as  $\text{C}_2\text{F}_6$  and  $\text{C}_3\text{F}_8$ .

The investigations on optical control processes concentrated on two mechanisms:

- 1) photodetachment
- 2) photoenhanced attachment

and their influence on the characteristics of externally and self sustained discharges.

## II. Opening Switch Concepts

The development and evaluation of new switch concepts and the utilization of new processes for external discharge control was a permanent issue during the entire research period. Individual processes considered in the last year are presented in the next two sections. A general overview of the field of diffuse discharge opening switches is presented in an invited review article which will be published in IEEE Transactions on Plasma Sciences (Appendix A). A short review was also presented at the IEEE Pulsed Power Conference, 1985 (Appendix B).



### III. E-Beam Controlled Diffuse Discharge Switch

The work on electron beam sustained discharges for switching applications in the last year concentrated on investigations with gas mixtures with an attachment rate increasing with  $E/N$ . All these gas mixtures show an increase of resistivity with increasing  $E/N$ . If the attachment rate increases strongly with  $E/N$ , a negative differential conductivity is also found.

Although such a characteristic has advantages for the closed phase and for the opening phase, it can cause several problems. One is the development of striations in the intermediate  $E/N$  range. This effect is discussed in a 1985 IEEE Pulsed Power Conference presentation (Appendix C) and in a paper which will be submitted to the Journal of Applied Physics (Appendix D).

Another effect is the interaction of an element with negative differential conductivity with a high impedance circuit. Investigations concerning this effect are presented in one of the 1985 IEEE Pulsed Power Conference presentations (Appendix B) and in a paper which will be submitted to the Journal of Applied Physics (Appendix E). The most recent results have also been submitted to two conferences in 1986 (Appendix F and G).

A third effect investigated is the interaction of the electron source (e-beam) with the attachers used in the gas discharge. This effect is discussed in two conference proceedings papers (Appendix B and H).

#### IV. Optically Controlled Discharges

The optical control mechanisms, considered to be most suitable for external discharge control, are photodetachment and optically enhanced attachment. The influence of these effects on the discharge characteristic has to be investigated over the full  $E/N$  range of interest, which means mainly for externally sustained discharges and the transition region to the self sustained discharge. The experimental setup used for these investigations is a transverse electrode configuration with a UV source incorporated into one of the electrodes, similar to a TEA laser. Such configurations can also be used as optically sustained discharge opening switches. The turn-on and turn-off characteristics of UV sources have therefore been investigated and are presented in a paper which will be submitted to the Journal of Applied Physics (Appendix I).

This setup in combination with a dye laser was used to investigate the influence of photodetachment on the characteristics of an externally sustained discharge. These investigations will be published in the Journal of Applied Physics (Appendix J).

SPARK GAP AND ARC DISCHARGE INVESTIGATIONS

(A.L. Donaldson, M. Ingram, M. Lehr,  
H. Krompholz, and M. Kristiansen)

Due to a change in personnel this part of the research program was modified considerably, in agreement with the Program Monitor, Major H. Pugh. Professor F. Williams moved to the University of Nebraska and Prof. H. Krompholz returned to Germany. Most of the originally proposed work was centered around Prof. Krompholz. We, therefore, concentrated on our previous erosion studies along with a smaller effort along the lines originally proposed, namely x-ray preionization of switch gases.

The high current facility used in some of the electrode erosion work was constructed with SDIO/DNA support and all future high current ( $\geq 100$  kA) work along these lines will be supported by that contract. The facilities were used on this (AFOSR) contract to provide some continuity with our previous low current (10's kA) studies and verify some of our predictions.

## A. ELECTRODE EROSION

(A.L. Donaldson, M. Lehr,  
H. Krompholz, and M. Kristiansen)

## I. Summary

The work performed during the last contract period has focused primarily on addressing the limitations on high current, high energy switches resulting from electrode erosion. A summary of the major accomplishments is outlined below with a more complete discussion given in the succeeding sections.

- Further materials testing in this low-current regime (10-20 kA) confirmed that crack formation in stainless steel could be explained by the presence of manganese stringers and eliminated by realignment of the arcing surface perpendicular to the stringer orientation.
- In conjunction with work supported by a SDIO-DNA contract, two new testing facilities were completed which allowed for peak currents up to 750 kA (280 kA has been tested to date).
- High current testing was carried out on several new materials, including 3 copper composites (CuC, CuZr, CuCrZr) as well as molybdenum, copper, and graphite. At least one of these materials (CuC) promises to offer superior erosion resistance at high current.

- The discontinuity effect (a rapid transition in electrode erosion rate as a function of peak current) was found to be a function of electrode area, material and the relative initial charging polarity.
- The significance of vapor jet heating of the opposite electrode as one of the major energy sources leading to electrode erosion was confirmed.
- An extensive library has been compiled on arc erosion (over 250 papers to date), including numerous translations from the Soviet literature (provided by the US Army FSTC, Mr. Larry Turner). Considerable interest for this bibliography has been expressed by the scientific community and an annotated bibliography is currently being prepared.

## II. Low Current Material Erosion Comparison

Four more materials were tested on the Mark II system (20 kA, 25  $\mu$ s, unipolar, 50,000 shots); Al, Cu, CuZr, and CuZrCr [1]. Figure 1 shows the relative performance of the materials compared with those previously tested. All three copper materials had very low erosion rates and were equal to or better than the previously best material, copper tungsten. Figures 2 and 3 show the surfaces of these electrodes and indicates that pure copper might give better voltage stability performance in that it yields a smoother surface after testing. As expected, aluminum was a poor performer, though not as bad as graphite. It was tested primarily to give results for one more pure element in order to allow for a

comparison of theoretical and experimental performances based on thermophysical properties.

Considerable effort was spent on analyzing the process of crack formation in stainless steel. The results were presented at the 5th IEEE Pulsed Power Conference and are given in Appendix K. Although later tests showed that stainless steel was not suitable for use in high current, high energy switches, the information concerning crack formation may be useful in those applications.

### III. High Current Erosion Measurements

In order to perform electrode erosion tests at higher currents (50-750 kA) the Mark V and Mark VI facilities shown in Fig. 4 were constructed. Both systems consist of a resistively charged capacitor bank connected in series to a water cooled test gap. When the capacitor bank is charged to the self-breakdown voltage of the spark gap it discharges through the test gap, producing a slightly damped oscillatory current wave form, as shown in Fig. 5. The current is given by the equation

$$i(t) = \frac{V_0}{\omega_0 L} e^{-Rt/2L} \sin \omega_0 t,$$

where  $V_0$  is the capacitor voltage,  $R$  and  $L$  are the circuit resistance and inductance and

$$\omega_0 = \sqrt{\frac{1}{LC} - \left(\frac{R}{2L}\right)^2}.$$

Thus, the inductance and resistance were kept to a minimum to guarantee maximum current for a given capacitance. The discharge current was varied by changing the system capacitance. Both Mark V and Mark VI were modular in design in that they used interchangeable spark gaps, header plates, etc. Basically the Mark VI capacitor bank consisted of up to six Mark V capacitor banks connected in parallel. The system operating parameters for these investigations are given below.

	<u>Mark V</u>	<u>Mark VI</u>
Peak Current (at 35 kV)	240 kA	600 kA
Energy/shot	1.6 - 8 kJ	1.6 - 48 kJ
Effective charge/shot	1-5 Coul	1-30 Coul
Capacitance	2-10 $\mu\text{F}$	2-60 $\mu\text{F}$

The first series of experiments consisted of investigating the rapid transition in the electrode erosion rate as a function of peak current which is known to take place for several electrode materials, including copper. This discontinuity in the erosion rate has been studied previously [2-10] for a wide range of currents and gas pressures. The primary explanation for the effect has been the increase in molten material ejection due to an increase in the current density at the electrodes. The purpose of the experiments performed at Texas Tech was twofold:

- 1) to further develop models for both electrode heating and material removal in the high current regime in order to make qualitative statements about scaling the erosion rate and

- 2) to enlarge the material database to include several more recently developed materials.

The experimental conditions for all the test results given in this report are as follows:

Gas	Air
Gap Spacing	1 cm
Total Coulomb Transfer	1155 Coul
Electrode Diameter	1.27, 2.54 cm
Gas Pressure	1-3 atm (varied to keep the breakdown voltage approximately constant at 32 kV)
Number of Shots	300-1500 (varied to keep the total Coulomb transfer constant for all experiments)
Capacitance	1.85-9.25 $\mu\text{F}$ (varied to study the effect of current, - peak current increases as the square root of the system capacitance)

The results for the first series of experiments are given in Figs. 6-8.

The effect of initial electrode polarity on the erosion of 1.27 cm diameter copper electrodes is shown in Fig. 6. A discontinuity in the anode erosion rate is easily observed with over an order of magnitude increase in the erosion rate occurring as the current is increased from 150 kA to 200 kA. Single shot and



cumulative damage patterns for the anode at several test currents are shown in Figs 9-11. The discontinuity seems to occur at the point at which the single shot damage pattern just begins to encompass the entire hemispherical electrode tip. For still higher current levels the arc is restricted by the electrode geometry to the same effective electrode area and thus the increase in current density leads to enhanced erosion by one of two mechanisms to be discussed later.

It is thought that at low currents the electrode erosion is dominated primarily by vaporization, whereas at higher currents the bulk of the erosion occurs in the molten phase. Examination of the electrode surfaces and the eroded debris shown in Figs. 12 and 13 tend to support this conclusion. Also, from Fig. 6, it is seen that the slope of the total erosion rate vs current increases as  $I^6$ , while the cathode erosion rate remains approximately constant in this transition region. This result seems to suggest that material is being transferred from the anode to the cathode in the transition region. Examination of the profiles of the electrodes shown in Fig. 14 indicates that not only is this true but that a significantly different mechanism for erosion is occurring, depending on the initial polarity. Keeping in mind that the discharge is oscillatory, with only slight damping, the question naturally arises - Why is there a polarity effect at all? After all, any effect which is polarity dependent would occur on each electrode alternately as the current reverses direction. The key to understanding this is realizing that this statement is only true if the initial conditions "seen" by each subsequent current

reversal are the same. In fact they are not. For example several important physical factors are fundamentally different during the first half cycle. First, during the initial rise of the current the arc is known to be in its most resistive phase since the gas is being ionized and electrode vapor is being released and heated to provide charge carriers for current conduction. Thus, a pulse of energy is delivered to the intergap region resulting from the product of the voltage (which falls from  $V_{\text{charge}}$  to  $V_{\text{arc}}$ ) and the current (rising from zero to its peak  $I_p$ ). All other current peaks on subsequent cycles occur after the voltage across the gap has collapsed to its minimum value. Secondly, the peaks in the current which occur later in the discharge are formed in a lower density, higher temperature gas, although the effect this has on the erosion or the energy delivered to the electrode is unknown. Finally the density of the individual current filaments is also likely to be a function of particular points in time on the current waveform as a result of both of the previous considerations. Thus, both the experimental results and physical reasoning seem to suggest that what occurs during the arc's formative stages in the first half cycle of the discharge plays a significant role in determining the degree of electrode erosion. It should be noted that under slightly different conditions the erosion pattern of the initial anode and cathode could be reversed. This tends to support the role of vapor jet erosion of the opposite electrode, mentioned in the last annual report [11], and will be discussed with some other experimental evidence in the section on vapor jet heating of the electrode.

Returning to the original set of experiments, the discontinuity effect was also studied as a function of the electrode diameter, as seen in the initial results shown in Fig. 7. The slope of the transition region is reduced from an  $I^6$  dependency for 1/2" diameter electrodes to approximately  $I^{3.5}$  for 1" diameter electrodes. The exact scaling will more than likely be a function of the geometry of the electrodes as well as several other factors, but it is evident that a critical parameter is the macroscopic current density  $I_p$ /electrode area. A similar conclusion was found by Gremmel [3] for lower currents, longer pulsewidths and by Belkin [6], at high currents.

Finally, Fig. 8 shows the effect of changing the electrode material from copper to graphite. It is believed that graphite does not have a transition region because it erodes via vaporization throughout the range of currents tested. The results are important for several reasons:

- 1) no apparent discontinuity in the erosion rate occurs for graphite in this current range,
- 2) there is a point, approximately 160 kA under these conditions, at which graphite performs substantially better than copper, thus a material which had given relatively poor erosion characteristics at low current was clearly the best material at high currents,
- 3) graphite is a material whose resistivity is almost two orders of magnitude higher than copper, which tends to rule out  $I^2R$  losses in the electrode as the dominant heating mechanism under these conditions.

Finally, a comparison of the erosion rates of all materials tested in this current regime is shown in Fig. 15. It is clear that both copper-graphite and graphite offer superior resistance to erosion. The question remains - Why? To answer this, several experiments were conducted to look at the two main mechanisms thought to be responsible for electrode erosion - vapor jet heating of the opposite electrode and its associated phenomena, and the interaction of current filaments leading to liquid droplet ejection in copper and molybdenum electrodes.

#### IV. Vapor Jet Effects

Vapor jets emanating from the electrode surface are thought to be a primary source for heating the opposite electrode and under some conditions for electrode erosion as well. A description of the vapor jet phenomena along with a review of the relevant literature was given in the last annual report [11]. Experiments designed to evaluate the role of vapor jets in electrode erosion were based on the following properties:

- 1) the smaller the diameter of the electrode the higher the jet energy (restricting the effective nozzle, which leads to higher velocities),
- 2) the larger the area of the opposite electrode the more energy is received by the electrode from the jet,
- 3) the lighter the atomic weight of the electrode producing the jet, the lower the jet energy.

The experiments consisted of changing the electrodes diameter from 2.54 cm to 1.27 cm and mixing materials (carbon anode copper cathode etc.). The results are given below.

## Vapor Jet Heating Experiments

Exp.				
No.	Anode Type	Cathode Type	Anode Loss (cm <sup>3</sup> )	Cathode Loss (cm <sup>3</sup> )
1	1" Cu	1" Cu	0.023	0.026
2	1/2" Cu	1/2" Cu	0.14	0.043
3	1/2" Cu	1" Cu	0.10	0.23
4	1" Cu	1/2" Cu	0.16	0.073
5	1/2" C	1" Cu	0.037	0.041

Experiments one and two were run to provide points of reference. Comparing the first three experiments we see that the cathode erosion is a strong function of the size of the opposite electrode with a smaller opposite electrode producing greater erosion. Experiment four indicates that this effect is more a function of size than of polarity. Finally, experiment five together with experiment three indicates that the material of the opposite electrode also affects the erosion with the lighter atomic weight, carbon producing significantly less erosion. All of these results would be correct if the vapor jet phenomenon plays a significant role in electrode erosion. Referring back to the earlier results of erosion versus electrode material it seems likely that carbon and carbon composite electrode materials perform well at high currents since their lower atomic weight reduces the energy transferred to the electrodes.

## V. References

1. Copper composite materials provided courtesy of the Nippert Company, 801 Pittsburgh Drive, Delaware, Ohio 43015, I.I. Koppinen, Director, a subsidiary of Outokumpu Oy.
2. W. Neumann, "On material loss in an aluminum disk electrode during high-intensity sparks", translated from Scientific Journal of the Humboldt University, Berlin, GDR, Mathematics and Natural Sciences Series, Nr. 5, Year 3, (1953/54).
3. H. Gremmel, "Das Abbrandverhalten der Elektroden von Starkstromlichtbogen bei kurzer Lichtbogendauer," Dissertation, Technische Hochschule Braunschweig, (1963).
4. G.S. Belkin and V. Ya. Kiselev, "Electrode Erosion in a Pulsed High Current Discharge," Sov. Phys. Tech. Phys. 11, pp. 280-283 (1966).
5. G.S. Belkin and V. Ya. Kiselev, "Influence of Electrode Material on Erosion at High Currents", Sov. Phys. Tech. Phys. 12, pp. 702-703 (1967).
6. G.S. Belkin and V. Ya. Kiselev, "Effect of the Medium on the Electrical Erosion of Electrodes at High Currents", Sov. Phys. Tech Phys. 23, pp. 24-27 (1978).
7. J.E. Gruber and R. Suess, "Investigation of the Erosion Phenomenon in High Current, High Pressure Gas Discharges", Institute fur Plasma Physik, Garching bei Munchen, IPP 4/22 (1969).
8. H.W. Turner and C. Turner, "Choosing Contact Materials", Electronics and Power, pp. 437-439 (1968).

9. G.M. Goncharenko and Ye. N. Prokhorov, "Erosion of Electrodes Due to Switching of Capacitor Bank Discharge Circuits", translated from Trudy, Moskovskogo Energeticheskogo Instituta, Tekhnika Vysokikh Naprazheniy, No. 114, Moscow, pp. 86-88 (1972).
10. R.B. Piejak, H. Wilhelmsen and S.R. Robertson, "Time-Resolved Studies of Anode Erosion by High-Current Density Arcs of Millisecond Duration", GTE Lab Report TR 82-567.2 (1982).
11. Final Report on Spark Gap Erosion, AFOSR Contract #84-0015 Texas Tech University (Dec. 20, 1984).
12. Poco Graphite Co., Decatur, TX.
13. Schwarzkopf Development Corp., Holliston, MA
14. Contacts Metals Welding Inc., Indianapolis, IN.
15. Carpenter Technology Corp., Reading PA.
16. DuDuCo KG, D 7530 Pforzheim, im Altgefall 12, GDR.

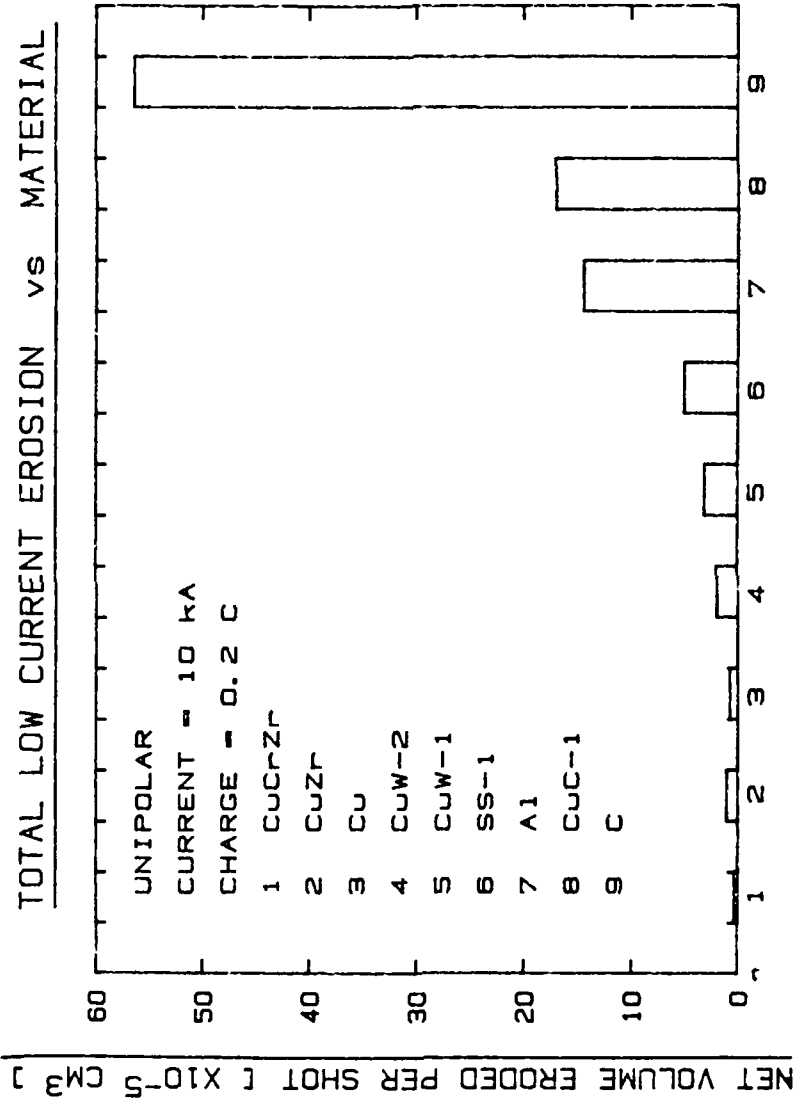
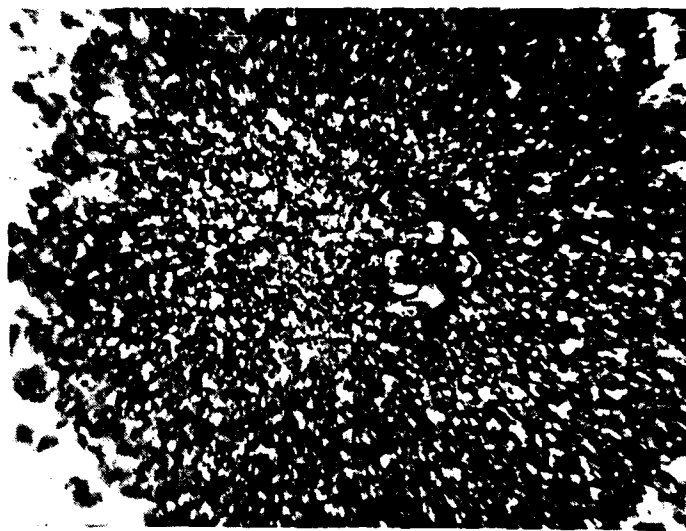


Fig. 1 Total Low Current Erosion vs Material

(C(ACF-10Q)12, CuC-1(DFP-1C)12 is 35% carbon by weight, CuW-1 (K-33)13 is 67% tungsten by weight, CuW-2 (3W3)14 is 68% tungsten by weight, SS-1 (304)15 is stainless steel).





5mm —————

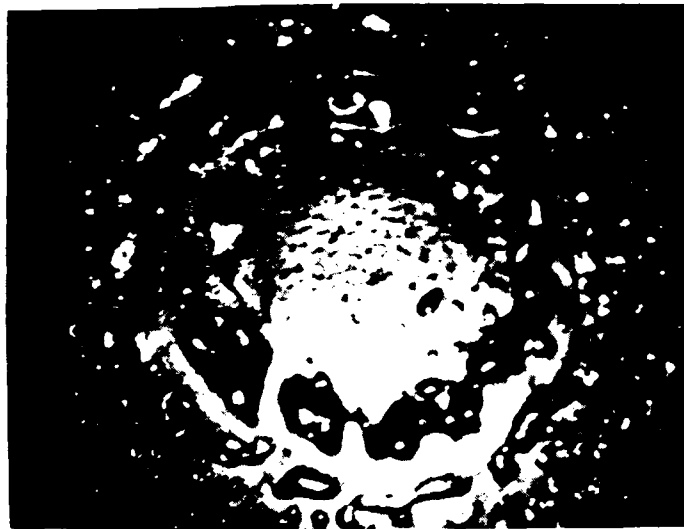
a) Aluminum anode, 50,000 shots



5mm —————

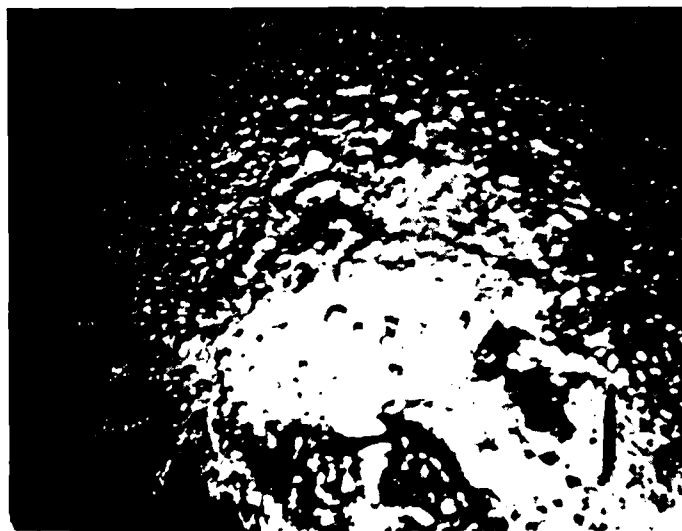
b) Copper anode, 50,000 shots

Fig. 2 Low Current Electrode Surface Damage



5mm |—————|

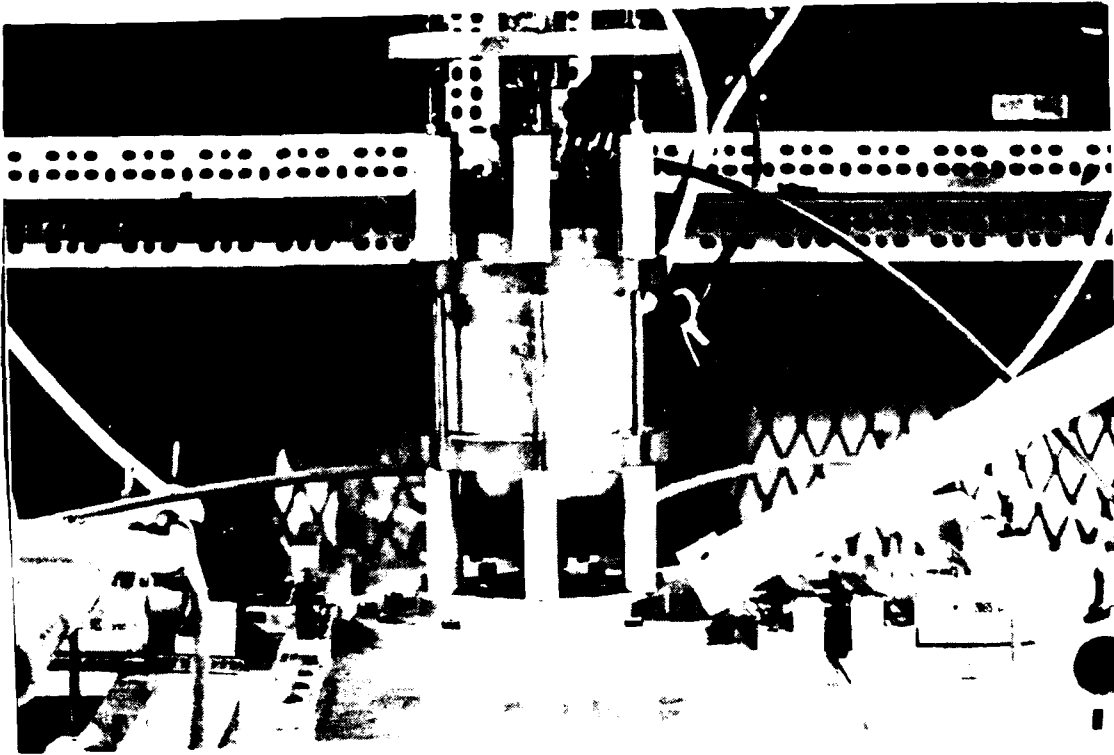
a) Copper Zirconium anode, 50,000 shots



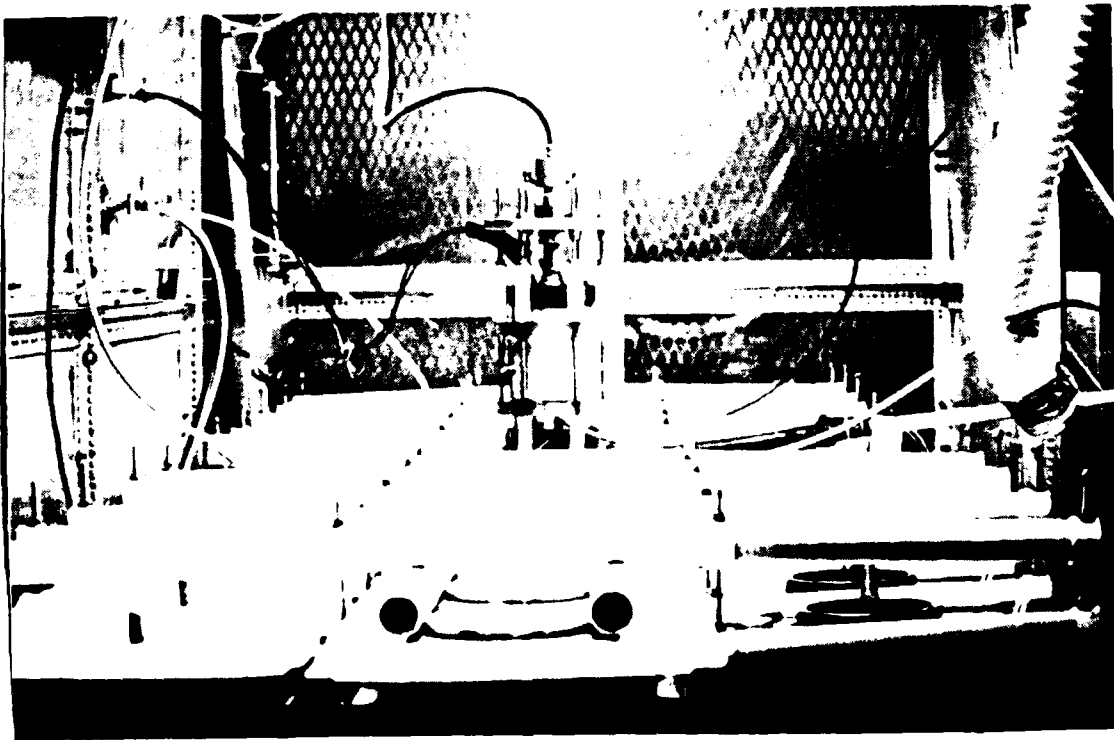
5mm |—————|

b) Copper Zirconium Chromium anode, 50,000 shots

Fig. 3 Low Current Electrode Surface Damage



a) Mark V, VI spark gaps



b) Mark VI capacitor bank

Fig. 4 Test Facilities

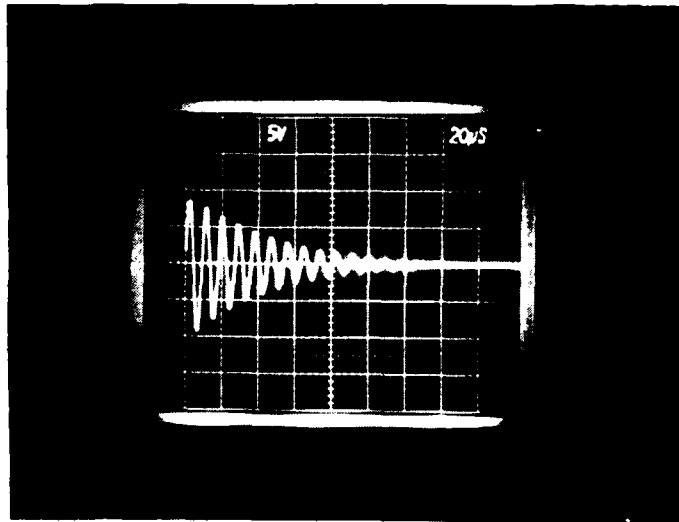


Fig. 5 Mark V Current Waveform ( $20 \mu\text{s}/\text{div.}$ ,  $120 \text{ kA}/\text{div}$ )

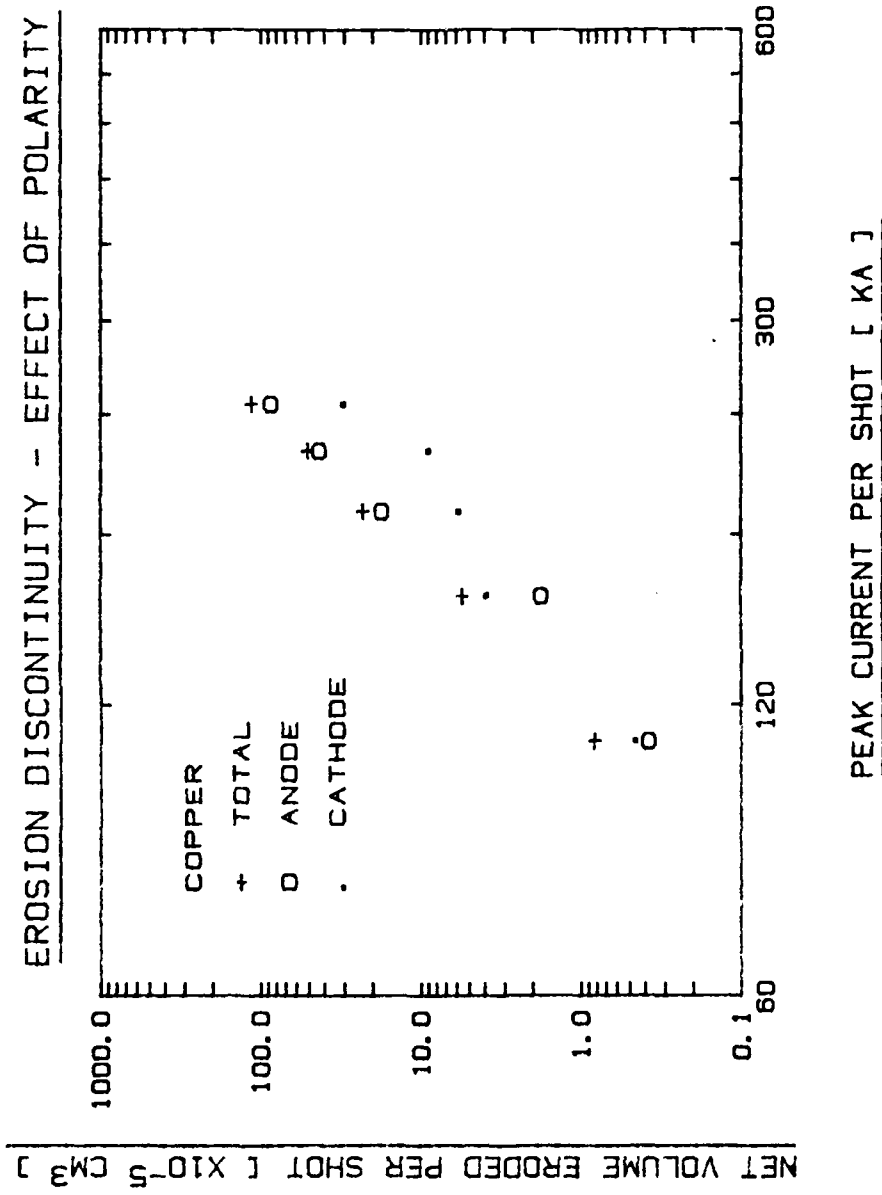


Fig. 6 Effect of Electrode Polarity on Electrode Erosion in the Transition Region

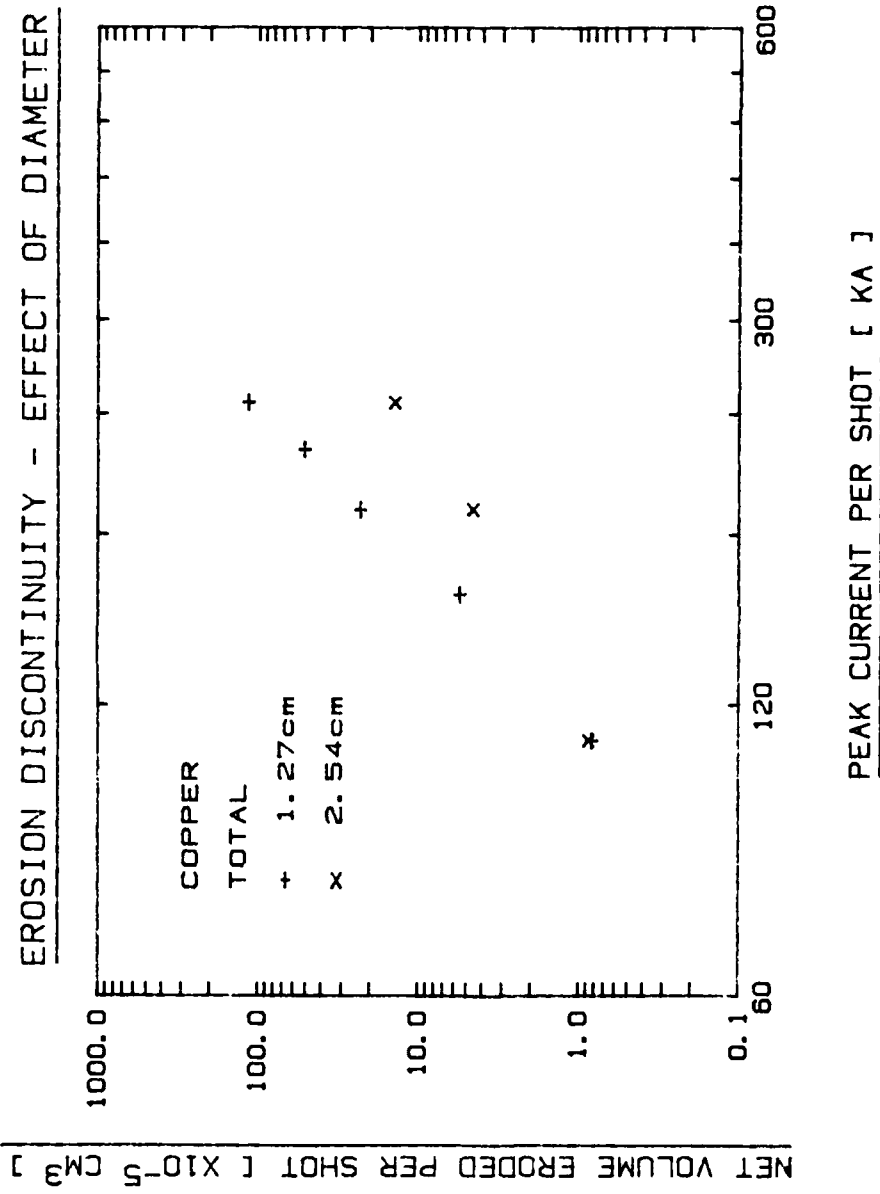


Fig. 7 Effect of Electrode Diameter on Electrode Erosion in the Transition Region

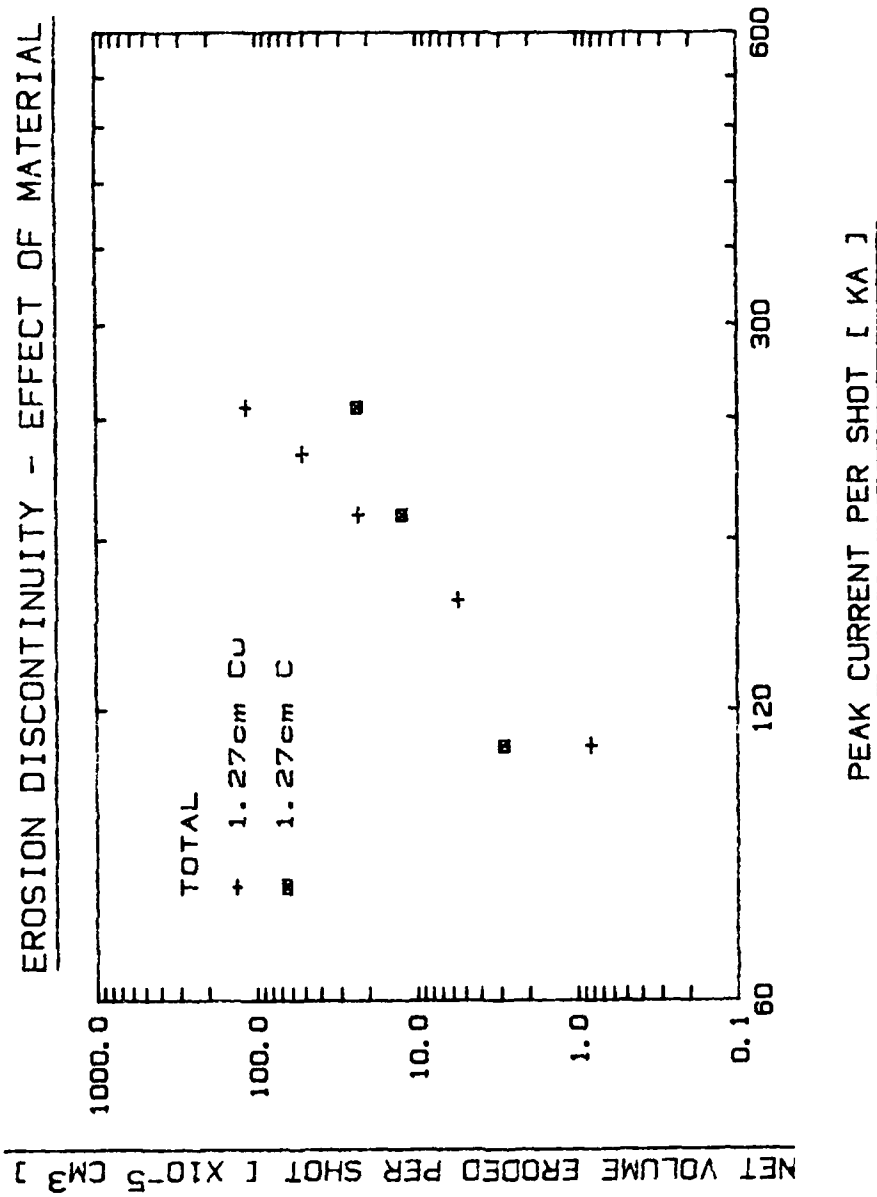
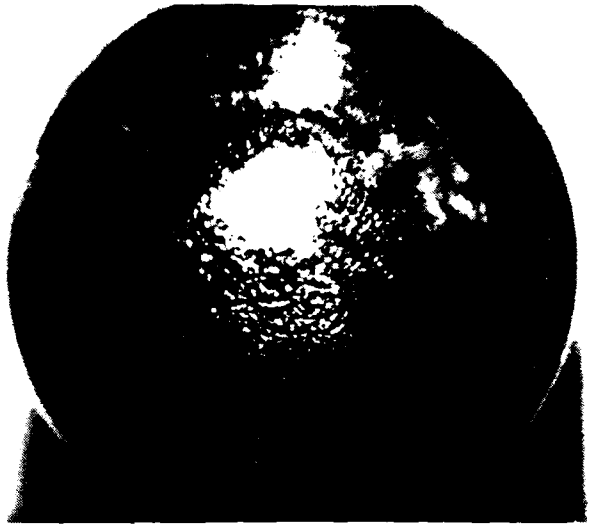
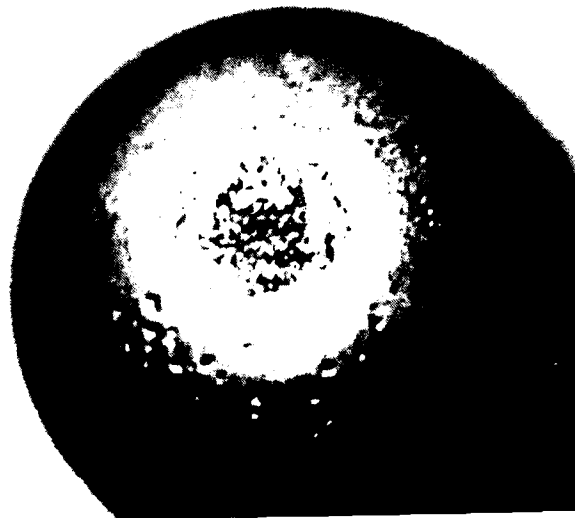


Fig. 8 Effect of Electrode Material on Electrode Erosion in the Transition Region



5mm

a) Single shot damage

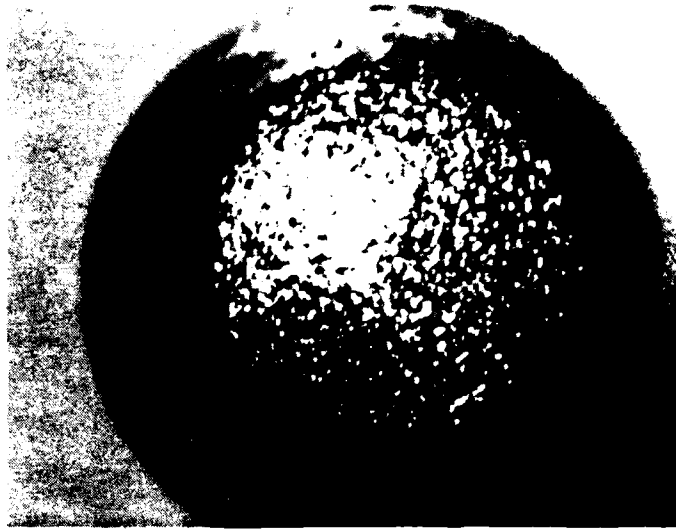


5mm

b) Cumulative damage, 1,500 shots

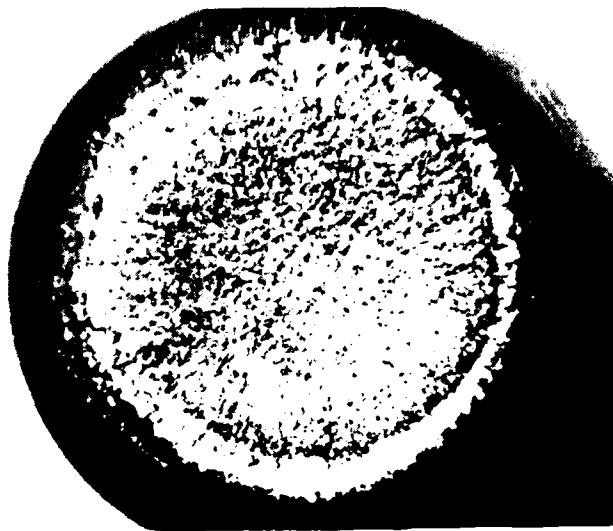
Fig. 9 Copper Anode Erosion at 110 kA





5mm

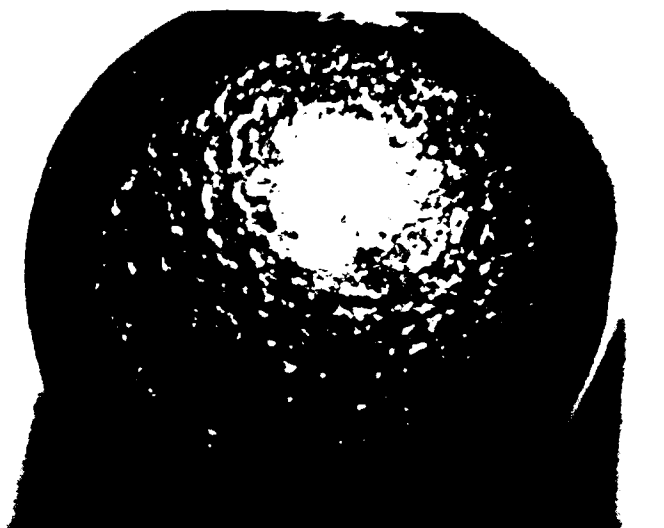
a) Single shot damage



5mm

b) Cumulative damage, 750 shots

Fig. 10 Copper Anode Erosion at 156 kA

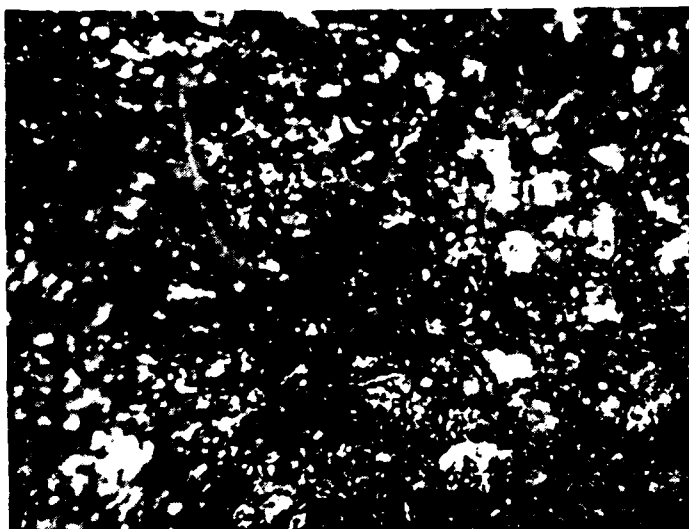


5mm |-----|  
a) Single shot damage



5mm |-----|  
b) Cumulative damage, 500 shots

Fig. 11 Copper Anode Erosion at 190 kA



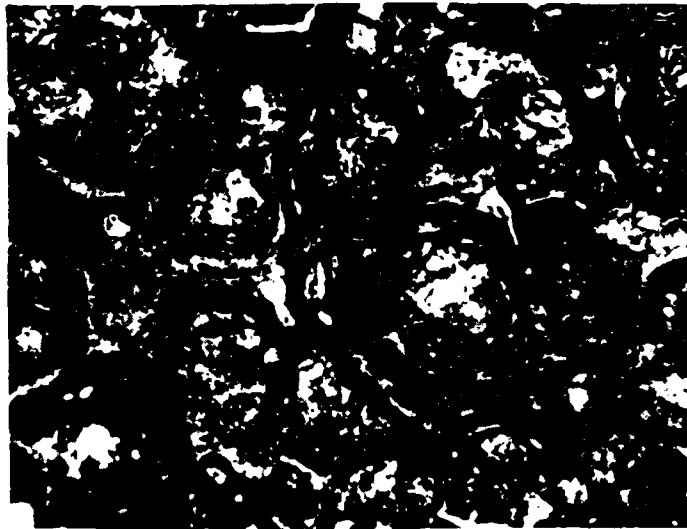
a) Surface, 0.5 mm



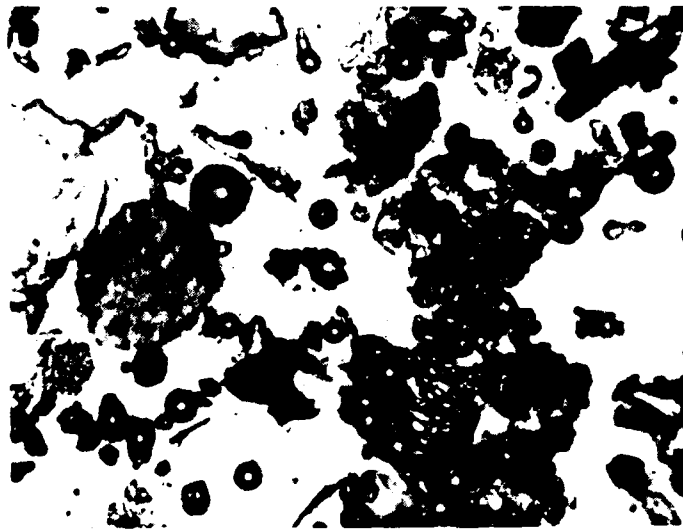
0.5 mm

b) Debris removed from gap

Fig. 12 Anode Erosion at 110 kA

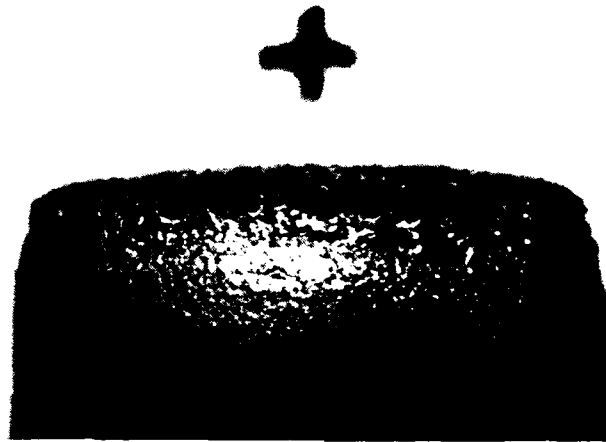


a) Surface, 0.5 mm



0.5 mm  
b) Debris removed from gap

Fig. 13 Copper Anode Erosion at 240 kA

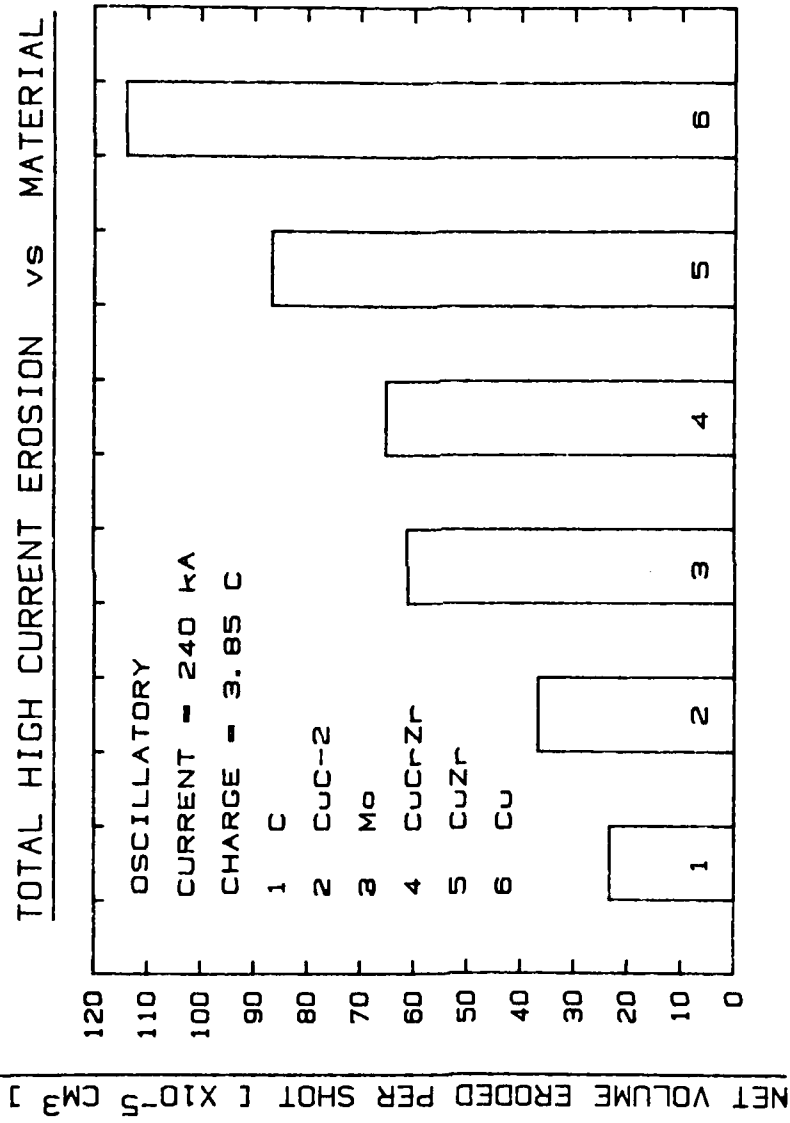


a) Anode, 5 mm



b) Cathode, 5 mm

Fig. 14 Copper Electrode Profiles after 300 shots



### ELECTRODE MATERIALS

Fig. 15 Total High Current Electrode Erosion vs Material  
(CuC-2 (Graphor 3)16 is 3% carbon by weight)

## B. X-RAY IONIZATION OF SWITCH GASES

(M. Ingram and M. Kristiansen)

X-rays have been successfully used to preionize various gas discharge lasers, providing known electron densities and volumes. This same method may be used to preionize spark gaps for triggering purposes. However, no data are available on the obtainable preionization densities in spark gap gases at greater than atmospheric pressure. Thus, a study was begun to measure the electron density in typical spark gap gases (Air,  $N_2$ ,  $SF_6$ ) and pressures (1, 3, 5 atmospheres) in order to predict the effectiveness of x-rays as a trigger source and provide known initial conditions in a spark gap for later studies.

We are currently investigating x-ray ionization of Air, Nitrogen,  $SF_6$ , and Argon. The x-ray source is a cold cathode, tungsten anode, flash x-ray tube manufactured by ITT. It is driven by a fast Marx bank at voltages up to 150 kV. Because of the large divergence of the tube, the x-rays are passed through a Soller slit (thin parallel stainless steel plates) to form a collimated rectangular beam. The x-rays are then introduced into a pressure chamber via a Plexiglas window (Fig. 1). The chamber contains the gas under study, and is used at pressures up to 5 atm. Inside the chamber is a large, flat, rectangular electrode (12 cm long) separated by the gas from a series of twelve small collection electrodes. Each small electrode is 8 mm long, separated by 2 mm and terminated in a 10 k resistor. When a potential is applied to these electrodes, the electrons generated

by the x-rays will drift toward the collection electrodes. By monitoring the current extracted from these electrodes, the ionization levels in the gas at various positions (from 1 to 12 cm) can be measured.

Results have been obtained for Argon and Nitrogen (Figs. 2 & 3). In Argon, with a 100 kV pulse applied to the tube,  $5 \times 10^7$  to  $2.5 \times 10^8$  ionized particles have been measured at pressures from 1 to 5 atm. At 150 kV tube voltage, the total number of electrons ranges from  $1 \times 10^8$  to  $5 \times 10^8$ , for the same pressures. For Nitrogen, at 100 kV tube voltage,  $1.3 \times 10^6$  to  $4.22 \times 10^6$  electrons were generated. For 150 kV,  $4.13 \times 10^6$  to  $9.14 \times 10^6$  electrons were generated.

In each of the above measurements, a peak in the ionization was found at typically 4.5 cm from the Plexiglas window, and then leveled off at about 6.5 cm. This is because the average photon energy is considerably lower than the maximum energy (tube voltage). At these lower energies, the absorption is greater. Absorption of higher energy photons remains nearly constant (and very small) through the length of the chamber, but the lower energy photons are absorbed more readily near the front end of the chamber.

No measurements have been obtained for air or  $\text{SF}_6$ , as was originally intended. This is because the strong attachment in these gases prevents any electrons from drifting across the gap and being collected. Rough approximations can be made however, by considering the atomic weights and densities of these gases. Since the absorption coefficient in  $\text{N}_2$  is slightly less than in



air, more electrons should be generated in air than in  $N_2$ . However, since air is 80%  $N_2$  and 20%  $O_2$ , the level should not be too different. Similarly,  $SF_6$  should produce more than Argon, since it is considerably denser.

This same x-ray tube has been incorporated into a spark gap to investigate the reliability of this source as a trigger mechanism (see Fig. 4). The tube is mounted on the ground electrode (top) so that the x-rays are admitted into the pressurized chamber along the axis of the electrodes. A 2" long hollow lead cylinder (I.D. = 4 mm) in the top electrode is used for collimation. The ground electrode is made of 1" diameter graphite with a hemispherical tip (graphite was chosen for its narrow selfbreak-down distribution and low x-ray absorption). Graphite and stainless steel were alternated for the high voltage electrode. The graphite electrode, because of its low x-ray absorption, will not eject any electrons when bombarded by x-rays; thus, the electrons generated in the gap can be considered as arising from the gas ionization. The stainless steel electrode will absorb x-rays very readily, and so acts as an additional source of electrons. Because of this, the gap polarity will also be considered.

Trigger delays ranged from 77 ns to 350 ns. In general, for graphite/graphite electrodes, delays ranged from 100 to 200 ns for air, and from 170 to 350 ns in Nitrogen. In every case, the triggered gap voltage was greater than 95% of  $V_{SB}$ . For the graphite/stainless steel combination with positive polarity, delays of 77 ns to 180 ns delays were measured, at voltages greater than 95%  $V_{SB}$ . For the same electrodes with a negative polarity, delays of

80 ns to 240 ns ( $> 75\% V_{SB}$ ) in air and 86 ns to 220 ns ( $> 95\% V_{SB}$ ) in Nitrogen were obtained. Obviously, this triggering scheme does not perform well, due to the low ionization of the gas. Since the gas absorbs lower energy x-ray photons better, a lower energy, higher intensity source may improve the performance.

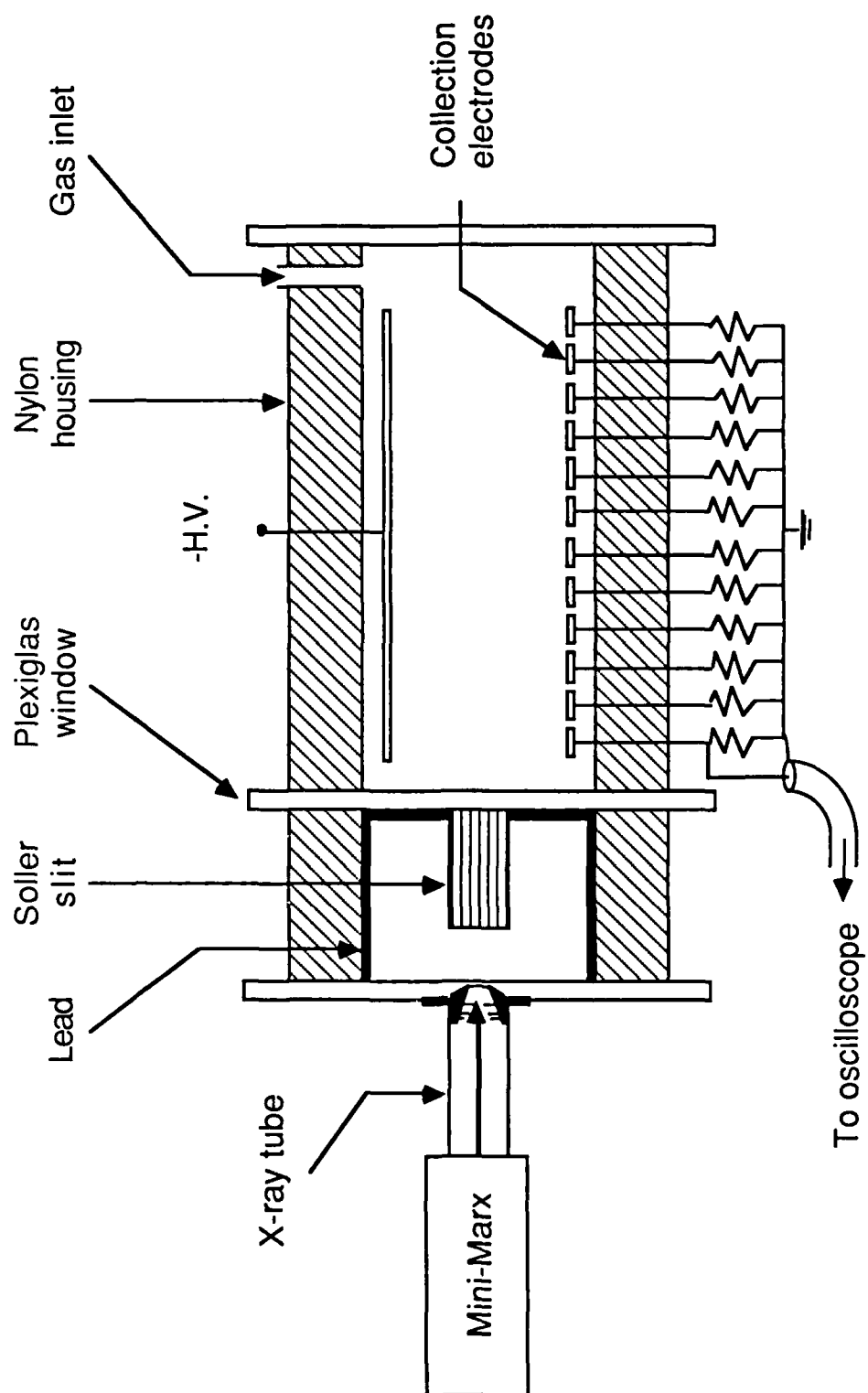
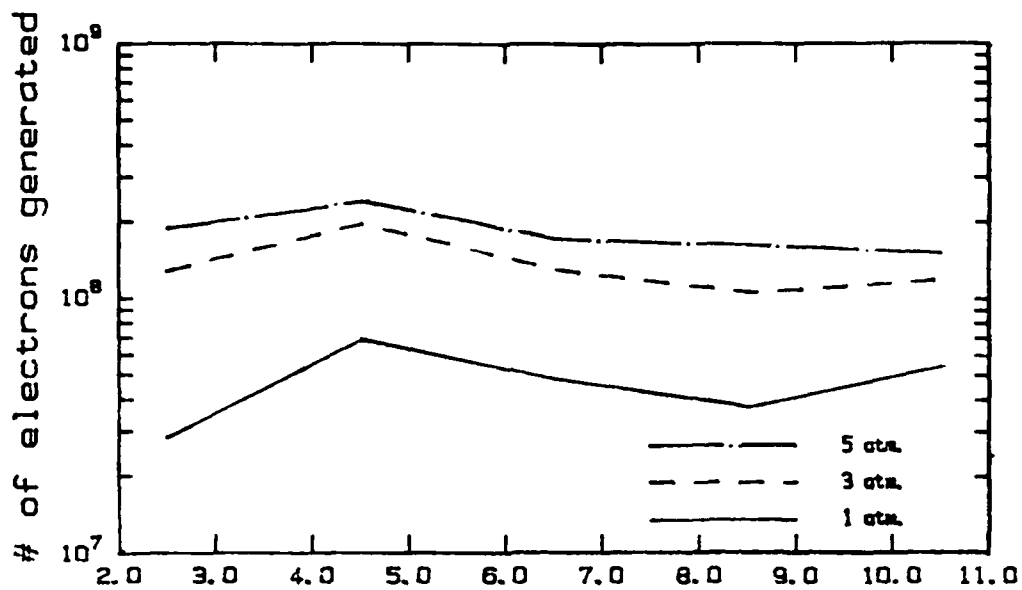
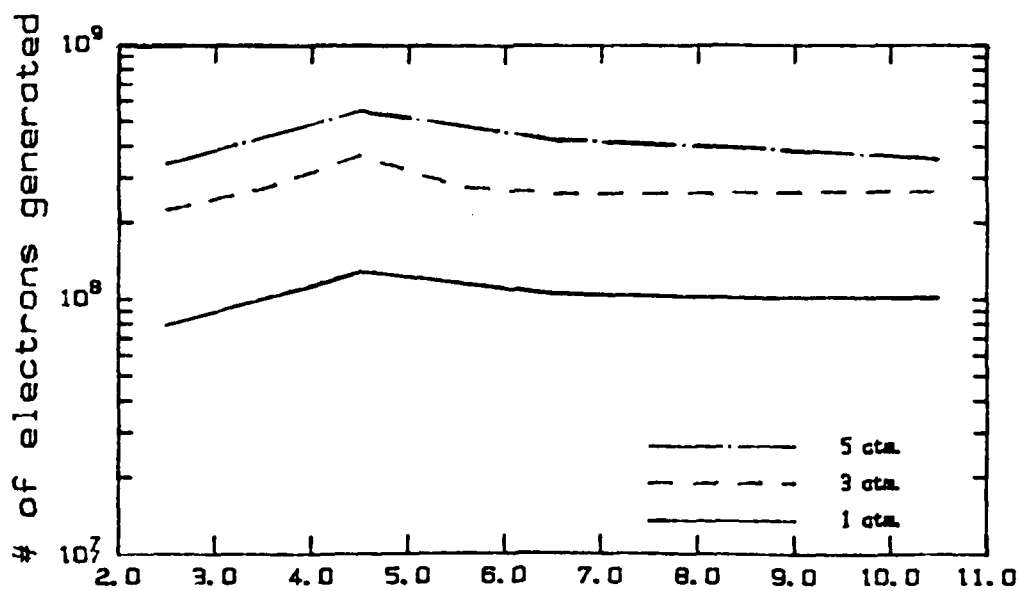


FIG. 1 : Ionization chamber.

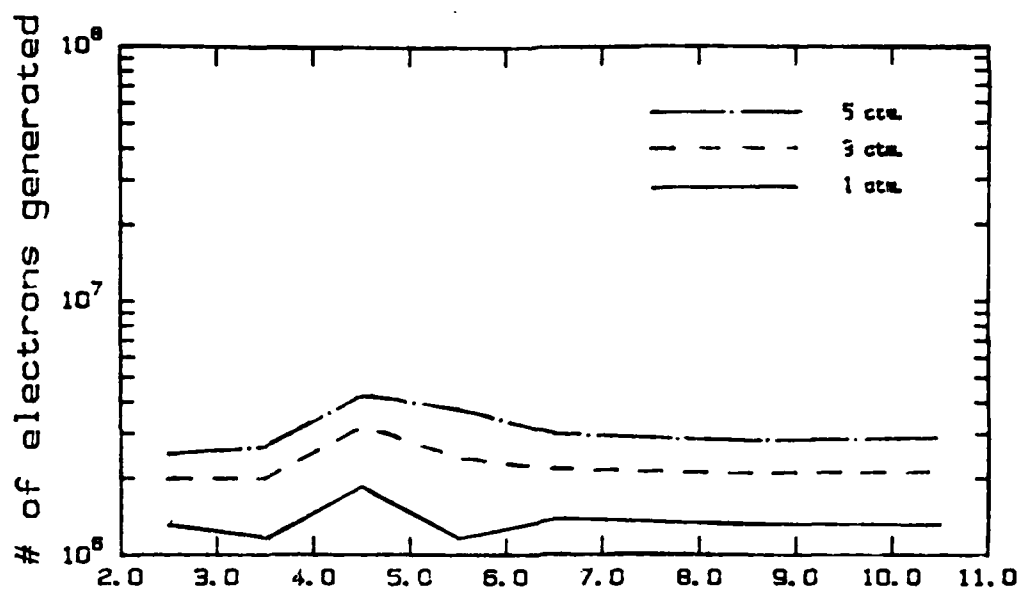


(a) Distance from source (cm) for 100kV.

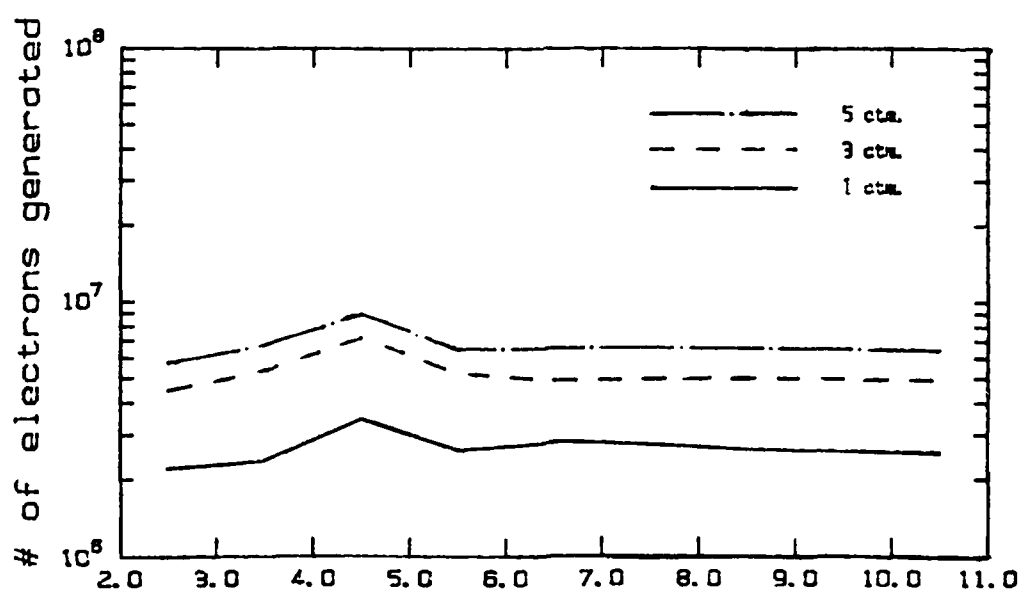


(b) Distance from source (cm) for 150kV.

Fig. 2 : Ionization vs. distance in Argon.



(a) Distance from source (cm) for 100kV.



(b) Distance from source (cm) for 150kV.

Fig. 3 : Ionization vs. distance in Nitrogen.

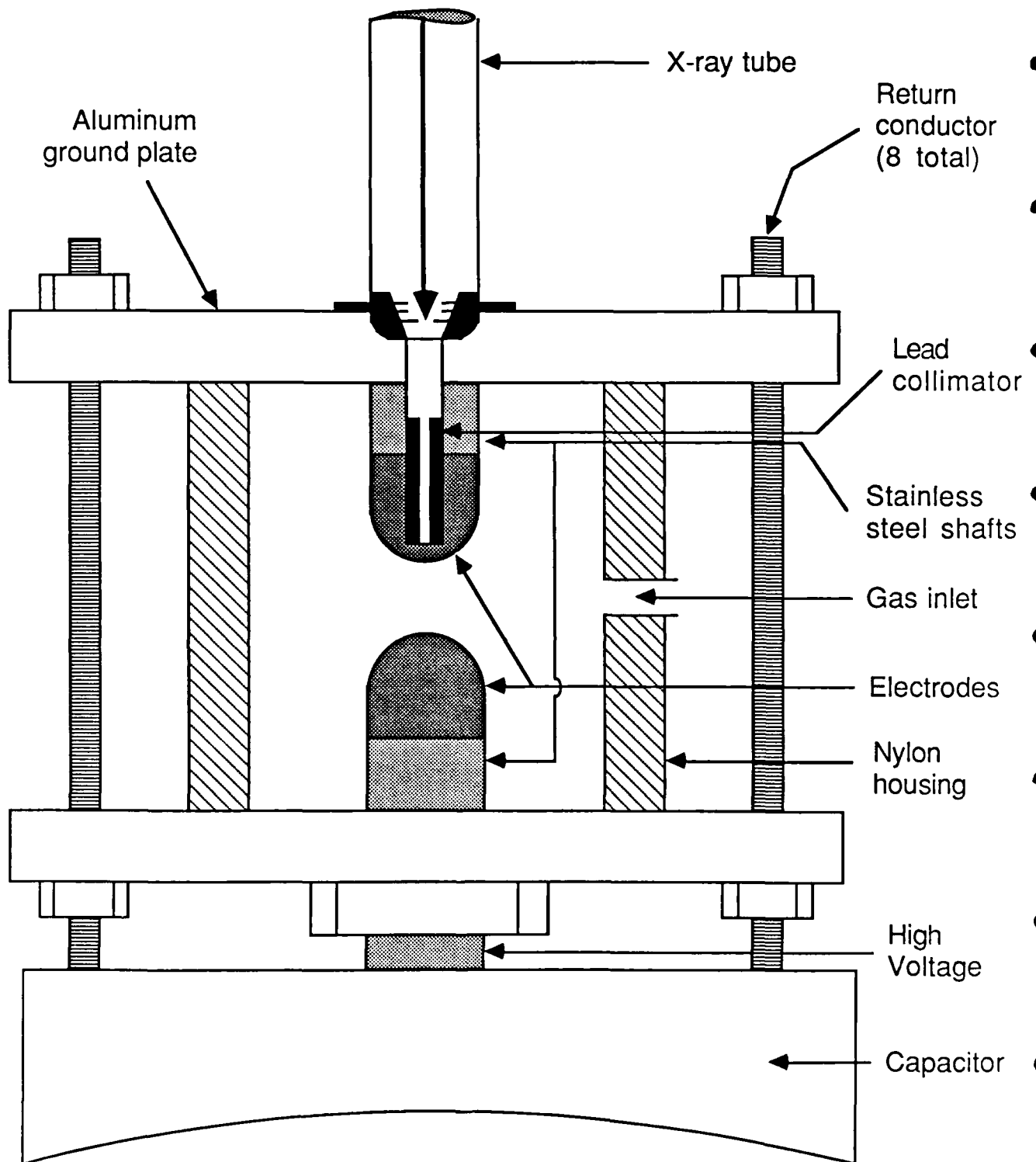


Fig. 4 : Spark gap assembly

EXPLORATORY CONCEPTS

(M. Ingram, P. Ranon, K. Ikuta\*, and M. Kristiansen)

I. Introduction

Since we did not obtain funds for the Raman shifter for our laser we were not able to carry out the main proposed investigation. Instead we concentrated on surface discharges and on the development of a new concept for injecting "bullets" in a railgun. Work is also underway on the proposed decrease of losses in microwave structures and should be completed within the next 1-2 months. The limits to channel currents in surface discharge switches has not been found. The limit is certainly much higher than we had expected and beyond our present switch capacity of about 250 kA. The work on surface discharges (insulator damage in intense discharge environments) will be continued with DNA/SDIO support.

---

\* Visiting Scientist from the Institute of Plasma Physics  
Nagoya University, Nagoya, Japan 464

## II. Surface Discharge Switching\*

(P. Ranon<sup>+</sup>, M. Kristiansen, and L. Hatfield)

During the first 6 months of fiscal year 1985, an existing surface discharge switch was modified to increase the current level from less than 10 kA to 130 kA in order to study the dynamic performances of insulators. Hold-off voltage versus the number of shots and the cold recovery voltage (hold-off voltage of the degraded insulator material after the surface was allowed to cool) were reported for: (1) G-10 (fiberglass poly laminate), (2) Delrin, and (3) Teflon. An experimental setup shown in Figure 1 was used to discharge a ringing current with a peak of 130 kA across the surface of insulator samples under test. The discharge current was determined by the hold-off voltage (initially set to approximately 40 kV) of the insulator material which was degraded by surface erosion.

The insulator performance results for G-10, Delrin, and Teflon are reported in the paper entitled "High Current Surface Discharge Switch", 5th IEEE Pulsed Power Conference (Appendix L) and are not duplicated here.

In the last months of the fiscal year 1985 additional funding was received from SDIO/DNA to study insulators for railguns at high currents and Coulomb transfer. Two additional surface

---

\* Work jointly supported by the AFOSR and SDIO/DNA

<sup>+</sup> USAF Officer (AFIT Student)



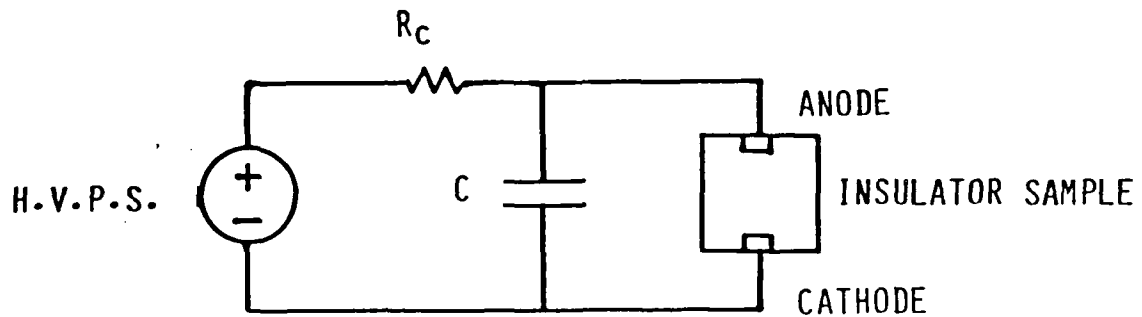
discharge switches as shown in Figs. 2 and 3, were designed and constructed using their funds. We presently have the capability of accommodating insulator samples up to 5 cm x 10 cm x 30 cm and peak discharge currents in excess of 200 kA (not all parameters simultaneously). Parameters of the discharge are (1)  $I_{\text{peak}} > 200$  kA, (2)  $f_0 = 435$  kHz, and current reversal of  $> 85\%$  (second current peak divided by the first current peak).

With the two newly constructed surface discharge switches, we plan to test the following materials in the first six months of F.Y. 1986:

- (1) Alumina Ceramics,
- (2) G-11,
- (3) Boron-nitride (possibly silicon-nitride)
- (4) Silicon Carbide, and
- (5) Kapton.

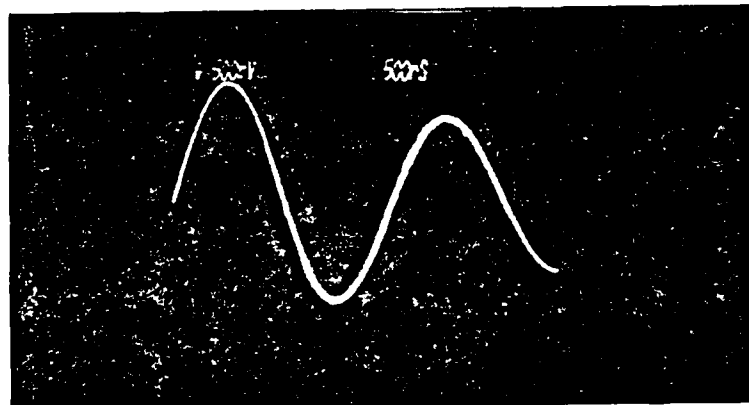
During the 2nd half of F.Y. 1986, a possible theoretical model of insulator erosion will be proposed based on experimental results obtained in the first half of F.Y. 1986. Most of this work will be supported by SDIO/DNA except as it applies specifically to high power switch performance.

TEST CONDITIONS  
SCHEMATIC OF EXPERIMENTAL CIRCUIT



- H.V.P.S. - HIGH VOLTAGE POWER SUPPLY (0-70 kV)  
 $R_c$  - CHARGING RESISTOR (100 k $\Omega$ )  
 $C$  - ENERGY STORAGE CAPACITOR (1.85  $\mu$ F)

SAMPLE CURRENT DISCHARGE WAVEFORM



- $I_{PEAK} = 200$  kA  
 $F_0 = 435$  kHz  
 $I_2/I_1 = 85\% + (I_1 - \text{FIRST PEAK}, I_2 - \text{SECOND PEAK})$

Fig. 1

PHOTOGRAPHS OF EXPERIMENTAL SET-UP

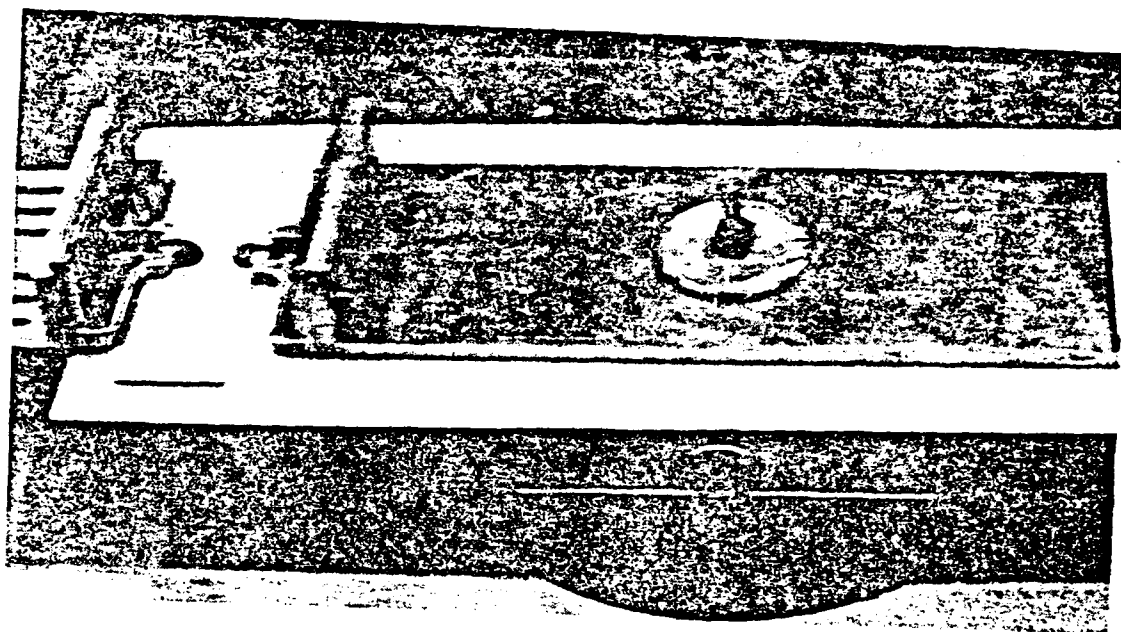


Fig. 2 140 kA MAX, 330 kHz RINGING DISCHARGE

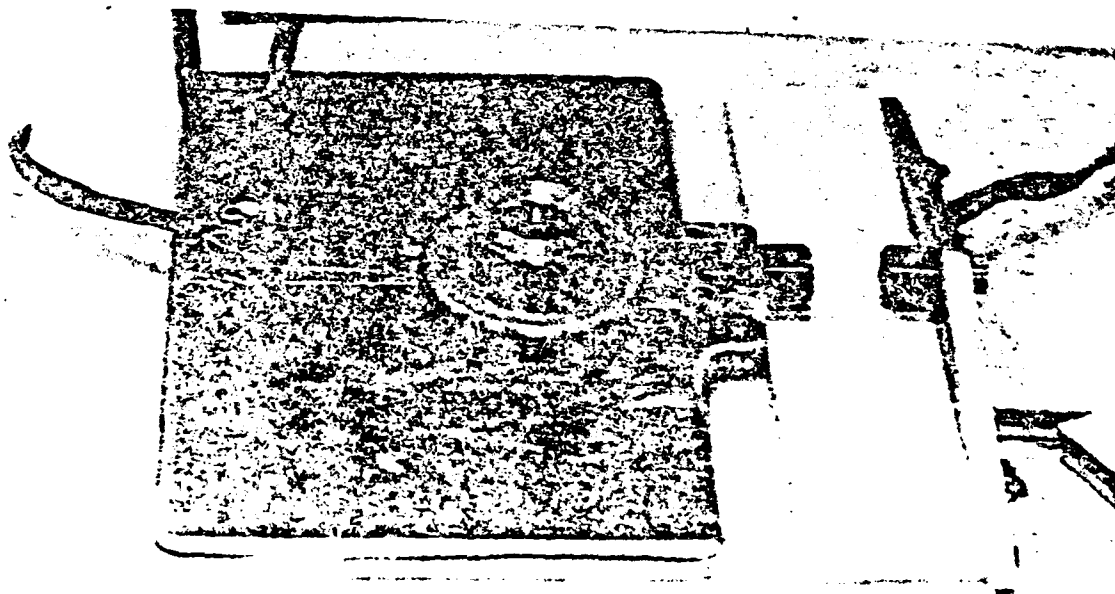


Fig. 3 200 kA +, 435 kHz RINGING DISCHARGE

### III. Conical Liner Implosion as a Projectile Injector for Mass Driver

(K. Ikuta and M. Kristiansen)

#### Introduction

A novel, high voltage injector concept for railguns has been developed. The resulting paper has been submitted for publication in the Japanese Journal of Applied Physics (Appendix M).

An important conclusion by the development is that it is possible to give a projectile an injection velocity of order  $1 \text{ km sec}^{-1}$  by use of the conical liner with its length of 25 cm. The necessary current for squeezing the cone is of the order  $10^6$  amperes for this injection velocity. An interesting case for the concept is the conical  $\theta$ -pinch injector in which the current along the liner can be driven by an induced electric field. In this case, repetitive injections of the projectiles into the railguns will become possible.

## Journal Papers and Conference Proceeding Papers

Published with AFOSR Support (1984-85)

H.C. Harjes, K.H. Schoenbach, G. Schaefer, M. Kristiansen, H. Krompholz, and D. Skaggs, "An Electron Beam Tetrode for Multiple, Submicrosecond Pulse Operation," Rev. Sci. Instr., vol. 55, pp. 1684-1686, Oct. 1984.

G. Schaefer, P. Husoy, K.H. Schoenbach, and H. Krompholz, "Pulsed Hollow-Cathode Discharge with Nanosecond Risettime," IEEE Trans. Plasma Sci, Vol. PS-12, pp. 271-274, Dec. 1984.

K.H. Schoenbach, G. Schaefer, M. Kristiansen, H. Krompholz, H.C. Harjes, and D. Skaggs, "An Electron-Beam Controlled Diffuse Discharge Switch," J. Appl. Phys., vol. 57, pp. 1618-1622, March 1985.

H. Krompholz, K.H. Schoenbach, and G. Schaefer, "Transmission Line Current Sensor," Proc. IEEE Conf. Instrumentation/Masurement Technology, Tampa, FL, March 1985.

G. Schaefer, B. Pashaie, P.F. Williams, K.H. Schoenbach, and H. Krompholz, "A New Design Concept for Field Distortion Trigger Spark Gaps," J. Appl. Phys., vol. 57, pp. 2507-2511, April 1985.

G. Schaefer and K.H. Schoenbach, "External Control of Diffuse Discharge Switches," Proc. 5th IEEE Pulsed Power Conf., Arlington, VA, June 1985, to be published.

K.H. Schoenbach, G. Schaefer, M. Kristiansen, H. Krompholz, D. Skaggs, and E. Strickland, "An E-Beam Controlled Diffuse Discharge Switch," Proc. 5th IEEE Pulsed Power Conf., Arlington, VA, June 1985, to be published.

M.R. Wages, G. Schaefer, K.H. Schoenbach, and P.F. Williams, "Streak Photographic Studies of Trigatron Triggered Breakdown," Proc. 5th IEEE Pulsed Power Conf., Arlington, VA, June 1985, to be published.

J.R. Cooper, K.H. Schoenbach, G. Schaefer, W.W. Byszewski, and J.M. Proud, "Magnetic Controlled Discharges for Switching Applications," Proc. 5th IEEE Pulsed Power Conf., Arlington, VA, June 1985, to be published.

A.L. Donaldson, M. Kristiansen, H. Krompholz, M.O. Hagler, L.L. Hatfield, G.R. Leiker, P.K. Predecki and G.L. Jackson, "Analysis of Electrode Surface Damage in High Energy Spark Gaps", Proc. 5th IEEE Pulsed Power Conf., Arlington, VA, June 1985, to be published.

P.M. Ranon, H. Krompholz, M. Kristiansen, and L.L. Hatfield, "High Current Surface Discharge Switch", Proc. 5th IEEE Pulsed Power Conf., Arlington, VA, June 1985, to be published.

B. Maas, H. Krompholz, M. Kristiansen, and M. Hagler, "Arc Current, Voltage, and Resistance in a High Energy, Gas-Filled Spark Gap", Proc. 5th IEEE Pulsed Power Conf., Arlington, VA, June 1985, to be published.

G. Schaefer, K.H. Schoenbach, M. Kristiansen, and H. Krompholz, "An Electron-Beam Controlled Diffuse Discharge Switch," Proc. XVIIth Int. Conf. on Phenomena in Ionized Gases, pp. 626-628, Budapest, Hungary, July 1985.

M.R. Wages, G. Schaefer, K.H. Schoenbach, and P.F. Williams, "Physical Triggering Mechanisms of Trigatron Spark Gaps," Proc. XVIIth Int. Conf. on Phenomena in Ionized Gases, pp. 638-640, Budapest, Hungary, July 1985.

A.L. Donaldson, E. Kristiansen, M. Kristiansen, A. Watson, and K. Zinsmeyer, "The Discontinuity in Electrode Erosion at Very High Currents", submitted to the 3rd Symposium on Electromagnetic Launch Technology, Austin, TX, April 1986.

P.M. Ranon, M. Kristiansen, M. Lehr, and L.L. Hatfield, "Insulator Damage in High Current Discharges", submitted to the 3rd Symposium on Electromagnetic Launch Technology, Austin, TX, April 1986.

Kazunari Ikuta and M. Kristiansen, "Conical Liner Implosion as a Projectile Injector for Mass Drivers", submitted to the Japanese Journal of Applied Phys., December 1985.

Interactionsa) Papers Presented

During the last contract period (October 1, 1983 - October 31, 1984), the following papers were presented, in addition to those listed as conference proceeding papers:

J.R. Cooper, K.H. Schoenbach, G. Schaefer, J.M. Proud, and W.W. Byszewski, "Magnetic Control of Low Pressure Glow Discharges," 37th Gaseous Electronics Conference, Boulder, CO, Oct. 1984.

M.R. Wages, P.F. Williams, G. Schaefer, and K.H. Schoenbach, "Streak Photographic Studies of Trigatron Triggered Breakdown," 37th Gaseous Electronics Conference, Boulder, CO, Oct. 1984.

-Invited- K.H. Schoenbach and G. Schaefer, "External Control of Diffuse Discharge Switches," 12th IEEE Int. Conf. Plasma Sci., Pittsburgh, PA, June 1985.

G. Reinking, G. Schaefer, K.H. Schoenbach, and G. Hutcheson, "Attachment of Initial Secondary Electrons in an Electron Beam Sustained Discharge", 12th IEEE Int. Conf. Plasma Sci., Pittsburgh, PA, June 1985.

J.R. Cooper, K.H. Schoenbach, and G. Schaefer, "Magnetic Control of Low Pressure Diffuse Discharges," Joint Symp. Swarm Studies and



Inelastic Electron Molecule Collisions, Lake Tahoe, NV, July 1985.

A.L. Donaldson, A. Watson, and M. Kristiansen, "Investigation of the Discontinuity effect in High Energy Spark Gap Erosion", 27th Annual Meeting APS Division of Plasma Physics, San Diego, CA, Nov. 1985.

G. Schaefer, K.H. Schoenbach, M. Kristiansen, and E. Strickland, "Negative Differential Conductivity in E-Beam Sustained Discharges", 27th Annual Meeting Division of Plasma Physics, San Diego, CA, Nov. 1985.

b) Consultative and Advisory Functions

During the 1984-85 contract period, the following functions were undertaken:

Dr. Kristiansen served on the USAF Scientific Advisory Board.

Dr. Kristiansen served on the USAF Ad Hoc Committee on "High Power Microwave Systems".

Dr. Kristiansen served on the USAF Ad Hoc Committee on the "Effects of HEMP on Military C<sup>3</sup>".

Dr. Kristiansen served on the USAF Ad Hoc Committee on "Basic Science".

Dr. Kristiansen was a member of the NASA Workshop on "Plasma Physics and Fusion Scientific Activity for the Space Station".

Dr. Kristiansen served as a consultant to LANL and LLNL.

Dr. Kristiansen worked with personnel from Maxwell Labs, WPAFB, and Boeing Co. to resolve a critical problem related to an Air Force project (see Appendix N).

c) Other Interactions

Numerous interactions with other universities, industry and government laboratories were carried out during the contract period. Our group effectively served as a coordination point for much of the ongoing work in high power gas discharges for switching applications in the U.S.

Professor H. Krompholz attended the IEEE Conf. on Instrumentation and Measurement Technology, Tampa, FL, March 1985.

Prof's. G. Schaefer and K.H. Schoenbach attended the 12th IEEE Int. Plasma Sci. Conf., Pittsburgh, PA, June 1985.

Prof. G. Schaefer visited the Department of Physics, University of Pittsburgh, PA, (Prof's. F. Biondi and R. Johnsen) June 1985.

Prof. G. Schaefer visited the Westinghouse Research Laboratory, Pittsburgh, PA, (Dr's. P. Chantry and L. Kline) June 1985.

Prof. G. Schaefer visited Oak Ridge National Laboratory, TN, (Prof. L. Christophorou) June 1985.

Prof's. M. Kristiansen, L. Hatfield, K.H. Schoenbach, and G. Schaefer attended the 5th IEEE Pulsed Power Conference in Arlington, VA, June 1985.

Prof's M. Kristiansen and G. Schaefer attended the Int. Conf on Phenomena in Ionized Gases, Budapest, Hungary, July 1985.

Prof. G. Schaefer visited the Karlsruhe Nuclear Research Center, West Germany (Prof's W. Schmidt and Citron), July 1985.

Prof. G. Schaefer visited the Department of Electrical Engineering, Thechnical University Darmstadt, West Germany (Prof. W. Pfeiffer), July 1985.

Prof. G. schaefer visited the High Voltage Institute, Technical University Braunschweig, West Germany (Prof. J. Salge), July 1985.

Prof. G. Schaefer visited the Air Force Weapons Laboratory, Albuquerque, NM (Chief Scientist Dr. A. Guenther) August 1985.

Prof. G. Schaefer participated in the Organizing Committee meeting for the Workshop "Research Issues in Power Conditioning", Los Angles, CA (Prof. M. Gundersen) Sept. 1985.

Prof. M. Kristiansen attended the Technical Program Review Meeting for the 5th IEEE Pulsed Power Conference, Wash., DC., Jan. 1985.

Prof. M. Kristiansen visited with Dr. B. Kulp, the Air Force Systems Command, Wash. DC, Jan 1985.

Prof. Kristiansen attended, by invitation, a NASA Workshop, and also met with Mr. L. Webster of the U.S. Army Ballistic Missile Defense, May 1985.

Prof. Kristiansen visited with personnel at Eglin AFB, Oct. 1985.

## ADVANCED DEGREES AWARDED

(1984-85)

1. Henry Charles Harjes, Ph.D., "An Electron Beam Controlled Diffuse Discharge Switch", May 1985.
2. Leo Erasmus Thurmond, M.S., "Photodetachment as a Discharge Control Mechanism in Gases Containing Oxygen", May 1985.
3. Brian Lane Maas, M.S., "Arc Current, Voltage, and Resistance in a High Energy, Gas-Filled Spark Gap", May 1985.
4. Randy Dale Curry, M.S. "Triggering of Surface Discharge Switches", August 1985.

SEMINARS  
1984-85

James A. Ionson	"The Policy and Technology of the Strategic Defense Initiative" May 2, 1985 Director, Innovative Science and Technology Office, SDIO Washington, DC
William G. Dunbar	"Insulating Materials Applications" "Space Applications of Insulating Materials" May 13, 1985 "Materials Testing" May 14, 1985 Boeing Aerospace Company Seattle, WA
Malcolm Buttram	"Spark Gap Stability" July 22, 1985 Sandia National Laboratories Albuquerque, NM
Giyuu Kido	"Generation and Application of Megagauss Fields" August 21, 1985 Tohoku University Sendai, Japan
Alan Watson	"Electrode Damage from Strong Transient Sparks by Surface Material Displacement in Hydro-magnetic Flow" September 12, 1985 University of Windsor Windsor, Ontario, Canada
Andrew K. Jonscher	"Dielectric Spectroscopy of Semi-Insulating Gallium Arsenide" October 10, 1985 University of London London, UK
Martin Gundersen	"Recent Progress in High Power Switch Research" October 25, 1985 University of Southern California Los Angeles, CA

Norwegian State TV, Oslo Norway

SDIO, Washington, DC  
LANL, Los Alamos, NM

## Boeing Aerospace Co, Seattle, WA

Univ. Texas at Arlington,  
Arlington, TX

" " " "

Tohoku University  
Sendai, Japan  
Taiwan, ROC

Taiwan, ROC

Mississippi State Univ,  
Starkville, MS

Toshiba Corp., Kawasaki, Japan

LLNL, Livermore, CA.

11	11	11
11	11	11

Kings College, London, UK

SUBMITTED TO IEEE TRANSACTIONS ON PLASMA SCIENCE

A REVIEW OF DIFFUSE DISCHARGE OPENING SWITCHES\*

G. SCHAEFER, SENIOR MEMBER IEEE AND  
K. H. SCHOENBACH, SENIOR MEMBER IEEE

Abstract

The basic operation principles of externally controlled diffuse discharges with respect to their application as opening switches are discussed. Discharge sustainment by electron and UV ionization and additional control mechanisms such as photodetachment and optically enhanced attachment are considered. Special emphasis is given electron beam controlled switches. For such systems, design criteria are discussed and a summary of experimental switch results is presented.

---

\*This work was supported by AFOSR and ARO.

G. Schaefer is with the Department of Electrical Engineering, Texas Tech University, Lubbock, Texas 79409-4439, and with Polytechnic Institute of New York, Farmingdale, New York 11735.

K. H. Schoenbach is with the Department of Electrical Engineering, Old Dominion University, Norfolk, Virginia 23508.

## I. INTRODUCTION

Inductive energy storage is attractive in pulsed power applications because of its intrinsic high energy density compared to capacitive storage systems. The key technological problem in developing inductive energy storage systems, especially for repetitive operation, is the development of opening switches. Promising candidates for repetitive opening switches are e-beam or laser controlled diffuse discharges.

In a "Diffuse Discharge Opening Switch," the switch medium is an externally sustained discharge. Most of the research on externally sustained, high pressure ( $> 1$  atm), diffuse discharges has been performed with respect to its application for molecular lasers. The most common sustainment method, the electron-beam (e-beam) controlled discharge technique, was used by Daugherty, Pugh, and Douglas-Hamilton in 1971 [1] to operate large volume, high energy CO<sub>2</sub> lasers. The use of diffuse discharges as fast closing and opening switches was first proposed in 1976 by Hunter [2] and Koval'chuk and Mesyats [3,4].

A schematic diagram of an externally controlled opening switch as part of an inductive energy storage system is shown in Figure 1. When the gas between the electrodes is ionized by an e-beam or by radiation, it becomes conductive, the diffuse discharge switch closes, and the inductor is charged. During conduction, the reduced electric field strength  $E/N$  is kept in a range where ionization through the discharge electrons is negligible. When the external ionization source is turned off, electron attachment and recombination processes in the gas cause the conductivity to decrease and the switch opens. Consequently, the current through the inductor is commutated into the load, and the voltage across the load increases according to the impedance ratio of load and storage system.



The most efficient method at this time to provide for plasma conductivity is the e-beam controlled discharge technique. Up to 50% of the electron beam energy can be converted directly into ionization energy [5]. The remaining energy mainly goes into excitation. The ionization efficiency can be increased further by using Penning gas mixtures, where part of the excitation energy is converted into ionization through Penning collisions [6]. The only way to reduce the conductivity in an e-beam sustained discharge is to turn off the e-beam. Optical control of diffuse discharges, on the other hand, allows changing of the conductivity in either direction [7]. By irradiating a discharge with radiation in the wavelength range corresponding to an atomic or molecular transition, the electric properties of the plasma can be modified through optogalvanic effects [8]. An attractive concept for an externally controlled diffuse discharge switch is to combine the advantages of both the e-beam and optical control to create an e-beam sustained, optically assisted switch [9].

## II. DISCHARGE ANALYSIS

### A. General Considerations

The goal of a discharge analysis of an externally sustained discharge for switching applications is to evaluate the time dependent impedance of the discharge for a given time dependent electron source in a given circuit. Such analysis will allow the optimization of gas mixtures and operation conditions. A complete discharge model must consider the bulk of the discharge and the fall regions, especially the cathode sheath. It must provide for steady state solutions and the transient behavior, and should include a stability analysis

of the discharge.

Model calculations aimed toward discharge applications for opening switches have concentrated mainly on the bulk of the discharge (zero-dimensional), on the influence of the proposed optimum gas properties ( $E/N$ -dependence of attachment coefficient and mobility), and on the transient behavior (time dependence) of the discharge in an inductive energy storage circuit [9-13]. Bulk discharge models are based on solving a set of rate equations for the charged particles and those excited particles which contribute to ionization. The steady state solution of the set of rate equations gives the (V-I)-characteristics of the discharge. For the evaluation of its transient behavior in a given circuit, the set of time dependent rate equations and the circuit equation must be solved simultaneously.

A simplified model of a spatially homogeneous discharge considers only the charged particles [12]. All ionization processes by the discharge electron are neglected and two-body dissociative attachment is considered to be the dominant attachment process. The rate equations are then given as:

$$\frac{dn_e}{dt} = S - k_{re} n_e n_+ - k_a N_a n_e \quad (1)$$

$$\frac{dn_+}{dt} = S - k_{re} n_e n_+ - k_{ri} n_+ n_- \quad (2)$$

$$\frac{dn_-}{dt} = k_a N_a n_e - k_{ri} n_+ n_- \quad (3)$$

$k_{re}$  and  $k_{ri}$  are the electron-ion and ion-ion recombination rate coefficients, respectively,  $k_a$  is the attachment rate coefficient,  $N_a$  is the attacher concentration in the gas mixture, and  $S$  is the source function (rate of

electron-ion pair production by the e-beam). Assuming charge neutrality in the discharge so that  $n_+ = n_e + n_-$ , and with the assumption that  $k_{re} = k_{ri} = k_r$ , the rate equation can be solved for the steady state electron density  $n_{eo}$ :

$$n_{eo} = \frac{S}{k_a N_a + \sqrt{S k_r}} \quad (4)$$

and for the steady state positive ion density  $n_{+o}$ :

$$n_{+o} = \sqrt{S/k_r} . \quad (5)$$

For electrons being the dominant current carriers, the conductivity is given as:

$$\sigma = \frac{e\mu S}{k_a N_a + \sqrt{S k_r}} , \quad (6)$$

where  $\mu$  is the electron mobility. This solution reduces to the attachment dominated solution for  $k_a N_a \gg k_r n_+$ :

$$\sigma_a = \frac{e\mu S}{k_a N_a} , \quad (7)$$

and the recombination dominated solution for  $k_a N_a \ll k_r n_+$ :

$$\sigma_r = e\mu \sqrt{\frac{S}{k_r}} . \quad (8)$$

Since the diffuse discharge is considered to be used as a switch, that

means as an element which controls the energy flow from an energy storage into a load, the power dissipated in the discharge should ideally be negligible compared to the power commutated to the load. This requires a high conductivity at a low reduced field strength  $E/N$ . The desirable gas properties for the conduction phase are therefore, according to equation (6), a large electron mobility and small attachment and recombination rate coefficients at low  $E/N$ .

In order to minimize losses during the transition from the conductive to the nonconductive state (opening phase) the switch conductance should decay as fast as possible. A simplified analysis of the opening phase is given by considering the rate of change in electron density (equation 1) for either recombination or attachment dominated discharges. For a non-attaching gas ( $k_a = 0$ ), the relative change of electron density  $n_e$  (and the switch conductivity  $\sigma$ ) is proportional to the instantaneous value of  $n_e$ :

$$\frac{dn_e/dt}{n_e} = -k_r n_e \quad (9)$$

i.e., the relative rate of change slows down with reduced electron density. In an attachment dominated discharge ( $k_a N_a \gg k_r n_e$ ) on the other hand, the relative rate of decay is not dependent on the electron density:

$$\frac{dn_e/dt}{n_e} = -k_a N_a \quad (10)$$

It can be controlled completely by the type and concentration of the electro-negative gas added to the buffer gas.

In order to achieve opening times of less than one microsecond at initial

electron densities  $n_e < 10^{-14} \text{ cm}^{-3}$ , the dominant loss mechanism must be attachment. That means that the switch gas mixture must contain an electro-negative gas. On the other hand, additives of attaching gases increase the power loss during conduction. Both low forward voltage drop and fast opening can be obtained by considering the  $E/N$  dependence of rate coefficients and transport coefficients, and choosing gases or gas mixtures which satisfy the following conditions [7,9,14,15].

1. For low values of the reduced field strength  $E/N$ , characteristic for the conduction phase, the electron drift velocity  $w$  should be large and the attachment rate coefficient  $k_a$  should be small in order to minimize losses.
2. With increasing  $E/N$ , characteristic for the opening phase of a switch in an inductive energy storage system, the attachment rate coefficient should increase and the electron drift velocity should decrease in order to support the switch opening process.
3. Additionally, the gas should have a high dielectric strength to hold off the expected high voltage across the switch when it opens.

#### B. Specific Gas Mixtures

Calculations on the discharge behavior of specific gas mixtures have been performed by several authors. Fernsler et al. [11] studied the influence of an admixture of an attacher ( $O_2$ ) to a buffer gas ( $N_2$ ) during the opening phase of the discharge. The attachment rate of the three-body attachment process ( $e + O_2 + N_2 \rightarrow O_2^- + N_2$ ) was considered to be dominant and independent of  $E/N$ . Shortening of switch opening with increasing attacher concentration was demonstrated.

Kline [12] presented calculations on discharges in  $N_2$ , Ar,  $N_2$ :Ar mix-

tures, and  $\text{CH}_4$  for the operation range of small e-beam current densities (some  $\text{mA/cm}^2$ ). The steady state analysis presents the discharge characteristic, the switch characteristic, and the current gain. The current gain in an e-beam sustained discharge is considered a figure of merit for the control efficiency of the diffuse discharge switch. It is defined as the ratio of switch current to sustaining e-beam current.

Kline's transient analysis of the diffuse discharge [12] incorporates the influence of an attacher; however, an attachment rate independent of  $E/N$  was considered. As a result of the calculations, methane was found to be the best of the switch gases studied since it exhibits a high electron drift velocity at low values of  $E/N$ . Figure 2 shows the measured and predicted e-beam switch waveforms in methane for the experimental conditions of Hunter (1976). The three different predictions result from different values for the recombination and attachment rates used in the calculations.

Schaefer et al. [9,13] presented calculations on discharges in  $\text{N}_2$  with  $\text{N}_2\text{O}$  as an attacher. These calculations concentrate on the influence of an attacher with an attachment rate increasing with  $E/N$ . It was demonstrated that such an attacher with sufficient concentration generates a discharge characteristic with a negative differential conductivity (NDC) in an intermediate  $E/N$ -range. This behavior has also been predicted for discharges in  $\text{N}_2$  with admixtures of  $\text{CO}_2$  or  $\text{O}_2$  as attachers [16]. Figure 3 shows the steady state  $E/N-j$  characteristic with the source function  $S$  as the variable parameter for an  $\text{N}_2/\text{N}_2\text{O}$  discharge [9]. Below  $\sim 3 \text{ Td}$ , the discharge is recombination dominated. Above  $\sim 3 \text{ Td}$ , the attachment rate increases, causing the conductivity to decrease (NDC). At high values of the source functions, the electron density will be high enough so that recombination is significant also in the  $E/N$  range with a high attachment rate and the negative differential

conductivity disappears.

The transient analysis shows that such a discharge characteristic allows to operate the discharge with low losses during the conduction phase in the  $E/N$  range below the threshold for attachment and to achieve fast opening times. Figure 4 shows the calculated time dependence of  $E/N$  and the current density  $j$  with the attacher concentration as the variable parameter. For the three smaller values of the attacher concentration (0.1%-0.75%), the discharge reaches the same low value of  $E/N$  where it is recombination dominated. The opening time decreases with attacher concentration, however, the closing time increases. For the higher values of the attacher concentration ( $\geq 1\%$ ) the discharge is obstructed to reach the low  $E/N$  range and stays attachment dominated, causing high losses. These results demonstrate that the desired attachment rate for low losses during conduction and for fast opening obstructs switch closing. Photodetachment is therefore discussed as additional control mechanism to overcome attachment during switch closure (see "Optical Control Mechanisms").

### III. BOUNDARY EFFECTS AND INSTABILITIES

The voltage drop across e-beam sustained diffuse discharges reaches from several hundred volts to several kilovolts, depending on operation conditions. An appreciable amount of the total voltage may be the cathode fall voltage [17-21]. The cathode fall voltage is a function of e-beam current, discharge current, gas type and pressure and electrode material [21]. For atmospheric pressure discharges and small gap distance, it can be considerably larger than the voltage across the bulk of the discharge. The addition of an attaching gas does not seem to increase the cathode fall voltage very much.

A theoretical investigation of the cathode fall in high pressure e-beam controlled discharges included secondary emission from the cathode and electron-impact ionization of metastable states [20]. The results showed that the cathode fall of an e-beam ionized discharge is very sensitive to the value of the cathode secondary emission coefficient, demonstrating the importance of the electrode properties.

Instabilities which lead to a glow-to-arc transition usually originate near the electrodes, a region of higher electric field intensity and lower electron density. Streamer formation is considered to begin with the formation of a filament of gas, heated to a temperature adequate to provide sufficient thermal ionization to become significantly conductive. Streamers can grow from cathode layer hot spots, and have been observed to originate on cathode protrusions [23]. The streamers subsequently propagate at speeds close to sonic, generally progressing with increasing velocity across the gap. An important feature of streamers in discharge gases is therefore that arcing can occur a considerable time after the e-beam current has been turned off [24].

The development of plasma instabilities in the bulk of the diffuse discharge was addressed by Haas [25,26], Nighan [27], and Bychkov et al. [10]. Two general models of bulk instabilities have been proposed, thermal and ionization. The thermal instability is due to local heating and dilution of the gas with subsequent increase in  $E/N$ , which in turn causes increased local energy deposition, etc. The ionization instabilities occur when in high field regions of the discharge, preferentially close to the electrodes, the regenerative ionization becomes comparable to the ionization caused by the external source. The times for the development for these instabilities range from hundreds of nanoseconds to milliseconds, depending on discharge para-



meters and filling pressure [28].

Discharges in mixtures containing electronegative gases can exhibit an attachment instability, if the attachment rate coefficient  $k_a$  is a rapidly increasing function of  $E/N$  [16,29]. A small local increase in the electric field intensity in such a gas mixture causes an increase in attachment which leads to a decrease of the electron density and therefore to a further increase in electric field. Ultimately, waves of high electric field in electron-depleted regions move across the discharge, resulting in current waves. The relevance of this instability is that the high local fields caused by the electron loss will greatly increase local heating, and streamers are initiated, growing toward both electrodes.

A problem related to instabilities in diffuse discharges is power loading [30]. The electrical energy density deposited in the gas is the product of discharge current density and electric field integrated over time. This energy is deposited in the form of kinetic energy of the gas molecules (gas heating) and in the internal degrees of freedom of the gas molecules. Experimental investigations have lead to the conclusion that an uniform discharge can be sustained until the gas temperature has increased to approximately 500 K [24]. After that point the uniform glow goes over to an arc.

There are attempts to quantify the fraction of the electrical energy input which results in gas heating as a function of  $E/N$  for timescales short compared to vibrational relaxation [31]. A major fraction of the energy input to molecular gases is consumed by vibrational excitation. Shirley and Hall [32] determined vibrational temperatures in  $H_2$  as a function of energy density deposited in the gas. They found vibrational temperatures of 1500 K to 1800 K for power loadings of several kJ/mole, or about  $0.1 \text{ J/cm}^3$  atm at 30 Td. The changes due to enhanced population in the high energy states of the gas

molecules will affect the behavior of the diffuse discharge switch, especially if attachers are used where the attachment cross section changes drastically with vibrational excitation as in HCl or H<sub>2</sub> [33,34].

#### IV. OPTICAL CONTROL OF DIFFUSE DISCHARGES

External control of a diffuse gas discharge, in general, means to make use of some mechanisms to influence the charge carrier balance in the discharge, in addition to those processes solely caused by the applied electric field. The control mechanism can be used to increase or to decrease the conductivity by controlling either the electron generation or depletion mechanism.

For opening switches, mainly externally sustained discharges are considered. An externally sustained discharge is operated in the E/N range where the ionization coefficient is negligible so that the electron generation process is given solely by the external source. Besides electron beams, UV radiation also has been used as a sustainment method for TEA-laser discharges [35-37]. Similar devices with glow discharges sustained by high power flash boards have also been investigated for switching applications [38-40]. The advantage of these devices is that the design and operation of a UV flashboard is significantly simpler than an electron beam gun. For an efficient impedance matching, a large number of sparks are operated in series [38]. A problem at this time is to achieve a fast cutoff of the ionization source. The propagation time for the exciting electric pulse through the flashboard [40] and the long afterglow of the flashboard [38] seem to limit the opening time to values above one microsecond.

An alternative would be to use lasers which allow a very precise timing.

Due to the high costs of laser photons, however, it seems to be inefficient at this time to use lasers as a sustainment method, especially if high photon energies are required. Lasers, on the other hand, offer the unique possibility to influence the density of specific states of one of the species generated in the discharge, and subsequently the generation and depletion mechanisms of electrons [8]. Laser discharge control for switching application is therefore considered only as an additional control for a specific phase of the switch cycle, where other means do not allow the optimization of the discharge properties. Laser control of diffuse discharges for opening switches is a very recent research field. Besides papers on concepts [7,8,13], model calculations on certain proposed systems [9,14], and investigations of basic processes suitable for switching applications [42,43], there are no results on operational switching devices available.

As discussed in the section on "Diffuse Discharge Analysis," the main effort concentrates on the optimization of the electron depletion through attachment. Although an optimization of the steady state phase and the opening phase is possible through tailoring the  $E/N$  dependence of the attachment rate coefficients, there are still problems related to the closing phase. Concepts on additional optical control, therefore, concentrate on attachment and its control in one of the transition phases. In principle, there are two different methods for optically controlling attachment: (1) to use photodetachment to overcome attachment [13], or (2) to use optically induced attachment in gases which otherwise would not have a strong attachment rate in the  $E/N$  range of interest [7].

#### A. Photodetachment

Just like photoionization, photodetachment is a nonresonant process which

in general requires much lower photon energies. The cross sections usually are not very high, requiring a high laser power. Therefore, photodetachment seems to be an appropriate process only if required for a short switch period in discharges sustained by other means (Schaefer et al., 1984).

A negative ion considered for photodetachment as a control mechanism is  $O^-$  [13]. The photodetachment cross section has a threshold at a photon energy of 1.47 eV and reaches a plateau of  $6.3 \cdot 10^{-18} \text{ cm}^2$  at approximately 2 eV [47]. Several molecules, such as  $O_2$ , NO, CO,  $N_2O$ ,  $NO_2$ ,  $CO_2$ , and  $SO_2$ , undergo dissociative attachment producing  $O^-$  (example:  $e^- + O_2 \rightarrow O^- + O$ ).

In fact, in all these gases or gas mixtures with these gases, competitive attachment processes exist or subsequent reactions of  $O^-$  will occur, producing molecular negative ions which in general have lower cross sections for photodetachment. In discharges in  $O_2$ , for example, the dominant molecular negative ion is  $O_2^-$  which is produced either through attachment in a three-body collision ( $e^- + O_2 + O_2 \rightarrow O_2^- + O_2$ ), which is the dominant attachment process at high pressures (Moruzzi and Phelps, 1966), or in a charge transfer collision with  $O^-$  ( $O^- + O_2 \rightarrow O_2^- + O$ ). The cross section for photodetachment of  $O_2^-$  is smaller by a factor of approximately 5 at 2 eV. Photodetachment experiments in low pressure  $O_2$  discharges and flowing afterglows showed that a fraction of 50% of the negative ions could be detached with laser pulses with an energy flux of  $35 \text{ mJ/cm}^2$  and a photon energy of 2.2 eV [13].

For attachers with a high attachment rate at high values of  $E/N$  and low or zero attachment rate at low values of  $E/N$ , photodetachment may be a suitable process to support a transition from a highly attaching state into a non-attaching state of an externally sustained discharge. The effect of laser photodetachment on the closing phase of an electron-beam sustained discharge in  $N_2$  containing an admixture of  $N_2O$  was calculated by Schaefer et al. [9].

Figure 5 shows the transient behavior of the discharge for an operation condition in which the closing phase is obstructed by attachment so that the discharge never reaches the low  $E/N$ -regime where it is not dominated by attachment. With a laser power density of  $10^7$  W/cm<sup>2</sup>, attachment is partially compensated and the discharge behaves similarly to one with a lower attachment concentration (compare with Figure 4). Since the laser is required only during the closing phase for about 10 ns, the power density of  $10^7$  W/cm<sup>2</sup> corresponds to an energy flux of 100 mJ/cm<sup>2</sup>. Since only a small fraction of the power is absorbed, this requirement can easily be fulfilled by a multipass or intracavity optical design.

#### B. Optically Enhanced Attachment

Optically enhanced attachment means to use a gas mixture with an additive of molecules, which in their initial state are very weak attachers, and to transfer these molecules through optical excitation and maybe some subsequent spontaneous transitions into species which act as a strong attacher. Optically enhanced attachment is a control mechanism considered for controlling the opening phase of diffuse discharge opening switches [7].

Certain attachers have a drastically increased attachment cross section in their rotational and/or vibrational excited states. This effect was first observed for dissociative attachment of SF<sub>6</sub> producing SF<sub>5</sub> [47,48]. An attachment rate constant  $k_a(T)$ , increasing with temperature  $T$ , is the clearest measure for the change of the cross section with vibrational and rotational excitation since the density of such excited molecules increases with  $T$ . There are several attachers known to show a strong increase of the attachment rate with increasing temperature [49,50].

As yet, there are no known measurements of attachment cross sections for

individual vibrational states. In experiments by Srivastava and Orient [51], however, it was demonstrated that monoenergetic electrons at least allow the excitation of specific modes of vibration, and subsequently the measurement of attachment cross sections of a special group of vibrational states. Bardsley and Wadehra [33] have calculated the cross section for the vibrational states ( $v = 0 - 3$ ) of HCl (Figure 6) from cross section measurements at different gas temperatures by Allan and Wong [50]. The population density of the rotational states was assumed to be a Boltzmann distribution at  $T = 300$  K. These data show that the attachment rate can be increased drastically using vibrational excitation, but this advantage disappears in HCl if the electron energy is larger than 0.5 eV. For switching application, one should look for molecules having their maximum attachment cross section in the ground state at a somewhat higher energy, depending on the E/N-range considered for the conduction phase of the switch.

For application in diffuse discharges, one also must consider that vibrational excitation also will result from electron collisions. As the discharge is considered to be cold, mainly collisions with molecules in the ground state occur. This is true for electrons as well as for excited molecules, which makes the excited state with the lowest energy the only excited species at considerable densities. Thus, an external control mechanism will work efficiently only if the significant increase of the attachment cross section in the considered electron energy range occurs for states ( $v > 1$ ) for two atomic molecules, or for larger molecules for states with energies well above that of the lowest lying excited state. Some possible mechanisms to produce molecules in vibrationally excited states which are not strongly created in a cold discharge are listed in Table V.

- (1) Optical vibrational excitation of higher lying states can be

accomplished through vibration-vibration energy transfer, through overtone excitation or excitation of combination states, and through multi-photon excitation. Such mechanisms can be found as excitation mechanisms of numerous optically pumped IR lasers. Examples are lasers, optically pumped with a CO<sub>2</sub> laser, in molecules such as CF<sub>4</sub>, NOCl, CF<sub>3</sub>I, and NH<sub>3</sub> [52]. To date, experiments have failed to demonstrate a significant increase of the attachment rate in an electron beam sustained discharge after irradiation with a pulsed CO<sub>2</sub> laser [43]. However, small increases of the resistivity ( $\sim 2\%$ ) of an externally sustained low current DC discharge containing C<sub>2</sub>H<sub>3</sub>F have been found after irradiation with a chopped low power ( $\sim 5 \text{ Wcm}^{-2}$ ) CW CO<sub>2</sub> laser [53].

(2) Single- and multi-photon dissociation of large molecules also has been shown to produce molecules in vibrationally excited states and also is used as an excitation mechanism for molecular gas lasers. Sirkin and Pimentel [54] demonstrated that photoelimination of HF from CH<sub>2</sub>CF<sub>2</sub>, CH<sub>2</sub>CHF, and other fluorinated hydrocarbons using an UV-flashlamp, would generate a significant fraction of the HF molecules in states  $v > 1$ . With chlorinated hydrocarbons, equivalent HCl molecules are produced [55]. Some of these processes have significant cross sections at the wavelength of the ArF-laser at 193 nm. Rossi, Helm, and Lorents [42] performed drift tube experiments to demonstrate the feasibility of these processes for controlling the electron balance. Figure 7 shows their experimental results. In a 100 torr mixture of helium with 100 mtorr C<sub>2</sub>HF<sub>3</sub> at low values of E/N ( $< 3 \text{ Td}$ ), they obtained an increase of the attachment rate of up to  $10^3$  with an ArF laser at 193 nm. Similar experiments were performed in C<sub>2</sub>H<sub>3</sub>Cl. Schaefer et al. [9] performed measurements in a DC discharge at low values of E/N (1-10 Td), which was externally sustained by helium plasma injection. In a gas mixture of 60 torr helium and 3% C<sub>2</sub>H<sub>3</sub>Cl, pulsed resistance changes of a factor of 5.5 were measured after

irradiating the discharge with a UV spark source through a quartz window.

(3) Electronic excitation can be transferred into vibrational excitation either through collisions or radiative processes (for a review see Houston, [56]). Collisional transfer subsequent to optical excitation has, for example, been used to operate a CO<sub>2</sub> laser. Petersen, Wittig, and Leone [57] used the following processes ( $\text{Br}_2 + h\nu \rightarrow \text{Br} + \text{Br}^*$  and consequent  $\text{Br}^* + \text{CO}_2 \rightarrow \text{Br} + \text{CO}_2^+ + \Delta E$ ), where the dominant excited states of CO<sub>2</sub> are the (10<sup>0</sup>1)- and (02<sup>0</sup>1)-state.

Electronic excitation and subsequent radiative transitions into highly vibrationally excited states have been used by Beterov and Fatayev [58] to show that vibrational excitation of I<sub>2</sub> can increase the attachment rate for dissociative attachment. Figure 8 depicts the excitation mechanism. The radiation from a frequency doubled Nd:YAG laser ( $\lambda = 532 \text{ nm}$ ) was used to excite the (B)-state. Intense Stokes fluorescence indicated a subsequent transition into highly vibrational excited states of the electronic ground state. Vibrational relaxation had to provide the population of the optimum vibrational states, resulting in an increase of the attachment rate by three or four orders of magnitude. Since the vibrational relaxation required times in the order of some 10  $\mu\text{s}$ , it also was suggested to use a stimulated resonant Raman process to excite directly the vibrational state with the highest attachment cross section.

For all proposed processes of optically enhanced attachment, it is very important to consider the attachment properties of the starting compound. A real advantage of optically enhanced attachment can be achieved only if the attachment rate is significantly increased over a wide E/N range. Also, the stability of the starting compound with respect to collisional processes in the  $\alpha$ -beam sustained discharge must be investigated. At this time, UV



photodissociation of molecules generating attaching fragments looks most promising.

## V. ELECTRON-BEAM CONTROL OF DIFFUSE DISCHARGES

### A. Electron Beam Considerations

Electron beams are the most commonly used ionization sources for externally sustained diffuse discharges. Typically, beam energies are in the 100-300 keV range with current densities up to several A/cm<sup>2</sup>. In order to generate the e-beam, it is necessary to have the electrodes in a vacuum of  $< 10^{-3}$  Torr for cold cathode operation and  $< 10^{-7}$  Torr for thermionic cathodes.

The electron generation mechanism at cold cathodes is usually field emission. With field-emitting cathodes, current densities of several hundred A/cm<sup>2</sup> can be obtained [59] at the expense, however, of limited pulse duration due to "diode closure" [60]. Diode closure is caused by plasma formation at the cathode. The plasma moves with velocities of  $2-5 \cdot 10^6$  cm/s toward the anode and "closes" the diode gap in typically 2-5  $\mu$ s.

Another cold cathode used for electron generation in e-beam controlled diffuse discharges is the wire-ion-plasma (WIP) electron gun [61-63]. The WIP gun cavity is filled with helium, typically at 10-20 mTorr. A positive pulse applied to the wire anode ionizes the helium in the plasma chamber. Helium ions are extracted and accelerated by the DC high voltage applied to the e-beam cathode. On helium impact, electrons are emitted from the cathode and accelerated by a high voltage. The e-beam current obtained in this device is typically 10 A over a cross section of 100 cm<sup>2</sup>.

Thermionic emitters offer the advantage of decoupling electron generation

and electron acceleration with (in principle) unlimited pulse length. The generation of pulse trains is possible by using a triode or tetrode configuration. In a tetrode with thoriated tungsten electrodes, current densities of up to  $4 \text{ A/cm}^2$  were obtained [64]. With dispenser type thermionic cathodes, values of  $300 \text{ A/cm}^2$  were reached [65,66].

The interface between electron gun and switch chamber is generally a thin (20 to 50  $\mu\text{m}$ ) foil backed by a support structure. The foil material should have low electron stopping power, and good thermal and mechanical properties. In Table 1, properties of different foil materials are listed (Eninger, 1981). A severe constraint for long e-beam pulses and/or repetitive operation is foil heating. In order to avoid structural fractures, the foil temperature must be limited. A foil heating analysis has been performed by Daugherty [67].

#### B. Design of an e-Beam Controlled Diffuse Discharge Switch

Because of the limited conduction time of an e-beam sustained discharge due to the development of instabilities and the time constraints of the e-beam source, it is proposed to use it as the main switch in a two-loop inductive energy storage circuit [9]. Figure 9 shows the schematic circuit with the charging loop and the discharge loop having only the inductor in common. The inductor is charged through the initially closed switch A. The e-beam is turned on when the current through the inductor has reached its maximum steady state value. Switch A now can open the charging circuit at relatively low switch voltage and commutate the current into the e-beam controlled discharge. If switch gases with low losses at low  $E/N$  are used, the efficiency of this commutation can be very high. Once the current is transferred into the diffuse discharge switch, the circuit can generate either a single pulse by closing switch B and simultaneously opening the diffuse discharge, or a pulse

train by repetitively closing and opening the diffuse discharge with switch B closed. In order to prevent loss currents in the load when the diffuse discharge is conducting (if the load impedance is comparable to diffuse discharge impedance), switch A could be replaced by a second e-beam controlled switch which opens and closes in a counter mode to the first switch.

The following design criteria for the e-beam sustained switch in such a circuit are based on a group report in the workshop proceedings on "Diffuse Discharge Opening Switches" [68]. For an efficient switch, the major electron loss in the conduction state will occur through recombination. Attachment is important only in onset and cutoff, steepening the current pulse. In steady state the electron density is well described by Equation (4) with  $k_a$  being neglected. The conductivity therefore is given by Equation (7) with Equation (14):

$$\sigma = e\mu \sqrt{\frac{\frac{dW}{dx} J_B}{eW_i}} \quad \text{with } \mu = \frac{v_d}{E_s} . \quad (11)$$

$v_d$  is the electron drift velocity,  $E_s$  is the electric field intensity in the diffuse discharge,  $J_B$  is the e-beam current density,  $dW/dx$  is the spatial rate of e-beam energy loss in the gas [69,70], and  $eW_i$  is the beam ionization energy of the gas [71].

In order to avoid glow-to-arc transition, the temperature in a molecular gas should not exceed  $T_0 = 500$  K. Assuming that any increase in gas temperature  $\Delta T$  is caused by Joule heating, leads to the relation:

$$\rho c_v \Delta T = \frac{J^2 \tau}{\sigma} , \quad (12)$$

$\rho$  being the gas density,  $c_v$  the specific heat, and  $\tau$  the conduction time. This relation allows estimation of an upper limit for the current density:

$$J_{\max} = \sqrt{(T_o - T_i) \frac{\rho c_v \sigma}{\tau}}, \quad (13)$$

where  $T_i$  is the initial temperature.

For a given total current  $I$ , this determines the switch diameter. The discharge gap length  $d$  is determined by the required switch holdoff voltage  $V_o$ :

$$d = \frac{V_o}{E_{\text{crit}}}. \quad (14)$$

Critical field strengths  $E_{\text{crit}}$  are in the order of 6-12 kV/cm at a pressure of 1 atm.

Calculations along this line were performed for a switch which carries 10 kA for a time of 50  $\mu$ s to charge a capacitor of 400 nF to a voltage of 250 kV [68]. A switch gas pressure of 10 atm in 90%  $\text{CH}_4$  and 10% Ar was assumed. The standoff capability of this mixture is  $E_{\text{crit}} \approx 5$  kV/cm at 1 atm. For a holdoff voltage of 250 kV, the gap length  $d$  must be at least 5 cm at a pressure of 10 atm. With an assumed e-beam current density of  $J_b \approx 140$  mA/cm<sup>2</sup> and an e-beam energy of 200 keV after passing the foil which separates e-beam gun and diffuse discharge switch, the discharge conductivity is  $\sigma = 2.1 \cdot 10^{-2}$  ( $\Omega$  cm)<sup>-1</sup> (equation 11). The maximum current density is according to equation (13)  $J_{\max} \approx 19$  A/cm<sup>2</sup>. For a total current of 10 kA, the switch area must be 531 cm<sup>2</sup>.

Using these data, the efficiency of the switch can be calculated. The

mean power transferred into the capacitor is  $P_{cap} = 250$  MW. The Joule losses in the diffuse discharge are  $P_{dis} = 45$  MW. The e-beam power dissipated in the switch is 15 MW. Allowing, conservatively, structure and foil e-beam losses to be 30%, the total required e-beam power is  $P_{eb} \approx 22$  MW. The efficiency is then given as

$$\mu = \frac{P_{cap}}{P_{cap} + P_{eb} + P_{dis}}, \quad (15)$$

which is about 80% for this diffuse discharge switch.

### C. Experimental Results

A summary of relevant experiments on e-beam controlled switches is given in Table 3. Listed are e-beam and switch parameters. The values for current gain and opening time are mostly approximate values which serve to define the range of operation for the respective experiment.

Early experiments on diffuse discharge switches were performed by Hunter [2] and Koval'chuk and Mesyats [4]. They used cold cathode e-beam emitters derived from laser experiments. With large e-beam current density, they achieved fast rise times and could afford to work with added attachers to get fast opening, at the expense of power gain. They did not use specially designed gases, however. Hunter [2] recognized the importance of having a gas with a high electron drift velocity and therefore chose methane. Methane has an electron drift velocity peaking at more than  $10^7$  cm/s at about 3 Td.

In later publications, several gas mixtures with optimized properties have been proposed for diffuse discharge opening switches [7,15,72-74]. Figure 10 shows electron attachment rate constants for several attachers in Ar and  $CH_4$  as buffer gas [74]. These gas mixtures exhibit also a negative

differential drift velocity region over a wide range of fractional concentrations of the attaching gas in the buffer gas as shown in Figure 11 for  $C_2F_6$  in Ar and  $CH_4$ , respectively. Consequently, the current density-reduced field strength ( $J$ - $E/N$ ) characteristics of e-beam sustained discharges in gas combinations of this type exhibit a pronounced negative differential conductivity range [75,76].

Another gas combination which was proposed as switch gas for e-beam sustained diffuse discharge opening switches is  $N_2O$  in  $N_2$  as buffer gas [7]. The gas mixture exhibits an  $E/N$  dependent electron decay rate which increases by more than a factor of 20 in the  $E/N$  range from 3-15 Td [77].

Work done at Wright-Patterson [18-21], at Hughes Laboratories [63], and at Westinghouse Laboratories [78] has concentrated on high gain systems with opening times in the microsecond range. At Wright-Patterson [18-21], special consideration was given to the cathode region and its influence on the discharge characteristic. Work at the Naval Research Lab [79-83] and at Texas Tech University [68,84-87] deals with repetitive or burst mode opening switch operation. Both groups concentrate on switches with opening times in the submicrosecond range, but try to achieve reasonable current gains ( $> 100$ ) by using suitable gas mixtures. At Texas Tech University, the interaction of discharge and circuit has been investigated for discharges with a strong negative differential conductivity such as in mixtures of Ar and  $C_2F_6$ . Figure 12 shows such a characteristic and demonstrates that the maximum current cannot be utilized in the burst mode in a high impedance system if the pulse separation is shorter than the discharge time of the inductor [87].

Opening switch experiments in discharge circuits including inductors have demonstrated the use of electron beam controlled diffuse discharges for the generation of high voltage pulses. For an experiment performed at Wright-

Patterson [88,89], a capacitor discharge current of up to 135 A was commutated into an inductive load after opening of the e-beam controlled switch. A short ( $\mu$ s) voltage pulse was generated, with its peak voltage exceeding the static breakdown voltage of the e-beam controlled discharge by more than 50% with a  $\text{CH}_4/\text{C}_2\text{F}_6$  gas mixture. An experiment performed as NRL [81] used an e-beam controlled diffuse discharge as the switch element in an inductive energy storage circuit. The storage inductor ( $1.5 \mu\text{H}$ ) was energized by a capacitor charged to 26 kV. Upon termination of the ionizing e-beam, the 10 kA discharge was interrupted, thereby generating a 280 kV, 60 ns voltage pulse across an open circuit (Figure 13). The gas mixture in the e-beam controlled switch was  $\text{CH}_4/\text{C}_2\text{F}_6$  at 5 atm. The current gain was about 10.

The experimental results demonstrate that diffuse discharge switches are suitable for the generation of high power pulses. In order to improve the efficiency of these switches (low losses during conduction at high current gain) and to minimize the opening time, it is important to utilize electron-molecule interactions in gas mixtures. Using "gas engineering" as a means to design switch gases should lead to improved switch performance, with current gain on the order of one hundred at opening times of less than 100 ns.

## REFERENCES

- [1] J. D. Daugherty, E. R. Pugh, and D. H. Douglas-Hamilton, "Bull. Amer. Phys. Soc.," vol. 16, p. 399, 1971.
- [2] R. O. Hunter, "Electron beam controlled switching," Proc. 1st IEEE Int. Pulsed Power Conf., Lubbock, TX, p. IC8-1, 1976.
- [3] B. M. Koval'chuk and G. A. Mesyats, "Rapid cutoff of a high current in an electron-beam-excited discharge," Sov. Tech. Phys. Lett., vol. 2, p. 252, 1976.
- [4] B. M. Koval'chuk and G. A. Mesyats, "Current breaker with space discharge controlled by electron beam," Proc. 1st IEEE Int. Pulsed Power Conf., Lubbock, TX, p. IC7-1, 1976.
- [5] D. R. Shure and J. T. Verdeyen, "Energy distributions in electron-beam produced nitrogen plasmas," J. Appl. Phys., vol. 47, p. 4484, 1976.
- [6] K. Nakanishi, L. G. Christophorou, J. G. Carter, and S. R. Hunter, "Penning ionization ternary gas mixtures for diffuse discharge switching applications," J. Appl. Phys., vol. 58, p. 633, 1985.
- [7] K. H. Schoenbach, G. Schaefer, M. Kristiansen, L. L. Hatfield, and A. H. Guenther, "Concepts for optical control of diffuse discharge opening switches," IEEE Trans. Plasma Sci., vol. PS-10, p. 246, 1982.
- [8] A. H. Guenther, "Optically controlled discharges," Proc. ARO Workshop on Repetitive Opening Switches, Tamarron, CO, p. 48, 1981.
- [9] G. Schaefer, K. H. Schoenbach, H. Krompholz, M. Kristiansen, and A. H. Guenther, "The use of attachers in electron-beam sustained discharge switches--Theoretical considerations," Lasers and Particle Beams, vol. 2, p. 273, 1984.
- [10] Yu. I. Bychkov, Yu. D. Korolev, and G. A. Mesyats, "Pulse discharges in gases under conditions of strong ionization by electrons," Sov. Phys. Usp., vol. 21, p. 944, 1978.
- [11] R. F. Fernsler, D. Conte, and I. M. Vitkovitsky, "Repetitive electron-beam controlled switching," IEEE Trans. Plasma Sci., vol. PS-8, p. 176, 1980.
- [12] L. E. Kline, "Performance predictions for electron-beam controlled on/off switches," IEEE Trans. Plasma Sci., vol. PS-10, p. 224, 1982.
- [13] G. Schaefer, P. F. Williams, K. H. S. F. Williams, K. H. Schoenbach, and J. T. Mosley, "Photodetachment as a control mechanism for diffuse discharge switches," IEEE Trans. Plasma Sci., vol. PS-11, p. 263, 1983.



- [14] K. H. Schoenbach, M. Kristiansen, E. E. Kunhardt, L. L. Hatfield, and A. H. Guenther, "Exploratory concepts of opening switches," Proc. ARO Workshop on Repetitive Opening Switches, Tamarron, CO, p. 65, 1981.
- [15] L. G. Christophorou, S. R. Hunter, J. G. Carter, and R. A. Mathis, "Gases for possible use in diffuse-discharge switches," Appl. Phys. Lett., vol. 41, p. 147, 1982.
- [16] A. D. Barkalov and G. G. Gladush, "Domain instability of a non-self-sustaining discharge in electronegative gases, I. Numerical calculations," High Temp., vol. 20, p. 16; "II. Theoretical Analysis," High Temp., vol. 20, p. 172, 1982.
- [17] J. J. Lowke and D. K. Davies, "Properties of electric discharges sustained by a uniform source of ionization," J. Appl. Phys., vol. 48, p. 4991, 1977.
- [18] P. Bletzinger, "Electron beam switching experiments in the high current gain regime," Proc. 3rd Int. Pulsed Power Conf., Albuquerque, NM, p. 81, 1981.
- [19] P. Bletzinger, "E-beam experiments--Interpretations and extrapolations," Proc. ARO Workshop on Diffuse Discharge Opening Switches, Tamarron, CO, p. 112, 1982.
- [20] M. R. Hallada, P. Bletzinger, and W. Bailey, "Application of electron-beam ionized discharges to switches--A comparison of experiment with theory," IEEE Trans. Plasma Sci., vol. PS-10, p. 218, 1982.
- [21] P. Bletzinger, "Scaling of electron beam switches," Proc. 4th IEEE Pulsed Power Conf., Albuquerque, NM, p. 37, 1983.
- [22] Yu. I. Bychkov, Yu. D. Korolev, G. A. Mesyats, A. P. Khuzeev, and I. A. Shemyakin, "Volume discharge excited by an electron-beam in an Ar-SF<sub>6</sub> mixture, I. Beam controlled discharge," Izvestiya Vysshikh Uchebnykh Zavedenii, vol. 7, p. 898; "II. Cascade ionization discharge," Izvestiya Vysshikh Uchebnykh Zavedenii, vol. 7, p. 77, 1979.
- [23] Yu. D. Korolev, G. A. Mesyats, and A. P. Khuzeev, "Electrode phenomena preceeding the transition of non-selfmaintaining diffuse discharge to a spark," Sov. Phys. Dokl., vol. 25, p. 573, 1980.
- [24] D. H. Douglas-Hamilton, "Some instabilities in non-self-sustained gas discharges," Proc. US-FRG Joint Seminar on Externally Controlled Diffuse Discharges, Bad Honnef, FRG, p. 43, 1983.
- [25] R. A. Haas, "Plasma stability of electric discharges in molecular gases," Phys. Rev. A, vol. 8, p. 1017, 1973.
- [26] R. A. Haas, "Stability of excimer laser discharges," in Applied Atomic Collision Physics, Volume 3: Gas Lasers (E. W. McDaniel and W. L. Nighan, eds.), Academic Press, 1982.

- [27] W. L. Nighan, "Stability of high-power molecular laser discharges," in *Principles of Laser Plasmas* (G. Bekefi, ed.), John Wiley & Sons, 1976.
- [28] E. E. Kunhardt, "Basic topics of current interest to switching for pulsed power applications," in *Gaseous Dielectrics IV* (L. G. Christophorou and M. O. Pace, eds.), Pergamon Press, New York, 1983.
- [29] D. H. Douglas-Hamilton and S. A. Mani, "Attachment instability in an externally ionized discharge," *J. Appl. Phys.*, vol. 45, p. 4406, 1974.
- [30] L. C. Pitchford, "Power loading effects in gas discharge models," *Proc. US-FRG Joint Seminar on Externally Controlled Diffuse Discharges*, Bad Honeff, FRG, p. 148, 1983.
- [31] A. P. Napartovich, V. G. Naumov, and V. M. Shashkov, "Heating of gas in a combined discharge in a flow of nitrogen, *Sov. Phys. Dokl.*, vol. 22, p. 35, 1977.
- [32] J. A. Shirley and R. J. Hall, "Vibrational excitation in  $H_2$  and  $D_2$  electric discharges," *J. Chem. Phys.*, vol. 67, p. 2419, 1977.
- [33] J. N. Bardsley and J. M. Wadehra, private communication, 1982.
- [34] J. M. Wadehra, "Effect of rot-vibrational excitation on dissociative attachment of  $H_2$ ," *35th Gaseous Elec. Conf.*, 1982.
- [35] H. Seguin and J. Tulip, "Photoinitiated and photosustained laser," *Appl. Phys. Lett.*, vol. 21, p. 414, 1972.
- [36] D. R. Shure and S. A. Wutzke, "UV sustained CO laser discharge, II. Discharge studies," *J. Appl. Phys.*, vol. 52, p. 3858, 1981.
- [37] D. R. Shure, "UV sustained CO laser discharge, I. Photoionization studies," *J. Appl. Phys.*, vol. 52, p. 3855, 1981.
- [38] W. M. Moeny and M. von Dadelszen, "UV-sustained glow discharge opening switch experiment," *Proc. 5th IEEE Pulsed Power Conf.*, Arlington, VA, 1985.
- [39] C. M. Young, M. von Dadelszen, J. M. Elizondo, J. W. Benze, M. M. Moeny, and J. G. Small, "Investigation of a UV-sustained radial glow discharge opening switch," *Proc. 5th IEEE Pulsed Power Conf.*, Arlington, VA, 1985.
- [40] G. Z. Hutchenson, J. R. Cooper, E. Strickland, G. Schaefer, and K. H. Schoenbach, "A UV-sustained discharge for opening switches," to be published, 1986.
- [41] G. Schaefer, K. H. Schoenbach, P. Tran, J. Wang, and A. H. Guenther, "Computer calculations of the time dependent behavior of diffuse discharge switches," *Proc. 4th IEEE Pulsed Power Conf.*, Albuquerque, NM, p. 714, 1983.

- [42] M. J. Rossi, H. Helm, and D. C. Lorents, "Photoenhanced electron attachment in vinylchloride and trifluorethylene at 193 nm," Appl. Phys. Lett., 1984.
- [43] F. L. Eisele, "Photon induced electron attachment," Final Report, AFWAL-TR-85-2015, 1984.
- [44] S. J. Smith, Proc. 4th Int. Conf. Ionization Phenomena in Gases, p. IC-219, 1960.
- [45] D. S. Burch, S. J. Smith, and L. M. Branscomb, "Photodissociation spectroscopy of  $O_2^-$ ," J. Chem. Phys., vol. 112 p. 171, 1958.
- [46] L. M. Branscomb, S. J. Smith, and G. Tisone, G., "Oxygen metastable atom production through photodetachment," J. Chem. Phys., vol. 43, p. 2906, 1965.
- [47] C. L. Chen and P. J. Chantry, "Photon-enhanced dissociative electron attachment in  $SF_6$  and its isotopic selectivity," J. Chem. Phys., vol. 71, p. 3897, 1979.
- [48] R. Barbe, J. P. Astruc, A. Lagreze, and J. P. Schermann, "Spectral and temperature dependence of laser induced dissociative attachment in  $SF_6$ ," Laser Chem., vol. 1, p. 17, 1982.
- [49] W. E. Wentworth, R. George, and H. Keith, "Dissociative thermal electron attachment of some aliphatic chloro, bromo, iodo compounds, J. Chem. Phys., vol. 51, p. 1791, 1969.
- [50] M. Allan and S. F. Wong, "Dissociative attachment from vibrationally and rotationally excited HCl and HF," J. Chem. Phys., vol. 74, p. 1687, 1981.
- [51] S. K. Srivastava and O. J. Orient, "A double e-beam technique for collision studies from excited states: Application to vibrationally excited  $CO_2$ ," Phys. Rev. A, vol. 27, p. 1209, 1983.
- [52] J. J. Tise and C. Wittig, "Optically pumped molecular lasers in the 11-17 micron region," J. Appl. Phys., vol. 49, p. 61, 1978.
- [53] G. Z. Hutcheson, C. Holmberg, B. Pashale, G. Schaefer, and K. H. Schoenbach, " $CO_2$  laser enhanced resistivity in externally sustained discharges containing admixtures of  $C_2H_3F$  and  $NH_3$ ," to be published.
- [54] E. R. Sirkin and G. C. Pimentel, "HF rotational laser emission through photoelimination from vinyl fluoride and 1,1-difluoroethene," J. Chem. Phys., vol. 75, p. 604, 1981.
- [55] M. J. Berry, "Chlorethylene photochemical lasers: Vibrational energy content of HCl molecular elimination products," J. Chem. Phys., vol. 61, p. 3114, 1974.

- [56] P. L. Houston, "Electronic to vibrational energy transfer from excited halogen atoms," in *Photoselective Chemistry--Part 2* (J. Jortner, R. D. Levine, and S. R. Rice, eds.), John Wiley & Sons, 1981.
- [57] A. B. Peterson, C. Wittig, and S. R. Leone, "Electronic to vibrational pumped CO<sub>2</sub> laser operating at 4.3, 10.6, and 14.1  $\mu$ m," *J. Appl. Phys.*, vol. 47, pp. 1051-1054, March 1976.
- [58] I. M. Beterov and N. V. Fatayev, "Optogalvanic demonstration of state-to-state dissociative electron capture rate in I<sub>2</sub>," *Opt. Comm.*, vol. 40, p. 425, 1982.
- [59] J. E. Eninger, "Broad area electron beam technology for pulsed high power gas lasers," *Proc. 3rd IEEE Pulsed Power Conf.*, Albuquerque, NM, p. 499, 1981.
- [60] T. J. Orzechowski and G. Bekefi, "Current flow in a high-voltage diode subjected to a crossed magnetic field," *Phys. Fluids*, vol. 19, p. 43, 1976.
- [61] W. M. Clark, "Ion plasma electron gun research," HRL Final Report, ONR Contract N00014-77-C-0484, 1977.
- [62] G. Wakalopoulos and L. Gresko, "Pulsed WIP electron gun, Final Report--Design Phase," HAC Report No. FR-79-73-735, UCRL, 1979.
- [63] H. E. Gallagher and R. J. Harvey, "Development of a 1-GW electron-beam controlled switch," *Proc. 16th Power Modulator Symp.*, Arlington, VA, p. 158, 1984.
- [64] C. H. Harjes, K. H. Schoenbach, G. Schaefer, M. Kristiansen, H. Krompholz, and D. Skaggs, "Electron-beam tetrode for multiple, submicrosecond pulse operation," *Rev. Sci. Instrum.*, vol. 55, p. 1684, 1984.
- [65] R. Petr, and M. Gundersen, "Field emission cathode for high current beams," *Lasers and Particle Beams*, vol. 1, p. 207, 1983.
- [66] J. L. Cronin, "Modern dispenser cathodes," *Proc. IEEE*, vol. 128, p. 19, 1982.
- [67] J. D. Daugherty, "Electron beam ionized lasers," in *Principles of Laser Plasmas* (G. Bekefi, ed.), John Wiley & Sons, Inc., 1976.
- [68] D. H. Douglas-Hamilton, "Diffuse discharge production--Group report," *Proc. ARO Workshop on Diffuse Opening Switches*, Tamarron, CO, p. 169, 1982.
- [69] M. J. Berger and S. M. Seltzer, "Tables of energy-losses and ranges of electrons and positrons," *NAS-NRC Publication 1133*, p. 205, 1964.
- [70] ICRU Report 37, "Stopping Powers for Electrons and Positrons, International Commission on Radiation Units and Measurements," ICRU Publications, 7910 Woodmont Ave., Suite 1016, Bethesda, MD 20814, 1984.

- [71] D. C. Lorents and R. E. Olson, "Excimer formation and decay processes in rare gases," SRI Semiannual Tech. Rep. No. 1, Stanford Research Institute, 1971.
- [72] L. C. Lee and F. Li, "Shortening of electron conduction pulses by electron attachers  $O_2$ ,  $N_2O$ , and  $CF_4$ ," J. Appl. Phys., vol. 56, p. 3169, 1984.
- [73] S. R. Hunter, J. G. Carter, J. L. Christophorou, and V. K. Lakdawala, "Transport properties and dielectric strengths of gas mixtures for use in diffuse discharge opening switches," in Gaseous Dielectrics IV (L. G. Christophorou and M. O. Pace, eds.), Pergamon Press, New York, 1984.
- [74] A. M. Efremov and B. M. Koval'chuk, "A non-self-consistent electron-beam controlled discharge in methane," Izvestiya Vysshikh Uchebnykh Zavedeni, vol. 4, p. 65, 1982.
- [75] G. Schaefer and K. H. Schoenbach, "External control of diffuse discharge switches," Proc. 5th IEEE Pulsed Power Conf., Arlington, VA, 1985.
- [76] B. E. Strickland, K. H. Schoenbach, G. Schaefer, O. Ishihara, and M. Kristiansen, "Domain instability in an E-beam controlled diffuse discharge switch exhibiting negative differential conductivity," to be published, 1986.
- [77] L. C. Lee, C. C. Chiang, K. Y. Tang, D. L. Huestis, and D. C. Lorents, "Gaseous electronic kinetics for e-beam excitation of  $Cl_2$ , NO and  $N_2O$  in  $N_2$ ," 2nd Annual Rept. on Coord. Res. Program in Pulsed Power Physics, Dept. Elec. Engineering, Texas Tech Univ., Lubbock, TX, p. 189, 1981.
- [78] J. F. Lowry, L. E. Kline, and J. V. R. Heberlein, "Electron-beam controlled on/off discharge characterization experiments, Proc. 4th IEEE Pulsed Power Conf., Albuquerque, NM, p. 94, 1983.
- [79] R. J. Commisso, R. F. Fernsler, V. E. Scherrer, and I. M. Vitkovitsky, "Electron-beam controlled discharges," Trans. Plasma Sci., vol. PS-10, p. 241, 1982.
- [80] R. J. Commisso, R. F. Fernsler, V. E. Scherrer, and I. M. Vitkovitsky, "Application of electron-beam controlled diffuse discharges to fast switching," Proc. 4th IEEE Pulsed Power Conf., Albuquerque, NM, p. 87, 1983.
- [81] R. J. Commisso, R. F. Fernsler, V. E. Scherrer, and I. M. Vitkovitsky, "Inductively generated, high voltage pulse using an electron beam controlled opening switch," Appl. Phys. Lett., vol. 47, p. 1056, 1985.
- [82] V. E. Scherrer, R. J. Commisso, R. F. Fernsler, L. Miles, and I. M. Vitkovitsky, "The control of breakdown and recovery in gases by pulsed electron beams," in Gaseous Dielectrics III (L. G. Christophorou, ed.), Pergamon Press, New York, 1982.

- [83] V. E. Scherrer, R. J. Commisso, R. F. Fernsler, and I. M. Vitkovitsky, "Study of gas mixtures for e-beam controlled switches," in Gaseous Dielectrics IV (L. G. Christophorou and M. O. Pace, eds.), Pergamon Press, 1984.
- [84] K. H. Schoenbach, G. Schaefer, M. Kristiansen, H. Krompholz, H. Harjes, and D. Skaggs, "Investigations of e-beam controlled diffuse discharges," in Gaseous Dielectrics IV (L. G. Christophorou and M. O. Pace, eds.), Pergamon Press, New York, 1984.
- [85] K. H. Schoenbach, G. Schaefer, M. Kristiansen, H. Krompholz, H. Harjes, and D. Skaggs, "An e-beam controlled diffuse discharge switch," Proc. 16th Power Modulator Symp., Arlington, VA, p. 152, 1984.
- [86] K. H. Schoenbach, G. Schaefer, M. Kristiansen, H. Krompholz, H. Harjes, and D. Skaggs, "An electron-beam controlled diffuse discharge switch," J. Appl. Phys., vol. 57, p. 1618, 1985.
- [87] G. Schaefer, K. H. Schoenbach, M. Kristiansen, B. E. Strickland, R. A. Korzekwa, and K. R. Rathbun, "Interaction of discharge and circuit in an electron beam controlled diffuse discharge opening switch," to be published, 1986.
- [88] P. Bletzinger, "Operation of externally ionized discharges at high electric fields," GEC 1985, Monterey, CO, Abstract H4, 1985.
- [89] P. Bletzinger, "Determination of breakdown voltages and instabilities in electron beam ionized discharges," Proc. 5th IEEE Pulsed Power Conf., Arlington, VA, 1985.

AD-A169 113

COORDINATED RESEARCH PROGRAM IN PULSED POWER PHYSICS

2/3

(U) TEXAS TECH UNIV LUBBOCK PULSED POWER LAB

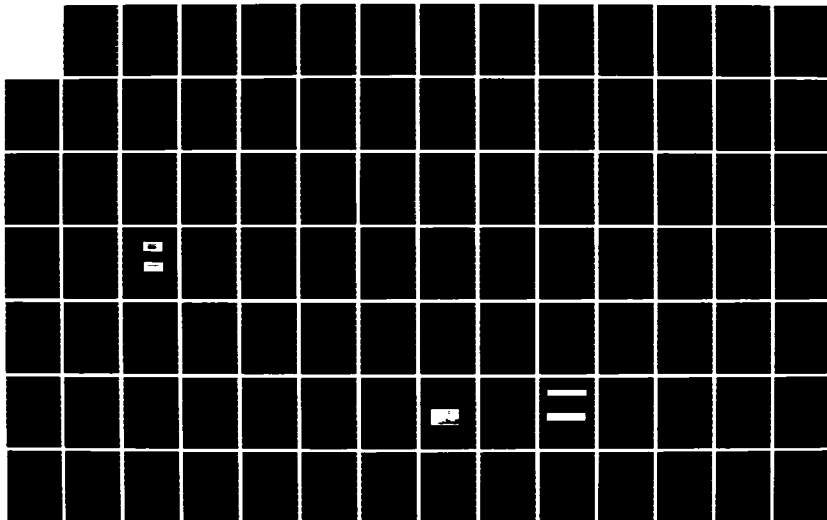
M KRISTIANSEN ET AL. 20 DEC 85 AFOSR-TR-86-0305

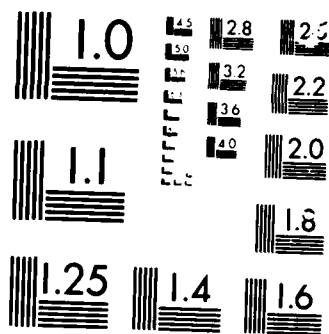
UNCLASSIFIED

AFOSR-84-0032

F/G 10/2

NL





MICROCOPY

CHART



## FIGURE CAPTIONS

- Fig. 1. Schematic of an externally controlled opening switch as part of an inductive energy storage system.
- Fig. 2. Measured and predicted e-beam switch waveforms in methane [2,12].
- Fig. 3. Calculated steady state  $E/N$ - $j$  characteristics for an e-beam sustained discharge in  $N_2$  with an  $N_2O$  fraction of 1%. The variable parameter is the electron generation rate [9].
- Fig. 4. Time dependence of  $E/N$  (top) and current density (bottom) of an e-beam sustained discharge in 1 atm  $N_2$  with admixtures of  $N_2O$ . The e-beam is on for  $0 \leq t \leq 100$  ns. The variable parameter is the  $N_2O$  fraction in % [9].
- Fig. 5. Time dependence of  $E/N$  (top) and current density (bottom) of an e-beam sustained, laser photodetachment assisted discharge in 1 atm  $N_2$  with an  $N_2O$  fraction of 1%. The e-beam and laser are on for  $0 \leq t \leq 100$  ns. The variable parameter is the laser power density [9].
- Fig. 6. Theoretical cross section for  $e + HCl \rightarrow H + Cl^-$ , depending on electron energy for the vibrational states ( $v=0-3$ ), assuming a Boltzmann distribution over rotational states at  $T=300$  K [33].
- Fig. 7. Attachment coefficient for trifluoroethylene. The solid dots give the values for the unexcited sample (200 mTorr of  $C_2F_3H$  in 200 Torr helium). The open circles represent the data for the excited sample (100 mTorr of  $C_2F_3H$  in 100 Torr helium). The attachment coefficients are expressed in terms of the unexcited trifluorethylene pressure [42].
- Fig. 8. Some potential curves for  $I_2$  and  $I_2^-$  and the scheme of excitation of vibrational levels [58].
- Fig. 9. Schematic circuit for an e-beam sustained discharge switch in an inductive energy storage system [9].
- Fig. 10. Total electron attachment rate constants as a function of the mean electron energy  $\langle \epsilon \rangle$  for several perfluoroalkanes and perfluoroethers measured in buffer gases of  $N_2$  and Ar [73].
- Fig. 11. Electron drift velocity  $w$  versus  $E/N$  for several (a)  $C_2F_6/Ar$  and (b)  $C_2F_6/CH_4$  gas mixtures [73].
- Fig. 12. Load lines and current density  $j$  versus reduced electric field strength  $E/N$  obtained with different load lines [87].
- Fig. 13. System current, e-beam current, and switch voltage for an e-beam controlled switch using 5 atm of  $CH_4$  with 1%  $C_2F_6$  [81].

Table 1  
Photoenhanced Electron Attachment

---

(1) VIBRATIONAL EXCITATION

- (a) Single-Photon Excitation plus Energy Transfer
  - (b) Overtone and Combination Band Excitation
  - (c) Multi-Photon Excitation
- 

(2) PHOTODISSOCIATION

- (a) Single-Photon - UV
  - (b) Multi-Photon - IR
- 

(3) ELECTRONIC EXCITATION

- (a)  $E \rightarrow V, R$  Collisions
  - (b)  $E \rightarrow V, R$  Transitions, Radiative
-

Table 2  
Properties of Foil Material Candidates [59]

FOIL MATERIAL	ADVANTAGE	DISADVANTAGE
Beryllium	Very Low Z High Conductivity	Highly Toxic Available only in Small Pieces, Expensive ( $\sim \$50/\text{in}^2$ )
Kapton	Low Z	Very Low Conductivity Disintegrates from Electron Radiation
Aluminum	Relatively Low Z High Conductivity	Low Strength at $T > 200^\circ \text{C}$
Titanium (Pure and Alloy)	High Strength	Low Conductivity Relatively High Z
Steel	High Strength	Low Conductivity High Z
Inconel 718	Very High Strength	Low Conductivity High Z
Composite E.G. Cu or Al CLAD Ti	Combines High Strength with High Conductivity	Difficulty to Fabricate in Uniform Layers with Good Bonding

Table 3

Summary of Data on Relevant Experiments  
on e-Beam Controlled Switches

INSTITUTE, REFERENCES	E-BEAM SYSTEM	E-BEAM CURRENT DENSITY $J_B$ [A/cm <sup>2</sup> ]	E-BEAM ENERGY $E_B$ (keV)	GASES	SWITCH CURRENT DENSITY $J_S$ [A/cm <sup>2</sup> ]	CURRENT GAIN	OPENING TIME
High Current Electr. Dept., Tomsk, USSR (Koval'chuk and Mesynts [3,4])	Cold Cathode	1.5	330	Natural Gas: CH <sub>4</sub> :C <sub>2</sub> H <sub>6</sub> :C <sub>3</sub> H <sub>8</sub> : O <sub>2</sub> :CO <sub>2</sub> : other hydrocarbons	15	~ 10	200 ns
(Efremov and Koval'chuk [47])	Thermionic Cathode, Tetrode	0.014	135	CO <sub>2</sub> :N <sub>2</sub> :He	30	1000	3 $\mu$ s - 5 $\mu$ s
Maxwell Labs San Diego, CA (Hunter [2])	Cold Cathode	2-5	250	CH <sub>4</sub>	27	5	400 ns
AFWL, Wright Patterson (Bletzinger [19,21])	Hot Matrix Cathode	0.02	175	N <sub>2</sub> , Ar, CH <sub>4</sub> with C <sub>2</sub> F <sub>6</sub> , C <sub>3</sub> F <sub>8</sub> , NF <sub>3</sub> , CF <sub>4</sub> , CCl <sub>4</sub>	2	100-1000	10 $\mu$ s - 1 $\mu$ s
Westinghouse R&D Ctr. Pittsburgh, PA (Lowry et al. [78])	WIP-gun	< 0.1	150	CH <sub>4</sub>	1.9	380	> 1 $\mu$ s (with inductor in switch loop)
Hughes Research Laboratories Malibu, CA (Gallagher & Harvey [63])	WIP-gun	< 0.035	150	CH <sub>4</sub>	20	< 1000	> 1 $\mu$ s (with inductor in switch loop)
Naval Research Lab, Washington, DC (Commisso et al. [80])	Cold Cathode, 200 ns and ~ 1 $\mu$ s pulse durations	0.2-5	200	CH <sub>4</sub> , N <sub>2</sub> N <sub>2</sub> :O <sub>2</sub> Ar:O <sub>2</sub> CH <sub>4</sub> :C <sub>2</sub> F <sub>6</sub>	< 50	10-20	50 ns - 100 ns
Texas Tech University Lubbock, TX (Schoenbach et al. [86], Schaefer et al. [87])	Thermionic Cathode, Tetrode, pulse train	0.1-1.0	250	N <sub>2</sub> :N <sub>2</sub> O N <sub>2</sub> :SO <sub>2</sub> N <sub>2</sub> :CO <sub>2</sub> Ar:C <sub>2</sub> F <sub>6</sub>	< 15	~ 15	50 ns

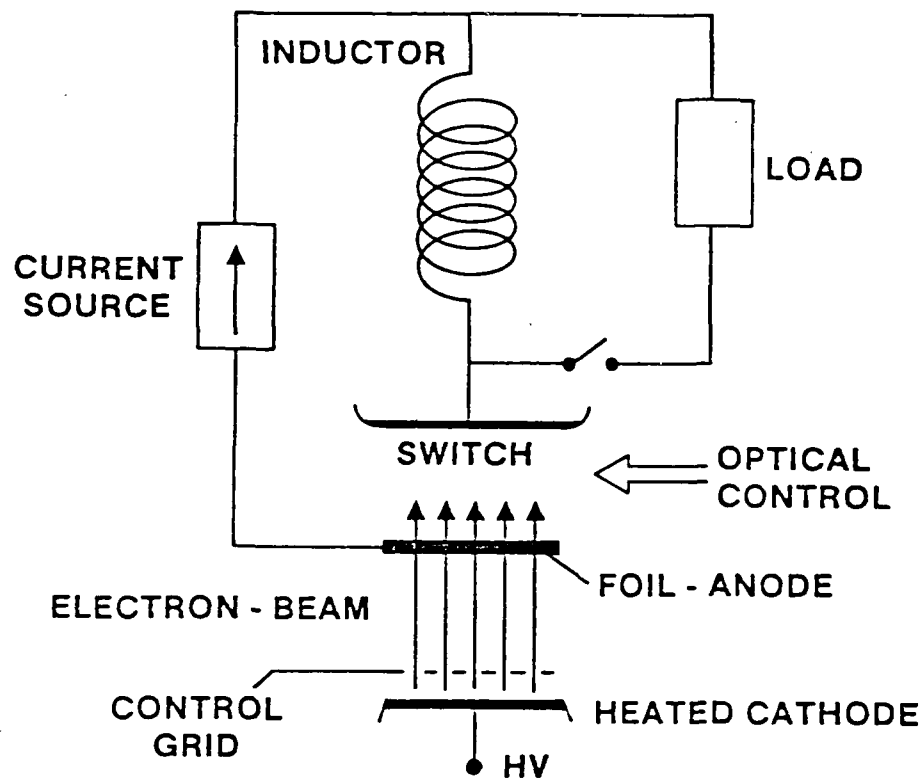


Fig. 1. Schematic of an externally controlled opening switch as part of an inductive energy storage system.

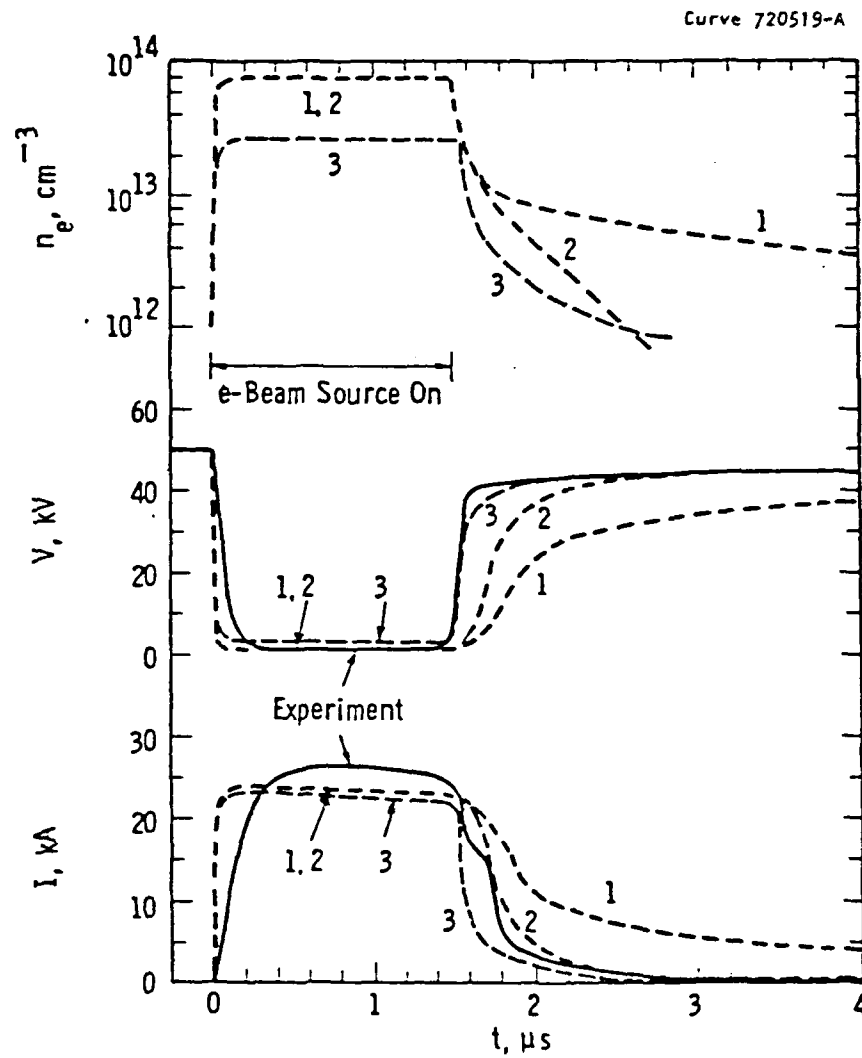


Fig. 2. Measured and predicted e-beam switch waveforms in methane [2,12].

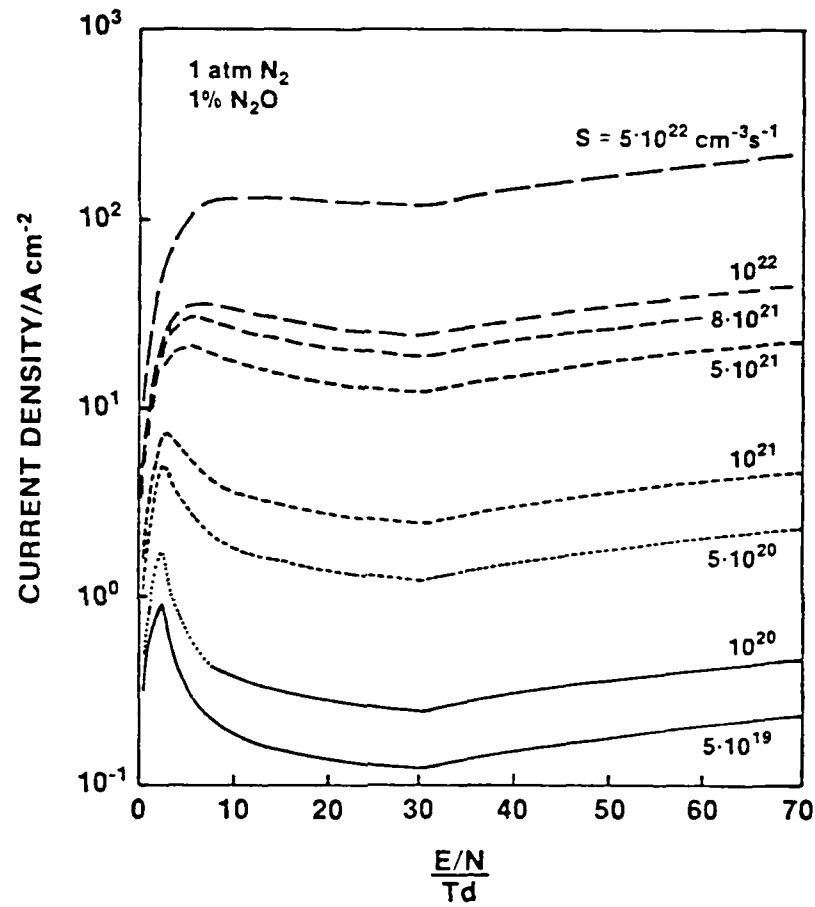


Fig. 3. Calculated steady state  $E/N$ - $j$  characteristics for an e-beam sustained discharge in  $N_2$  with an  $N_2O$  fraction of 1%. The variable parameter is the electron generation rate [9].

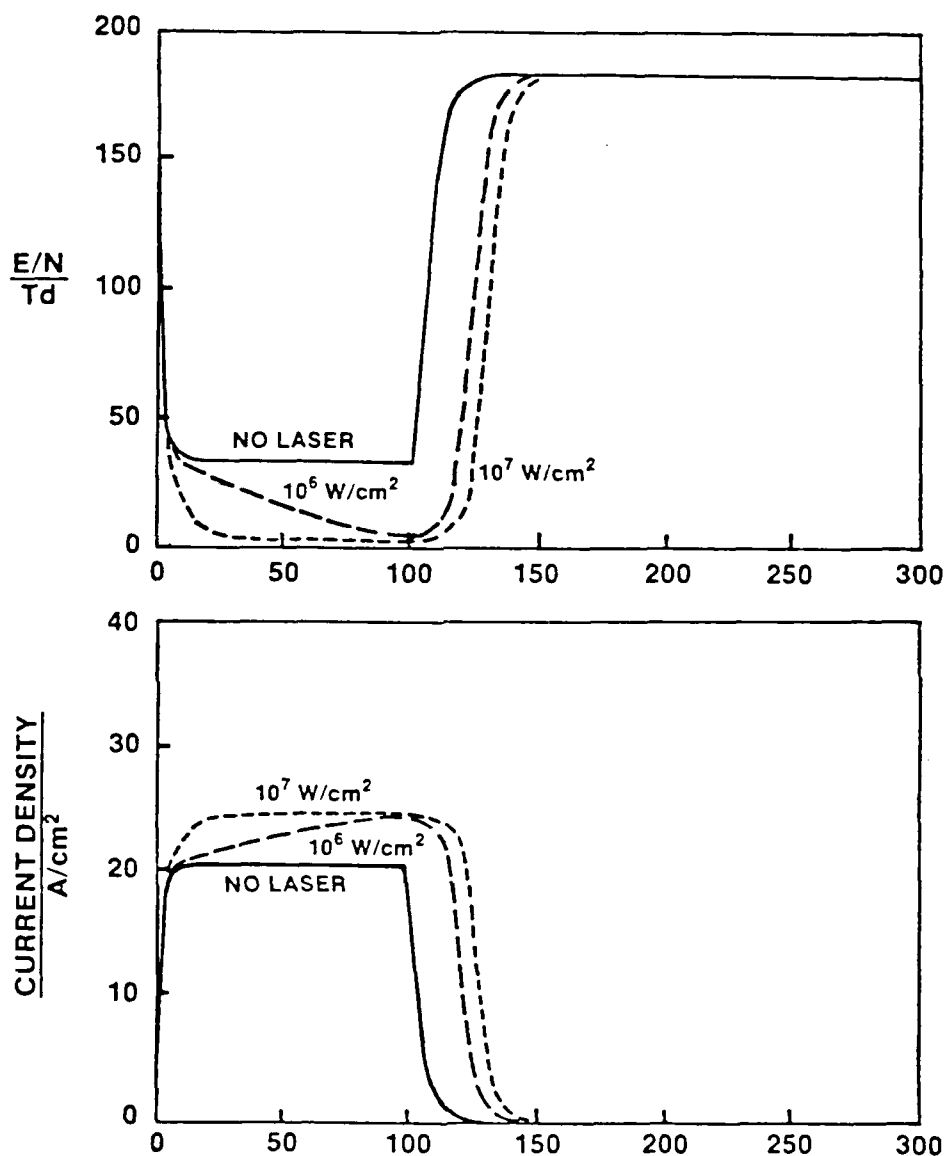


Fig. 4. Time dependence of  $E/N$  (top) and current density (bottom) of an e-beam sustained discharge in 1 atm  $N_2$  with admixtures of  $N_2O$ . The e-beam is on for  $0 \leq t \leq 100$  ns. The variable parameter is the  $N_2O$  fraction in % [9].



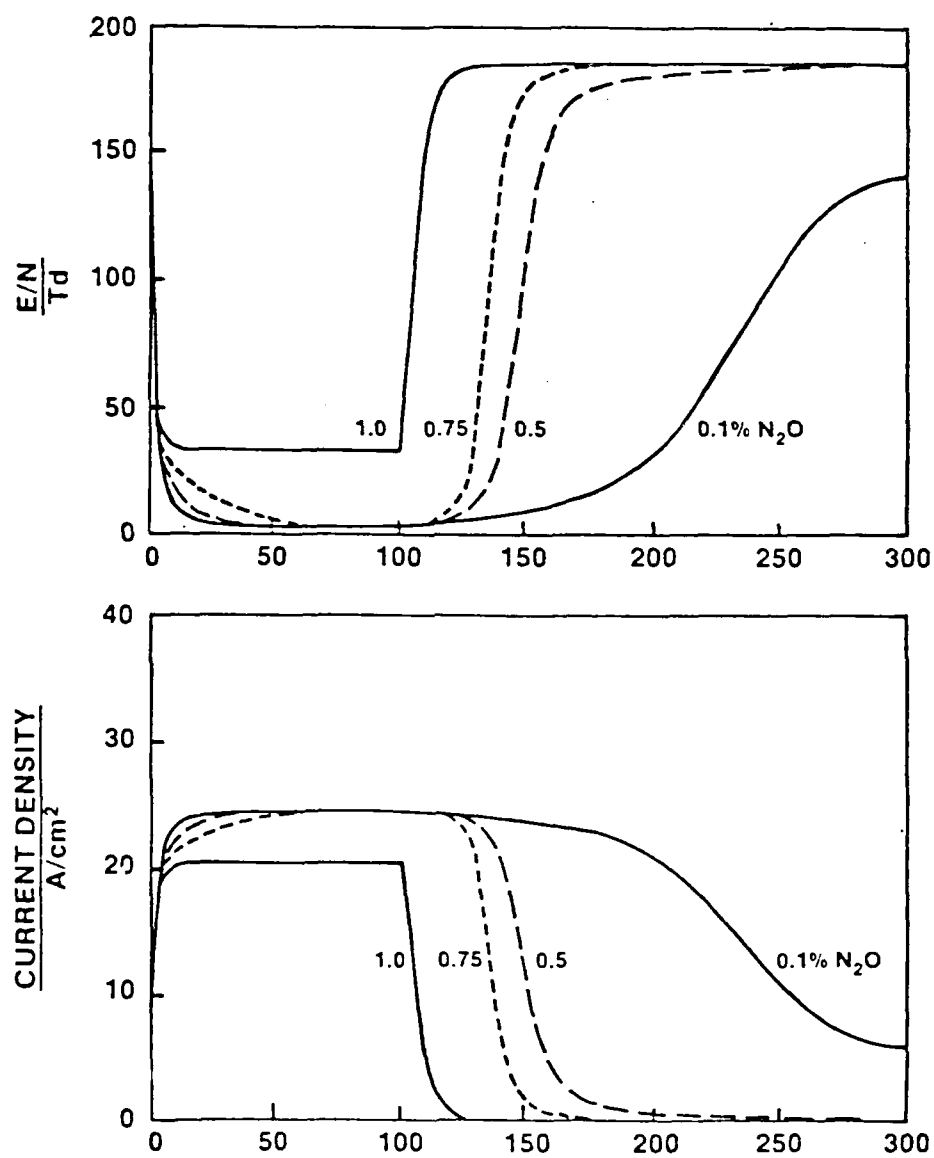


Fig. 5. Time dependence of  $E/N$  (top) and current density (bottom) of an e-beam sustained, laser photodetachment assisted discharge in 1 atm  $N_2$  with an  $N_2O$  fraction of 1%. The e-beam and laser are on for  $0 \leq t \leq 100$  ns. The variable parameter is the laser power density [%].

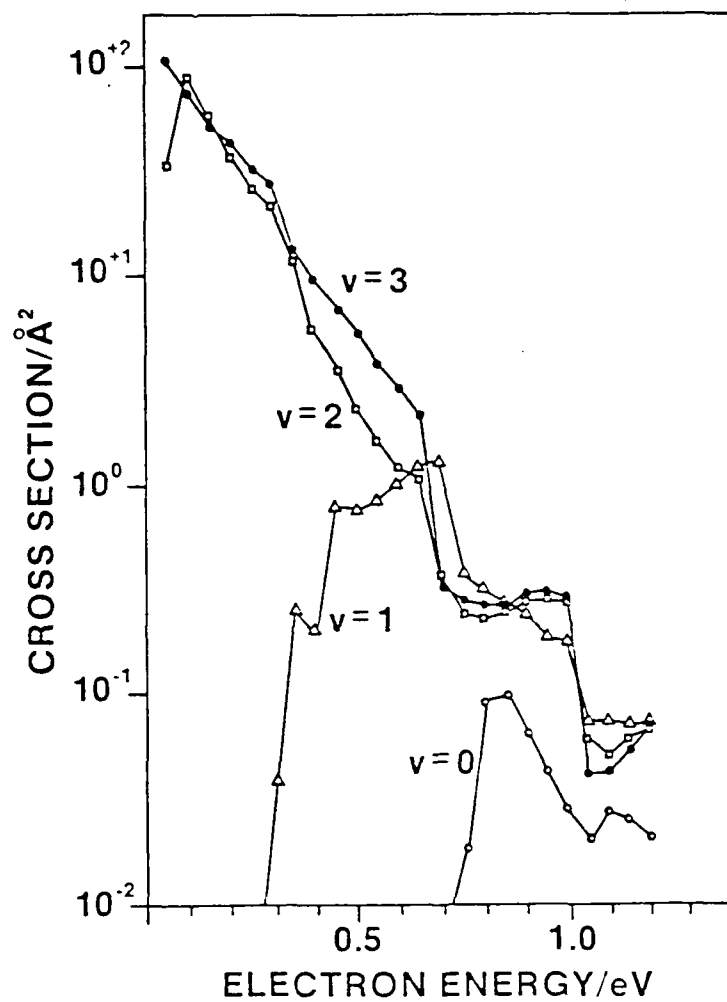


Fig. 6. Theoretical cross section for  $e + \text{HCl} \rightarrow \text{H} + \text{Cl}^-$ , depending on electron energy for the vibrational states ( $v=0-3$ ), assuming a Boltzmann distribution over rotational states at  $T=200$  K [33].

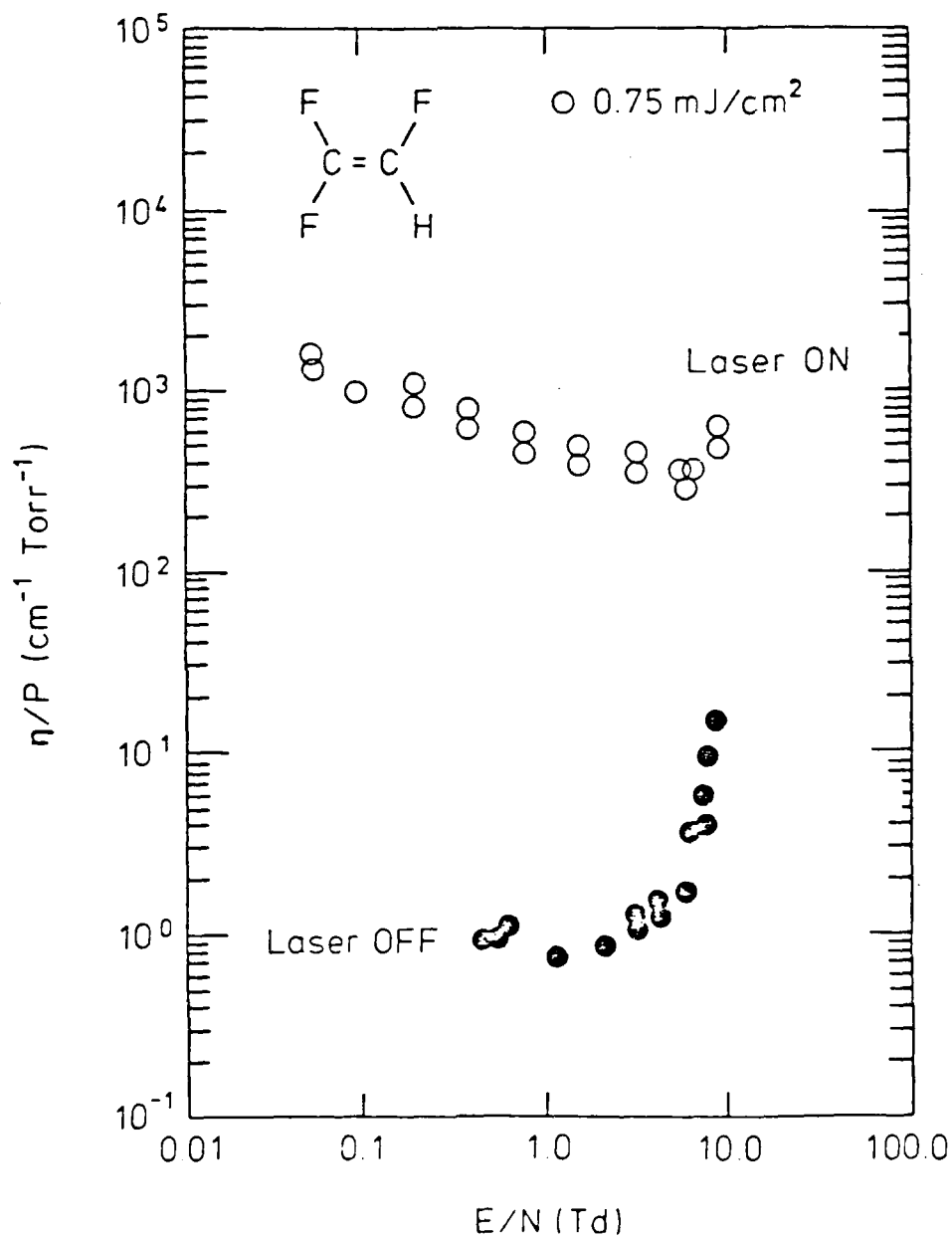


Fig. 7. Attachment coefficient for trifluoroethylene. The solid dots give the values for the unexcited sample (200 mTorr of  $C_2F_3H$  in 200 Torr helium). The open circles represent the data for the excited sample (100 mTorr of  $C_2F_3H$  in 100 Torr helium). The attachment coefficients are expressed in terms of the unexcited trifluoroethylene pressure [42].

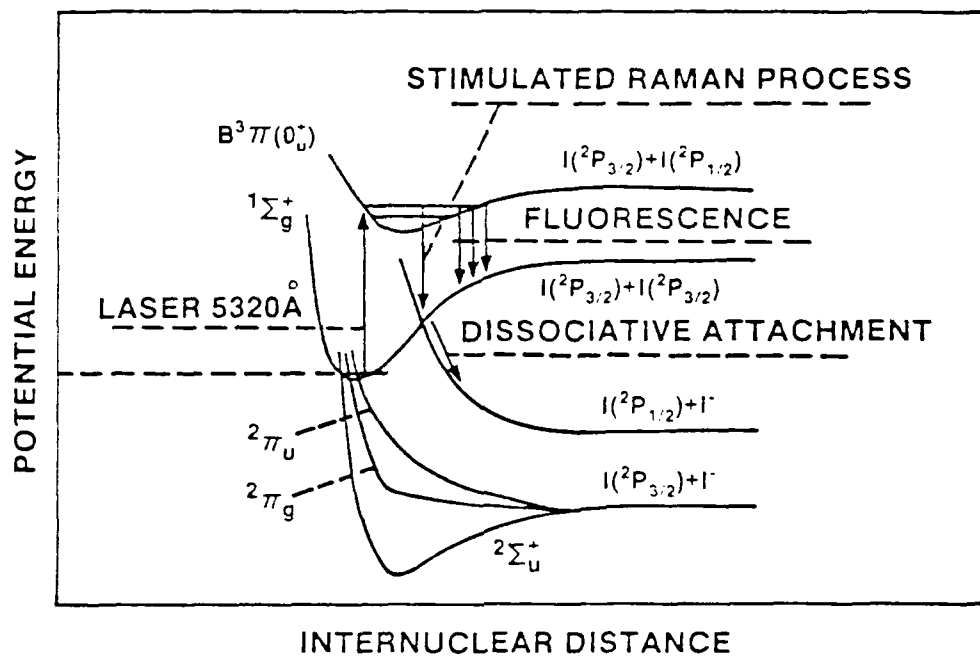


Fig. 8. Some potential curves for  $I_2$  and  $I_2^-$  and the scheme of excitation of vibrational levels [58].

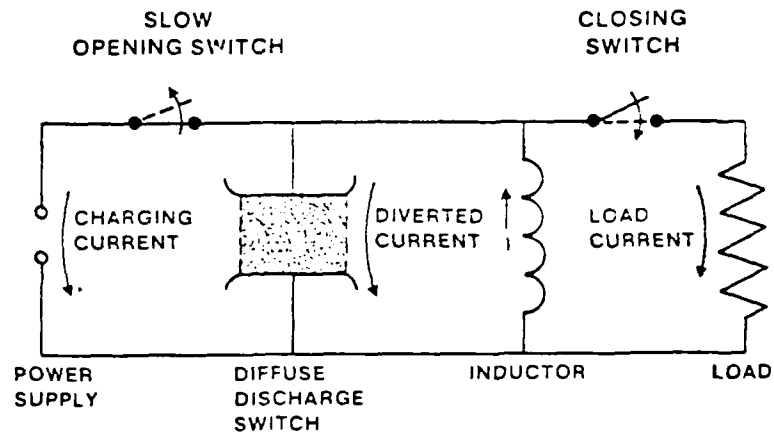


Fig. 9. Schematic circuit for an e-beam sustained discharge switch in an inductive energy storage system [9].

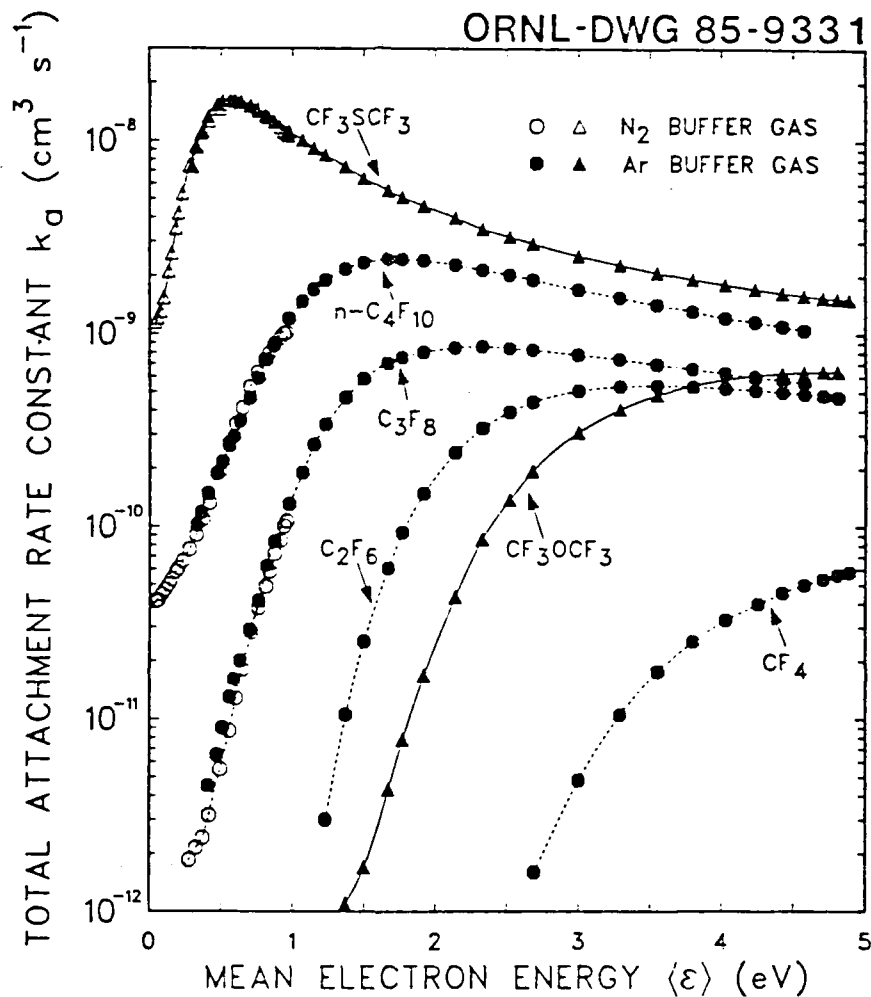


Fig. 10. Total electron attachment rate constants as a function of the mean electron energy  $\langle \epsilon \rangle$  for several perfluoroalkanes and perfluoroethers measured in buffer gases of  $\text{N}_2$  and  $\text{Ar}$  [73].

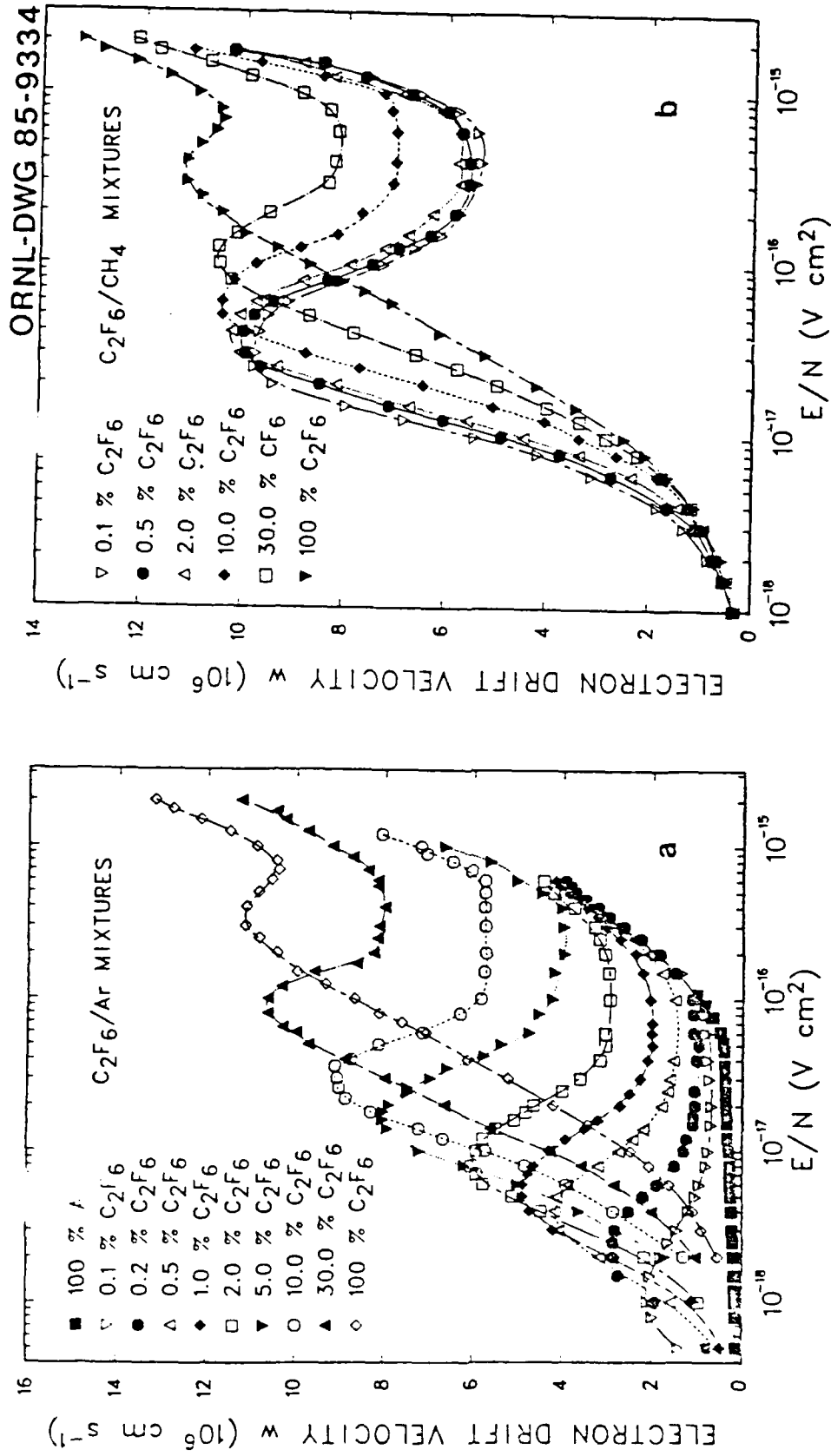


Fig. 11. Electron drift velocity  $w$  versus  $E/N$  for several (a)  $C_2F_6/Ar$  and (b)  $C_2F_6/CH_4$  gas mixtures [73].

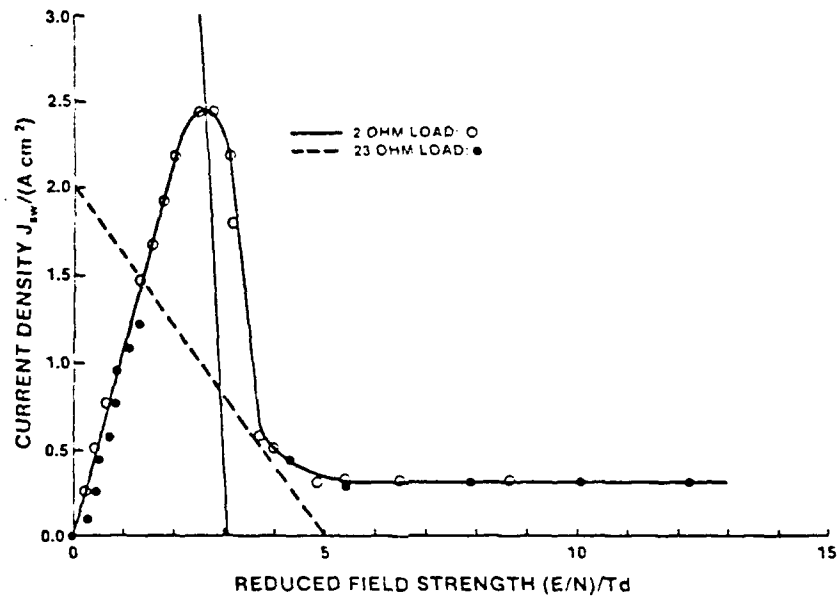


Fig. 12. Load lines and current density  $j$  versus reduced electric field strength  $E/N$  obtained with different load lines [87].



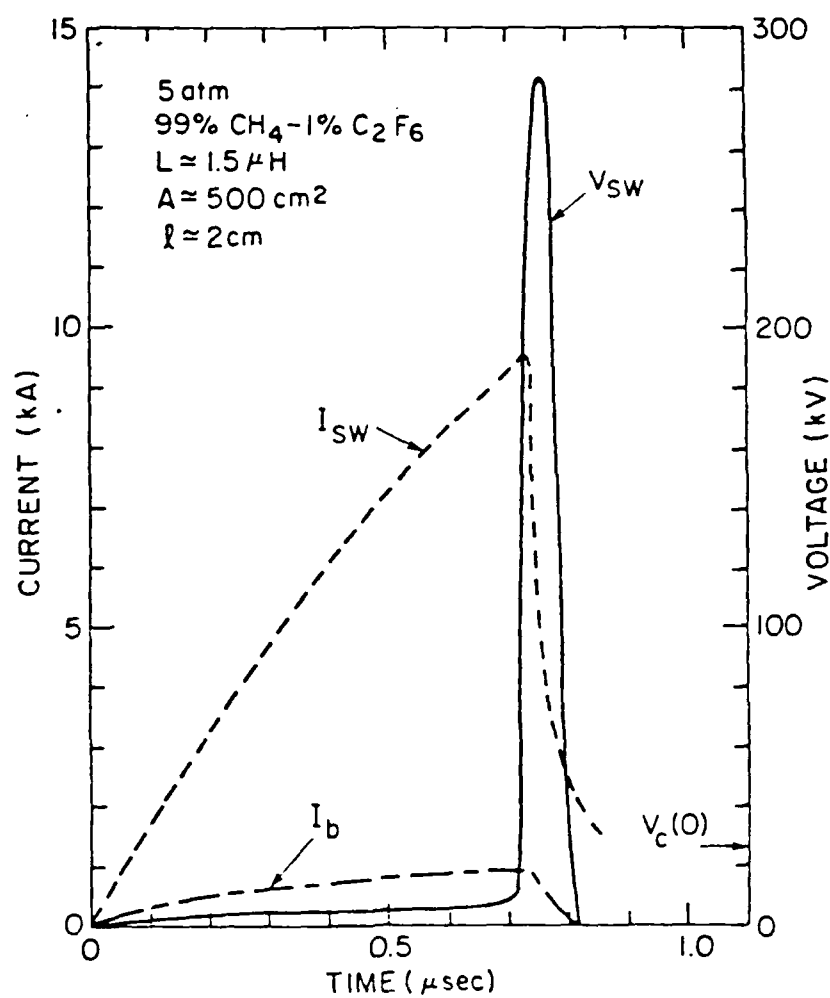


Fig. 13. System current, e-beam current, and switch voltage for an e-beam controlled switch using 5 atm of CH<sub>4</sub> with 1% C<sub>2</sub>F<sub>6</sub> [81].

## EXTERNAL CONTROL OF DIFFUSE DISCHARGE SWITCHES

G. Schaefer and K. H. Schoenbach  
Texas Tech University, Department of Electrical Engineering  
Lubbock, Texas 79409

**Abstract:** Electron-beam sustained diffuse discharges have attracted considerable interest as submicrosecond opening switches for inductive energy storage systems. Opening is accomplished through turning off the ionizing e-beam. In order to increase the switch efficiency (switch current/e-beam current) at high hold-off voltages and to reduce the opening time, attachers are used with a high attachment rate at high values of  $E/N$  and a low attachment rate at low values of  $E/N$ . These attachers will decrease the net source term and will obstruct the closing phase. Additional control through photodetachment and optically enhanced attachment will also allow to optimize the closing phase. The results of model calculations and experimental studies on various control mechanisms are discussed.

Introduction

In recent years there has been an increasing interest in the development of fast, repetitive, opening switches which would allow the use of inductive energy storage in repetitively operated pulsed power systems. Opening switch concepts that show promise for fast repetitive operation are based on the external control of the electron generation and depletion mechanisms in a diffuse discharge. Such control mechanisms can be the sustainment by electron beams and radiation sources, optical control of the electron depletion mechanisms, or external magnetic field to control the internal ionization processes. This paper gives an overview of the mentioned control mechanisms and discusses the requirements for the optimization of such systems.

Externally Sustained Discharges

An externally sustained discharge switch makes use of the electrons produced by an external source (electron-beam, UV radiation, or x-rays). The voltage across the gas discharge is always kept well below the value required for internal ionization. Figure 1 shows the general time dependence of some of the important discharge quantities through one full switch cycle, assuming that the time dependent source function has a trapezoidal shape with a steep rise and fall (Fig. 1a). The electron density (Fig. 1b), and consequently the current density will initially be zero and the switch is open. A constant source function  $S$  will then increase the electron density in the closing phase until it approaches a new steady state condition given by the balance of the electron generation and depletion mechanisms. In this state the current density reaches its maximum and the switch is closed. When the source is turned off the electron depletion mechanism will cause a decrease of the electron density and consequently of the current density in the opening phase until the initial state with approximately zero electron density is reached again. Since this device is operated in an inductive energy storage system the voltage and the reduced field strength  $E/N$  will drop to a lower value when the switch is conducting and will increase when the conduction is reduced (s. Figure 1c).

Steady State Conditions

In the closed phase the switch is supposed to have a resistivity as low as possible at a low voltage drop across the switch and consequently at a low value of  $E/N$ . This requires a high electron mobility and an electron depletion rate as low as possible at low values of  $E/N$ . Recombination can not be controlled significantly except by keeping the electron density low, but any further losses such as attachment have to be avoided. In the opening phase the switch has to withstand a high voltage. This means that strong electron losses must occur at very low electron densities at high values of  $E/N$ . This can be accomplished by an attacher with a high attachment rate at high values of  $E/N$ . The mobility of the electrons in the high  $E/N$  range is of minor importance since the electron density approaches zero. A decreasing mobility with increasing  $E/N$ , however, will improve the transition into the high  $E/N$  range. The two steady state phases therefore require an  $E/N$  dependence of the mobility and attachment rate as shown in Figure 2a [1,2].

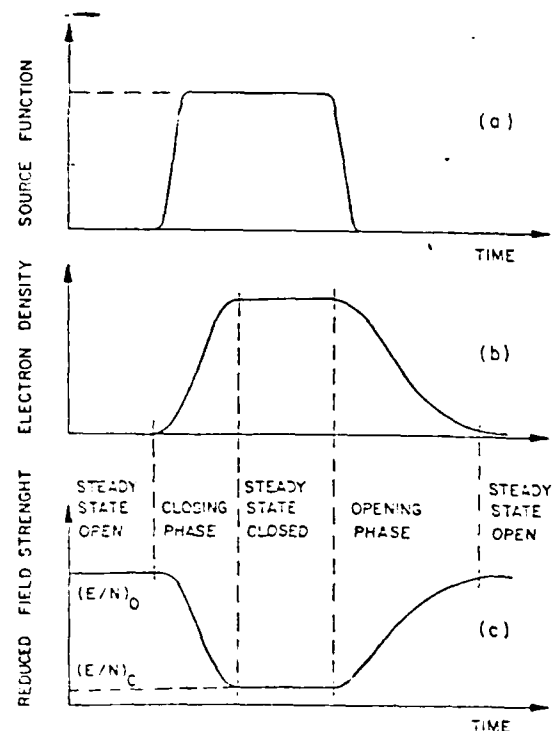


Fig. 1. Schematic time dependence of the electron source (a), electron density (b), and reduced electric field strength (c) in an externally sustained diffuse discharge for switching applications.

Although one never intends to operate the switch as an externally sustained discharge at high values of  $E/N$  one can calculate and measure the steady state resistivity and  $(J-E/N)$  characteristic for the full  $E/N$  range as shown in Figure 2b and c. The part of the discharge characteristic at high values of  $E/N$  has important consequences on the opening and closing phases as discussed later.

The required attachment characteristics can cause undesired losses if an electron beam is used as a discharge sustainer source. An attachment rate as shown in Figure 2a is given if the attachment cross section has its maximum above, but close to the energy range of the electron energy distribution function at the low value of the reduced field strength in the closed phase  $(E/N)_c$ , as shown in Figure 3. Since there is no overlap of the electron energy distribution function with the attachment cross section no attachment will occur. When  $E/N$  is increased, the electron energy distribution function is shifted towards higher energies and the attachment rate increases.

The initial secondary electrons produced by the high energy electron beam have an energy distribution over a wide energy range as shown in Figure 3 [3], and only a small fraction is produced in the energy range of the steady state electron energy distribution. A significant fraction (approximately 80% for the attach  $N_2O$  in a  $N_2$  buffer gas) is generated above the energy range of the attachment cross section. These electrons will during their relaxation move through the energy range where attachment can occur. The probability for attachment of these electrons will

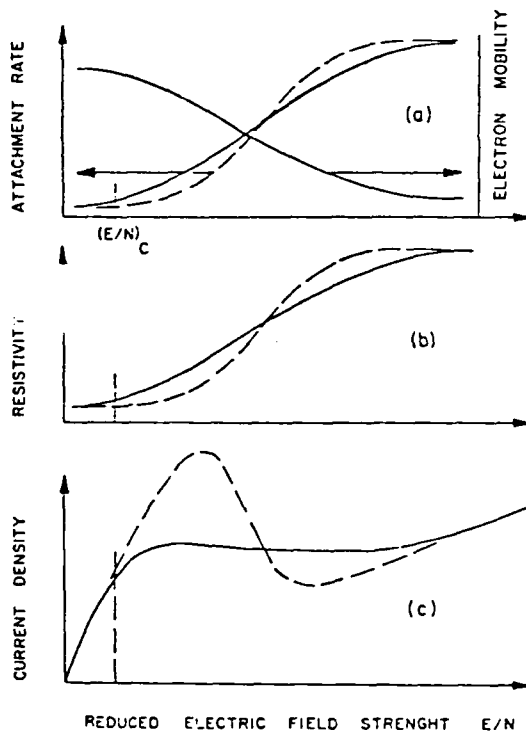


Fig. 2. Schematic  $E/N$  dependence of attachment rate and electron mobility (a), resistivity (b), and current density (c) in an externally sustained diffuse discharge for switching applications.

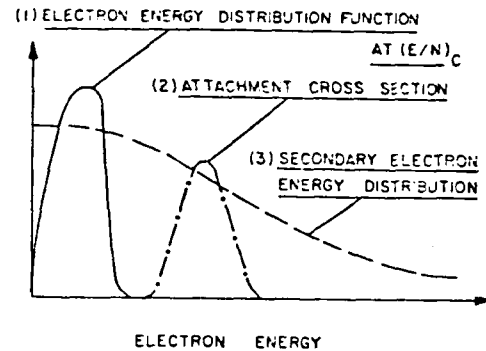


Fig. 3. Schematic electron energy dependence of the steady state electron energy distributions at low  $E/N$ , the attachment cross section, and the distribution function of the initial secondary electrons in an electron beam sustained discharge.

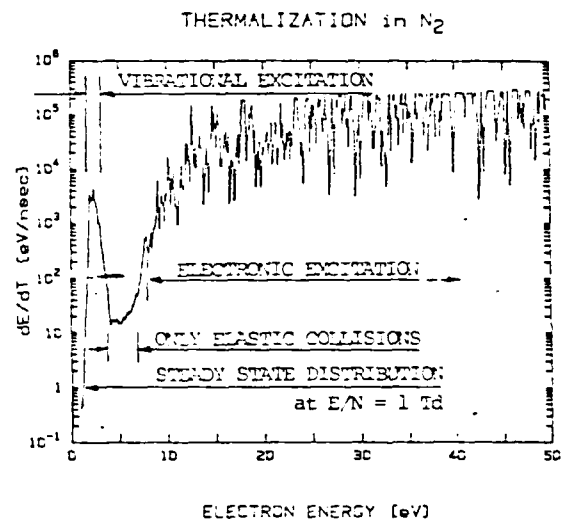


Fig. 4. Average velocity of relaxing electrons in energy space of relaxing electrons generated at 100 eV in  $N_2$  at  $E/N = 1 \text{ Td}$ .

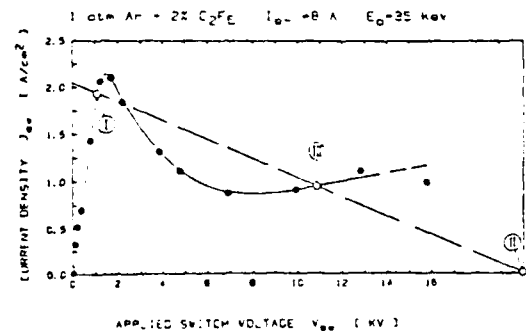


Fig. 5. Measured Current-Voltage characteristic of an electron beam sustained discharge in a mixture of 2%  $C_2F_6$  in 1 atm Argon.

then depend on their velocity in energy space in the energy range where attachment is dominant. Figure 4 shows the calculated average velocity of the electrons in energy space,  $dE/dt$ , during relaxation in  $N_2$  for initial energies of 100 eV [4]. This velocity is very high ( $> 10^3$  eV/ns) in energy ranges with strong inelastic cross section but significantly lower (10 eV/ns) in the 3-7 eV range where  $N_2$  has no significant inelastic cross sections. Attachment of the initial secondary electrons in a  $N_2$  buffer gas will therefore be significant if the attacher has its maximum cross section in the 3-7 eV range (example  $SO_2$ , approximately 10% are attached with 2%  $SO_2$  in  $N_2$ ) and much less significant if the maximum cross section is below 3 eV but above the steady state distribution (example  $N_2O$ ) [4]. Attachment of the initial secondary electrons has therefore to be considered using a correction factor in the source function, and these losses can be minimized by using an appropriate mixture of an attacher with a buffer gas as discussed above.

### Opening and Closing Phases

The opening phase starts when the electron source is turned off. Since the opening phase starts at the  $(E/N)_c$  value of the closed state, the electron depletion rate and consequently the rise of  $E/N$  will initially be slow until the system reaches the  $E/N$  regime where attachment dominates the electron losses. Since the performance of an inductive energy storage system strongly depends on the rise of the switch resistance  $dR/dt$  the attachment rate should have a steep rise with  $E/N$  (dashed line in Figure 2a). Such a gas mixture will cause a negative differential conductivity ( $d(E/N)/dJ$ ) in an intermediate  $E/N$  range as shown in Figure 2c. Such a characteristic, however, can cause problems for the closing phase. Figure 5 shows the measured V-I characteristic of an electron beam sustained discharge in a mixture of 1 atm Ar and 2%  $C_2F_6$  [5]. The optimum operation condition for the switch in the closed phase is at the maximum current in the low resistance regime at low values of  $E/N$  as indicated in condition (I). The suitable open condition (II) is given by a voltage of approximately 20 kV (at 1 atm and 1 cm discharge length), well below the hold-off voltage. In a good approximation an inductive energy storage system can be considered as having a transmission line characteristic. This means that the system will move on a straight line. When the source is turned on the system will therefore only approach condition (III) in Figure 5 with a lower current density and strong losses (high value of  $E/N$ ) [6]. To avoid this problem different approaches can be taken. One approach is to compromise with respect to the closing and opening phase using a gas mixture with a less steep increase of the attachment rate with  $E/N$  resulting in a weak negative differential conductivity (solid lines in Figure 2). A second possibility is to tailor the time dependence of the source function [6]. An electron beam with an increased current density in the beginning of the e-beam pulse will shift the J-E/N characteristic towards higher J-values for a short time to allow the system to reach the low  $E/N$  value c (I), before it approaches its steady state condition. Other solutions are to use additional external control mechanisms which alter the attachment properties of the gas mixture in a specific switch period.

### Optical Control Mechanisms

Optical control of diffuse discharges for switching applications, especially for opening switches, is a very recent research field. Besides

papers on concepts [7,8], model calculations on certain proposed systems [6], and numerous papers on basic processes suitable for switching applications, there are no results on operational switching devices available. Especially laser are attractive light sources allowing the generation of high power densities, precise illumination of the discharge volume, and precise timing. Due to the high costs of laser photons, however, especially if high photon energies are required, it seems to be inefficient at this time to use lasers for sustainment. Optical discharge control for switching application is therefore considered only as an additional control for a specific phase of the switch cycle, where other means do not allow the optimization of the discharge properties.

As discussed it is possible to optimize the operation conditions of an electron beam sustained diffuse discharge switch with respect to the steady state phases and the opening phase through tailoring the  $E/N$  dependance of the attachment rate coefficients, but this optimization causes problems with respect to the closing phase. Concepts on additional optical control, therefore, concentrate on attachment and its control in one of the transition phases. In principle, there are two different methods of optical control of attachment: to use photodetachment to overcome attachment, or to use optically induced attachment in gases which otherwise do not have a strong attachment rate in the  $E/N$  range of interest.

Photodetachment can be used as a method to overcome attachment in a well defined discharge period. A negative ion considered for photodetachment as a control mechanism is  $O^-$  [7]. Several molecules, such as  $O_2$ ,  $NO$ ,  $N_2O$ ,  $NO_2$ ,  $CO_2$ , and  $SO_2$ , undergo dissociative attachment producing  $O^-$ . In all gases or gas mixtures with these gases, however, competitive attachment processes exist or subsequent reactions of  $O^-$  will occur, producing molecular negative ions, which in general have lower cross sections for photodetachment.

Photodetachment experiments in low pressure  $O_2$  discharges and flowing afterglows showed that, for example, a fraction of 50% of the negative ions could be detached with laser pulses with a energy flux of 35 mJ/cm<sup>2</sup> at 565 nm [7]. For attachers with a high attachment rate at high values of  $E/N$  and low or zero attachment rate at low values of  $E/N$  (s. Figure 2) photodetachment may be a suitable process to support a transition from a highly attaching state into a non-attaching state of an externally sustained discharge [6].

Optically enhanced attachment means to use a gas mixture with an additive of molecules, which in their initial state are very weak attachers, and to transfer these molecules through optical excitation and may be some subsequent spontaneous transitions into species which act as strong attachers. Optically enhanced attachment is a control mechanism considered for controlling the opening phase of diffuse discharge opening switches. Some attachers show a drastically increased attachment cross section if excited into vibrational states. For HCl [9] and  $I_2$  [10] for example the attachment enhancement factor through excitation can be larger than  $10^3$ . There are many ways to create attachers excited into vibrational states. Only two optical methods are mentioned here, which have been used before for the pumping lasers operating between vibrational states:

(1) Optical vibrational excitation of higher lying states can be accomplished through overtone excitation or excitation of combination states, and

through multi-photon excitation. Such mechanisms can be found in numerous excitation mechanisms of optically pumped IR lasers. Some examples are lasers operating in gases such as  $\text{CF}_4$ ,  $\text{NOCl}$ ,  $\text{CF}_3\text{I}$ , and  $\text{NH}_3$ , pumped by a  $\text{CO}_2$  laser [11].

(2) Photodissociation of large molecules has shown to produce molecules in vibrationally excited states and is also used as excitation mechanism for molecular gas lasers. Examples are HF lasers pumped by photoelimination of HF from  $\text{CH}_2\text{CF}_2$  and  $\text{CH}_2\text{CHF}$ , using a UV-flashlamp [12]. Some of these processes have significant cross sections at the wavelength of the ArF-laser at 193 nm. Rossi et al. [8], performed a drift tube experiment to demonstrate the feasibility of these processes for controlling the electron balance in a discharge. In 100 torr Helium with 100 mtorr  $\text{C}_2\text{H}_2\text{F}_3$  at low values of  $E/N$  ( $< 3 \text{ Td}$ ), they obtained an increase of the attachment rate of up to  $10^3$  with an ArF laser. Similar experiments were performed in  $\text{C}_2\text{H}_3\text{Cl}$ . Schaefer et al. [13], performed measurements in a dc glow discharge at low values of  $E/N$  (0.5-5 Td), which was externally sustained by a Helium plasma injection. In a gas mixture of 60 Torr Helium and 3%  $\text{C}_2\text{H}_3\text{Cl}$ , pulsed resistance changes of a factor of 3.5 were measured after irradiating the discharge with a UV spark source.

#### Summary

Externally sustained diffuse discharges are promising candidates for fast, repetitive, opening switches. Low losses in the conduction phase, fast opening, and high hold-off voltages can be accomplished by using attachers with a high attachment rate at high values of  $E/N$  and a low attachment rate at low values of  $E/N$ . The optimization of the closing phase requires additional control mechanisms. Possible processes are photodetachment and optically enhanced attachment.

#### Acknowledgement

This work was supported jointly by AFOSR and ARO and in part by NSF.

#### References

- [1] K. H. Schoenbach, G. Schaefer, M. Kristiansen, L. L. Hatfield and A. H. Guenther, "Concepts for Optical Control of Diffuse Discharge Opening Switches," IEEE Trans. Plasma Sci., vol. PS-10, pp. 246-251, Dec. 1982.
- [2] L. G. Christophorou, S. R. Hunter, J. G. Carter, and R. A. Mathis, "Gases for Possible Use in Diffuse Discharge Switches," Appl. Phys. Lett., vol. 41, pp. 147-149, July 1982.
- [3] A. E. S. Green and T. Sawada, "Ionization Cross Sections and Secondary Electron Distribution," J. Atmosph. Terr. Phys., vol. 34, pp. 1719-1728, 1972.
- [4] G. Reinking, G. Schaefer, K. H. Schoenbach and G. Hutcheson, "Attachment of Initial Secondary Electrons in an Electron Beam Sustained Discharge," IEEE Int. Conf. Plasma Sci., 1985.

- [5] K. H. Schoenbach, G. Schaefer, M. Kristiansen, H. Krompholz, D. Skaggs and E. Strickland, "An E-Beam Controlled Diffuse Discharge Switch," Proc. 5th IEEE Pulsed Power Conf., 1985.
- [6] G. Schaefer, K. H. Schoenbach, H. Krompholz, M. Kristiansen, and A. H. Guenther, "The Use of Attachers in Electron Beam Sustained Discharge Switches - Theoretical Considerations," Laser and Particle Beams, vol. 2, pp. 273 - 291, 1984.
- [7] G. Schaefer, P. F. Williams, K. H. Schoenbach, and J. T. Mosley, "Photodetachment as a Control Mechanism for Diffuse Discharge Switches," IEEE Trans. Plasma Sci., vol. PS-11, pp. 263-265, Dec. 1983.
- [8] M. J. Rossi, H. Helm, and D. C. Lorents, "Photoenhanced Electron Attachment of Vinylchloride and Trifluoroethylene at 193 nm," Appl. Phys. Lett., submitted 1985.
- [9] J. N. Bardsley and J. M. Wadehra, private communication, 1982.
- [10] I. M. Beterov and N. V. Fatayev, "Optogalvanic Demonstration of State-to-State Dissociative Electron Capture Rate in  $\text{I}_2$ ," Opt. Comm., vol. 40, pp. 425-429, Feb. 1982.
- [11] J. J. Tsee and C. Wittig, "Optically Pumped Molecular Lasers in the 11-17 micron Region," J. Appl. Phys., vol. 49, pp. 61-64, Jan. 1978.
- [12] E. R. Sirkin, and G. C. Pimentel, "HF Rotational Laser Emission Through Photoelimination from Vinyl Fluoride and 1, 1-Difluoroethene," J. Chem. Phys., vol. 75, pp. 604-612, July 1981.
- [13] G. Schaefer, K. H. Schoenbach, and P. F. Williams, to be published.

## 54th IEEE PULSED POWER CONFERENCE

## AN E-BEAM CONTROLLED DIFFUSE DISCHARGE SWITCH

K. H. Schoenbach, G. Schaefer, M. Kristiansen,  
H. Krompholz, D. Skaggs and E. Strickland  
Texas Tech University, Department of Electrical Engineering/Computer Science  
Lubbock, Texas 79409

**Abstract:** The control efficiency and the response time of electron-beam controlled diffuse discharges is to a large extent determined by atomic and molecular properties of the switch gas composition. An e-beam tetrode was used to study switch gas properties for submicrosecond opening switches. Electrical measurements were performed with various switch gas mixtures containing small amounts of electronegative gases. Of particular interest were mixtures of  $\text{N}_2\text{O}:\text{N}_2$  and  $\text{C}_2\text{F}_6:\text{Ar}$ . In both gas mixtures the resistivity increases with electric field strength. This effect is particularly strong in a mixture of 2%  $\text{C}_2\text{F}_6$  in 1 atm Ar, where an increase of 25 was obtained in a reduced field strength range of  $1 \text{ Td} < E/N < 20 \text{ Td}$ . The current decay times or opening times with this mixture were below 100 ns. Optical time resolved investigations of discharges in  $\text{C}_2\text{F}_6:\text{Ar}$  showed the occurrence of striations which were perpendicular to the discharge axis. These luminous layers in the discharge can be explained as domain formations similar to those observed in direct semiconductors as e.g. the Gunn-effect in GaAs.

Introduction

Electron-beam controlled diffuse discharges can be used as fast, repetitively operated closing and opening switches. The concept is as follows: The gas between the electrodes conducts when the ionizing e-beam is injected and the switch closes. The switch voltage remains below the self-breakdown voltage, so that avalanche ionization is negligible. Thus the discharge is completely sustained by the e-beam. When the e-beam is turned off, electron attachment and recombination processes in the gas cause the conductivity to decrease and the switch opens.

In order to achieve opening times of less than a microsecond at initial electron densities of  $n_e < 10^{14} \text{ cm}^{-3}$ , the dominant loss must be attachment. That means that the switch gas mixture must contain an electronegative gas which, however, lowers the efficiency of the switch. It causes a reduction of the current gain (switch current/e-beam current) proportional to the opening time. If the switch is part of an inductive energy circuit, both high current gain and fast opening can be obtained by choosing gas mixtures which satisfies the conditions [1,2,3]:

- For low values of the reduced field strength  $E/N$  (conduction phase) the gas mixture should have a high drift velocity  $v_d$  and low attachment rate  $k_a$ .
- For high  $E/N$  values (opening phase) the gas mixture should have lower drift velocities and high attachment rate coefficients.

Experimental Setup

For the investigation of e-beam controlled conductivity in a high pressure gas mixture with properties as discussed above, a discharge system was constructed with an e-beam tetrode as control element [4]. A schematic cross-section of the tetrode and the discharge chamber is shown in Fig. 1. The e-beam cathode is located in the Pyrex cylinder between the two plates of a stripline and consists of an

electrically heated array of thoriated tungsten filaments. At a filament temperature of 2100 K, the e-beam current density is about  $4 \text{ A/cm}^2$  over the  $100 \text{ cm}^2$  cross-sectional area of the beam. The temporal structure of the e-beam is controlled by means of a control grid which allows the generation of a pulse train with pulse duration and pulse separation in the 100 ns time range. For some investigations the e-beam was operated as a cold cathode system, which provided e-beam current pulses of 15 A with a pulse duration of ~400 ns.

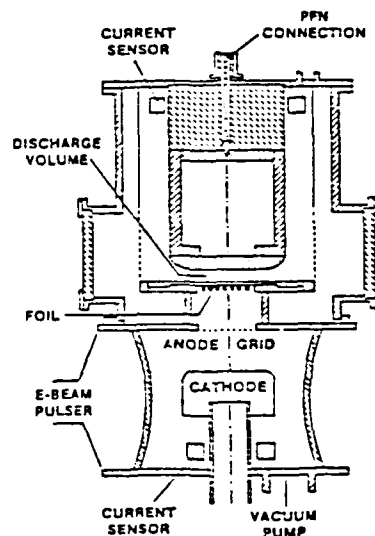


Fig. 1. Cross Section of E-Beam Tetrode and Switch Chamber.

The e-beam voltage is applied to the anode by a two-stage Marx generator, which delivers a maximum voltage of 250 kV with a 5 ns risetime and with an exponential decay time constant of about 2.5 microseconds into a 300 Ohm load. After passing through a 25  $\mu\text{m}$  titanium foil and a 12.5  $\mu\text{m}$  aluminum foil, which serves as an electrode in the diffuse discharge switch, the e-beam generates a diffuse plasma between the electrodes in the stainless steel discharge chamber. The current through the plasma is provided by a 2 Ohm pulse forming network.

Measurements of the e-beam current and the switch current were performed by means of transmission line current transformers [5]. Voltages were measured with fast resistive voltage dividers. In order to get information on the spatial structure of the discharge an image converter camera was built [6] using an ITT image converter diode type F4109. The camera has a high sensitivity of 225  $\mu\text{A/m}$  and a high spatial resolution of 45  $\mu\text{p/mm}$ . The shutter time was about 10 ns.

### Experimental Results

Diffuse discharge experiments were performed in  $N_2O$ ,  $SO_2$ , and  $CO_2$  with  $N_2$  as buffer gas, and  $C_2F_6$  in Ar. The source term, the number of electrons produced per  $cm^3$  second, was in the range of  $10^{20} cm^{-3}s^{-1}$  to  $10^{21} cm^{-3}s^{-1}$ . The voltage applied at the PFN was varied between 100 Volts and 20 kV. The switch electrode gap was kept constant at 3.5 cm. Most of the measurements were performed with the  $N_2O:N_2$  gas mixture. This gas combination was for one expected to satisfy the conditions for switch gases nicely (see introduction) and secondly it allowed modeling of the diffuse discharge [7], since a complete set of cross sections is available for  $N_2$  [8] and the plasma chemistry in a mixture of  $N_2$  and  $N_2O$  appeared to be relatively simple.

Figure 2 shows the influence of the attacher concentration ( $N_2O$ ) on the opening time. For high  $N_2O$  concentrations (3 %) the switch current replicates the e-beam current, except for the tail. The tail is caused by the current carried by positive and negative ions. The current gain is about 2 for this attacher concentration. For concentrations of .7 % the fall time ( $1/e$  -time) increases to approximately 100 ns. For .1 % it is in the order of 500 ns. The gain increases to values of 9 and 12, respectively.

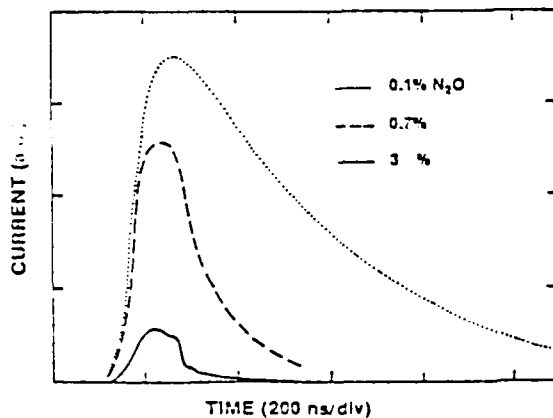


Fig. 2. Normalized Switch Current for Different Attacher Concentrations. Demonstrating the Strong Effect of the Attacher on the Current Decay (Opening Time).

Figure 3 shows the experimentally obtained current density ( $j$ ) values (dots) versus reduced field strength  $E/N$  for the e-beam sustained discharge under steady state conditions in 1 atm  $N_2$  with .7%  $N_2O$ . The curve represents calculated values [9] which were critically depending on available attachment rate coefficients or cross sections [10,11,12]. The good coincidence between model and experiment was obtained with attachment cross sections measured by Chantry [12].

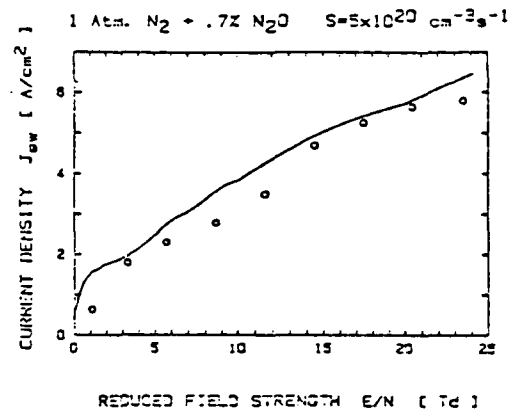


Fig. 3. Current Density  $j$  versus Reduced Field Strength  $E/N$  for a Discharge in  $N_2O:N_2$  (Calculated Curve and Experimental Data Points).

In Fig. 4 the experimental and theoretical data are plotted in a resistivity  $\rho_0$  versus  $E/N$  diagram. The desired opening switch effect, an increase in resistivity with increasing electric field, is obtained with the  $N_2O:N_2$  gas mixture. However, the increase is moderate: about 2.5 over a field strength

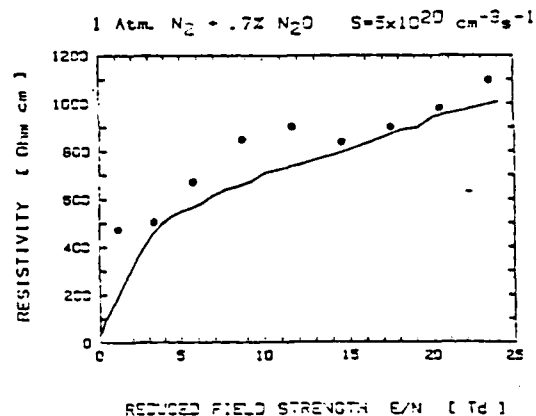


Fig. 4. Discharge Resistivity  $\rho_0$  versus  $E/N$  for a Discharge in  $N_2O:N_2$  (Calculated Curve and Experimental Data Points.)

range of 25 Td. The strong deviation of the lowest experimental value from the computed curve is probably due to the fact that the cathode fall was not included in our model. Gas combinations of  $SO_2$  and  $CO_2$  with  $N_2$  as buffer gas showed even smaller changes in resistivity at comparable opening times.

A group of very promising gases, what the opening switch conditions concerns (see introduction), were proposed by Christophorou et al., [3]. The total attachment rate constant  $k_a$  is plotted versus mean electron energy  $\epsilon$  in Fig. 5. Measurements performed with the gas mixture of 2 %  $C_2F_6$  in 1 atm Ar as buffer gas gave as a result a very strong increase in resistivity with field strength (Fig. 6). Decay (opening) times for this mixture were below 100 ns. The mixture seems to be relatively stable.

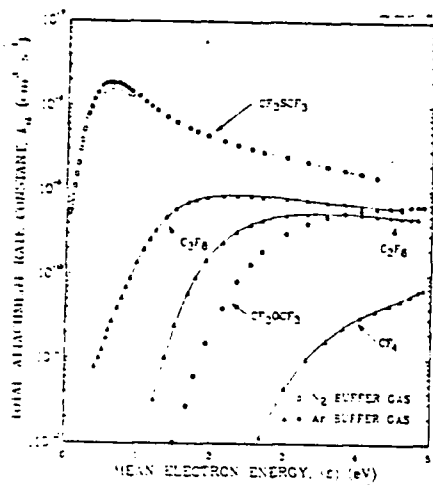


Fig. 5. Gases with Strong Increase of Attachment Rate Coefficient with Electron Energy [13].

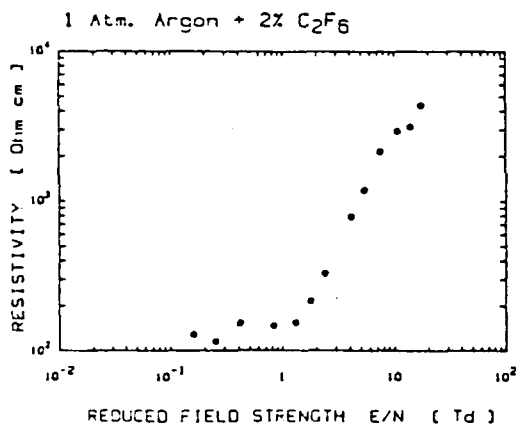


Fig. 6. Discharge Resistivity  $\rho_0$  versus  $E/N$  for a Discharge in  $C_2F_6:Ar$ .

Reproducible results at an e-beam voltage of 150 kV were obtained for 150 shots without changing the gas.

The current density ( $j$ ) versus reduced field strength ( $E/N$ ) curve for this gas mixture is shown in Fig. 7. It contains a region with very pronounced negative differential conductivity (NDC). The effect which causes NDC in externally sustained diffuse discharges containing attachers is due to the increased generation of negative ions, that means

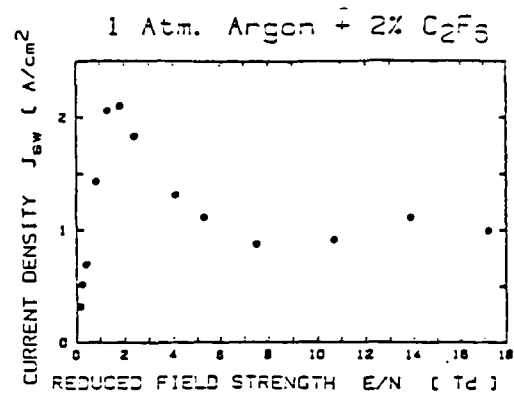


Fig. 7. Current Density  $j$  versus Reduced Field Strength  $E/N$  for a Discharge in  $C_2F_6:Ar$ .

negative charges with increased mass, above a certain electron energy. A similar effect is known and widely applied for high frequency generation and amplification in semiconductors, as e.g. GaAs [14]. The negative differential conductivity in semiconductors is caused similarly as in diffuse discharges by an increase in the effective mass of the electrons at higher electron energies [15]. The presence of NDC in semiconductors causes homogeneous material to become electrically heterogeneous thus causing high field dipole domains to form and propagate through the semiconductor (Gunn-effect).

The same effect, formation of high field domains, can be expected in externally sustained discharges with gas mixtures such as  $C_2F_6$  in Ar. In order to prove this, the discharge was optically recorded by means of an image converter camera with a shutter time of 10 ns. Figure 8a shows side-on photographs of the discharge at different times after e-beam turn-on, Fig. 8b the corresponding photometer curves along the discharge axis. The discharge was biased so that the point of operation was in the NDC-region of the  $j$ - $E/N$  characteristic (Fig. 7). The pictures show clearly the development of a highly luminous layer in the cathode region of the discharge. Its profile is dependent on the bias voltage; for bias points on the left hand side of the current density maximum the discharge appears homogeneous.

We consider the region of high luminosity as a high field domain, a region of enhanced energy dissipation, similar to the ones observed in semiconductors. The reduction in the width of these structures can be explained by the more than linear increase in the attachment rate coefficient in the NDC-region. A propagation of the high field domains in anode direction could not be observed. The reasons are the shot-to-shot variations in the structure which did not allow exact timing and the expected relatively slow motion of the layer ( $v = 10^2 - 10^3$  cm/s).

The development of high field domains has probably little effect on the opening switch behavior of an e-beam controlled discharge; however, it may lead to more applications for these type of discharges. The analogy to the Gunn effect in GaAs points to the initiation of e-beam sustained discharges as high power, high frequency oscillators and amplifiers. Preliminary calculations indicate power levels of  $> 100$  kW at frequencies  $< 1$  GHz.



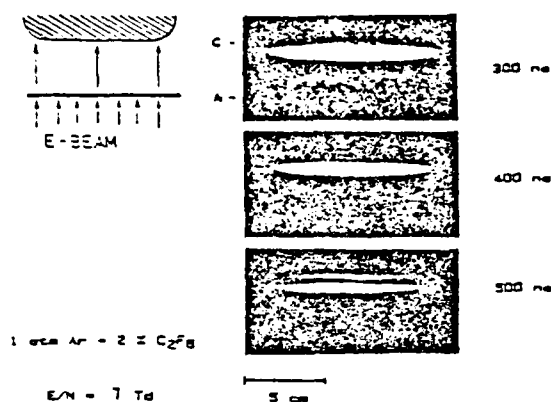


Fig. 8a Temporal Development of Striations in the E/N Range with Negative Differential Conductivity.

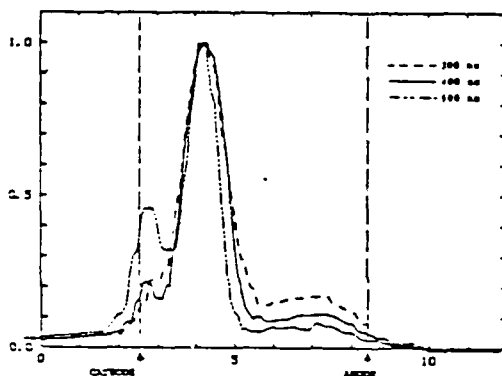


Fig. 8b. Photometer Curves of the Discharge Along the Discharge Axis.

#### Summary

Different gas mixtures were tested for their use in diffuse discharge opening switches. Results were obtained with a mixture of  $C_2F_6$  and Ar as buffer gas. For a mixture of 2%  $C_2F_6$  in 1 atm Ar opening times of less than 100 ns were measured. The increase in resistivity was almost two orders of magnitude in a field strength range up to 25 Td. The current gain for this gas combination at a pressure of 5 atm and e-beam energies of 165 keV would be about 100. The current density-reduced field strength characteristic of the e-beam controlled discharge in  $C_2F_6$ :Ar has a distinct region with negative differential conductivity. This effect causes the formation of luminous striations in the discharge. The analogy between this type of discharge and semiconductors, which exhibit NDC, might lead to applications for externally sustained diffuse discharges as high power oscillators and amplifiers.

#### Acknowledgement

This work was supported by Army Research Office and Air Force Office of Scientific Research.

#### REFERENCES

- [1] K.H. Schoenbach, G. Schaefer, E.E. Kunhardt, L.L. Hatfield, and A.H. Guenther, "An Optically Controlled Diffuse Discharge Switch", in Proc. 3rd IEEE Int. Pulsed Power Conf. (Albuquerque, NM, 1981), p. 142 (IEEE Catalog 81CH1662-6).
- [2] K.H. Schoenbach, G. Schaefer, M. Kristiansen, L.L. Hatfield, and A.H. Guenther, "Concepts for Optical Control of Diffuse Discharge Opening Switches", IEEE Trans. Plasma Sci., vol. PS-10, p. 246, 1982.
- [3] L.G. Christophorou, S.R. Hunter, J.G. Carter, and R.A. Mathis, "Gases for Possible Use in Diffuse Discharge Switches", Appl. Phys. Lett., vol. 41, p. 147, 1982.
- [4] C.H. Harjes, K.H. Schoenbach, G. Schaefer, M. Kristiansen, H. Krompholz, and D. Skaggs, "Electron-Beam Tetrode for Multiple, Submicrosecond Pulse Operation", Rev. Sci. Instrum., vol. 55, p. 1684, 1984.
- [5] H. Krompholz, J. Doggett, K.H. Schoenbach, J. Genl, C. Harjes, G. Schaefer, and M. Kristiansen, "Nanosecond Current Probe for High-Voltage Experiments", Rev. Sci. Instrum., vol. 55, p. 127, 1984.
- [6] The image converter camera was designed and built by M. Michel, Technische Hochschule Darmstadt, Germany.
- [7] G. Schaefer, K.H. Schoenbach, H. Krompholz, M. Kristiansen, and A.H. Guenther, "The Use of Attachers in Electron-Beam Sustained Discharge Switches - Theoretical Considerations", Laser and Particle Beams, vol. 2, p. 237, 1984.
- [8] A.V. Phelps, private communication.
- [9] G. Schaefer et al., to be published.
- [10] L.C. Lee, C.C. Chiang, K.Y. Tang, D.L. Huestis, and D.C. Lorents, "Gaseous Electronic Kinetics for E-beam Excitation of  $Cl_2$ , NO, and  $N_2O$  in  $N_2$ ", Second Annual Report on Coord. Res. Program in Pulsed Power Physics, Dept. Electrical Engineering, Texas Tech University, Lubbock, TX (1981).
- [11] L.C. Lee and F. Li, "Shortening of Electron Conduction Pulses by Electron Attachers  $O_2$ ,  $N_2O$ , and  $CF_4$ ", J. Appl. Phys., vol. 56, p. 3169, 1984.
- [12] P.J. Chantry, "Temperature Dependence of Dissociative Attachment in  $N_2O$ ", J. Chem. Phys., vol. 51, p. 3369, 1969.
- [13] L.G. Christophorou, S.R. Hunter, J.G. Carter, S.M. Spyrou, V.K. Lakdawla, "Basic Studies of Gases for Diffuse-Discharge Switching Applications," Proceedings IEEE Pulsed Power Conf., p. 702, 1983.
- [14] J.B. Gunn, "Microwave Oscillations of Current in III-V Semiconductors," Solid State Communications vol. 1, p. 88, 1963.
- [15] B.K. Ridley, and T. B. Watkins, "The Possibility of Negative Resistance Effects in Semiconductors," Proc. Phys. Soc., vol. 78, p. 293 1961 and C. Hilsum, "Transferred Electron Amplifiers and Oscillators," Proc. IEEE, vol. 50, p. 185, 1962.

TO BE SUBMITTED IN JOURNAL OF APPLIED PHYSICS

DRAFT

Domain Instability in an E-beam Controlled Diffuse  
Discharge Switch Exhibiting Negative Differential  
Conductivity

B. E. Strickland,<sup>a)</sup> K. H. Schoenbach,<sup>b)</sup> G. Schaefer,<sup>c)</sup>  
O. Ishihara, M. Kristiansen, and R. A. Korzekwa.  
Department of Electrical Engineering  
Texas Tech University, Lubbock, Texas 79409

ABSTRACT - In externally sustained diffuse discharges in gas mixtures containing admixtures of electronegative gases, the discharge characteristic (current density versus reduced field strength) exhibits negative differential conductivity (NDC) depending on the source function and the concentration of the attacher. In discharges exhibiting NDC, electron depleted domains of high field intensity are formed in the discharge.

This paper presents the results of electrical and optical measurements performed on an e-beam sustained diffuse discharge in gas mixtures of Argon and  $C_2F_6$  at 1 atm. The steady state current density versus reduced field strength exhibits a strong negative differential conductivity in the  $E/N$  range of  $2.5 \text{ Td} < E/N < 5 \text{ Td}$ . Time resolved photographs of the discharge taken in

this E/N range show luminous layers perpendicular to the discharge axis. These experimental results are compared with numerical predictions.

---

Present address:

- a) Maxwell Laboratories Inc., San Diego, CA 92123
- b) Old Dominion University, Norfolk, VA 23508
- c) Polytechnic Institute of New York,  
Farmingdale, NY 11735

## INTRODUCTION

In recent years interest has grown in the use of inductive energy storage devices in pulsed power systems because inductive devices have intrinsically higher energy densities than capacitors. In order to use an inductive energy storage device in a pulsed power system, an opening switch is required to transfer the energy from the inductor to the load. In order to use it in a repetitive pulsed power system, the opening switch should have the ability to perform in a controlled repetitive mode of operation. Furthermore, it is desirable for the switch to have a high current carrying ability (kA), a high voltage stand off capability (kV), low losses in the conduction phase, and a long lifetime. Electron-beam controlled diffuse discharges show promise for use as repetitively operated switches in inductive energy storage systems.

In order for a diffuse discharge switch to have the previously mentioned properties, it is necessary to properly engineer the gas mixture used in the switch. To obtain low losses in the conduction phase, it is necessary that the gas has a high electron mobility and a low electron loss rate at low reduced field strength ( $E/N$ ) which corresponds to the conduction phase. Furthermore, to improve the opening and stand off capabilities of the switch, it is desirable to have a gas with a low electron mobility and a high attachment rate at higher values of  $E/N$  which correspond to the opening and hold off phases. For the switch to achieve fast opening times, electronegative gases or attachers must be used in the switch gas mixture. To satisfy the conditions previously mentioned, it has been suggested to use attachers that have a low attachment rate at low  $E/N$  and a high attachment rate at high  $E/N$  [1]. The use of such

attachers in e-beam controlled diffuse discharge switches and their effect on the current-voltage (I-V) characteristics of the switch has been theoretically investigated by Schaefer, et al. [1]. The results show that a switch which utilizes attachers with a strongly increasing attachment rate as a function of  $E/N$  will have an I-V characteristic which exhibits negative differential conductivity (NDC) depending on the magnitude and energy of the ionization source and the concentration of attacher.

Negative differential conductivity is also a characteristic of semiconductors exhibiting the Gunn Effect. There, isolated domains with high electric field intensity propagate across the semiconductor material [2]. Therefore, it is of interest to determine if the domains present in a diffuse discharge [3, 4, 5, 6] which exhibits NDC have the same properties as the domains in semiconductors.

#### ELECTRICAL INVESTIGATIONS

In order to study electron-beam controlled conductivity in a high pressure diffuse discharge containing small amounts of electronegative gases, a repetitive electron-beam controlled diffuse discharge switch experiment has been constructed and used to investigate promising gases for opening switches [7].

The e-beam system consists of an e-beam gun inside of a Pyrex chamber that is located between the two parallel plates of the e-beam pulser's transmission line. The stainless steel switch chamber is located above the e-beam system as shown in Fig. 1.

The e-beam gun is a tetrode that consists of a dispenser cathode, a control grid, a screen grid, and the anode. The electron source or cathode is a  $BaO_2$

dispenser cathode capable of emitting  $4 \text{ A/cm}^2$  uniformly over the  $100 \text{ cm}^2$  area of the cathode at a temperature of 950 K. The temporal structure of the e-beam is controlled by a control grid that is driven by a transmission line pulser capable of generating a pulse train with a variable pulse duration and separation. In addition, a d.c. biased screen grid shields the control grid from the effects of induced voltage by the anode or e-beam pulser.

The e-beam pulser consists of a two-stage Marx generator that is capable of delivering a maximum output voltage of 250 kV with a risetime of 5 ns and a decay time of 2.5  $\mu\text{s}$  into a 300 ohm load.

The diffuse discharge is generated in a stainless steel chamber that has been tested up to 4 atmospheres. A 25  $\mu\text{m}$  titanium foil serves as the interface between the high pressure switch chamber and the high vacuum e-beam chamber. A 12  $\mu\text{m}$  aluminum foil functions as the lower electrode while the upper electrode is made of stainless steel. A 2-ohm pulse forming network with a maximum output voltage of 60 kV supplies the current through the discharge plasma.

Transmission line current transformers [8,9] and fast resistive current probes were used to measure the e-beam current and switch current, respectively. Fast resistive voltage dividers were utilized as voltage probes.

While operating the e-beam gun as a cold cathode diode, which relies only on field emission for electron production, electrical investigations were performed on a high pressure diffuse discharge in a gas mixture of 2%  $\text{C}_2\text{F}_6$  in 1 atm Argon which is a promising switch gas candidate [10]. The impedance of the switch system was held constant at 4 ohms. In the cold cathode diode mode, the source function, which is the number of electrons produced per  $\text{cm}^3$  second, was in the range of

$2-3 \times 10^{19} \text{cm}^{-3} \text{s}^{-1}$ . The electrode gap spacing was maintained at a constant 3.9 cm while the applied voltage was varied from 0 to 15 kV.

The steady state current density ( $J$ ) versus reduced field strength ( $E/N$ ) characteristic for a gas mixture of 2%  $\text{C}_2\text{F}_6$  in 1 atm Ar is shown in Fig. 2. This characteristic contains a pronounced negative differential conductivity (NDC) in the reduced field strength range of  $2.5 \text{ Td} < E/N < 5 \text{ Td}$  where the attachment rate for this gas mixture increases strongly with  $E/N$ .

It has been discussed before that gas mixtures of Argon and a molecular gas such as Nitrogen exhibit a drift velocity with maximum at low values of  $E/N$  [11, 12, 13]. Such gas mixtures can generate a negative differential conductivity without the use of any attachers. Therefore, we performed experiments in Argon with 2% and 5% Nitrogen. A comparison of the  $J$  versus  $E/N$  characteristics is shown in Fig. 3. No negative differential conductivity was observed with Nitrogen admixtures in the range of 2-5%. Also, in previous experiments performed under the same conditions using various mixtures with attachers such as  $\text{CO}_2$ ,  $\text{SO}_2$ , or  $\text{N}_2\text{O}$  in 1 atm  $\text{N}_2$ , the steady state  $J$  versus  $E/N$  characteristic did not yield a region of NDC [14, 15]. In order to obtain a high pressure diffuse discharge whose steady state  $J$  versus  $E/N$  exhibits a strong NDC characteristic, it is necessary to use a gas mixture with an attachment rate that increases strongly with  $E/N$  such as  $\text{C}_2\text{F}_6:\text{Ar}$  and  $\text{C}_3\text{F}_8:\text{Ar}$  mixtures [16].

#### OPTICAL INVESTIGATIONS

The formation of high field domains can be expected in e-beam sustained diffuse discharges that exhibit a NDC characteristic [3, 4, 5, 6, 16, 17, 18, 19]. It can

be expected that in regions of high field intensity, the number of excited atoms or molecules is increased causing an increased level of emission processes. In order to investigate the possible formation of such domains in our discharge, time resolved photographs were taken at various times during the discharge while using various bias conditions.

Time resolved photographs of discharges were taken using a high speed, high resolution image converter camera that consisted of a proximity focusing diode manufactured by ITT with a Tektronix roll film back mounted on the rear of the diode [20]. A krytron switched, Blumlein pulser was used to deliver a 10 kV, 10 ns rectangular pulse to the diode; consequently, the camera has a shutter speed of 10 ns. The diode has a resolution of 45 lp/mm. Optical investigations were performed on discharges containing gas mixtures of 2%  $C_2F_6:Ar$  and 5%  $N_2:Ar$ .

The diffuse discharge containing 2%  $C_2F_6:Ar$  was investigated in three operation regions: the region of positive differential conductivity, (PDC), corresponding to the  $E/N$  range of  $0 \text{ Td} < E/N < 2.5 \text{ Td}$  as shown in Fig. 2; the region of negative differential conductivity, (NDC), corresponding to the  $E/N$  range of  $2.5 \text{ Td} < E/N < 5 \text{ Td}$ ; and the region of approximately zero differential conductivity, (ZDC), corresponding to the  $E/N$  range  $5 \text{ Td} < E/N < 12 \text{ Td}$ .

A time resolved photograph of the discharge biased at 2 Td so that it would operate in the PDC region is shown in Fig. 4a. This photograph at a time of 400 ns illustrates that the discharge is homogeneous or has no field domains other than the cathode fall for bias points to the left of the current density maximum. Furthermore, the discharge was homogeneous throughout the duration of the 500 ns discharge current pulse.



With the discharge biased at 5 Td so that it would operate in the region of NDC, time resolved photographs were taken at 100 ns intervals throughout the duration of the discharge current. Figure 4b illustrates the discharge at a time of 400 ns. At any point of operation in this region, the discharge is not homogeneous. This photograph shows a distinct luminous layer perpendicular to the discharge axis.

Time resolved pictures of the discharge biased at 9 Td so that it would operate in the ZDC region of the attachment dominated stage of operation were taken which illustrated the occurrence of striations similar to those observed in the NDC region.

In order to obtain qualitative information about the position of these luminous layers or striations as a function of time, photodensitometer plots were made from the negative of each photograph. The normalized photodensitometer plots along the discharge axis corresponding to the photographs taken at 9 Td are shown in Fig. 5.

These results show that the domain forms at the cathode and propagates toward the anode with a constant shape and velocity  $V_D = 1.95 \times 10^6$  cm/sec. The domain velocity is approximately equal to the electron drift velocity as predicted by Douglas-Hamilton [19]. Similar results were obtained for any bias point in the attachment dominated stage of discharge operation. As predicted by Barkalov and Gladush [3] the domain velocity is independent of applied voltage while the amplitude and width of the domain is proportional to the applied field.

From the photographs shown, it is evident that the shape and position of the striations vary with applied voltage. Therefore, discharges were photographed at a constant time of 400 ns throughout the E/N range of  $2 \text{ Td} < E/N < 12 \text{ Td}$ . The position of the striation with

respect to the anode as a function of applied voltage is shown in Fig. 6.

Time resolved photographs were also taken of a discharge containing a mixture of 5% N<sub>2</sub> in 1 atm Ar. These pictures revealed a homogeneous discharge like that shown in Fig. 4a for the gas mixture of 2% C<sub>2</sub>F<sub>6</sub> in 1 atm Ar in the positive differential conductivity region.

#### MODEL

The spatial dependence of a diffuse discharge can be described by the space dependent one dimensional continuity equations

$$\begin{aligned} \frac{\partial n_e}{\partial t} + \frac{\partial}{\partial x} \mu_e n_e E = S + k_i N_a n_e \\ - k_a N_a n_e - \beta_{ei} n_e n_+ \end{aligned} \quad (1)$$

$$\begin{aligned} \frac{\partial n_+}{\partial t} - \frac{\partial}{\partial x} \mu_+ n_+ E = S + k_i N_a n_e \\ - \beta_{ii} n_+ n_- - \beta_{ei} n_e n_+ \end{aligned} \quad (2)$$

$$\begin{aligned} \frac{\partial n_-}{\partial t} + \frac{\partial}{\partial x} \mu_- n_- E = k_a N_a n_e \\ - \beta_{ii} n_+ n_- \end{aligned} \quad (3)$$

and Poisson's equation

$$\frac{\partial E}{\partial x} = \frac{-e}{\epsilon_0} (n_+ - n_- - n_e), \quad E > 0 \quad (4)$$

where  $n_e, n_-$ , and  $n_+$  are the densities of electrons, negative ions, and positive ions;  $\mu_e, \mu_-$ , and  $\mu_+$  are the corresponding mobilities;  $S$ , the source function, is the rate at which electrons are produced by the external source;  $B_{ei}$  and  $B_{ii}$  are the electron-ion and ion-ion recombination rate coefficients respectively; and  $e$  is the charge of an electron. We must adjoin to the system of equations (1)-(4) the boundary conditions at the electrode surfaces and the equations governing the external circuit. The boundary conditions are

$$\mu_e n_e(0, t) = \gamma \mu_+ n_+(0, t),$$

$$n_-(0, t) = 0$$

and

$$n_+(L, t) = 0$$

where  $\gamma$  is the secondary-emission coefficient at the cathode. The equations governing the external circuit are

$$j(t) = \frac{e}{L} \int_0^L (\mu_e n_e + \mu_+ n_+ + \mu_- n_-) E dx$$

and

$$\int_0^L E dx = U_0 = \text{constant}$$

where  $U_0$  is the supply voltage and  $L$  is the interelectrode gap length.

In order to investigate the formation of domains in a diffuse discharge of interest for pumping CO<sub>2</sub> lasers,

Barkalov and Gladush [3] solved the mathematical model previously discussed for a discharge containing a mixture of  $N_2+O_2$  which exhibited NDC.

When a voltage  $U_0$  was applied to the discharge which corresponded to the electric field  $E$  in the  $E/N$  range of where the discharge is attachment dominated, a domain formed completely at the cathode and moved with constant velocity, amplitude, and shape along the interelectrode gap as shown in Fig. 7. The sloping line of Fig. 7 (a-c) indicates that the domain moves at a constant velocity,  $V_0 = 6 \times 10^5$  cm/sec. Upon reaching the anode, the domain merges with the anode. The voltage released by the merging process is redistributed between a new domain growing at the cathode and the discharge column as shown in Fig. 7d. This merging process causes the current in the external circuit to increase until the new domain is completely formed at the cathode. The new domain picks off voltage from the discharge column which causes the current to fall to its minimum value. The current remains constant while the domain is moving along the interelectrode gap.

These calculations revealed that as the applied voltage was further increased there was a proportional increase in the width of the domain as shown in Fig. 7b. Furthermore, the domain velocity was independent of applied voltage. Since the domain width increases with increasing voltage, the period of the current oscillation becomes smaller with increasing voltage [3].

By implementing the implicit finite difference methods to numerically solve the system of equations (1)-(4), the results of Barkalov and Gladush have been reproduced.

This computer code has been modified to solve the system of equations (1)-(4) for a discharge in a gas mixture of 2%  $C_2F_6$  in Ar at a total pressure of 1 atm.

The basic gas data for this gas mixture were obtained from Christophourou et al [10].

## CONCLUSIONS

E-beam controlled diffuse discharges used as fast opening switches are operated in gas mixtures containing small additives of electronegative gases. Attachers which have a strongly increasing attachment rate will cause the discharge to exhibit a NDC characteristic depending on the magnitude of the source function and the concentration of attacher gas. Gas mixtures which cause a NDC characteristic in an intermediate E/N range are most suitable for diffuse discharge opening switches which are operated in a single shot mode where the inductor is recharged after each shot.

If an e-beam sustained diffuse discharge which exhibits NDC is operated in a range of E/N where the discharge is attachment dominated, moving domains of high field intensity will be formed in the discharge. The velocity of these domains is independent of applied voltage while the amplitude and shape are proportional to the applied field. Current and voltage oscillations can be expected in applications where the discharge conducts longer than the transit time of a domain moving across the discharge. This might make it possible to use such discharges as high power oscillators.

## ACKNOWLEDGMENT

This work was jointly supported by AFOSR and ARO under contract AFOSR 84-0032.

## REFERENCES

1. Schaefer, G., Schoenbach, K., Krompholz, H., and Kristiansen, M., Guenther, A., "The use of attachers in electron-beam sustained discharge switches - theoretical considerations," *Laser and Particle Beams*, Vol. 2, pp. 273-291, (1984).
2. Bar-Lev, A., Semiconductors and Electronic Devices, Englewood Cliffs: Prentice-Hall Inc., pp. 329-334, (1979).
3. Barkalov, A. D., and Gladush, G. G., "Domain Instability of a Non-self-sustaining Discharge in Electronegative Gases," Translated from *Teplofizika Vysokikh Temperatur*, Vol. 20, pp. 19-24, (1982).
4. Barkalov, A. D., and Gladush, G. G., "Domain Instability in a Non-Self-Sustaining Discharge in Electronegative Gases," Translated from *Teplofizika Vysokikh Temperatur*, Vol. 20, pp. 201-206, (1982).
5. Barkalov, A. D., and Gladush, G. G., "Spontaneous oscillations in a discharge in an electronegative gas," *Sov. Phys. Tech. Phys.*, Vol. 24, pp. 1203-1206, (1979).
6. Bekefi, G., Editor, Principles of Laser Plasmas, New York: John Wiley and Sons, p. 283, (1976).
7. Harges, C. H., Schoenbach, K. H., Schaefer, G., Kristiansen, M., Krompholz, H., and Skaggs, D., "Electron-Beam Tetrode For Multiple, Submicrosecond Pulse Operation," *Rev. Sci. Instrum.*, Vol. 55, pp. 1684-1686, (1984).
8. Krompholz, H., Doggett, J., Schoenbach, K. H., Gahl, J., Harges, C., Schaefer, G., and Kristiansen, M., "Nanosecond Current Probe for High-Voltage Experiments," *Rev. Sci. Instrum.*, Vol. 55, pp. 127-128, (1984).
9. Krompholz, H., Schoenbach, K., and Schaefer, G., "Transmission Line Current Sensor," *Proc. IMTC-IEEE Instrum. and Meas. Tech. Conf.*, pp. 224-227, (1985).
10. Christophourou, L., Hunter, S., Carter, J., Spyrou, S., and Lakdawla, V., "Basic Studies of Gases for Diffuse Discharge Switching Applications," U. S. - F.R.G. Joint Seminar on Externally Controlled Diffuse Discharges, pp. 103-132, (1983).

11. Long, W. H., Jr., Bailey, W. F., and Garscadden, A., "Electron drift velocities in molecular-gas-rare-gas mixtures," *Phys. Rev.*, Vol. A-13, pp. 471-475, (1976).
12. Haddad, G. N., "Drift Velocities of Electrons in Nitrogen-Argon Mixtures," *Aust. J. Phys.*, Vol. 36, pp. 297-303, (1983).
13. Petrovic', Z. Lj., Crompton, R. W., and Haddad, G. N., "Model Calculations of Negative Differential Conductivity in Gases," *Aust. J. Phys.*, Vol. 37, pp. 23-24, (1984).
14. Schoenbach, K. H., Schaefer, G., Kristiansen, M., Krompholz, H., Harjes, H. C., and Skaggs, D., "An electron-beam controlled diffuse discharge switch," *J. Appl. Phys.*, Vol. 57, pp. 1618-1622, (1985).
15. Schoenbach, K., Schaefer, G., Kristiansen, M., Krompholz, H., Harjes, H., and Skaggs, D., "Investigations of E-beam Controlled Diffuse Discharges," *Proc. 4th Gaseous Dielectrics Conf.*, pp. 246-253, (1984).
16. Hunter, S. R., Carter, J. G., Christophourou, L. G., and Lakdawala, V. K., "Transport Properties and Dielectric Strengths of Gas Mixtures for use in Diffuse Discharge Opening Switches," *Proc. 4th Gaseous Dielectrics Conf.*, pp. 224-237, (1984).
17. Lopantseva, G. B., Pal', A. F., Persiantsev, I. G., Polusnkin, V. M., Starostin, A. N., Timofeev, M. A., and Treneva, E. G., "Instability of an externally sustained discharge in mixtures of argon with molecular gases," *Sov. J. Plasma Phys.*, Vol. 5, pp. 767-773, (1979).
18. Petrushevich, Yu. V., and Starostin, A. N., "Domain instability in mixtures of inert and molecular gases," *Sov. J. Plasma Phys.*, pp. 463-368, (1981).
19. Douglas-Hamilton, D. H., and Mani, S. A., "Attachment instability in an externally ionized discharge," *J. Appl. Phys.*, Vol. 45, pp. 4406-4415, (1974).
20. The image converter camera was designed and constructed by M. Michel, Technische Hochschule Darmstadt, FRG.

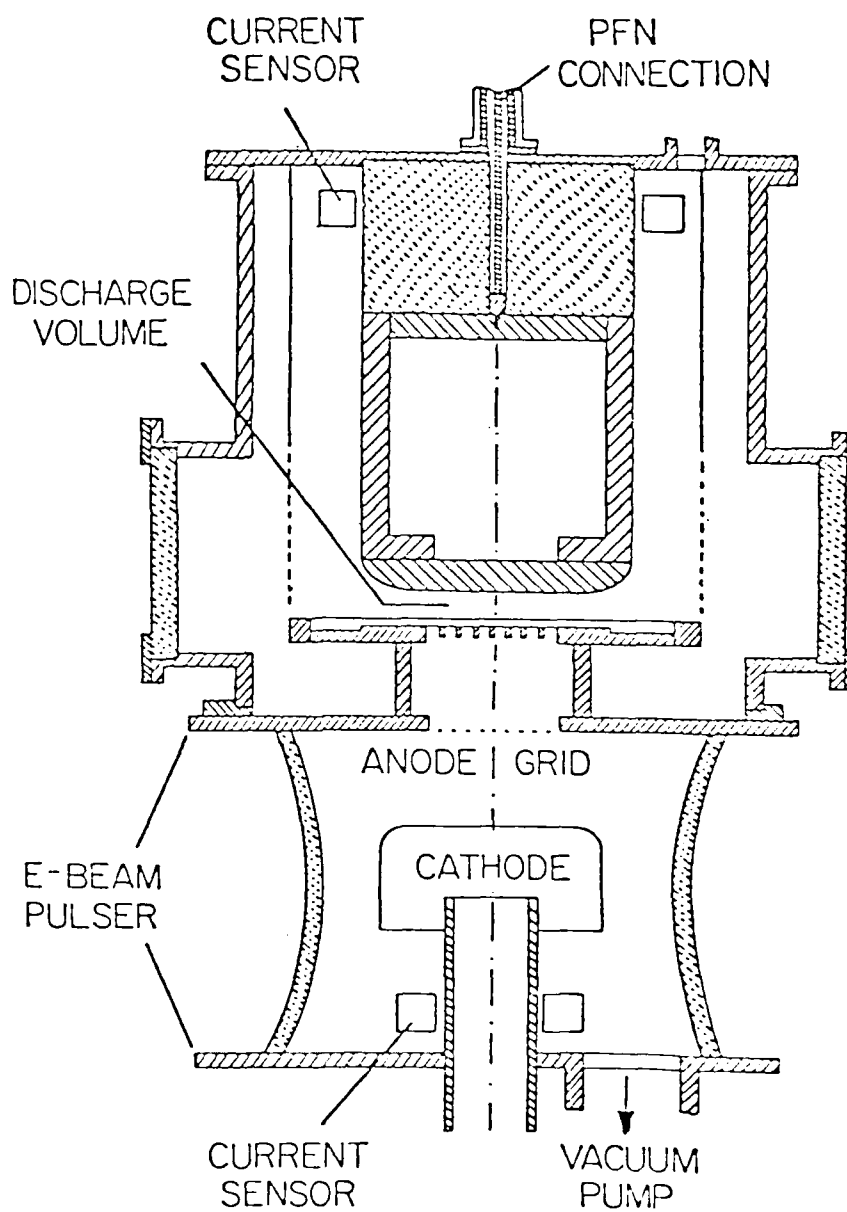


Figure 1 Cross sectional view of e-beam and switch systems.



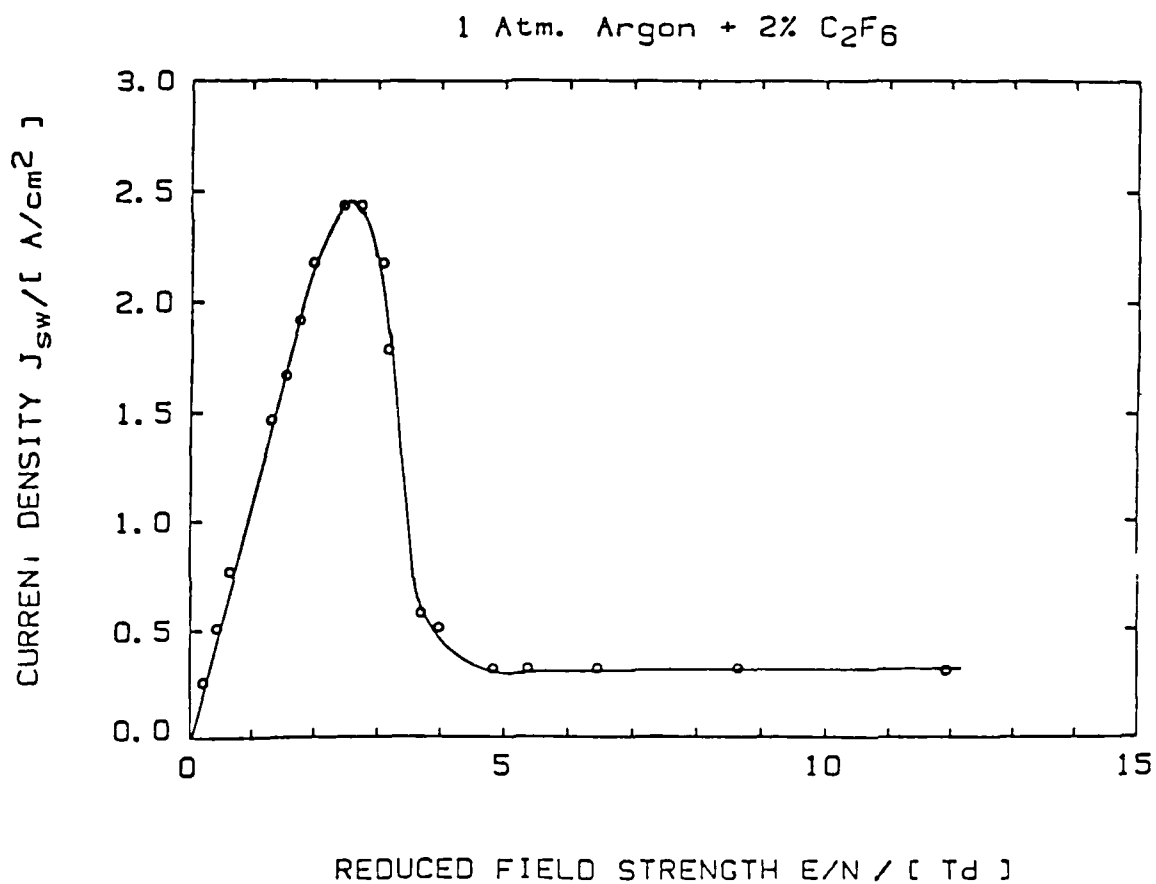


Figure 2 Steady state  $J$  versus  $E/N$  for a discharge in 2% C<sub>2</sub>F<sub>6</sub>:Ar at 1 atm.

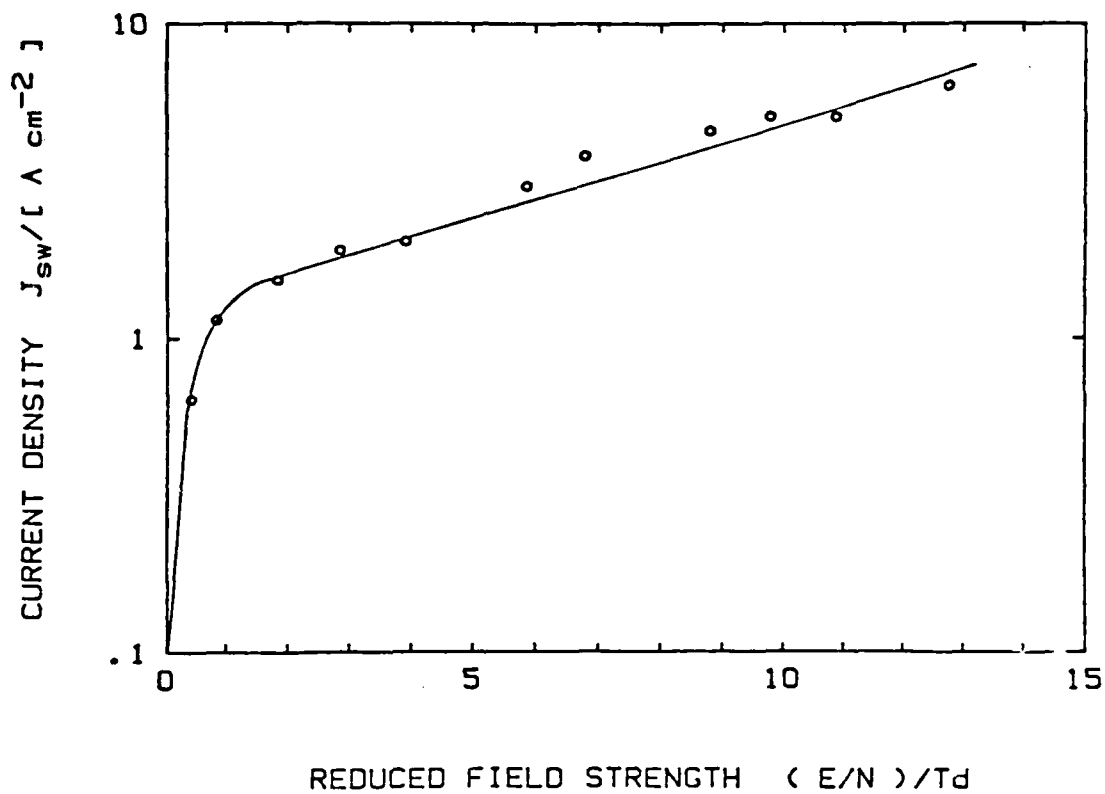
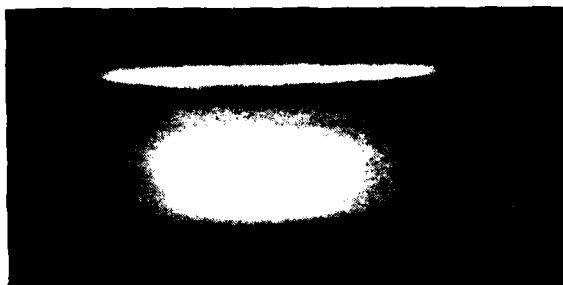


Figure 3 Steady state  $J$  versus  $E/N$  for a discharge in 5%  $N_2$ :Ar at 1 atm.



(a)



(b)

Figure 4 Photograph of discharge taken (a) at 2 Td in the positive differential conductivity region and (b) at 5 Td in the NDC region.

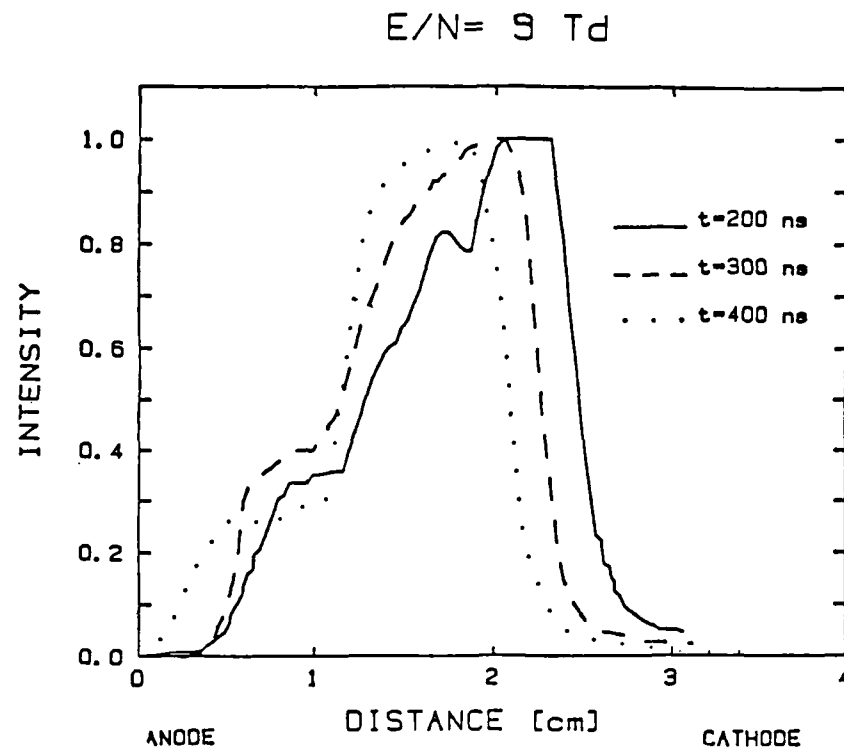


Figure 5 Photodensitometer curves of the discharge along the discharge axis at 9Td

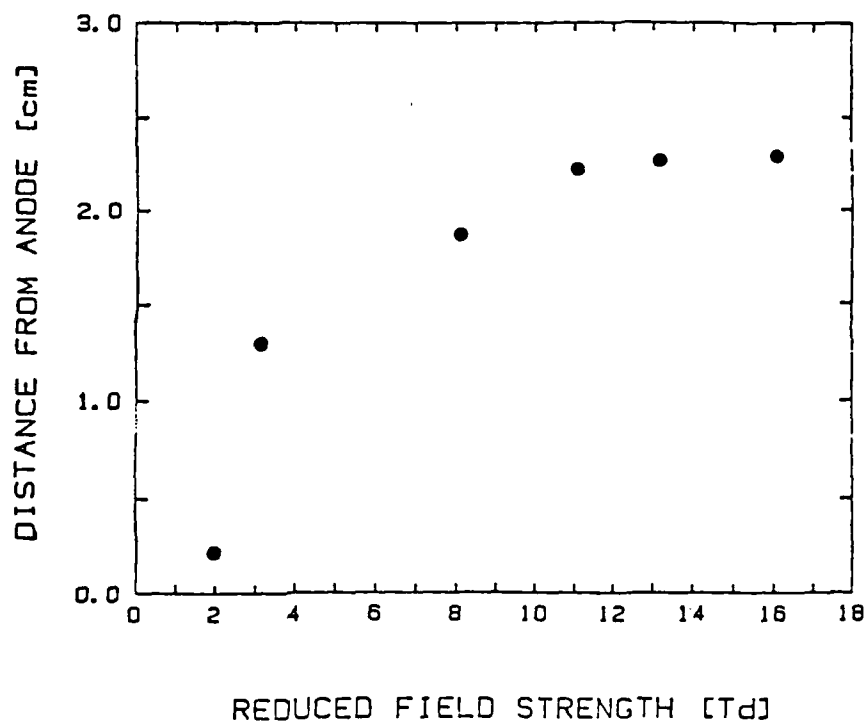


Figure 6 Position of striation as a function of reduced field strength,  $E/N$ .

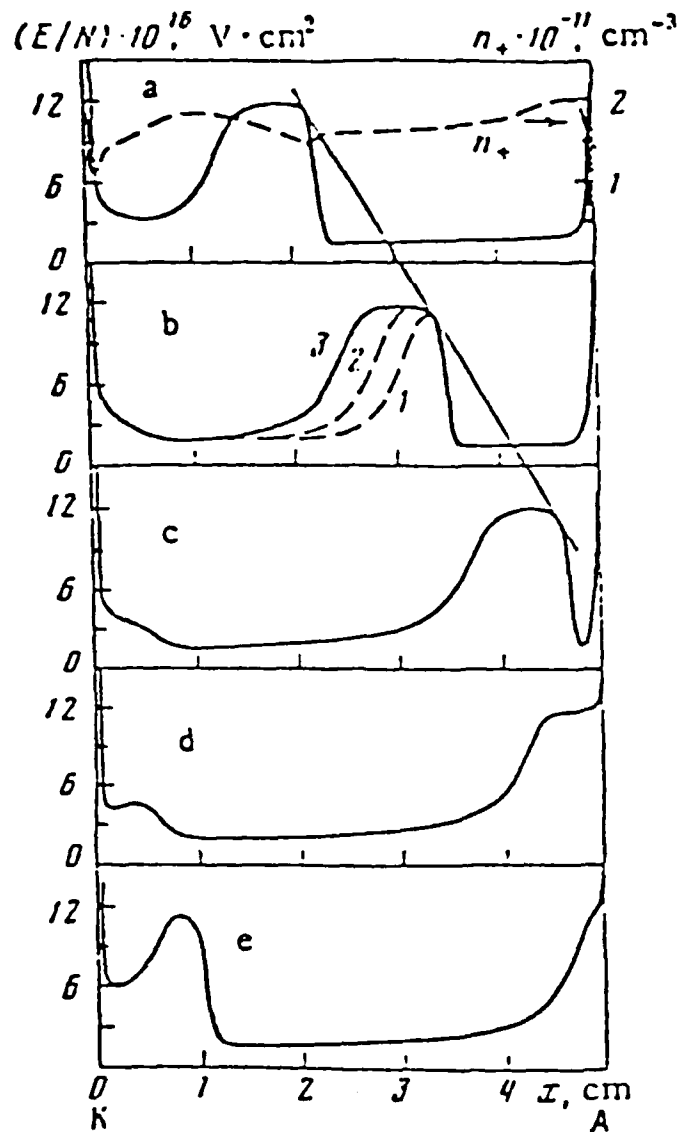


Figure 7. Distribution of  $E/N$  (curves a-e) and  $n_+$  (a) in discharge gap with  $E/N = 4.8 \cdot 10^{-16} \text{ V} \cdot \text{cm}^2$  (Problem 1,  $V_0 = 10^5 \text{ cm/sec}$ ); current density at times: a) 0; b) 2  $\mu\text{sec}$ ; c) 4  $\mu\text{sec}$ ; d) 5  $\mu\text{sec}$ ; e) 6  $\mu\text{sec}$ . [1)  $(E/N) \cdot 10^{16} = 3.3 \text{ V} \cdot \text{cm}^2$ ; 2) 3.9; 3) 4.8]; d) 5; e) 6. These values correspond to the points in Fig. 4c. [3].

To be Submitted to Applied Physics Letters

DRAFT

THE INFLUENCE OF THE CIRCUIT IMPEDANCE ON AN ELECTRON-BEAM  
CONTROLLED DIFFUSE DISCHARGE WITH A NEGATIVE DIFFERENTIAL  
CONDUCTIVITY

G. Schaefer, a) K. H. Schoenbach, b) M. Kristiansen,  
B. E. Strickland, c) R. A. Korzekwa, and G. Z. Hutcheson  
Department of Electrical Engineering  
Texas Tech University  
Lubbock, Texas 79409-4439, USA

ABSTRACT - The use of attaching gases in an externally sustained diffuse discharge opening switch with a low attachment rate at low values of  $E/N$  and a high attachment rate at high values of  $E/N$  allows the discharge to operate with low losses in the closed switch phase and to achieve fast opening after the sustainment source is turned off. Such an attacher generates a  $J$ - $E/N$  characteristic with a negative differential conductivity in an intermediate  $E/N$  range. Such a characteristic obstructs the closing process of the discharge if it is operated in a high impedance system. Experiments demonstrating these effects are presented for electron beam sustained discharges in mixtures of Argon and  $C_2F_6$ .

- 
- a) Present address: Department of Electrical Engineering  
Polytechnic Institute of New York  
Farmingdale, NY 11735
- b) Present address: Department of Electrical Engineering  
Old Dominion University  
Norfolk, VA 23508
- c) Present address: Maxwell Laboratories  
San Diego, CA 92123

Inductive energy storage is attractive in pulsed power applications because of its intrinsic high energy density compared to capacitive storage systems. The key technological problem in developing inductive energy discharge systems, especially for repetitive operation, is the development of opening switches. Promising candidates for repetitive opening switches are e-beam or laser controlled diffuse discharges.

An e-beam controlled diffuse discharge switch opens when the e-beam is turned off. The switch opening time is determined by the electron loss processes: recombination and attachment. In order to achieve opening times of less than a microsecond at initial electron densities  $n_e < 10^{14} \text{ cm}^{-3}$ , the dominant loss process must be attachment, which means that the switch gas mixture must contain an electro-negative gas. On the other hand, additives of attachers increase the power losses during conduction. Both low forward voltage drop and fast opening can only be obtained by choosing gases or gas mixtures which satisfy the following conditions [1-3]:

- (1) For low values of the reduced field strength  $E/N$  (conduction phase) the gas mixture should have a high drift velocity  $v_d$  and low attachment rate coefficient  $k_a$ .
- (2) For high  $E/N$  values (opening phase) the gas mixture should have low drift velocities and high attachment rate coefficients.

It has been discussed before that such gas properties cause a discharge characteristic (current density  $J$  versus reduced electric field strength  $E/N$ ) with a strong negative differential conductivity [2,4]. Such a characteristic is equivalent to a strong increase of the discharge resistivity with increasing  $E/N$ . Gas mixtures, for example, which show the above mentioned properties and were recommended for these applications are mixtures of Argon or  $\text{CH}_4$  and  $\text{C}_2\text{F}_6$  or  $\text{C}_3\text{F}_8$  [2]. Some of these gas mixtures have been used for switching experiments in electron-beam sustained discharges [5,6]. The experiments presented here were performed with mixtures of Argon and  $\text{C}_2\text{F}_6$ .



The experimental setup used for our investigations is an electron-beam controlled diffuse discharge switch with an electron-beam tetrode for multiple, submicrosecond pulse operation [7,8]. The discharge itself is driven by a 2 Ohm pulse forming network, and series resistors are used to simulate high impedance systems. The discharge characteristics were investigated with a 2 Ohm system. Figures 1 and 2 show the discharge characteristics and the resistivities for different mixing ratios of Argon and  $C_2F_6$ . The source function was kept constant at a value of  $S = 1.3 \cdot 10^{20} \text{ cm}^{-3} \text{ s}^{-1}$ . The current density reaches a maximum in the E/N range of 2-3 Td, depending on the  $C_2F_6$  concentration and the source function, S. With further increasing E/N up to approximately 5 Td the current density decreases. The discharge resistivity increases in this E/N range by a factor of approximately 20. The increase of resistivity is more pronounced with increasing  $C_2F_6$  concentration. It is mainly caused by the attachment properties of  $C_2F_6$  and not by the E/N dependence of the drift velocity. Also mixtures of Argon and Nitrogen have a drift velocity with a maximum at low values of E/N, however, these mixtures did not show a negative differential conductivity. The drift velocity, however, seems to influence the magnitude of the current maximum at low  $C_2F_6$  concentrations since the characteristic for 0.5%  $C_2F_6$  shows a lower maximum current than for 2%  $C_2F_6$ . Since the maximum of the current density indicates the optimum operation range for the steady state conducting phase one can conclude that the optimum Ar- $C_2F_6$  mixture contains approximately 2%  $C_2F_6$ .

It should also be mentioned that the self breakdown voltage increases with increasing  $C_2F_6$  concentration. The E/N values at self breakdown were 8 Td, 12 Td, 15 Td, and > 20 Td for  $C_2F_6$  concentrations of 0.5%, 2%, 5%, and 10%, respectively.

It is interesting to notice that a similar discharge characteristic has been found in optically sustained discharges using the same gas mixtures. Figure 3 shows the

characteristics for 10% C<sub>2</sub>F<sub>6</sub> in Argon in an e-beam sustained discharge with a source function of  $S=1.3 \cdot 10^{20} \text{ cm}^{-3}\text{s}^{-1}$  and for an optically sustained discharge with a source function of  $S = 1.6 \cdot 10^{19} \text{ cm}^{-3}\text{s}^{-1}$ . In the case of the optically sustained discharge approximately 350 ppm dimethylaniline were used as an additive with low ionization potential. One would expect that the onset of the negative differential conductivity is more pronounced if the source function decreases since the influence of recombination is reduced [3]. According to Figure 3 the opposite is found. A significant difference between the two ionization sources is that the average energy of the electrons produce by the UV source is very low ( $\gg 1\text{eV}$ ) while the electrons produced by the e-beam have an average energy in the order of several eV. This effect in combination with attaching gases may have a significant effect on the electron energy distribution function and consequently on the onset of attachment with increasing E/N [9]. Also the additive of dimethylaniline may contribute to a change of the electron energy distribution.

If the specific switch application requires a burst of short pulses with a high repetition rate then the inductor is charged only once and the total length of the burst of pulses is in the order of the discharge time of the inductor. For this operating mode the inductor can be treated as a high impedance line and the closing and opening process have to follow the same high impedance load line [3]. Figure 4 shows the different load lines used and the experimental discharge results achieved with these load lines. It becomes obvious that the current maximum can not be utilized with a high impedance system in the repetitive mode.

The closing process is obstructed even for operating conditions for which the discharge can reach a low loss, low E/N state, since the closing process starts at high values of E/N where attachment is strong. This behavior is demonstrated in Figure 5. The characteristics measured with a 2 Ohm system and a 100 ohm system are shown. For the 2 Ohm system the

steady state values are obtained in less than 100 ns. For the 100 Ohm system the (E/N) values are plotted for 75 ns and for 350 ns after e-beam initiation. The ionizing electron beam had a risetime of approximately 10 ns and a nearly flat maximum over a pulse length of 400 ns [7]. The source function for these measurements again was  $S=1.3 \cdot 10^{20} \text{ cm}^{-3} \text{ s}^{-1}$ . Figure 5 demonstrates that those low loss, low E/N operation conditions which can be achieved with this high impedance system are reached only after a long closing period. This behavior was already predicted for  $\text{N}_2:\text{N}_2\text{O}$  mixtures [3].

We therefore have to conclude that gas mixtures which cause a negative differential conductivity in an intermediate E/N range are most suitable for diffuse discharge opening switches only if the system is operated in a single shot mode (recharging of the inductor after every shot). For a burst mode (several shots from a single inductor charging), however, the closing process is obstructed and the maximum possible current can not be utilized. For such an application a discharge characteristic is required where the current rises strongly with E/N up to the operation point of the discharge in the closed phase. Above this E/N value the current should stay constant or decrease slowly with E/N over a wide E/N range to assure a high self breakdown voltage. Ternary gas mixtures can be used with two attachers with attachment cross sections at different electron energies to produce such a flat characteristic over a wide E/N range and to achieve the same increase of resistivity. Another approach to solve this problem is to control the attachment externally [1,3].

This work was jointly supported by AFOSR and ARO under contract AFOSR 84-0032.

## REFERENCES

- [1] K. H. Schoenbach, G. Schaefer, M. Kristiansen, L. L. Hatfield, and A. H. Guenther, "Concepts for Optical Control of Diffuse Discharge Opening Switches," IEEE Trans. Plasma Sci., Vol. PS-10, pp. 246-251, 1982.
- [2] L. L. Christophorou, S. R. Hunter, J. A. Carter, and R. A. Mathis, "Gases for Possible Use in Diffuse Discharge Switches," Appl. Phys. Lett., Vol. 41, pp. 147-149, 1982.
- [3] G. Schaefer, K.H. Schoenbach, H. Krompholz, M. Kristiansen, and A. H. Guenther, "The Use of Attachers in Electron Beam Sustained Discharge Switches - Theoretical Consideration," Laser and Particle Beams, Vol. 2, pp. 273-291, 1984.
- [4] A. D. Barkalov and G. G. Gladush, "Domain Instability of a Non-Self-Sustaining Discharge in Electronegative Gases," Translated From Teplofizika Vysokikh Temperatur, Vol. 20, pp. 19-24, 1982.
- [5] P. Bletzinger, "Scaling of Electron Beam Switches," Proc. 4th IEEE Pulsed Power Conf., pp. 37-40, Albuquerque, NM 1983.
- [6] R. J. Comisso, R. F. Fernsler, V. E. Scherrer, and I. M. Vitkovitsky, "Application of Electron Beam Controlled Diffuse Discharges to Fast Switching," Proc. 4th IEEE Pulsed Power Conf., pp. 87-90, Albuquerque, NM 1983.
- [7] H. C. Harjes, K. H. Schoenbach, G. Schaefer, M. Kristiansen, H. Krompholz, and D. Skaggs, "An Electron Beam Tetrode for Multiple, Submicrosecond Pulse Operation," Rev. Sci. Instr., Vol. 55, pp. 1684-1686, 1984.
- [8] K. H. Schoenbach, G. Schaefer, M. Kristiansen, H. Krompholz, H. C. Harjes, and D. Skaggs, "An Electron-Beam Controlled Diffuse Discharge Switch," J. Appl. Phys., Vol. 57, pp. 1618-1622, 1985.
- [9] G. Schaefer and K. H. Schoenbach, "External Control of Diffuse Discharge Switches," Proc. 5th IEEE Pulsed Power Conf., Arlington, VA 1985.

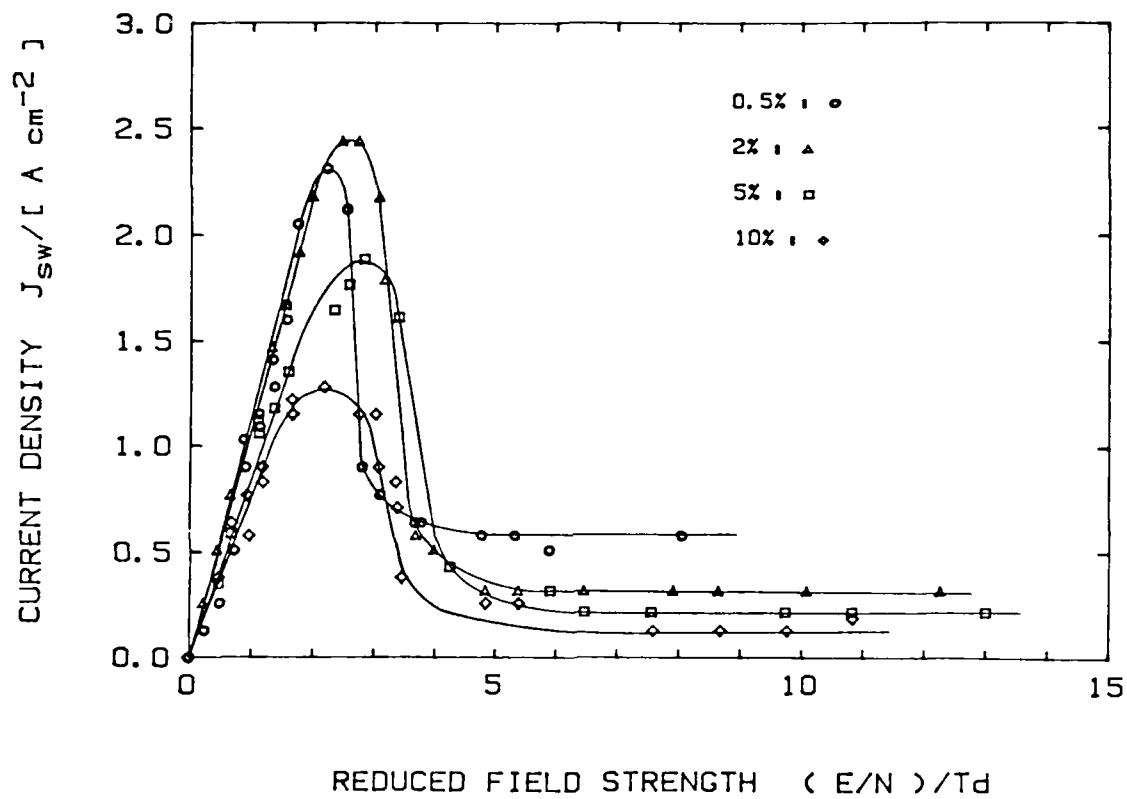


Fig. 1 Current density  $J$  versus reduced field strength  $E/N$  for an e-beam sustained discharge in Argon with admixtures of  $\text{C}_2\text{F}_6$ . The source function is  $S = 1.3 \cdot 10^{20} \text{ cm}^{-3} \text{ s}^{-1}$ . The variable parameter is the  $\text{C}_2\text{F}_6$  fraction.

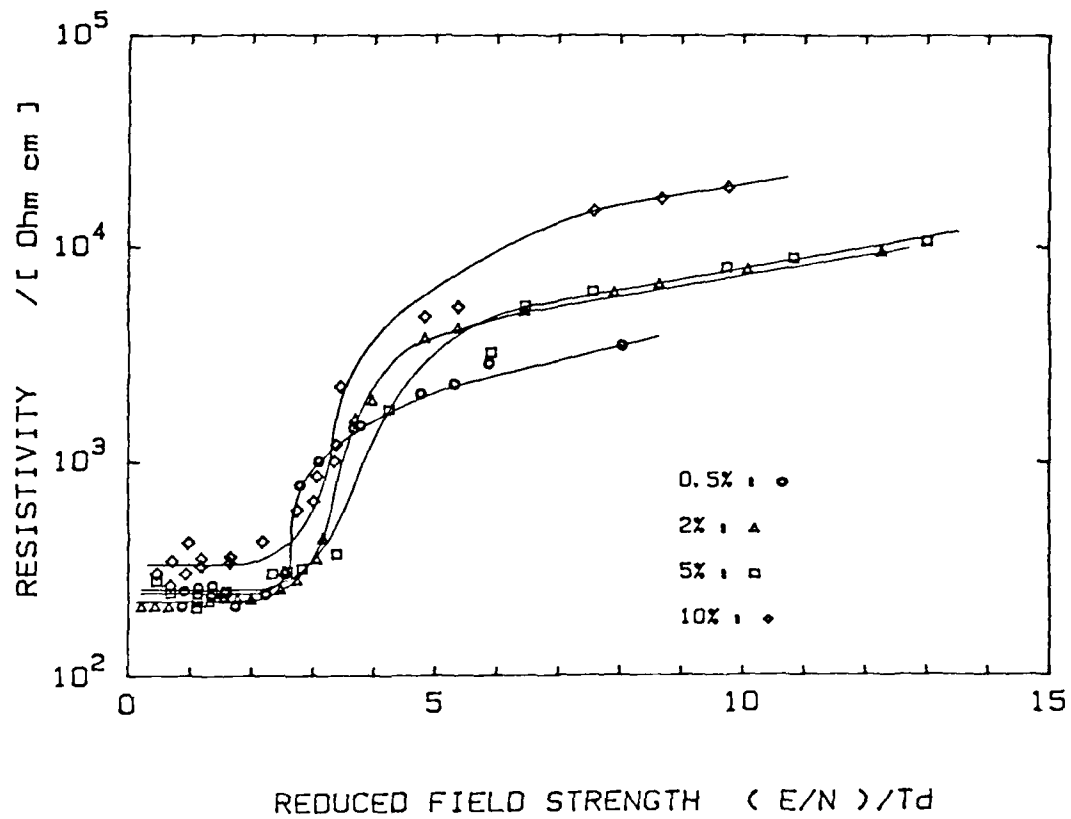


Fig. 2 Resistivity versus reduced field strength  $E/N$  for an e-beam sustained discharge in Argon with admixtures of C<sub>2</sub>F<sub>6</sub>. The source function is  $S = 1.3 \cdot 10^{20} \text{ cm}^{-3} \text{ s}^{-1}$ . The variable parameter is the C<sub>2</sub>F<sub>6</sub> fraction.

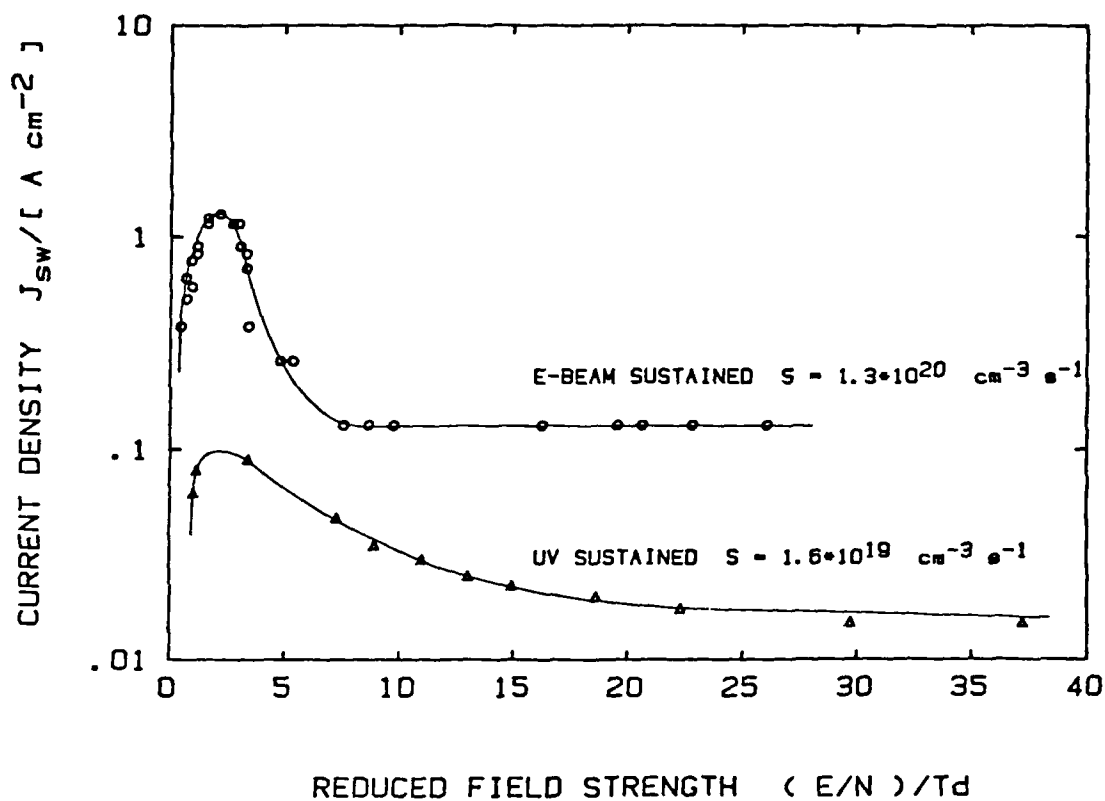


Fig. 3 Current density  $J$  versus reduced field strength  $E/N$  for an e-beam sustained discharge and for a UV sustained discharge in Argon with an admixture of 10%  $C_2F_6$ .

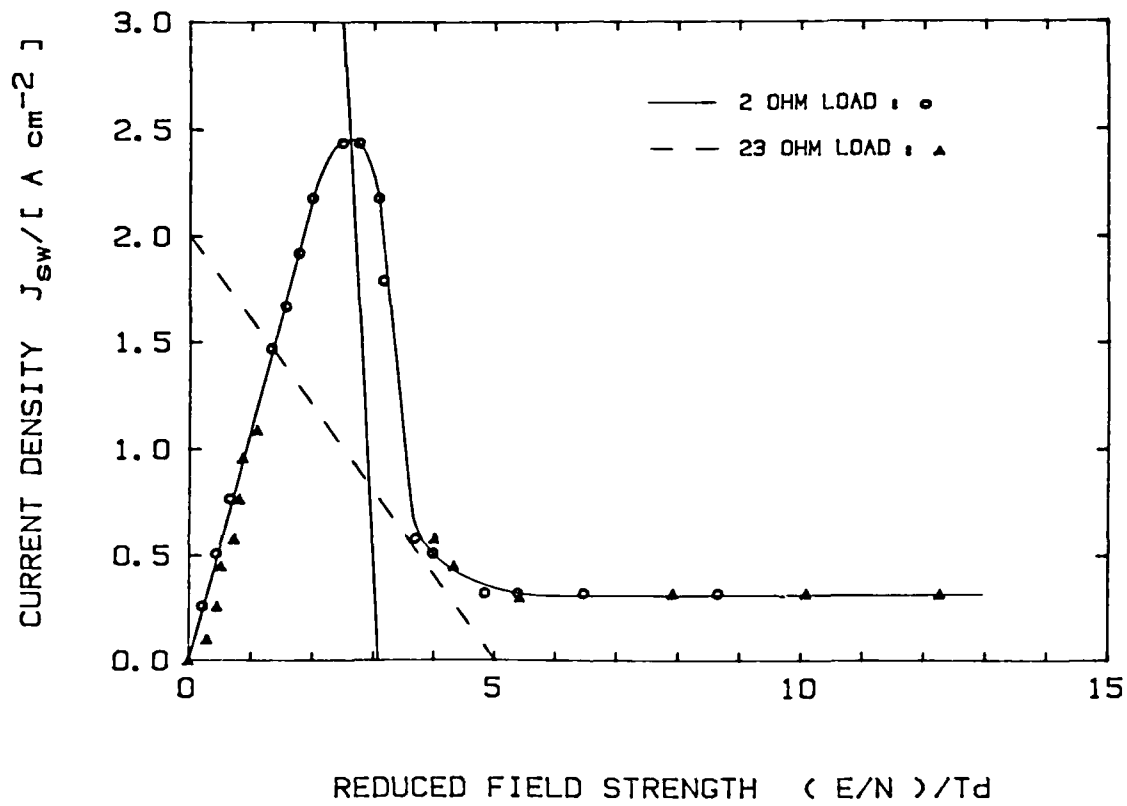


Fig. 4 Loadlines and current density  $J$  versus reduced electric field strength  $E/N$  for an e-beam sustained discharge in Argon with an admixture of 2%  $C_2F_6$ , obtained with different loadlines.



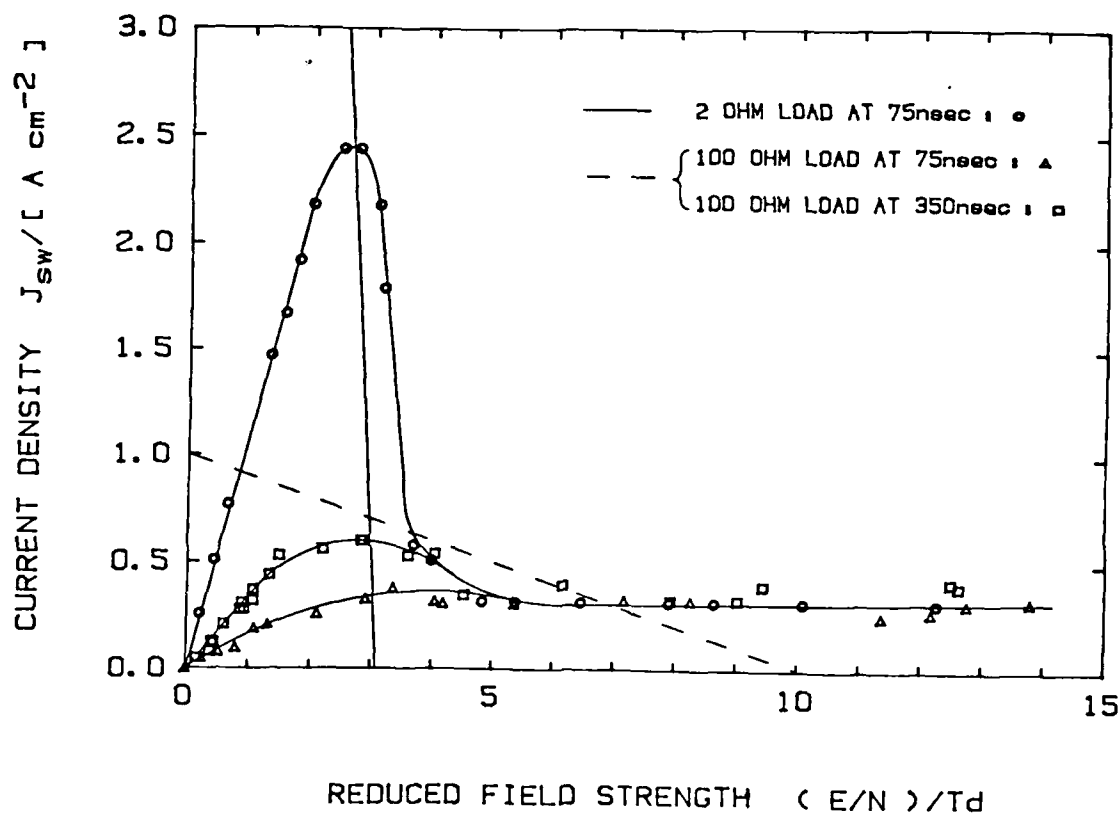


Fig. 5 Current density  $J$  versus reduced electric field strength  $E/N$  for an e-beam sustained discharge in Argon with an admixture of 2%  $C_2F_6$ , obtained at different times after e-beam initiation and with different loadlines.

Submitted to:

BEAMS'86 OSAKA, JAPAN, JUNE 1986

INTERACTION OF DISCHARGE AND CIRCUIT IN AN ELECTRON-BEAM CONTROLLED  
DIFFUSE DISCHARGE OPENING SWITCH\*

G. Schaefer,\*\* K. H. Schoenbach,\*\*\* M. Kristiansen,  
B. E. Strickland, R. A. Korzewka, and K. R. Rathbun  
Texas Tech University, Department of Electrical Engineering  
Lubbock, Texas 79409-4439, USA

Abstract

Inductive energy storage is attractive in pulsed power applications because of its intrinsic high energy density. The key technological problem is the development of repetitive opening switches. A promising candidate is the e-beam controlled diffuse discharge. An e-beam controlled diffuse discharge switch opens when the e-beam is turned off. In order to achieve short opening times the switch gas mixture must contain an attacher. Both low forward voltage drop and fast opening can only be obtained by choosing gas mixtures which satisfy the following conditions:

- (1) For low values of the reduced field strength  $E/N$  (conduction phase) the gas mixture should have a high drift velocity  $v_d$  and low attachment rate coefficient  $k_a$ .
- (2) For high  $E/N$  values (opening phase) the gas mixture should have low drift velocities and high attachment rate coefficients.

Such gas properties cause a discharge characteristic (current density  $j$  versus reduced electric field strength  $E/N$ ) with a strong negative differential conductivity. Experiments performed with mixtures of Argon and  $C_2F_6$  are presented. For switch applications requiring a burst of short pulses the inductor is charged only once and the total length of burst of pulses is in the order of the discharge time of the inductor. For this operating mode the inductor can be treated as a high impedance line and the closing and opening process have to follow the same high impedance load line. Here the closing process is obstructed since it starts at high values of  $E/N$  where attachment is strong, and the maximum possible current can not be utilized, as demonstrated in experiments performed with varying system impedance. As a solution, ternary gas mixtures can be used with two attachers with attachment cross sections at different electron energies to produce a flat characteristic over a wide  $E/N$  range. Another approach discussed is to control the attachment externally.

\* Supported by AFOSR/ARO

\*\* Polytechnic Institute of New York, New York, USA

\*\*\* Old Dominion University, Norfolk, Virginia, USA

### Appendix G

#### NEGATIVE DIFFERENTIAL CONDUCTIVITY IN AN ELECTRON-BEAM CONTROLLED DIFFUSE DISCHARGE FOR SWITCHING APPLICATIONS\*

G. Schaefer, K. H. Schoenbach, M. Kristiansen, B. E. Strickland  
and R. A. Korzekwa

Department of Electrical Engineering  
Texas Tech University  
Lubbock, Texas 79409-4439, USA

Inductive energy storage is attractive in pulsed power applications because of its intrinsic high energy density compared to capacitive storage systems. The key technological problem in developing inductive energy discharge systems, especially for repetitive operation is the development of opening switches. Promising candidates for repetitive opening switches are e-beam or laser controlled diffuse discharges.

An e-beam controlled diffuse discharge switch opens when the e-beam is turned off. The switch opening time is determined by the electron loss processes in the diffuse discharge: recombination and attachment. In order to achieve opening times of less than a microsecond at initial electron densities  $n_e < 10^{14} \text{ cm}^{-3}$ , the dominant loss process must be attachment, which means that the switch gas mixture must contain an electro-negative gas. On the other hand, additives of attachers increase the power losses during conduction. Both low forward voltage drop and fast opening can only be obtained by choosing gases or gas mixtures which satisfy the following conditions:

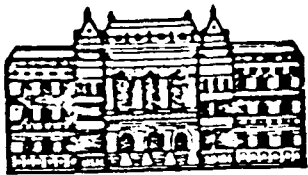
---

\*Supported by AFOSR/ARO

(1) For low values of the reduced field strength  $E/N$  (conduction phase) the gas mixture should have a high drift velocity  $v_d$  and low attachment rate coefficient  $k_a$ .

(2) For high  $E/N$  values (opening phase) the gas mixture should have low drift velocities and high attachment rate coefficients.

In recent experiments gas mixtures have been investigated containing Ar or  $CH_4$  as a buffer gas and  $C_2F_6$  as an attacher. It was demonstrated that these gas mixtures exhibit a discharge characteristic (current density  $j$  versus reduced electric field strength  $E/N$ ) with a strong negative differential conductivity in an intermediate  $E/N$  range. For Ar -  $C_2F_6$  mixtures, for example, the current density reaches a maximum in the  $E/N$  range of 2-3 Td, depending on the  $C_2F_6$  concentration and the source function. With further increasing  $E/N$  up to approximately 10 Td the current density decreases. This negative differential conductivity is more pronounced with increasing  $C_2F_6$  concentration. It is caused by the attachment properties of  $C_2F_6$  and not by the  $E/N$  dependent mobility of mixtures of Ar with molecular gases since Ar- $N_2$  mixtures did not show this negative differential conductivity. The maximum of the current density indicates the optimum operation range for the steady state conducting phase. However, it was demonstrated that this maximum cannot be reached with gas mixtures with high attacher concentrations and in systems with high impedance which are typical for inductive energy storage systems. Additional control mechanisms or three component gas mixtures are discussed as alternatives.



XVII  
International  
Conference on  
Phenomena in  
Ionized  
Gases  
Budapest  
1985

# AN ELECTRON-BEAM CONTROLLED DIFFUSE DISCHARGE SWITCH

G. Schaefer, K. H. Schoenbach, M. Kristiansen, and H. Krompholz

Department of Electrical Engineering  
Texas Tech University  
Lubbock, Texas 79409

Inductive energy storage is attractive in pulsed power applications because of its intrinsic high energy density compared to capacitive storage systems. The key technological problem in developing inductive energy discharge systems, especially for repetitive operation is the development of opening switches. Promising candidates for repetitive opening switches are e-beam or laser controlled diffuse discharges [1]. The schematic diagram of an electron-beam controlled opening switch as part of an inductive storage system is shown in Fig. 1 [2]. The switch chamber is filled with a gas of pressures of 1 atm and above. The gas between the electrodes conducts and allows charging of the inductor only when an ionizing e-beam is injected into the gas. When the e-beam is turned off, electron attachment and recombination processes in the gas cause the conductivity to decrease and the switch opens.

The switch opening time, after e-beam turn-off, is determined by the electron loss processes in the diffuse discharge: recombination and attachment. In order to achieve opening times of less than a microsecond at initial electron densities  $<10^{14} \text{ cm}^{-3}$ , the dominant loss process must be attachment, which means that the switch gas mixture must contain an electronegative gas. On the other hand, additives of attachers increase the

power losses during conduction. Both low forward voltage drop and fast opening can only be obtained by choosing gases or gas mixtures which satisfy the following conditions [1,3,4,]:

- (1) For low values of the reduced field strength  $E/N$  (conduction phase) the gas mixture should have a high drift velocity  $v_d$  and low attachment rate coefficient  $k_a$ .
- (2) For high  $E/N$  values (opening phase) the gas mixture should have lower drift velocities and high attachment rate coefficients.

Along with these considerations, several gas mixtures have been proposed for diffuse discharge opening switches. For our theoretical investigations  $\text{N}_2$  was chosen as a buffer

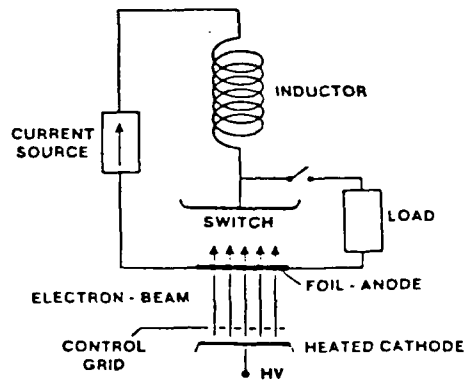


Fig. 1. Schematic of an e-beam controlled diffuse discharge opening switch.

gas with  $N_2O$ ,  $SO_2$ , and  $CO_2$  as the added attachers which satisfy the above mentioned conditions. Experiments were performed in the same gas mixtures and in mixtures of Argon and  $C_2F_6$  [3].

Calculations of the steady-state discharge characteristics were performed with the relative attacher concentration in the buffer gas as the parameter. Figure 2 shows the current density  $j$  versus reduced field  $E/N$  characteristics for different  $N_2O$  concentrations in an  $N_2$  buffer gas. The total pressure is 1 atm. At small  $E/N$ , below 4 Td, the electron loss is due to recombination only. At about 4 Td the attachment rate coefficient rises steeply. This

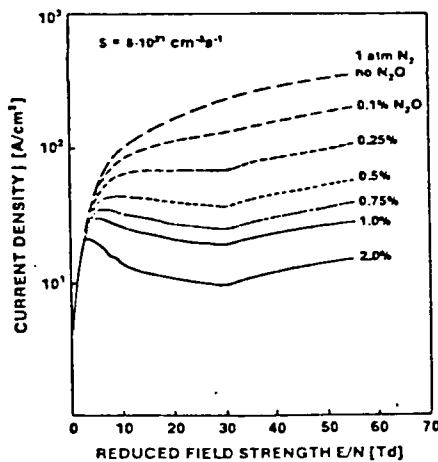


Fig. 2. Calculated steady-state  $j$  vs  $E/N$  characteristics for an e-beam sustained discharge in  $N_2$  with admixtures of  $N_2O$ . The electron generation rate is  $8 \times 10^{21} \text{ cm}^{-3} \text{ s}^{-1}$ . The parameter is the  $N_2O$  fraction in percent (see Ref. 4).

means that, for reasonably high attacher concentrations in the buffer gas, the losses increase drastically, causing a negative slope in the current-voltage characteristics. At 30 Td, where the attachment rate coefficient is assumed to level off, recombination becomes more important again, as demonstrated by the change in the slope of  $j$  vs  $E/N$ , at this value. In experiments the strongest negative slope in the current-voltage characteristics was found in Argon with admixtures of  $C_2F_6$ , while in  $N_2$  with admixtures of  $N_2O$  this effect was not well pronounced.

Figure 3 shows the influence of attacher concentration ( $N_2O$ ) on the switch current. For high  $N_2O$  concentrations (3%) the switch current pulse replicates the e-beam current pulse, except for the tail. The tail may be caused by the current carried by positive and negative ions. The current gain (switch current/electron beam current) is about 2 for this high attachment concentration.

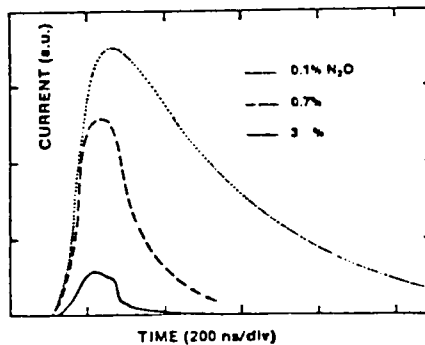


Fig. 3. Time dependence of switch current with  $N_2O$  concentration as the variable parameter.

For concentrations of 0.7%, the fall time ( $1/e$ -time) increases to approximately 100 ns. For 0.1% it is on the order of 500 ns. The gain increases to values of 9 and 12 for 0.7% and 0.1%  $N_2O$ , respectively.

Further calculations were performed to investigate the influence of the attacher on the electron generation mechanism. For an electron beam sustained discharge operated at low values of  $E/N$  the energy of the initial secondary electrons may be well above the energy range of the steady state electron energy distribution, and also above the energy range in which the attacher used has a significant attachment cross section. These initial secondary electrons will subsequently during their relaxation move through the energy range where attachment may occur even if the steady state distribution function does not overlap with the attachment cross section.

Monte Carlo calculations for a gas mixture of  $N_2$  and attachers such as  $N_2O$  and  $SO_2$  showed that at 3 Td the average time for an 8eV electron to reduce its energy to 2eV is  $\sim 2.5 \times 10^{-10}$  s. This time is almost exclusively spent in the energy range above 4eV where  $N_2$  does not have significant inelastic cross sections. This causes a significant difference of the influence of the two attachers mentioned.  $SO_2$  has its maximum attachment cross section at  $\sim 4.5$  eV. In a mixture of 90%  $N_2$  and 10%  $SO_2$  more than 20% of the initial secondary electrons are attached if they are generated at energies above 5eV. In a mixture of 90%  $N_2$  with 10%  $N_2O$  attachment of the initial second-

ary electrons can nearly be neglected ( $< 5\%$ ), since the attachment cross section of  $N_2O$  has its maximum at  $\sim 2.3$  eV in the range where  $N_2$  has its large inelastic cross sections.

#### References

1. K. H. Schoenbach, G. Schaefer, M. Kristiansen, L. L. Hatfield, and A. H. Guenther, IEEE Trans. Plasma Sci. PS-10, 246 (1982).
2. C. H. Harjes, K. H. Schoenbach, G. Schaefer, M. Kristiansen, H. Krompholz, and D. Skaggs, Rev. Sci. Instrum. 55, 1684 (1984).
3. L. L. Christophorou, S. R. Hunter, J. A. Carter, and R. A. Mathis, Appl. Phys. Lett. 41, 147 (1982).
4. G. Schaefer, K. H. Schoenbach, H. Krompholz, M. Kristiansen, and A. H. Guenther, Laser Part. Beams 2, 273 (1984).

TO BE SUBMITTED TO IEEE TRANSACTIONS ON ELECTRON DEVICES

DRAFT

TIME DEPENDENT EMISSION FROM A SPARK ARRAY USED AS AN  
IONIZATION SOURCE FOR DIFFUSE DISCHARGES

G. Z. Hutcheson, J. R. Cooper, B. E. Strickland,<sup>a)</sup>  
G. Schaefer,<sup>b)</sup> and K. H. Schoenbach<sup>c)</sup>

Department of Electrical Engineering  
Texas Tech University  
Lubbock, TX 79409-4439, USA

ABSTRACT - This paper discusses the use of a spark array as an ionization source for diffuse discharges. A linear array of twenty bare spark gaps was constructed and tested to determine the turn-on and turn-off characteristics using streak photography and high resolution time resolved photography. The experimental results indicate that the turn-on time is dominated by the serial breakdown of the spark gaps in the array, and the turn-off time is dominated by the decay time of the plasma produced by each spark gap. The application for UV initiated discharges is discussed.

- a) Present address: Maxwell Laboratories  
San Diego, CA 92123
- b) Present address: Department of Electrical Engineering  
Polytechnic Institute of New York,  
Farmingdale, NY 11735
- b) Present address: Department of Electrical Engineering,  
Old Dominion University  
Norfolk, VA 23508



## INTRODUCTION

In recent years diffuse discharges have gained significant interest as lasing media and as switches (For reviews see [1,2]). In general, these discharges can be self-sustained or externally sustained. For self sustained discharges a preionization source is usually required to generate stable arc-free discharges, while in an externally sustained discharge ionization totally depends on the external source. Such an externally sustained discharge can be used as an opening and/or closing switch. Sustainment methods used are electron-beams, x-rays, and ultraviolet sources. In an externally sustained diffuse discharge opening switch the controlling mechanism ionizes the gas in the discharge, forming a conducting medium which continues to conduct as long as charged particles are present. Once the ionization source is removed, electron attachment and recombination processes in the gas cause the electron density to decrease and consequently the conductivity of the gas discharge decreases until the discharge ceases, thus forming an insulating medium.

The requirements for the operation of the external ionization source strongly depend on the specific applications. In the case of an externally initiated discharge it is mainly the turn-on characteristic of the ionization source which determines the performance of the discharge while in the case of an opening switch the turn-off characteristic and the charge carrier loss mechanisms determine the opening time.

In one of the experiments at Texas Tech University related to opening switches, additional external discharge control mechanisms using lasers are investigated. Such mechanisms are photodetachment and optically enhanced attachment. These processes have to be investigated over a wide E/N range from below 1 Td up to the self breakdown voltage of the discharge. These variations of E/N require the possibility to operate the discharge in the self

sustained and in the externally sustained mode. The experiments related to these effects are discussed elsewhere [3]. The subject of this paper is to discuss the properties of the used UV ionization source which are important for these applications.

#### UV SOURCE DESIGN CONSIDERATIONS

The optically controlled switch experiment used to study optogalvanic effects is shown schematically in Fig. 1. This experiment utilizes an ultraviolet radiation source which can be used as a preionizer for a self-sustained discharge or as the external ionization source for an externally sustained discharge. To produce a homogeneous self-sustained discharges at high pressure such as in TEA lasers it has been proven that the transverse homogeneity of the ionization source is one of the keys for arc free operation [1]. The best way to incorporate an ultraviolet source into a switch system is, therefore, to illuminate the discharge volume from behind one electrode [1]. This requires that the electrode be optically transparent or a mesh. Placing the ultraviolet source behind the electrode also assures that the maximum photoionization effect occurs directly between the parallel surfaces of the switch electrodes.

When operating gas discharges for lasers or switches it is desirable to maintain a constant gas environment in the discharge chamber. Arcs are good sources of ultraviolet radiation and can be created by surface discharges or bare sparks. Surface discharges are a good source of ultraviolet radiation; however, these discharges erode some part of the insulator surface with each discharge. The by-products of surface discharges can contaminate the discharge environment; therefore, a bare spark source should be used whenever it is important to maintain the integrity of the gas in the discharge chamber over a large number of shots.

In order to optimize the turn-on and turn-off characteristics and the efficiency of the source, a pulse

forming network providing a rectangular current pulse should be used and the impedance of the ultraviolet source after breakdown should be matched to the impedance of the pulse forming network which excites the source. To achieve fast breakdown of a spark gap, high applied voltages are also required. A stripline design allows optimization of these conditions. Since the impedance of an individual spark is in the order of 25 mOhms [4], many spark sources in series have to be incorporated into the transmission line (Figure 2). Nearly the full charging voltage will then be applied to each individual spark source before breakdown and the impedance of the line can be matched to all spark sources in series after breakdown. The impedance  $Z_0$  of the pulse forming network available for our experiment was 9.4 Ohm; therefore, approximately 375 individual spark sources would be needed to match the impedance using only the resistance of the sparks. Given the physical size limitations of our discharge chamber only 20 spark gaps in a linear array have been used. Therefore, an additional resistance was incorporated at the end of the array to match the impedance of the ultraviolet source to the pulse forming network and to avoid reflections. A feasible system can operate with a 2.5 Ohm pulse forming network and approximately 100 sparks in series.

Utilizing the above considerations, an ultraviolet source has been designed and constructed which consists of 20 individual bare spark gaps with approximately 1 mm gap spacing arranged in a linear array and terminated with an additional matching resistance. When the switch spark gap shown in Fig. 1 is triggered by a ruby laser, a pulse with a voltage of  $V_0/2$ , a current of  $I_0 = V_0/2Z_0$ , and pulse length of 10ns is delivered to the transmission line. The magnitude of the charging voltage  $V_0$  is usually kept below the dc breakdown voltage of the source as a whole (all spark gaps in series), but well above the dc breakdown voltage of a single spark gap. Since the individual spark gaps are incorporated into the transmission line, the array will breakdown in a

serial manner. The turn-on time of the entire ultraviolet source is, therefore, determined by the delay between the light emission from the first and last spark gap. This delay time will include the transit time of the pulse along the transmission line from the first to the last spark gap and the sum of the breakdown time of all spark gaps.

#### OPTICAL INVESTIGATIONS

In order to obtain knowledge about the turn-on and turn-off characteristics of the ultraviolet source as a function of the charging voltage  $V_0$  and to determine the time dependent relative intensity of the emitted light, two optical investigations were performed. First, streak photography was used to obtain information about the turn-on time of the source as a function of the charging voltage  $V_0$ . Second, high-speed, high-resolution time resolved photography was employed to determine the time dependent relative intensity characteristics of the source.

For each of the optical investigations performed, the experimental set-up was the same with the exception of the camera. The ultraviolet source was positioned so that it directly illuminated the lens of the camera. Delay generators were incorporated into the trigger circuitry of the experiment to allow for variation in the timing of the event with respect to the camera shutter. Each of the tests were performed in open air.

A TRW streak camera was used to investigate the turn-on characteristics of the source. A streak photograph of the ultraviolet source with a charging voltage of 33 kV is shown in Fig. 3. The streak photograph illustrates that the linear array of spark gaps breakdown serially. The dim area in the center region of the streak photograph is due to an imperfection in the photocathode of the streak camera and not due to the source itself. The turn-on time of the source for a given charging voltage can be determined by considering the writing rate or streak rate of the camera and the distance

between the beginning of the streaks made by the first and last spark gaps of the source. The picture shown in Fig. 3, for example, shows that the turn-on time of the source with a charging voltage of 33 kV is 15.5 ns. Similar streak photographs were taken of the source with charging voltages varying which were varied from 23-35 kV. Figure 4 illustrates the dependence of the turn-on time of the ultraviolet source on the charging voltage.

The time resolved photographs of the ultraviolet source were made using a high-speed, high-resolution image converter camera. The camera consists of a proximity focusing diode manufactured by ITT with a Tektronix roll film back mounted on the rear of the diode [5]. A krytron switched transmission line pulser was used to deliver a 10 kV, trapezoidal pulse with a rise and fall time of approximately 5 ns and a half width of approximately 10 ns to the diode. Consequently, the camera had a shutter speed of 10 ns. The diode has a high resolution of 45 lp/mm. Figure 5 contains two photographs which were taken at different times. Figure 5a was taken during the turn-on phase and illustrates again that the spark gaps breakdown in succession. Figure 5b, taken with reduced sensitivity, illustrates the ultraviolet source with all 20 spark gaps emitting light. Figure 5a and 5b were taken at 10 ns and 290 ns, respectively. Figure 6 depicts the relative intensity verses time for the first spark gap in the ultraviolet source. The data for this figure were obtained by making photodensitometer plots and correcting them for the different aperture settings and film speeds.

The total light emitted from the UV source is the superposition of the light emitted from the twenty individual sparks as shown in Figure 7. The linear section of the turn-on characteristic corresponds to the serial breakdown of the individual spark gaps and makes up for the most important part of the risetime (compare Fig. 3). The minimum risetime achieved was 14 ns for the array of 20 sparks with a charging

voltage of 35 kV. Considering that approximately 100 sparks in series are needed to match a 2.5 Ohm line, one should observe a risetime of approximately 70 ns. It should be mentioned that this is the risetime of the source function for the discharge as a whole. An individual volume element will experience a source function with a significantly shorter risetime since not all sparks contribute to ionization in a given volume element.

It is also important to note that the ultraviolet source continues to emit light for many hundreds of nanoseconds (90% to 10% in 700 ns) after the relatively short current pulse, which excites the source, has been removed. The breakdown of a spark gap produces a hot plasma, providing an increased free electron density which remains in the arc region until electrons are removed by recombination processes. Through recombination highly excited atoms or molecules are produced which decay optically. Thus, until the free electrons are removed by recombination, light will be emitted from the plasma remaining in the arc region.

#### DISCHARGE INVESTIGATIONS USING THE UV SOURCE

The ultraviolet source has been installed in our discharge chamber and has demonstrated its usefulness in three different modes. One experiment demonstrated that using the ultraviolet source as a preionizer allowed the system to operate in a self-sustained discharge mode. Another experiment illustrated that the ultraviolet source could be used as a sustainment mechanism in the presence of attaching gases which enabled our system to be operated as an ultraviolet sustained diffuse discharge switch. It should be noted here again that a switch which utilizes a spark gap as a sustainment mechanism may have limitations with respect to short turn-off times, because the ultraviolet source continues to emit ultraviolet radiation after the excitation current pulse has been removed [5].

The third mode discussed here more in detail is the UV initiated self-sustained discharge for laser applications. In this mode a DC voltage below self breakdown is applied to the discharge gap and the externally initiated discharge acts as the switch as well as the active medium for the laser. Several methods have already been used to initiate discharges such as overvolting with a high voltage trigger pulse [6,7], or UV or X-ray photoionization [8,9].

Using the optically controlled diffuse discharge experiment we have demonstrated externally initiated, matched discharges in gas mixtures containing different attachers. Here the experimental setup shown in Figure 1 is directly connected to a transmission line. This line is dc charged to a value  $V_0$  which is below the self-breakdown voltage, and above the operation voltage,  $V_d$ , of the self sustained discharge. For impedance matched operation the condition  $V_0 = 2V_d$  must be fulfilled.

Figure 8 shows the typical time dependence of current and voltage for matched operation. The current risetime is approximately 20 ns. With preionized discharges, triggered by a laser triggered spark gap, and utilizing the same experimental setup, risetimes down to approximately 10 ns were achieved. We therefore conclude that the risetime of the UV source, caused by the sequential breakdown of the spark array, imposes a limitation for the lowest possible risetime of UV initiated discharges using spark arrays.

## CONCLUSIONS

Spark arrays can be used as efficient ionization sources for externally initiated and externally sustained discharges. Efficient (impedance matched) devices require the operation of a large number of spark gaps in series ( $> 100$ ). The turn-on time of such a device is limited by the sequential breakdown of the individual gaps to values above approximately 70 ns. The turn-off time is limited by the

decay time of the plasma produced by the sparks. The designed device was successfully operated as a preionized self sustained, as an externally sustained, and as an externally initiated discharge.

#### ACKNOWLEDGEMENT

This work was jointly supported by AFOSR and ARO under AFOSR Grant No. 84-0032.



## REFERENCES

- [1] E. W. McDaniel and W. L. Nighan, eds. "Applied Atomic Collision Physics, volume 3 - Gas Lasers", Academic Press, 1982.
- [2] G. Schaefer and K. H. Schoenbach, "A Review of Diffuse Discharge Opening Switches," IEEE Trans. Plasma Sci., to be published in 1986.
- [3] G. Schaefer, G. Z. Hutcheson, K. H. Schoenbach, and P. F. Williams, "The Influence of Photodetachment on the VI-Characteristic of an Externally Sustained Discharge Containing Oxygen," J. Appl. Phys., to be published in 1986.
- [4] W. M. Moeny and M. von Dadelszen, "UV-Sustained Glow Discharge Opening Switch Experiments," Proc. 5th IEEE Pulsed Power Conf., Arlington, VA, June 1985.
- [5] The image converter camera was designed and built by M. Michel, Technische Hochschule Darmstadt, FRG.
- [6] R. S. Taylor and K. E. Leopold, "Magnetically Induced Pulser Laser Excitation," Appl. Phys. Lett., vol. 41, pp. 335-337, Sept. 1985.
- [7] R. S. Taylor and K. E. Leopold, "Microsecond Duration Optical Pulses From a UV-Preionized XeCl Laser," Appl. Phys. Lett., vol. 47, pp. 81-83, July 1985.
- [8] O. deWitte, B. Lacour, and C. Vannier, "Switchless TE Gas Lasers," Conf. Lasers and Electro-Optics, Digest of Technical Papers, Washington, D. C., April 1982.
- [9] B. Lacour and C. Vannier, "X-ray Photoswitching of a 1-J Excimer Laser," Conf. Lasers and Electro-Optics, Digest of Technical Papers, Baltimore, MD, May 1985.

## FIGURE CAPTIONS

- Figure 1 Schematic representation of the optically controlled diffuse discharge switch experiment.
- Figure 2 Schematic representation of the spark array ultraviolet radiation source.
- Figure 3 Streak photography of the ultraviolet source with a charging voltage of 33kV (in air).
- Figure 4 Turn-on time (i.e. propagation time of the arc development) of the ultraviolet source as a function of charging voltage.
- Figure 5 Time resolved photographs of the ultraviolet source (a) prior to complete turn-on and (b) after turn-on.
- Figure 6 Relative intensity versus time relationship for the first spark gap of the ultraviolet source with a charging voltage of 33 kV.
- Figure 7 Relative intensity versus time relationship for the whole UV source with a charging voltage of 33 kV (visible spectral range).
- Figure 8 Time dependence of current and voltage for a UV initiated discharge in a CO<sub>2</sub> laser mixture (Ar: N<sub>2</sub>: CO<sub>2</sub>=125: 26: 1).

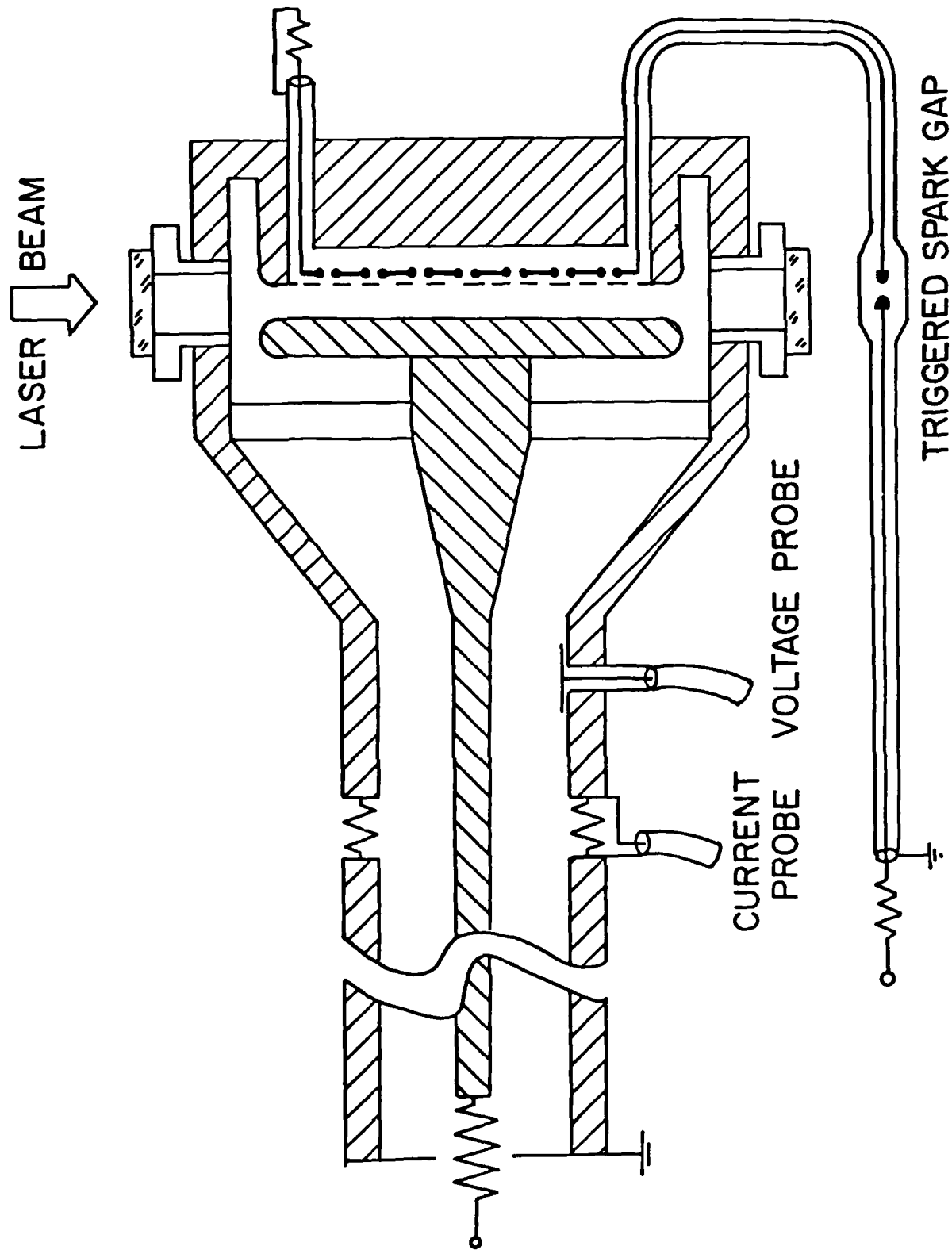


Figure 1 Schematic representation of the optically controlled diffuse discharge switch experiment.

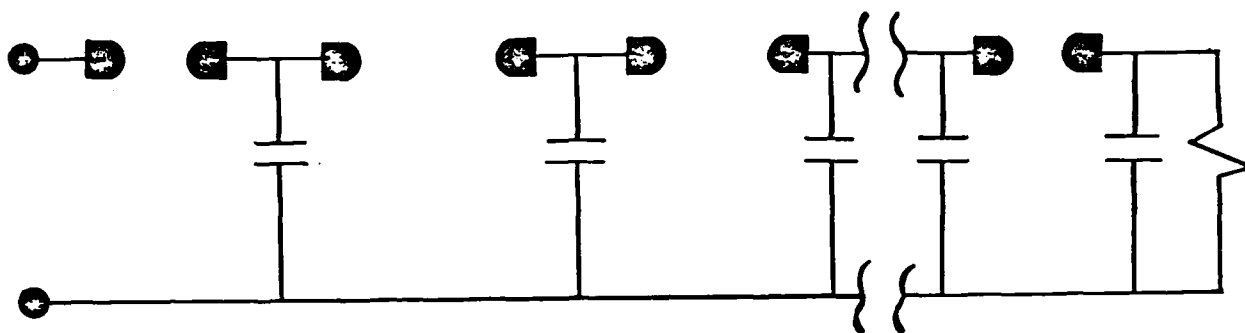


Figure 2 Schematic representation of the spark array ultraviolet radiation source.

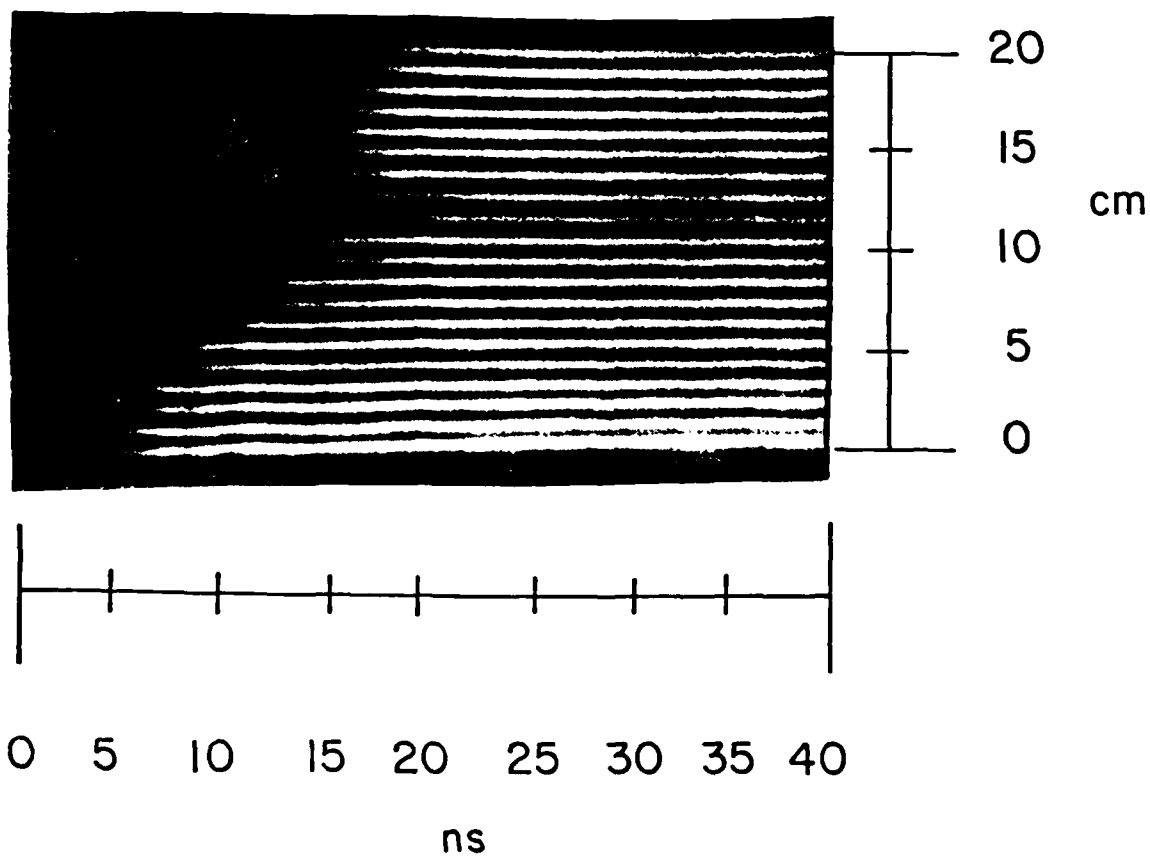


Figure 3 Streak photography of the ultraviolet source with a charging voltage of 33kV (in air).

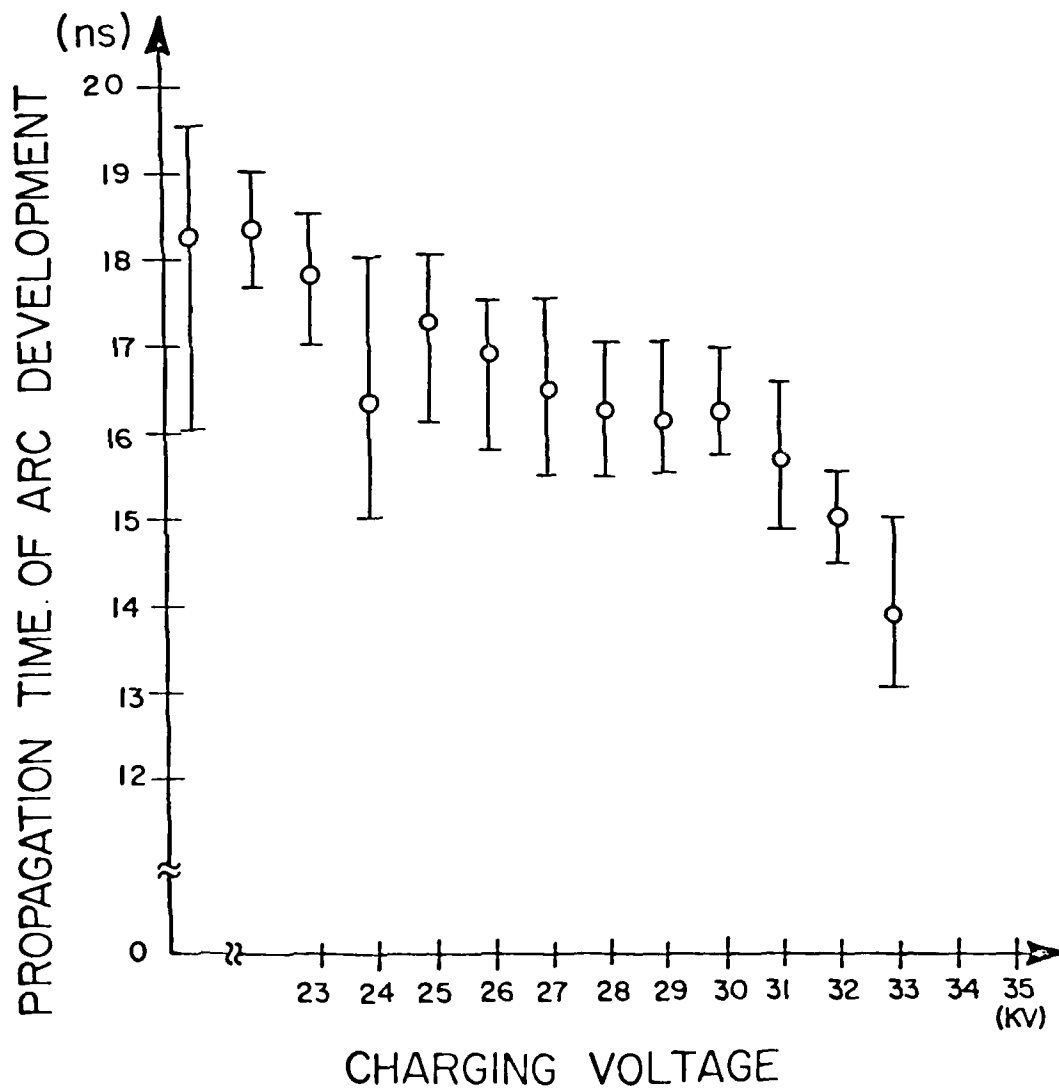
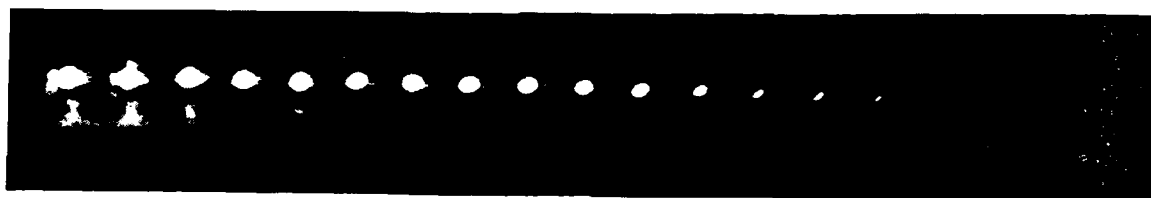
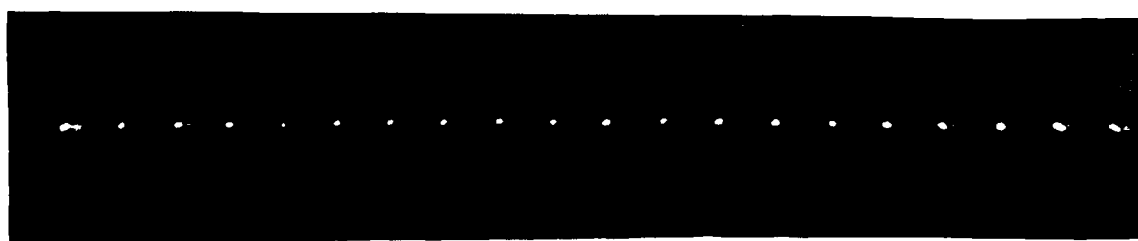


Figure 4 Turn-on time (i.e. propagation time of the arc development) of the ultraviolet source as a function of charging voltage.



(a)



(b)

Figure 5 Time Resolved Photographs of the Ultraviolet Source a) Prior to Complete Turn-on b) After Turn-on.

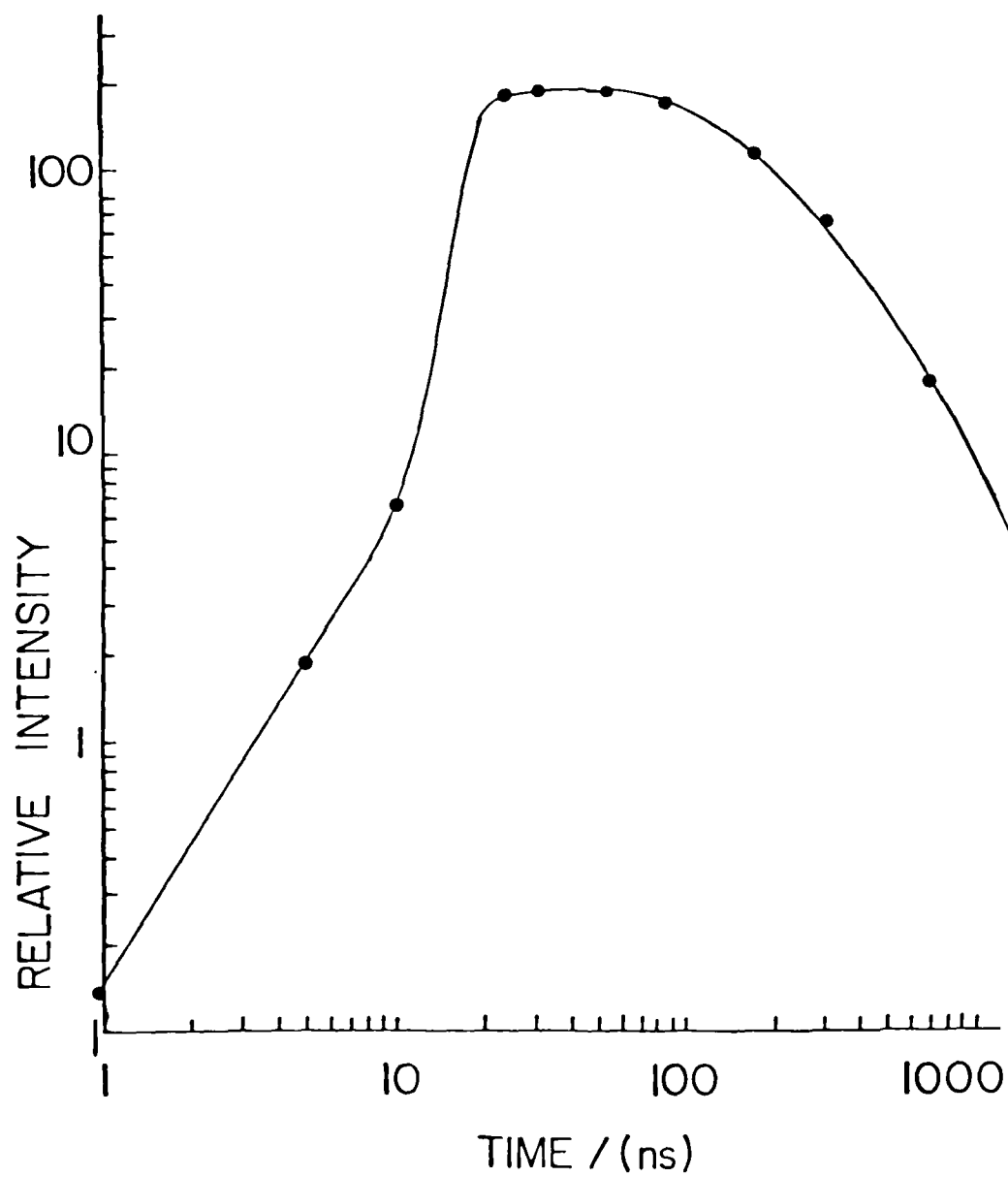


Figure 6 Relative intensity versus time relationship for the first spark gap of the ultraviolet source with a charging voltage of 33 kV.

## RELATIVE INTENSITY (VISIBLE SPECTRAL RANGE)

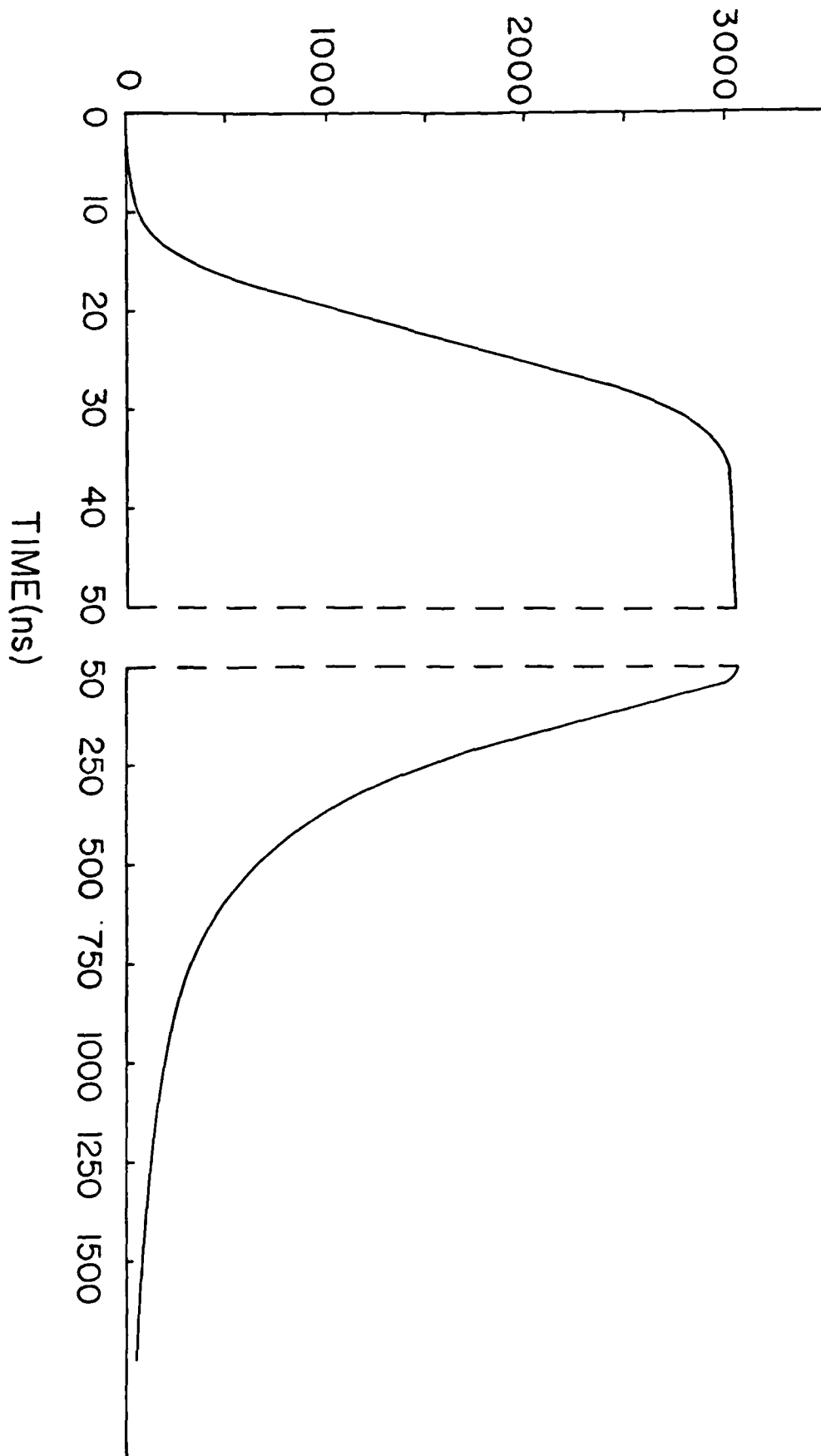


Figure 7 Relative intensity versus time relationship for the whole UV source with a charging voltage of 33 kV (visible spectral range).



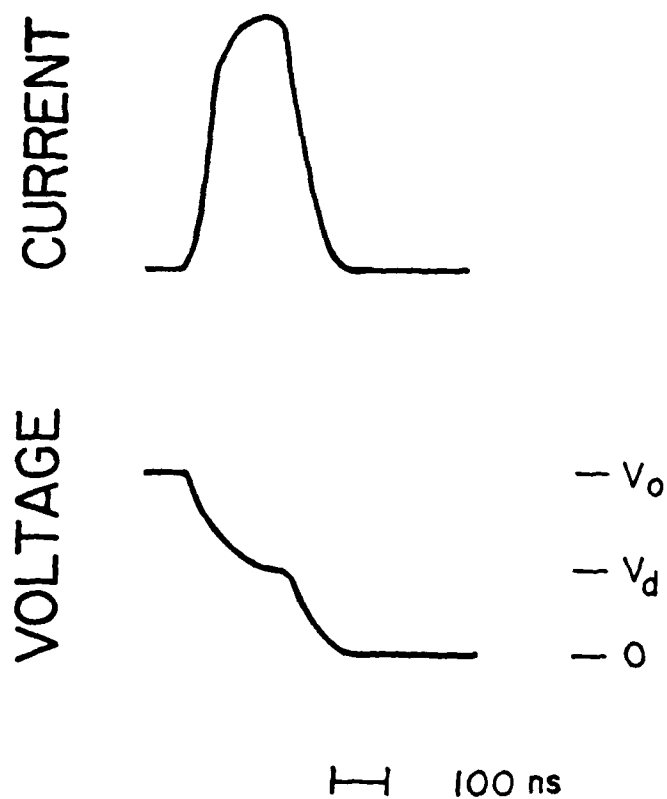


Figure 8 Time dependence of current and voltage for a UV initiated discharge in a  $\text{CO}_2$  laser mixture (Ar:  $\text{N}_2$ :  $\text{CO}_2$ =125: 26: 1).

TO BE SUBMITTED TO JOURNAL OF APPLIED PHYSICS

DRAFT

THE INFLUENCE OF PHOTODETACHMENT ON THE VI-  
CHARACTERISTICS OF AN EXTERNALLY SUSTAINED DISCHARGE  
CONTAINING OXYGEN

G. Schaefer,<sup>a)</sup> G. Z. Hutcheson, K. H. Schoenbach,<sup>b)</sup>  
and P. F. Williams<sup>c)</sup>

Department of Electrical Engineering  
Texas Tech University, Lubbock, TX 79409-4439

Abstract - Externally sustained discharges can be used in opening and closing switch applications for producing bursts of energy in pulsed power systems. Admixtures of attachers with a low attachment rate at low values of  $E/N$  and a high attachment rate at high values of  $E/N$  will allow a low loss operation in the conduction phase as well as rapid opening when the external sustaining source is terminated, however, losses will increase in the closing transition when the external sustaining source is turned-on. Photodetachment has been proposed as an additional control mechanism to overcome these losses in the closing transition. This paper presents measurements on photoionization sustained discharges in argon and nitrogen containing admixtures of  $O_2$  under the influence of laser radiation in the visible where the photodetachment cross section of  $O^-$  has a plateau. Strong changes of VI-characteristics and of the current risetime have been observed. The influence of parameters such as percentage of  $O_2$  and  $N_2$ , and laser power is presented.

- 
- a) Present address: Department of Electrical  
Engineering,  
Polytechnic Institute of New  
York,  
Farmingdale, NY 11735
- b) Present address: Department of Electrical  
Engineering,  
Old Dominion University  
Norfolk, VA 23508
- c) Present address: Department of Electrical  
Engineering  
University of Nebraska - Lincoln  
Lincoln, NE 68588-0511

## I. INTRODUCTION

Inductive energy storage is attractive in pulsed power applications because of its intrinsic high energy density compared to capacitive storage systems. The key technological problem in developing inductive energy storage systems especially for repetitive operation is the development of a fast opening and closing switch. Diffuse discharges have advantages for switching because of their low inductance, small electrode erosion and heating rates and moderate energy density which offer the possibility of external control of the opening and closing process by means of electron beams and/or lasers. To achieve short opening times in an externally sustained discharge with electron densities in the range  $n_e \leq 10^{15} \text{ cm}^{-3}$  attachers have to be used. Attachers with a high attachment rate at high values of  $E/N$  and a low attachment rate at low values of  $E/N$  will allow fast opening when the electron beam is turned off and low losses in the conduction phase [1, 2]. Such an attacher, however, increases the closing time and increases the losses during closure if switch closure has to be performed in a high impedance system. This effect has been demonstrated in calculations on discharges in  $N_2$  containing  $N_2O$  [3] and in experiments on discharges in Argon containing  $C_2F_6$  [4]. It has been proposed that photodetachment can be used to overcome these losses during closure [3, 5]. The influence of photodetachment will mainly influence the discharge characteristics in an intermediate  $E/N$  range. At low values of  $E/N$  attachment will not dominate the discharge if the attacher used has the properties as mentioned above. At high values of  $E/N$  - above self breakdown - ionization through the discharge electrons will dominate [6]. For applications as a repetitive closing and

opening switch the discharge therefore has to be operated at low values of  $E/N$ , not influenced by attachment, in the conduction phase and at intermediate values of  $E/N$ , well below self-breakdown and subsequently dominated by attachment in the non-conducting phase and the transitions between these two phases. The influence of photodetachment can subsequently be demonstrated by measuring the VI-characteristics and the current risetime under the influence of photodetachment.

## II. EXPERIMENTAL SETUP

The experimental setup used for our experiments is shown in Figure 1 [7]. The major component is the discharge chamber with a TEA-laser electrode configuration (variable gap distance,  $d = 3.5\text{--}10\text{ mm}$ , active electrode width,  $w = 20\text{ mm}$ , electrode length,  $l = 200\text{ mm}$ ). The electrodes of this chamber are connected to a 93 Ohm line which is charged to a voltage below self-breakdown of the discharge gap. A resistor in series is used to vary the system impedance. A spark array UV source is located behind a screen in one of the main electrodes. The UV source is fired by synchronously discharging eight charging cables into eight transmission cables which are terminated by the UV source. This UV source can produce light pulses with 5 ns risetime and nearly constant emission over several 100 ns if sufficient long charging cables are used. When the UV source is fired an externally sustained discharge will be initiated in the discharge chambers. Current and voltage probes in the main line allow the evaluation of the time dependence of current, voltage, and impedance of the discharge. Side on windows at the discharge chamber allow the illumination of the discharge volume with a flashlamp pumped dye laser.

This laser produces pulses of approximately 1000 ns length and nearly constant power of 1 MW over the central 400 ns. With a cavity dumping resonator also short pulses of 20 ns length and 10 MW power can be obtained. The time dependent measurements of current and voltage across the discharge, with and without laser, allow the evaluation of the influence of photodetachment on the VI-characteristics and on the transient behavior of the discharge.

### III. EXPERIMENTAL RESULTS AND DISCUSSION

The measurements reported here were performed in mixtures of argon and nitrogen with admixture of oxygen as the attacher. Attachers producing  $O^-$  as the dominant negative ion have been proposed to be suitable, since  $O^-$  has a relatively high photodetachment cross section for photons of approximately 2 eV [8] which can be produced efficiently with flashlamp pumped dye lasers.

The mixture of argon and nitrogen optimizes the ionization efficiency of the UV source. Nitrogen is known to increase the UV yield of the spark source [9] while the admixture of argon allows increased the penetration depth of the ionizing radiation. The ionization efficiency was further enhanced by using N,N dimethylaniline as an additive with low ionization potential.

The first set of experiments was performed to evaluate the influence of attachment on the steady state VI - characteristic of the discharge. For these experiments the system impedance was kept small compared to the impedance of the discharge. One set of data was taken without the laser. For the second set of data with the laser the UV source was fired when the laser power had reached its constant value. The gap spacing

was 3.5 mm and the laser power density was approximately  $8 \times 10^5 \text{ W/cm}^2$  over the cross section of the discharge.

Figure 2 shows an example of such a measurement. The gas mixture used generates a negative differential conductivity in an intermediate E/N range which is believed to be the consequence of an attachment coefficient strongly increasing with E/N. At higher values of E/N the current increases drastically. In this E/N range ionization through discharge electrons is already significant and, therefore, represents the transition to the self-sustained discharge.

No influence of the laser on the discharge characteristic is observed in the low E/N range where no dissociative attachment occurs. This is especially true for the gas mixture not containing any oxygen. The influence of the laser starts in the range where the current density is at a minimum, and with the laser this minimum of the current density is less pronounced. The strongest changes of the current density at constant values of E/N are observed in the transition regime to the self-sustained discharge. Such measurements allow the evaluation of the laser influence ( $\Delta J = J_L(\text{with laser}) - J_0(\text{without laser})$ ) depending on E/N.

Figures 3-6 show the experimental results for different gas mixtures. In Figures 3 and 4 the  $\text{O}_2$  concentration is the variable parameter. Higher oxygen concentrations produce a more pronounced negative differential conductivity (Fig. 3) and also the influence of the laser on the current density increases (Fig. 4). In Figures 5 and 6 the admixture of  $\text{N}_2$  is the variable parameter. The current density of the externally sustained discharge increases significantly with increasing  $\text{N}_2$  concentration (Fig. 5). This effect is the consequence of the higher UV yield of spark sources. The strongest negative differential conductivity is found for an  $\text{N}_2$  admixture of 2.6%. This

mixture also showed the strongest influence of the laser. This may be due to the fact that the attachment cross section for dissociative attachment of  $O_2$  has its maximum above the  $N_2$  cross sections for vibrational excitation of  $N_2$  and therefore admixtures of nitrogen will reduce the attachment rate.

Figure 7 shows the influence of the laser power on the current density. These measurements were performed at an  $E/N = 53$  Td in 13.2%  $O_2$ , 2.6%  $N_2$ , 84.2% Ar at 1 Atm where the laser had its strongest influence.

#### IV. CONCLUSION

The experiments presented demonstrate that externally sustained discharges in mixtures of argon and nitrogen, containing admixtures of oxygen exhibit a negative differential conductivity in an intermediate  $E/N$  range. This effect is believed to be the consequence of the attachment coefficient for the dissociative process ( $e+O_2+O^-+O$ ), increasing strongly with  $E/N$  in this range.

Photodetachment with a visible laser can be used to significantly change the discharge characteristic. This behavior was predicted with calculations on discharges containing  $N_2O$  [3]. According to these calculations an especially significant influence of photodetachment on the closing characteristics of an externally sustained discharge in a high impedance system is expected. Experiments on the transient behavior of the discharge are presently being performed.

#### ACKNOWLEDGMENT

This work was supported jointly by AFOSR and ARO under AFOSR Grant No. 84-0032.



## REFERENCES

- [1] K. H. Schoenbach, G. Schaefer, M. Kristiansen, L. L. Hatfield and A. H. Guenther, "Concepts for Optical Control of Diffuse Discharge Opening Switches," IEEE Trans. on Plasma Science, vol. PS-10, pp. 246-251, Dec. 1982.
- [2] L. L. Christophourou, S. R. Hunter, J. A. Carter, And R. A. Mathis, "Gases for Possible Use in Diffuse-Discharge Switches," Appl. Phys. Lett., vol. 41, pp. 147-149, 1982.
- [3] G. Schaefer, K. H. Schoenbach, H. Krompholz, M. Kristiansen, and A. H. Guenther, "The Use of Attachers in Electron Beam Sustained Discharge Switches - Theoretical Consideration," Laser and Particle Beams, vol. 2, pp. 273-291, 1984.
- [4] G. Schaefer, K. H. Schoenbach, M. Kristiansen, B. E. Strickland, R. A. Korzekwa, and G. Z. Hutcheson, "The Influence of the Circuit Impedance on an Electron-Beam Controlled Diffused Discharge with a Negative Differential Conductivity," submitted for publication in Appl. Phys Lett.
- [5] G. Schaefer, P. F. Williams, K. H. Schoenbach, and J. Moseley, "Photodetachment as a Control Mechanism for Diffuse Discharge Switches," IEEE Trans. on Plasma Sci., vol. PS-11, pp. 263-265, Dec. 1983.
- [6] R. T. VanBrunt and M. Misakian, "Role of Photodetachment in Initiation of Electric Discharges in SF<sub>6</sub> and O<sub>2</sub>," J. Appl. Phys., vol. 54, pp. 3074-3079, June 1983.
- [7] R. Cooper, G. Hutcheson, M. Kristiansen, G. Schaefer, K. H. Schoenbach, and A. H. Guenther, "Multi-Spark Preionization Source for Diffuse Discharges Containing Attachers," Proc. 4th IEEE Int. Pulsed Power Conf., Albuquerque, NM, June 1983.
- [8] L. M. Branscomb, S. J. Smith, and G. Tisone, "Oxygen Metastable Atom Production Through Photodetachment," J. Chem. Phys., vol. 43, p. 2906, 1965.
- [9] H. J. J. Seguin, D. McKen, and J. Tulip, "Photon Emission and Photoionization Measurements in the CO<sub>2</sub> Laser Environment," J. Appl. Phys., vol. 28, pp. 487-489, May 1976.

## FIGURE CAPTIONS

- Figure 1. Experimental setup for UV sustained, photodetachment controlled discharge.
- Figure 2. VI - characteristics of UV sustained discharges in 7.9% O<sub>2</sub>, 2.6% N<sub>2</sub>, and 89.5% Ar at 1 Atm without and with laser - photodetachment.
- Figure 3. VI - characteristics of UV sustained and UV initiated discharges for several concentrations of O<sub>2</sub> with 2.6% N<sub>2</sub> and balance of Ar to make 1 Atm.
- Figure 4. The influence of the laser on the current density ( $\Delta J/J$ , where  $\Delta J = J_L$  (with laser) -  $J_0$  (without laser)) versus charging voltage of the transmission line for various concentrations of O<sub>2</sub> with 2.6% N<sub>2</sub> and balance of Ar to make 1 Atm.
- Figure 5. VI - characteristics of UV sustained and UV initiated discharges for varying concentrations of N<sub>2</sub>, with 5.3% O<sub>2</sub> and balance of Ar to make 1 Atm.
- Figure 6. The influence of the laser on the current density ( $\Delta J/J$ , where  $\Delta J = J_L$  (with laser) -  $J_0$  (without laser)) versus charging voltage on the transmission line for various concentrations of N<sub>2</sub> with 5.3% O<sub>2</sub> and balance of Ar to make 1 Atm.
- Figure 7. Current densities for varying laser intensities in 13.2% O<sub>2</sub>, 2.6% N<sub>2</sub>, and 84.2% Ar at 1 Atm and an E/N = 53 Td.

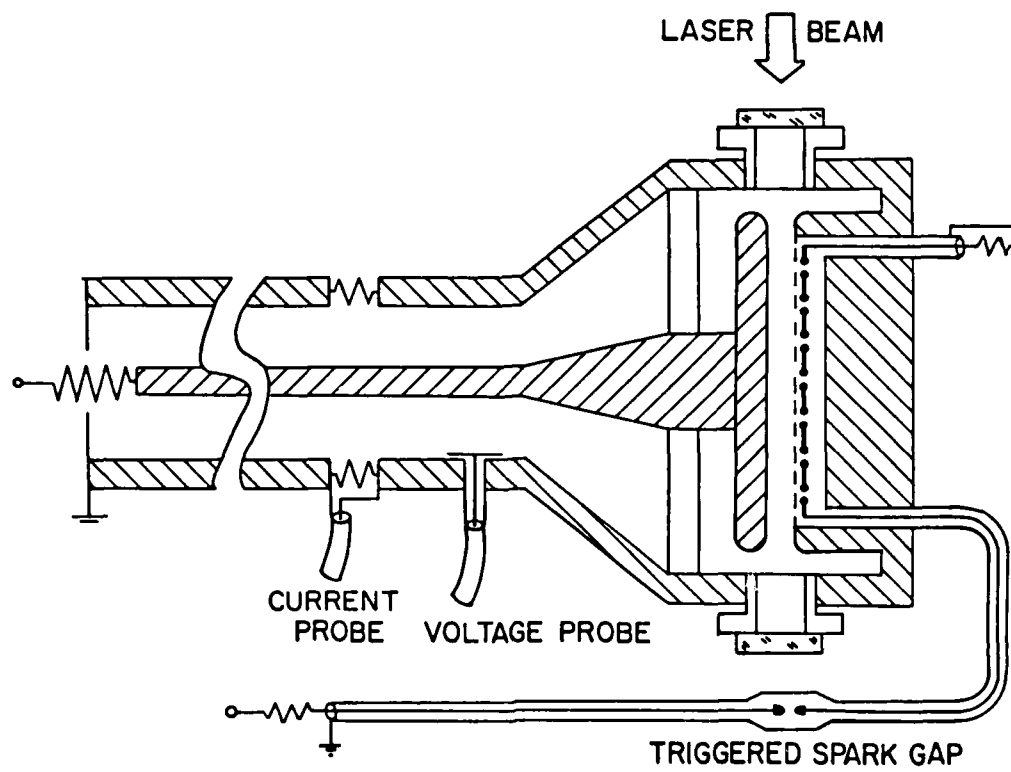


Figure 1. Experimental setup for UV sustained, photodetachment controlled discharge.

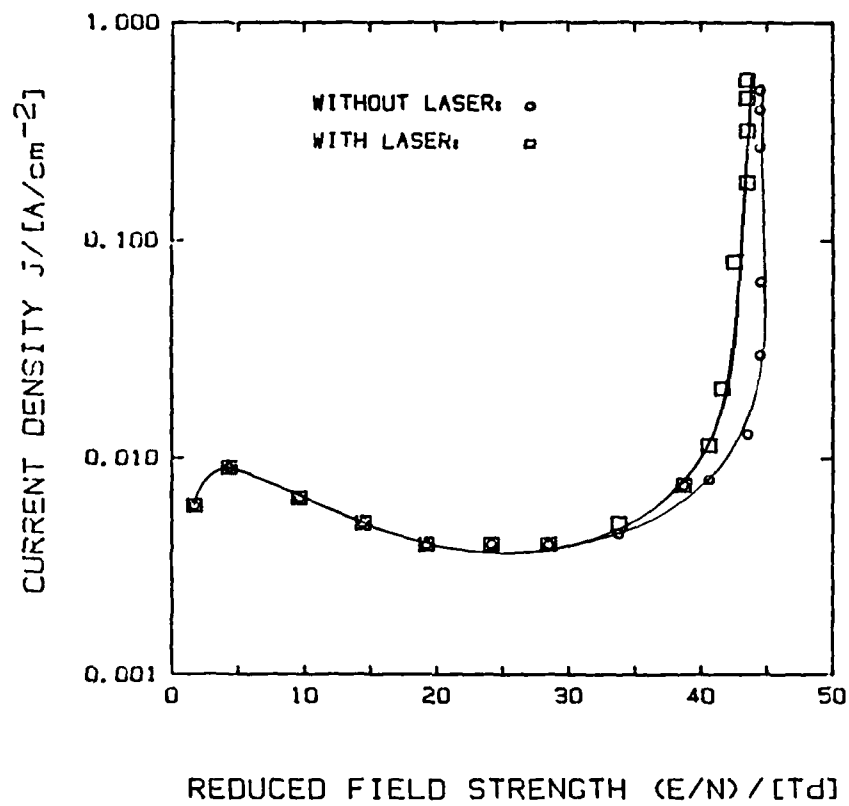


Figure 2. VI - characteristics of UV sustained discharges in 7.9% O<sub>2</sub>, 2.6% N<sub>2</sub>, and 89.5% Ar at 1 Atm without and with laser - photodetachment.

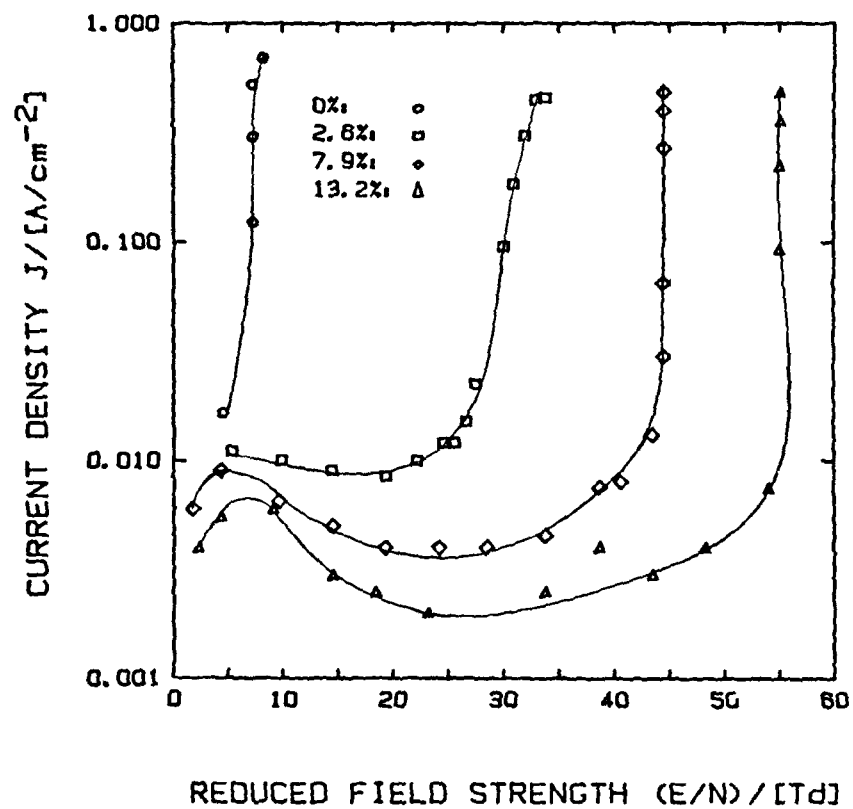


Figure 3. VI - characteristics of UV sustained and UV initiated discharges for several concentrations of  $\text{O}_2$  with 2.6%  $\text{N}_2$  and balance of Ar to make 1 Atm.

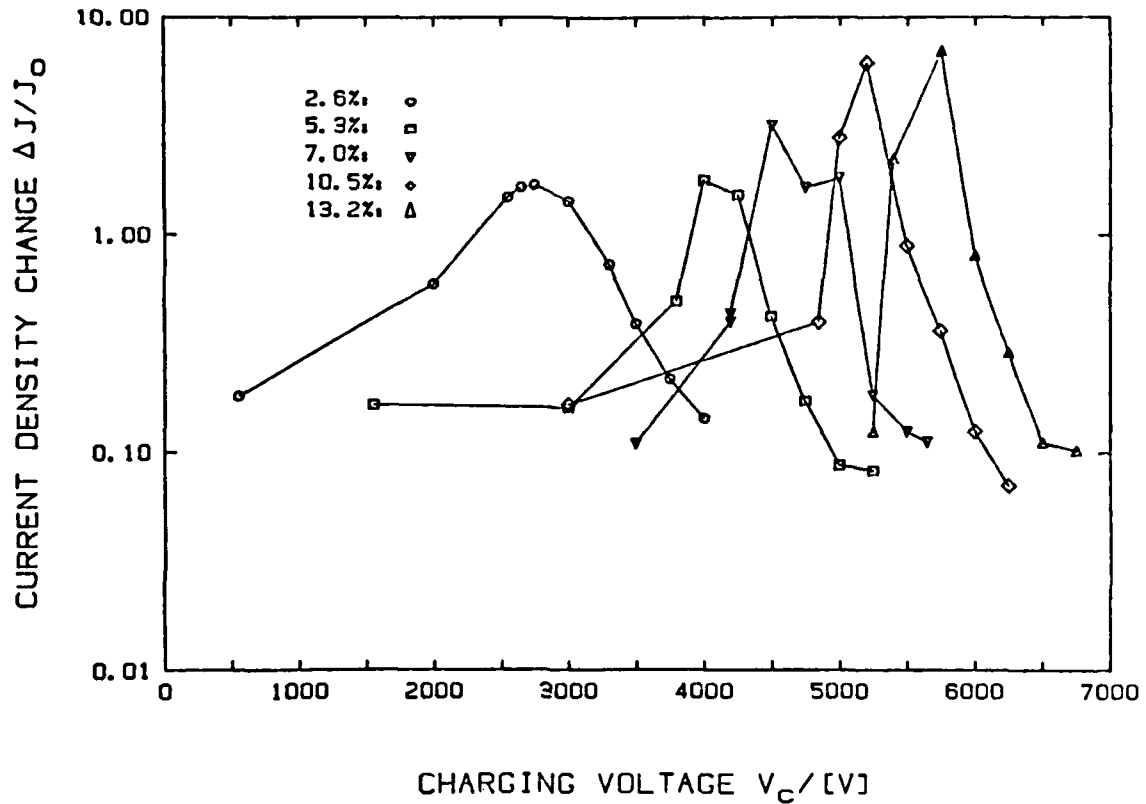


Figure 4. The influence of the laser on the current density ( $\Delta J/J$ , where  $\Delta J = J_L$  (with laser) -  $J_0$  (without laser)) versus charging voltage of the transmission line for various concentrations of  $O_2$  with 2.6%  $N_2$  and balance of Ar to make 1 Atm.

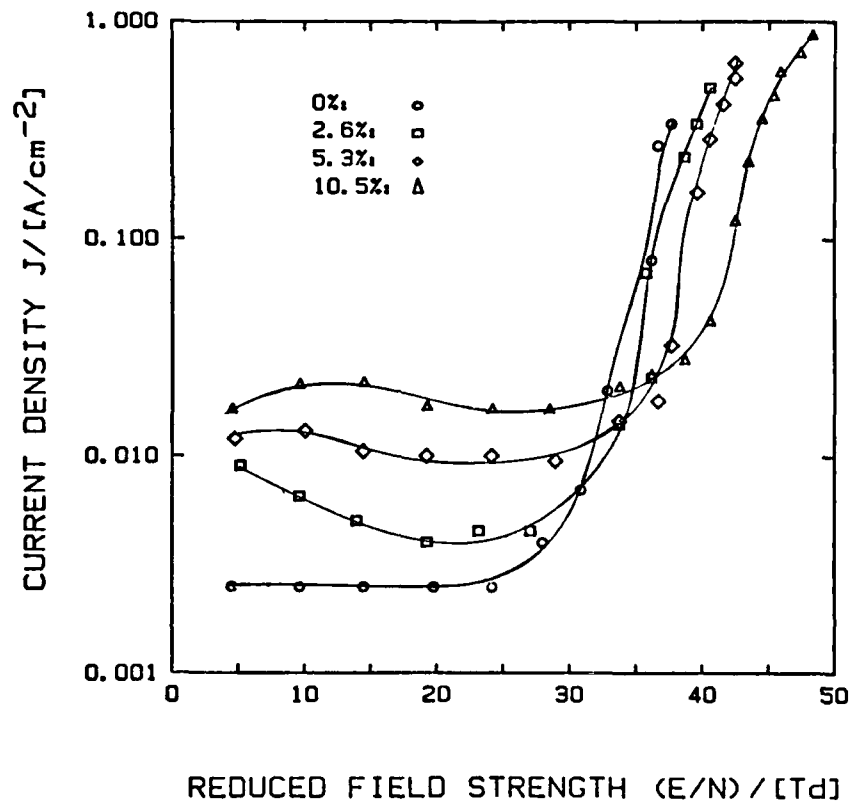


Figure 5. VI - characteristics of UV sustained and UV initiated discharges for varying concentrations of  $\text{N}_2$ , with 5.3%  $\text{O}_2$  and balance of Ar to make 1 Atm.

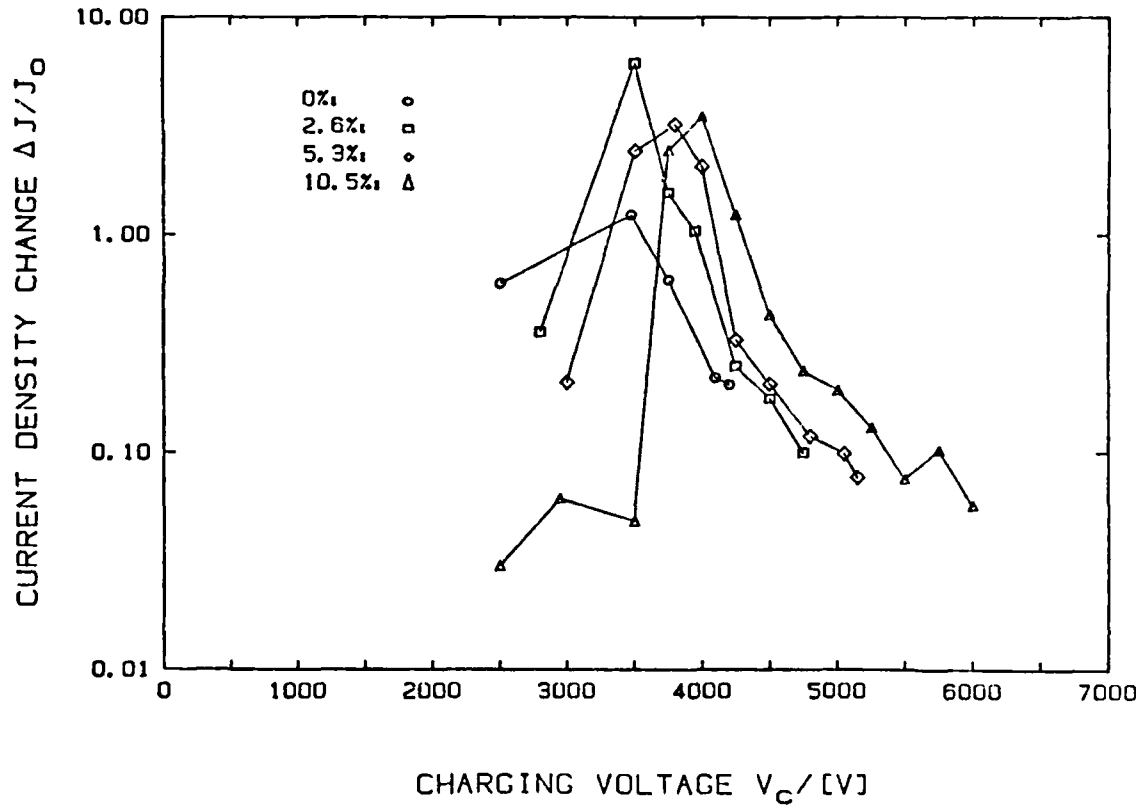


Figure 6. The influence of the laser on the current density ( $\Delta J/J$ , where  $\Delta J = J_L$  (with laser) -  $J_0$  (without laser)) versus charging voltage on the transmission line for various concentrations of  $N_2$  with 5.3%  $O_2$  and balance of Ar to make 1 Atm.



AD-A169 113

COORDINATED RESEARCH PROGRAM IN PULSED POWER PHYSICS

3/3

(U) TEXAS TECH UNIV LUBBOCK PULSED POWER LAB

M KRISTIANSEN ET AL. 20 DEC 85 AFOSR-TR-86-0305

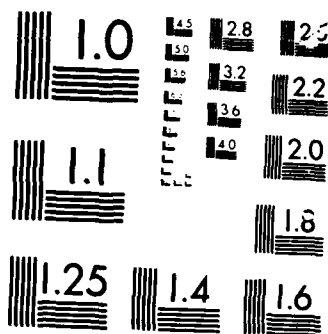
UNCLASSIFIED

AFOSR-84-0032

F/G 10/2

NL





MICROCOPY

CHART

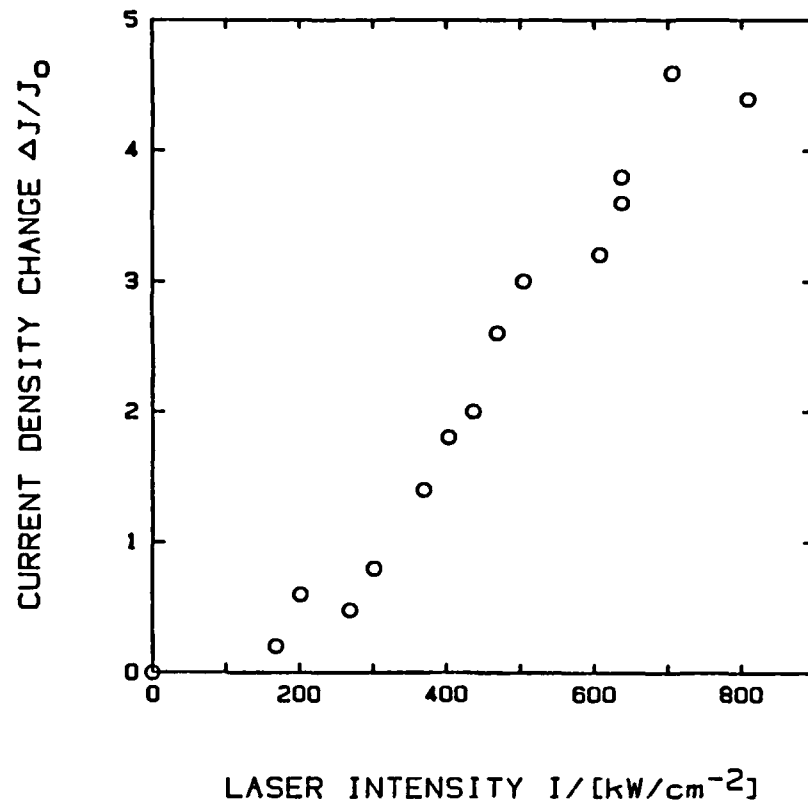


Figure 7. Current densities for varying laser intensities in 13.2% O<sub>2</sub>, 2.6% N<sub>2</sub>, and 84.2% Ar at 1 Atm and an E/N = 53 Td.

## Appendix K

Analysis of Electrode Surface Damage  
in High Energy Spark Gaps\*

A. L. Donaldson, M. Kristiansen, H. Krompholz, and M. O. Hagler  
Department of Electrical Engineering/Computer Science  
L. L. Hatfield and G. R. Leiker  
Department of Physics  
Texas Tech University  
Lubbock, Texas 79409 USA  
P. K. Predecki  
University of Denver  
Denver, Colorado 80208 USA  
G. L. Jackson  
The BDM Corporation  
Huntsville, Alabama 35805 USA

Abstract

The surfaces of stainless steel electrodes used in a high energy, gas-filled spark gap have been analyzed using Auger Electron Spectroscopy (AES) and Scanning Electron Microscopy (SEM). The analysis of electrode cross-sections revealed areas of enhanced erosion and crack formation as a result of temperature cycling of the arc and enhanced chemical attack along manganese "stringers" which were present in the stainless steels. The depth of the cracks was considerably less in nitrogen (20  $\mu\text{m}$ ) than in air (30  $\mu\text{m}$ ) and except at the cracks the damage was generally less than 10  $\mu\text{m}$ . The use of low sulphur steels and cutting the electrodes so that the stringers ran parallel to the surface both proved to be effective means of eliminating crack formation, thus reducing the chance of electrode failure.

Introduction

The surface damage and subsequent electrode erosion resulting from high energy arcs has been of interest for a considerable time as a major factor limiting the lifetime of spark gaps used as switching components in a variety of pulsed power systems. Recent work on electromagnetic launchers ("rail guns") has renewed the interest in understanding electrode erosion, especially for very high currents (> 100 kA). The work reported here contains results on material effects likely to play a role in electrode reliability in the high current regime.

In order to thoroughly study the processes and effects resulting in electrode surface damage, the following questions should be addressed:

- \* What effect was observed?
- \* What is its importance to spark gap performance (via electrode erosion for example)?
- \* What is (are) the cause(s)?
- \* How can it be corrected/altered/designed around?

A listing of some of the surface alterations which have occurred are given in Table I along with a brief summary of their significance.

\*Supported by AFOSR

Table I  
Listing of Surface Damage/Alteration Effects

Effect	Significance
Material Removal (Erosion)*	Increase in Breakdown Voltage
Micro Cracks (Hexagonal "Riverbed")*	Possible Fracturing of Electrode, Bulk Material Removal; Subsequent Failure to Operate
Material Transfer Electrode to Electrode*	Surface Stability & Erosion Rate; A Function of Opposite Electrode
Macro Cracks*	Fracturing of Electrode Subsequent Failure to Operate
Macro Protrusions	Reduction in Breakdown Voltage
Micro Protrusions	Alteration of Breakdown Voltage Stability
Chemical Compound Formation on Surface	Alteration of Breakdown Voltage Stability
Micro Craters	None, Except the Sum Leads to Net Material Removal

\*Likely to be of increasing importance at very high currents.

Specifically, the work reported here will concentrate primarily on one of these effects, namely, surface cracking and the resulting hexagonal structure in stainless steel.

Experimental Setup

The electrode erosion experiments described below were performed on the Mark II energy storage and spark gap system. The spark gap was coaxial in design and was essentially like the one shown in Figure 1. Some modifications have been made to allow for water cooling of the electrodes and inner gap housing in order to remove the bulk heat at high repetition rates and also Coulomb transfer.) The spark gap was designed for frequent electrode and insulator replacement and to allow for accurate control of the electrode alignment and gap spacing.

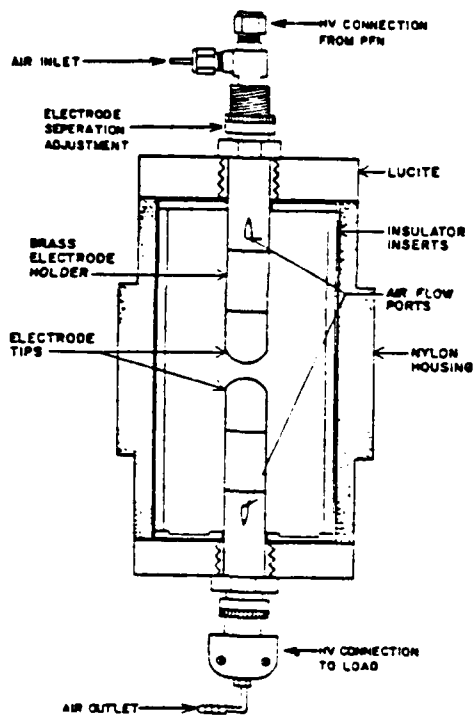


Figure 1. Mark II spark gap (original).

The hemispherically shaped electrodes are all 2.5 cm in diameter and were attached to a stainless steel (304) electrode holder. The insulator inserts provide protection for the main gap housing and studies of the surfaces of these inserts have given information about the insulator damage resulting from the discharge byproducts [1]. A detailed description of the spark gap assembly and diagnostic systems are given elsewhere [2]; however, the operating parameters for the gap are summarized in Table II.

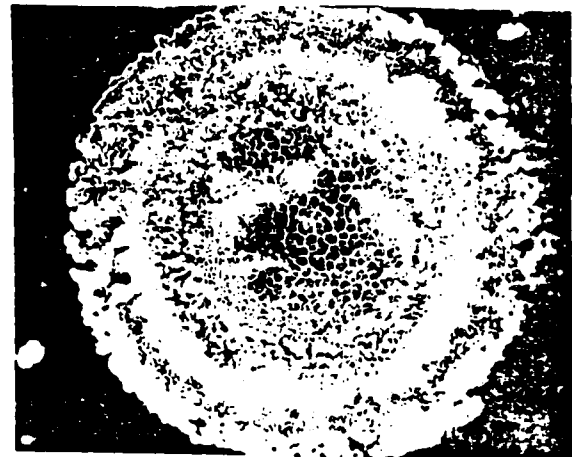
Table II  
Mark II Operating Conditions

Gap Spacing	< 0.75 cm
Voltage	< 30 kV
Current	< 25 kA
Capacitance	21 $\mu$ F
Charge/Shot	0.6 Coul
Energy/Shot	< 9 kJ
Pulse Width	25 $\mu$ s
Rep-Rate	5 pps
Pressure	1 atm (absolute)

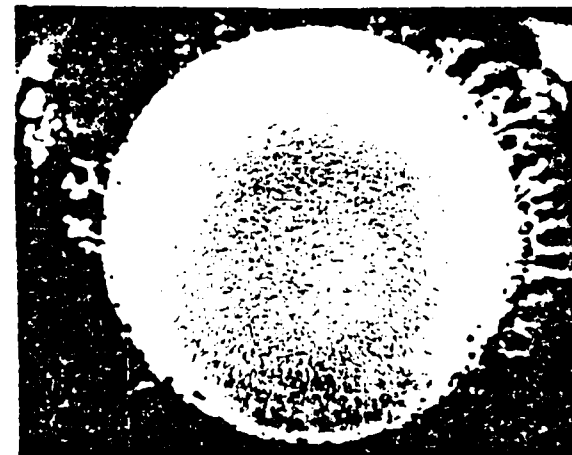
The analysis of the electrodes was performed using several pieces of equipment including a PHI model 595 Auger Electron Spectrometer, a JEOL JSM-2 Scanning Electron Microscope and an Olympus BHM Optical Microscope.

#### Results

Previous experiments performed by the authors [3] have shown that stainless steel (304) electrodes subjected to 50,000 shots showed a significant reduction in electrode erosion (1.5 to 0.7  $\mu$ m<sup>3</sup>/coul) when the switching gas was changed from air to nitrogen. The surfaces of these electrodes, shown in Figure 2a,b,c indicate a regular surface pattern with tracks similar in appearance to a dried up river bed.



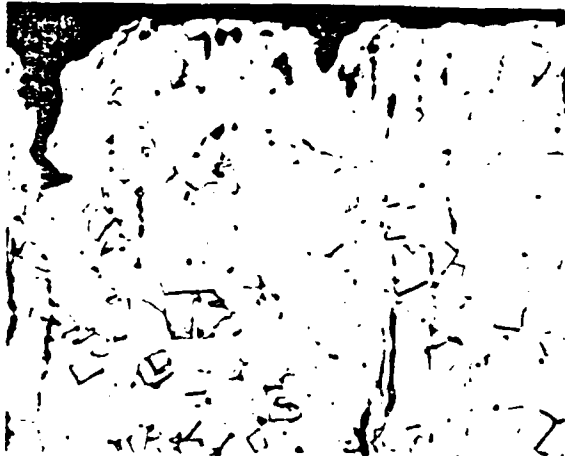
(a) 2 mm

(b) 200  $\mu$ m

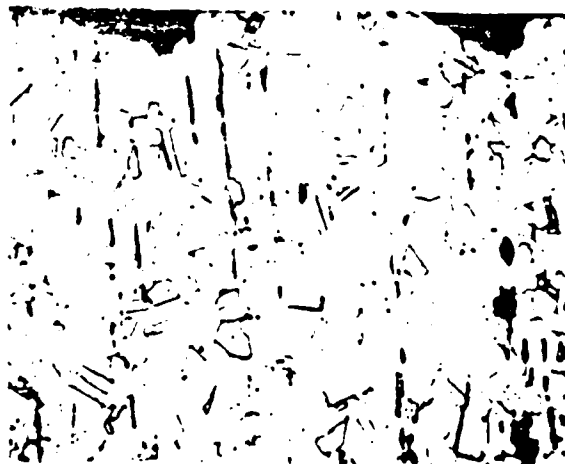
(c) 2 mm

Figure 2. Surfaces of stainless steel (304) cathode: (a) in air, low magnification; (b) in air, high magnification; (c) in nitrogen, low magnification.

The cross sections of these electrodes, shown in Figure 3a,b reveal cracks with depths of approximately 80  $\mu\text{m}$  for electrodes run in air and 20  $\mu\text{m}$  for electrodes run in nitrogen. At first it was thought that the cracks were due solely to temperature cycling in the material with the "hexagonal" pattern resulting from the biaxial tensile forces present during resolidification of the molten surface. (A simple calculation showed that a temperature change of 200°C could lead to crack formation.)



(a) 50  $\mu\text{m}$



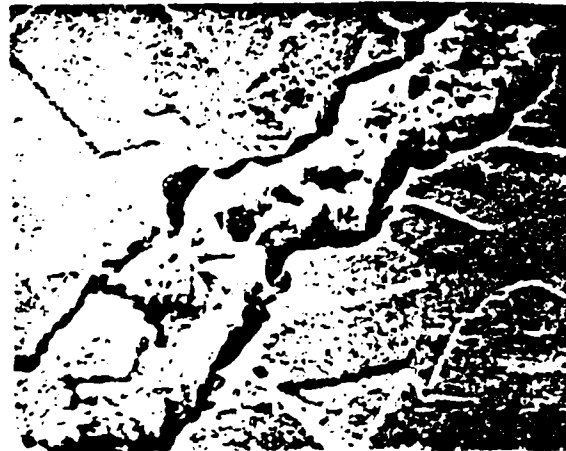
(b) 50  $\mu\text{m}$

Figure 3. Cross sections of stainless steel (304) cathode: (a) in air; (b) in nitrogen.

However, further examination of the cracks shown in Figure 4a,b revealed that the crack orientation was coincident with manganese "stringers" present in the steel, which are perpendicular to the surface (parallel to the length of the rod from which the electrode tip was cut).



(a) 50  $\mu\text{m}$



(b) 5  $\mu\text{m}$

Figure 4. Cross sections of stainless steel (304) cathode in air: (a) on the outer edge; (b) SEM photograph at region examined by Auger analysis.

Auger analysis of the cracks indicated that the manganese acted as a "getter" for the sulphur present in the steel which at high temperatures resulted in a chemical reaction leading to material removal at the manganese sites. However, since many more manganese sites exist than those occurring just at the cracks, it was concluded that the resulting surface formation was a combination of both temperature cycling and chemical attack.

To validate the importance of the stringers, an experiment was performed using a cathode (304) which was cut so that the stringers ran parallel to the surface of the steel and in a mode which had the original orientation to serve as a control. The resulting surfaces shown in Figure 5a,b indicated that no surface tracking occurred in the cathode (as expected), whereas the anode remained the same.

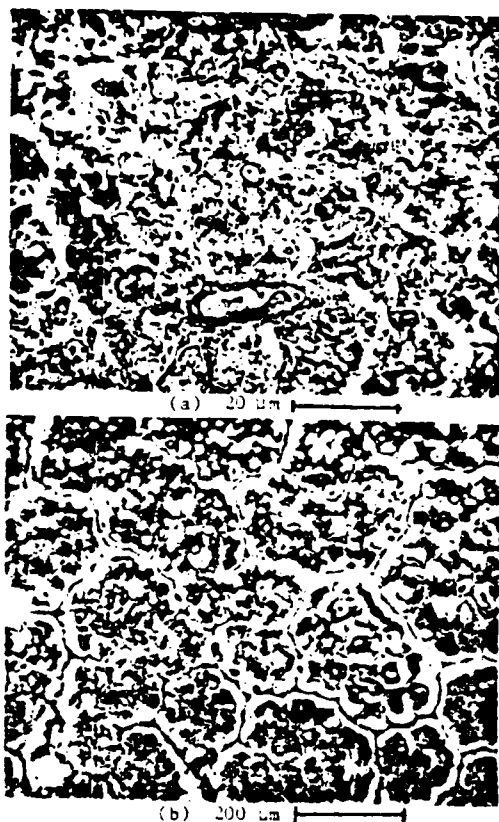


Figure 5. Surfaces of stainless steel (304) in air: (a) cathode--cut so that stringers ran parallel to the surface; (b) anode--the same as previous runs.

In addition, at the suggestion of the steel manufacturer, a second steel was tried (316) which might have lower sulphur content. The results, shown in Figure 5a,b, also indicate an absence of cracks, although no significant reduction in bulk erosion occurred.

One should not conclude from these experiments that surface cracking requires the presence of manganese stringers or even chemical attack--any mechanism which leads to a weakening of the material surface during temperature cycling can prove sufficient to produce the observed structure. Indeed, crack formation has been observed by the authors and others in electrodes made of copper in a tungsten matrix [3-5] and tantalum [6], although the processes leading to the surface cracking are unclear.

Examination of electrodes run for 2,000, 10,000 and 50,000 shots indicated that the depth of the cracks increases with shot number and, although the damage at 50,000 shots (80 μm cracks) was not enough to produce catastrophic failure of the electrode, it is quite plausible that for normal switching use (100 to 1000 shots) crack formation could present a significant materials problem.

#### Acknowledgments

The authors would like to thank M. McNeill for her work on the manuscript and M. Chanirao, L. Hark, L. Jordan, L. Stephenson, H. Tanumiharita, and B. Tucker for their work on the data acquisition system and experimental facility.

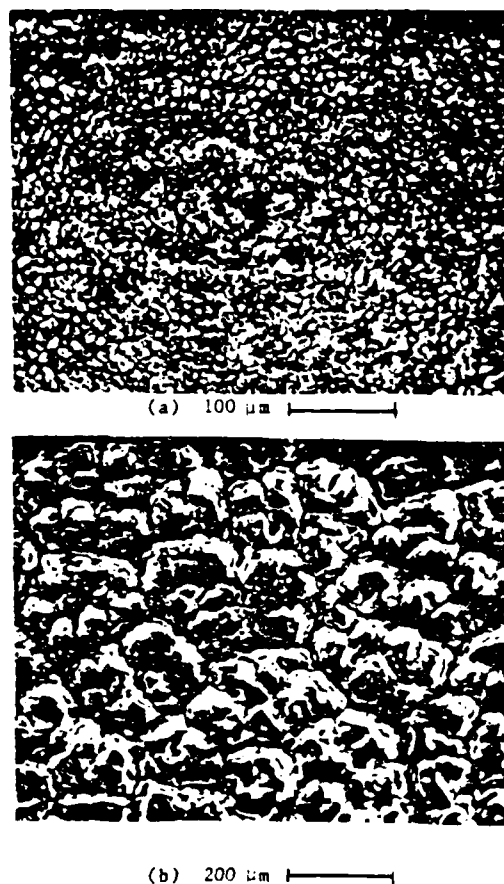


Figure 6. Comparison of cathode surfaces of two different stainless steels: (a) 316; (b) 304.

#### References

- [1] G. L. Jackson, L. Hatfield, M. Kristiansen, M. Hagler, A. L. Donaldson, G. Leiker, R. Curry, R. Ness, L. Gordon and D. Johnson, "Surface Studies of Dielectric Materials Used in Spark Gaps," *J. Appl. Phys.* **55** (1) (1984).
- [2] A. L. Donaldson, "Electrode Erosion in a High Energy Spark Gap," Master's Thesis, Texas Tech University (August 1982).
- [3] A. L. Donaldson, M. O. Hagler, M. Kristiansen, L. L. Hatfield and G. L. Jackson, "Electrode Erosion Phenomena in a High Energy Pulsed Discharge," *IEEE Trans. on Plasma Science*, **PS-12** (1), pp. 28-38 (March 1984).
- [4] Y. Suzuki, Y. Kawakita, M. Kume and M. Kawai, "A 150 kV, 100 kA Spark Gap Switch for Marx Generators," in *Proc. 3rd IEEE Int. Pulsed Power Conf.* (Albuquerque, NM), pp. 444-447 (June 1981).
- [5] M. T. Magnusson, "Erosion and formation of cracks in W/Cu Impregnated Materials of Different Tungsten Grain Size," *ETZ (A)*, **98**, pp. 239-240 (1977).
- [6] E. I. Zolotarev, V. Mukhin, L. E. Polyanskii and V. N. Traneznikov, *Sov. Phys. Tech. Phys.* **21**, pp. 340-344 (1978).

# HIGH CURRENT SURFACE DISCHARGE SWITCH

P.M. Ranon, H. Krompholz, M. Kristiansen  
Department of Electrical Engineering/Computer Science  
L.L. Hatfield  
Department of Physics and Engineering Physics  
Texas Tech University  
Lubbock, Texas 79409

## Abstract

The erosion of several dielectrics has been investigated in a single channel surface discharge switch (SDS). The switch was operated in an oscillating circuit in a self break mode (capacitance 1.85  $\mu$ F, charged to 40 kV, peak current 130 kA, charge transfer .74 C/shot, frequency 300 kHz). Delrin, Teflon, and the epoxy-fiberglass laminate G-10 were used as dielectric surfaces with Copper-Tungsten (K33) electrodes. Repetition rates on the order of 1/3 pulse per second (pps), which increased during operation as the surface eroded and the breakdown voltage decreased, were used. Delrin withstood 100 shots before the 1.6 mm thick sample melted through. Teflon eroded at a lesser rate. G-10 samples quickly shattered or developed a carbonized track which lowered the breakdown voltage to 5 kV.

current waveforms are damped RLC in nature, with their amplitudes determined by the charging voltage. The best results of 130 kA peak current and 0.74 Coulombs/shot charge transfer were obtained across a 3.5 cm gap.

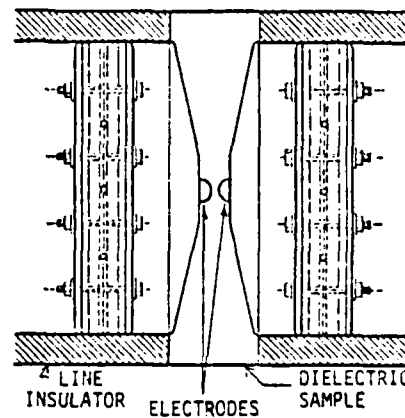
## Introduction

Very little information can be found on insulators which have been tested to repetitive high level currents in excess of MA's, but various dielectric materials are considered as insulators in pulsed power applications due to their availability and cost. G-10, for example, has been used in rail guns, primarily due to its ease of machining and mechanical strength. In such an application, the G-10 is subjected to MA current levels at a very low rep-rate. The present experiment uses field enhanced electrodes which confine currents in excess of 100 kA to a highly localized region on the insulator surface.

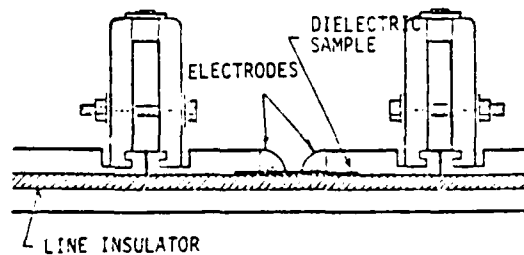
The purpose of this paper is to describe the erosion of Delrin, Teflon, and G-10 as they were subjected to high current levels. Hold-off voltage characteristics of the three dielectric materials were measured and are reported. It is interesting to note the drastic difference of 130 kA switching effects on the dielectrics as compared to previous 5 kA switching studies. G-10 for example, exhibited the best characteristics for 5 kA switching [1], but was the poorest for 130 kA switching. Despite the gross erosion pattern left on the its samples, Delrin exhibited far superior performance compared to G-10. Finally, Teflon exhibited the best overall characteristics of the three materials tested.

## Experimental Arrangement

As shown in Fig. 1, the dielectric samples were inserted into a 5 Ohm, 1 m long strip line. The electrodes, made of K 33, can be continuously adjusted to accommodate gap separations from 0 to 30 cm. The strip line shown is 20.3 cm wide and the separation is provided by a Blue Nylon dielectric, 30.5 cm wide and .65 cm thick. The energy storing, 1.85  $\mu$ F, Scyllac capacitor, shown in Fig. 2, is integrated into the strip line and can store 1.48 kJ of energy when charged to 40 kV. The DC charged SDS, operated in air, is allowed to self break at about 40 kV initially, and allowed to free run, at about 1/3 pps, as determined by the self break voltage which decreased as the dielectric surface eroded away. Both the voltage and



(a) Top View



(b) Side View

Fig. 1 Surface Discharge Switch



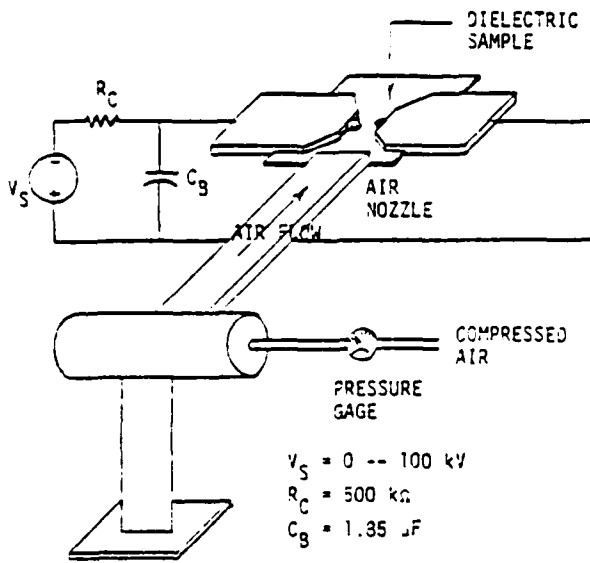


Fig. 2 Experimental Setup

### Results

#### G-10

1) Hold-off voltage, 2) total charge transferred, and 3) total energy transferred are plotted against the number of shots for a typical G-10 sample in Fig. 3. After the first few preconditioning shots, the hold-off voltage dropped quite drastically. As shown in Fig. 4, two different levels of forced air cooling is compared to no cooling with no significant improvement. Fig. 5 shows the cold recovery after the surface has been allowed to cool, but not long enough for the surface charge to be discharged (surface resistance of sample times the capacitance  $\gg$  cooling time). Visual inspection by the naked eye of the G-10 samples with a severely reduced hold-off voltage (approximately 1/10 of initial hold-off voltage), showed signs of a carbonized track approximately 0.5 mm wide burned between the two electrodes, as shown in Fig. 6.

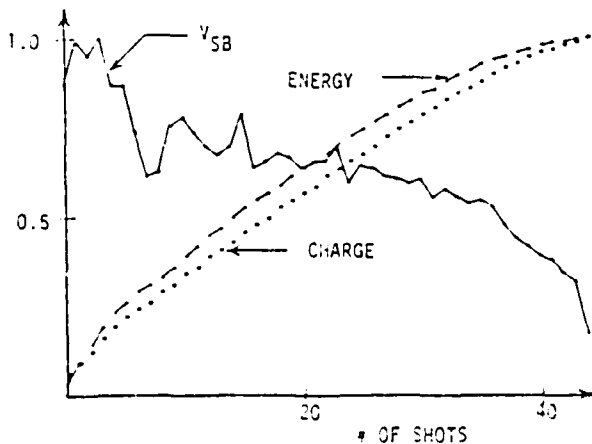


Fig. 3 Typical G-10 Hold-off Voltage Plot

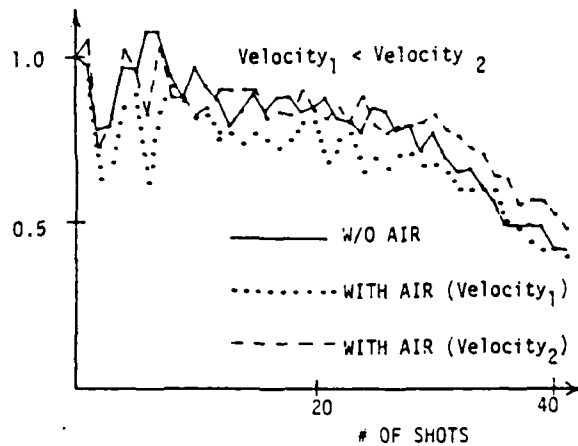


Fig. 4 Effect of Forced Air Cooling on G-10

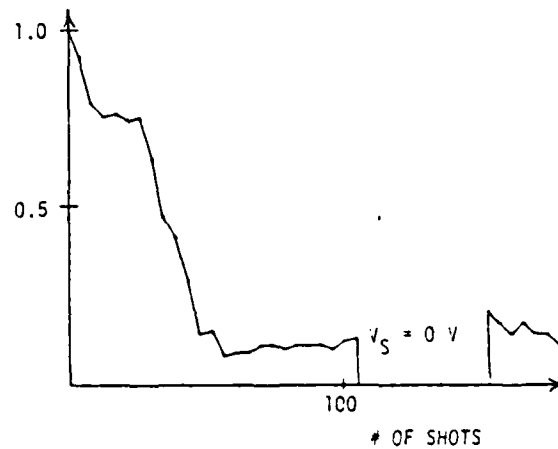


Fig. 5 Cold Recovery of G-10.

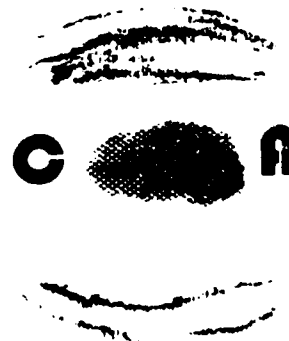


Fig. 6 Erosion Pattern on G-10

Delrin

1) Hold-off voltage, 2) total charge transferred, and 3) total energy transferred are plotted against the number of shots for a non air cooled Delrin sample in Fig. 7. In the case of air cooled samples, there is quite an impressive improvement over the non air cooled sample, as can be seen in Fig. 8. Cold recovery of Delrin using the same method as in the G-10 sample, shows that the material can recover, unlike the G-10 sample. A non air cooled sample is plotted to show the cold recovery of Delrin in Fig. 9. A typical erosion pattern on Delrin is shown in Fig. 10 and it can be seen that the erosion pattern is rather uniform. It is interesting to note that Nylon 66 samples were also tested and showed almost identical patterns overall to those of Delrin and thus not reported separately here.

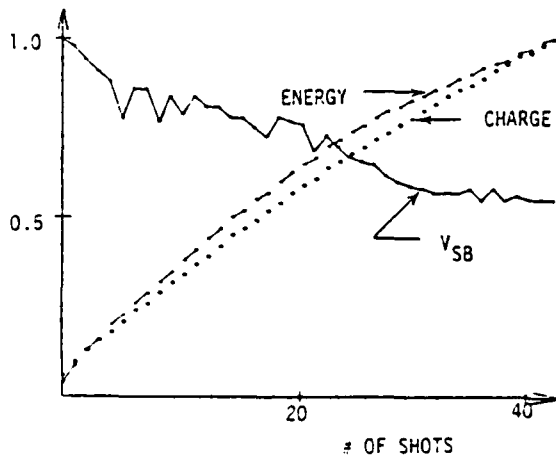


Fig. 7 Non Air Cooled Delrin Hold-Off Voltage Plot

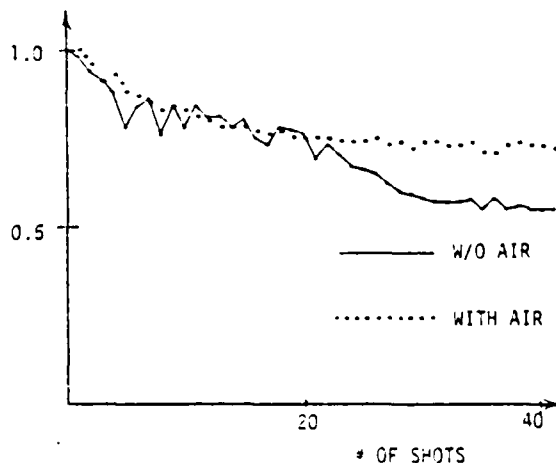


Fig. 8 Effect of Forced Air Cooling on Delrin

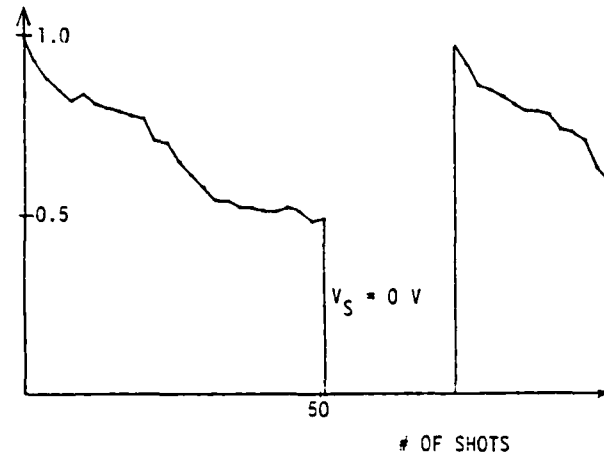


Fig. 9 Cold Recovery of Delrin



Fig. 10 Erosion Pattern on Delrin

Teflon

In Fig. 11, 1) Hold-off voltage, 2) total charge transferred, and 3) total energy transferred are plotted against the number of shots for a non air cooled Teflon sample. As can be seen from the figure, the hold-off voltage remained consistently high throughout the run. Forced air cooling on Teflon samples seemed to have an effect as it did for the Delrin, but the results did not seem as significant due to the consistently high hold-off voltage. Due to this high hold-off voltage characteristics, it is difficult to determine whether the Teflon has actually recovered for the test shown in Fig. 13. Figure 14 shows the erosion pattern left on a Teflon sample.

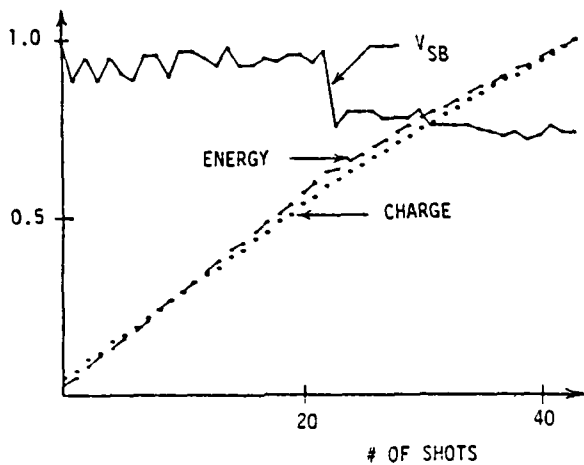


Fig. 11 Non Air Cooled Teflon Hold-Off Voltage Plot

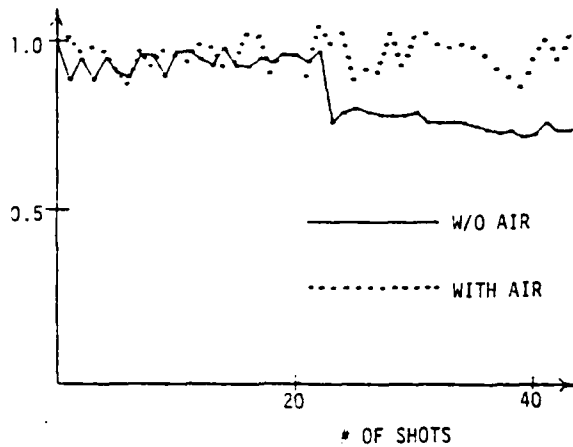


Fig. 12 Effect of Forced Air Cooling on Teflon

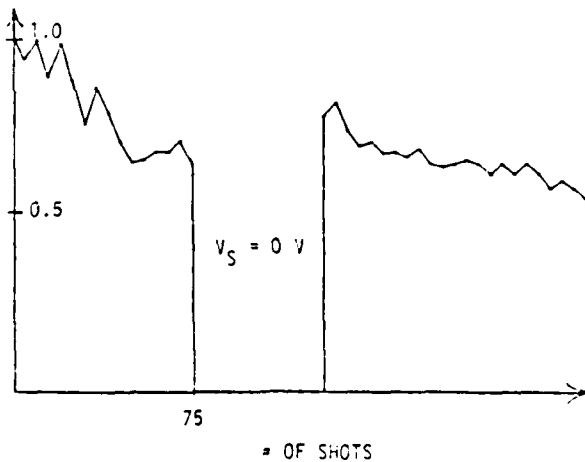


Fig. 13 Cold Recovery of Teflon



Fig. 14 Erosion Pattern on Teflon

#### Discussion of Results

Johnson [2], measured no significant reduction of the hold-off voltage of G-10 and Delrin at relatively low current levels even after exposing them to several thousand shots at current levels of a few thousand Amperes. It is clearly evident that the erosion of dielectric materials depend very heavily on the maximum current as is especially evident for G-10. For Delrin, the hold-off voltage depends very heavily on the surface temperature and not the physical volumetric erosion. With no prior reports on Teflon it is impossible to make any type of contrasting comparison but Teflon seems very promising as a high current insulator for these types of applications.

#### Acknowledgment

This work was supported by the Air Force Office of Scientific Research and the Army Research Office. The authors would like to extend their appreciation to Stephen Whiteside, Mike Ingram, Marie Byrd, and Tom Morris for their technical support.

#### References

1. R.D. Curry, Master's Thesis, Texas Tech University, (May, 1984).
2. D. Johnson, Master's Thesis, Texas Tech University, (1982).

Conical Liner Implosion as a  
Projectile Injector for Mass Drivers\*

Kazunari IKUTA (a) and Magne KRISTIANSEN

Department of Electrical Engineering/  
Computer Science  
Texas Tech University  
Lubbock, Texas 79409

ABSTRACT

An electro-magnetic method for injecting a projectile into a mass driver using a conical liner is proposed.

---

\* This work was supported by the AFOSR and ARO

(a) Institute of Plasma Physics  
Nagoya University  
Nagoya, Japan 464

Most of the serious problems for electro-magnetic accelerators of projectiles, such as rail guns<sup>1)</sup> and ablation mass drivers<sup>2,3)</sup> occur at the low velocity section of the accelerator, since most of the electrode erosion occurs in this low velocity section of the accelerators. Here the low velocity means the velocity lower than about  $1 \text{ km s}^{-1}$ . This is because of the fact that the heat load on the surface of the electrode in the low velocity section becomes extremely high since it is approximately inversely proportional to the projectile velocity.

In order to minimize this problem, the projectile should have a high injection speed into the accelerator. Using light gas guns as injectors to give an initial speed to the projectile, however, induces other complicated problems since these guns also inject large amounts of gas into the discharge chamber where the armature propels the projectile. This can, for instance, cause restrike at the breech of the gun. The initial projectile speed should, therefore, be caused by other means than using gas pressure.

Another serious problem is the stiffness of the accelerator. The operating stress for accelerator rails and insulators must be low enough to avoid unacceptable mechanical distortions. This later problem must be solved by the careful choices and the development of the materials. We do not discuss this problem in this work.

The purpose of the present letter is to propose a new method of injecting projectile into electromagnetic accelerators. At the exit of the injectors, the projectile should have the velocities of the order of a few  $\text{km s}^{-1}$  in order to avoid the electrode erosion of the main accelerator.

A potential alternative method for imparting the necessary injection speed to the projectile is to use an imploding conical liner which squeezes an insulating working fluid (e.g. oil) into the accelerator instead of the gas. The driven fluid can then give the forward thrust to the projectile. This principle of conical liner injector is shown in Fig. 1.

The dynamic behavior of the metallic cone is as follows. Once the switch is turned on, the current flows along the conical surface (conical z-pinch). As long as the current is sufficiently high, the cone is compressed by the magnetic pressure, as shown in Fig. 2. The eventual change of the cone geometry squeezes the fluid into the barrel and the projectile, which, together with the ablator, is propelled by the fluid.

An estimate of the attainable velocity is as follows. The equation of motion of the conical shell, driven by the fluid, the ablator, and the projectile is approximately described by

$$M \frac{d^2 z}{dt^2} = \frac{\mu_0 I^2}{2\pi} g, \quad (1)$$

where  $M$  is the total mass including the fluid, the ablator and the projectile,  $I$  is the total current along the conical shell,  $\mu_0$  is the magnetic permeability of vacuum,  $z$  is the distance along the cone, and  $g$  is a constant of order unity. Here the mass of the moving shell is neglected. If the length of the cone is  $h$  and the current is supplied by a constant current source, the final velocity,  $v_0$ , obtained is

$$v_o = \left( \frac{\mu_o g h}{\pi M} \right)^{1/2} \quad (2)$$

If the required speed for the injection is  $v_o \approx 10^3$  m/s, Eq. (2) is reduced to

$$\frac{I^2 h}{M} \approx 0.25 \times 10^{13} \quad (3)$$

in MKS unit. Specifically when the current,  $I$ , is  $10^6$  amperes and the mass,  $M$ , is 0.1 kg, the length of the cone becomes

$$h \approx 0.25 \text{ (meter)} \quad (4)$$

In conclusion, we have suggested a possible method for injecting the projectile into an electromagnetic mass driver without using gas pressure. The necessary cone for the acceleration of the projectile is acceptably short, provided that the driven current along the conical shell is of the order of  $10^6$  amperes. The quasi-steady current of order  $10^6$  amperes should be obtained by the method employed in the work<sup>1</sup>.

In addition it is possible to compress the liner by induced current azimuthally on the surface of the liner (conical  $\theta$ -pinch), although only the case of conical  $z$ -pinch compression of the liner

is discussed in this work. In spite of less efficient acceleration with a conical  $\theta$ -pinch than with a conical z-pinch, the non-destructible conical  $\theta$ -pinch accelerator is possible.



## Figure Captions

Fig. 1     Structure of injector using a metallic conical liner.

Fig. 2     Change of the shape of the metallic cone when current is driven along it. Note the formation of the stem.

## References

1.   S.C. Rashleigh and R.A. Marshall, J. Appl. Phys., 49, (1978) 2540.
2.   K. Ikuta: Jpn. J. Appl. Phys., 24, (1985) 862.
3.   K. Ikuta, M. Kristiansen and M.F. Rose: Submitted to J. Appl. Phys.

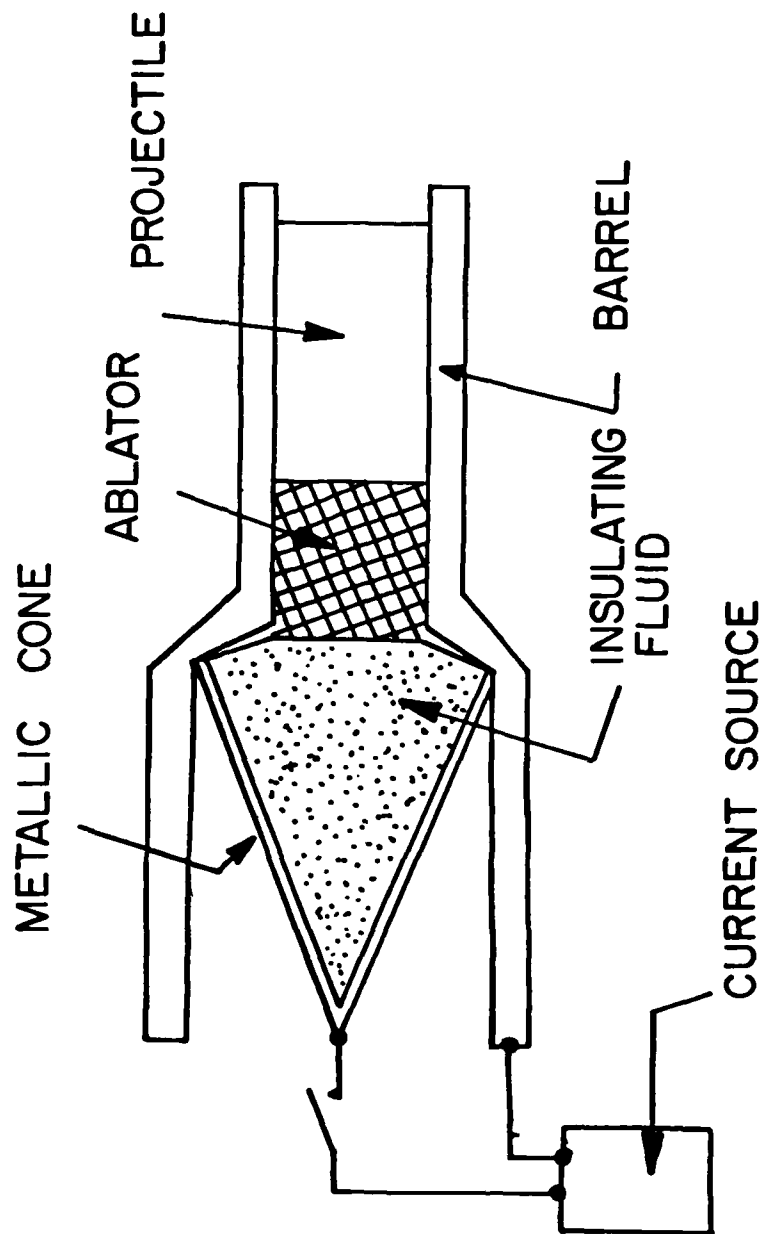


Fig. 1 Principle of Conical Liner Injection

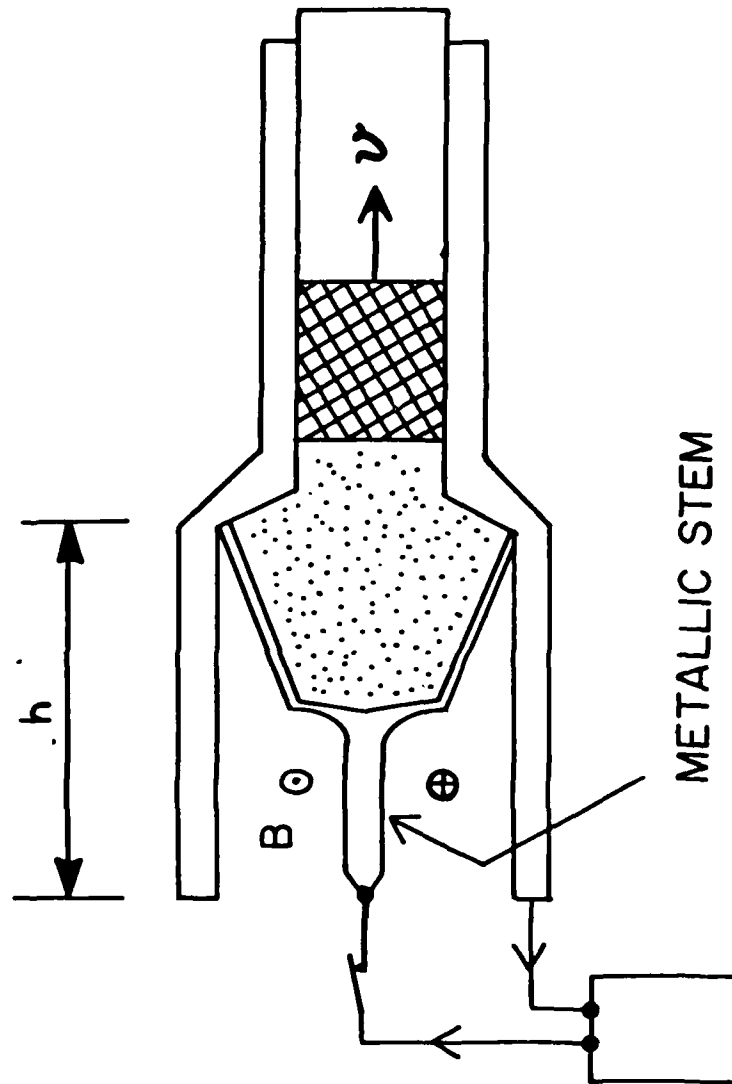


Fig. 2 Schematic of Cone Compression by Magnetic Pressure

JUN 10 1985



DEPARTMENT OF THE AIR FORCE  
AIR FORCE WRIGHT AERONAUTICAL LABORATORIES (AFSC)  
WRIGHT-PATTERSON AIR FORCE BASE, OHIO 45433

REPLY TO  
ATTN OF:

FI

5 JUN 1985

SUBJECT: Appreciation

TO: Dr Marion O. Hagler  
Chairman, Dept of Electrical Engineering  
Texas Tech University  
Lubbock, Texas 79409

1. The Flight Dynamics Laboratory of the Air Force Wright Aeronautical Laboratories wishes to express its appreciation to Dr M. Kristiansen, Head of the Plasma and Switching Laboratory, for his outstanding contributions to technical discussions held at Maxwell Laboratories, Inc., San Diego, CA, on 1 May 1985.

2. These discussions were conducted to solve problems with a pulsed power KrF laser triggered crowbar switch which is a critical component of a full threat lightning simulation generator. This generator is being built under contract for the Air Force's Atmospheric Electricity Hazards Protection Advanced Development Program (AFWAL/FIEA). These problems had plagued the contractor for over a month and had delayed the delivery of the generator. This delay was costing the Air Force money as it further delayed other Air Force contracted efforts.

3. Dr Kristiansen contributed significantly to the technical discussions at Maxwell Laboratories which resulted in a concise detailed plan of approach to solve the problems with this pulsed power switch. Prior to the discussions, Dr Kristiansen identified to the Air Force those individuals in the United States who could contribute most significantly to these discussions. He solicited and arranged the participation of Dr A. H. Guenther, Chief Scientist, Air Force Weapons Laboratory. Unable to attend the Thursday meetings due to prior commitments, he arrived two days early and set the stage for all discussions which followed. He determined concisely the problems, made significant recommendations and pre-briefed the other participants. As a result of his efforts, the technical discussions held on Thursday were a monumental success. Dr Kristiansen's superb technical abilities in the area of pulsed power and his extreme interest in solving this significant U.S. Air Force problem bring credit upon himself and Texas Tech University.

4. For providing his superb technical abilities, arranging his schedule to participate in the technical discussions and his outstanding contributions to the solution of this Air Force problem, the Flight Dynamics Laboratory is extremely grateful and wishes to express its appreciation to Dr Kristiansen, Head of the Texas Tech University Plasma and Switching Laboratory.

JAMES J. MATTICE  
Acting Director  
Flight Dynamics Laboratory

END

DTIC

7-86